



Centre for Research in String Theory
School of Physics and Astronomy

THESIS SUBMITTED FOR THE DEGREE OF
DOCTOR OF PHILOSOPHY

**Form factors and scattering amplitudes
in supersymmetric gauge theories**

MARTYNA MARIA JONES

Supervisors

PROF. GABRIELE TRAVAGLINI
PROF. ANDREAS BRANDHUBER

July 2018

*Pracę tę dedykuję pamięci dziadka Zbyszka,
który nauczył mnie, że w pierwszej wszystkie są dodatnie.*

Declaration

I, Martyna Maria Jones, confirm that the research included within this thesis is my own work or that where it has been carried out in collaboration with, or supported by others, that this is duly acknowledged below and my contribution indicated. Previously published material is also acknowledged below.

I attest that I have exercised reasonable care to ensure that the work is original, and does not to the best of my knowledge break any UK law, infringe any third party's copyright or other Intellectual Property Right, or contain any confidential material.

I accept that the College has the right to use plagiarism detection software to check the electronic version of the thesis. I confirm that this thesis has not been previously submitted for the award of a degree by this or any other university.

The copyright of this thesis rests with the author and no quotation from it or information derived from it may be published without the prior written consent of the author.

Signature:

A handwritten signature in black ink that reads "M. Jones". The signature is written in a cursive style with a large initial 'M' and a long, sweeping underline.

Date: September 16, 2018

Details of collaboration and publications:

This thesis describes research carried out with my supervisors, Prof. Gabriele Travaglini and Prof. Andreas Brandhuber, which was published in [1–4]. We collaborated with Dr. Brenda Penante on all of the aforementioned publications and with Dr. Donovan Young on [1]. Where other sources have been used, they are cited in the bibliography.

Abstract

The study of scattering amplitudes in the maximally supersymmetric Yang-Mills theory ($\mathcal{N} = 4$ SYM) is a thriving field of research. Since the reformulation of perturbative gauge theory as a twistor string theory by Witten, this area has witnessed a flurry of activity, leading to the discovery of a multitude of novel techniques, such as recursion relations and MHV diagrams, collectively referred to as on-shell methods. In parallel, many previously hidden properties and rich mathematical structures have been found, a powerful example of such being the dual superconformal symmetry.

It is natural to ask whether this understanding can be extended to phenomenologically relevant theories as well as other quantities. The goal of the present work is to apply the modern on-shell methods to calculations of form factors, with particular focus on those which are relevant for describing Higgs production in QCD from the point of view of an effective field theory. Specifically, our analysis will be carried out in supersymmetric gauge theories at two-loop level and will consist of several steps. We focus first on operators in the $SU(2|3)$ closed subsector of $\mathcal{N} = 4$ SYM, in particular two non-protected, dimension-three operators. We then move on to consider the trilinear operator $\text{Tr}(F^3)$ and a related descendant of the Konishi operator which contains $\text{Tr}(F^3)$, also in $\mathcal{N} = 4$ SYM. Finally, we concentrate on two-loop form factors of these two operators in theories with less-than-maximal supersymmetry. The result of our investigation shows an emergence of a small number of universal building blocks, ultimately related to the two-loop form factor of a trilinear half-BPS operator. This finding suggests that the most complicated, maximally transcendental part of Higgs plus multi-gluon amplitudes in QCD can be equivalently computed in a remarkably simple way by considering form factors of half-BPS operators in $\mathcal{N} = 4$ SYM.

Acknowledgements

First and foremost, it is a great pleasure to thank my supervisors, Prof. Gabriele Travaglini and Prof. Andreas Brandhuber for their guidance, support and encouragement during the course of my doctoral studies. Their wisdom, intuition and infectious enthusiasm for the subject were the driving force behind my research.

A very special thank you to a friend and a collaborator, Brenda Penante for her presence, kindness and good humour in sharing some of the struggles along the way. Thank you to Donovan Young for the collaboration in the early stages of my studies.

I would like to thank the fellow PhD students at Queen Mary University of London of many generations, in particular Luigi Alfonsi, Nadia Bahjat-Abbas, Nejc Ceplak, Ed Hughes, Arnau Koemans Collado, Zac Kenton, Zoltan Laczko, Chris Lewis-Brown, Linfeng Li, Paolo Mattioli, James McGrane, Emmanuele Moscato, Ray Otsuki, Felix Rudolph, Ricardo Stark-Muchao. Special thank you to Joe Hayling and Rodolfo Panerai for their friendship, which I hope will continue for many years to come, and help with preparation of this thesis. I would also like to thank fellow students of King's College London and Imperial College London, in particular Simone Noja and Max Zimmermann for their long-standing support, encouragement and friendship.

I wish to extend my gratitude to the faculty and staff members at Queen Mary University of London who made my time here a very enjoyable experience. In particular, many thanks to David Berman, Sarah Cows, Jessica Henry, Lucie Langley, Sanjaye Ramgoolam, Karen Stoneham, John Sullivan, Steve Thomas and Isabel Wood.

Many thanks to friends, fellow instructors and students at Total Krav Maga and other clubs of Krav Maga Global in the UK and worldwide to whom I owe much of my peace of mind over the course of the past four years.

To my family, I owe the greatest debt of gratitude. To my husband, Ben, for his love, encouragement and support which went as far as proofreading parts of this thesis. To my parents, Marcin and Kasia, my sisters, Marysia, Malgosia and Maja, and my grandmothers, Basia and Bozenka. This journey has been a long one and they have helped me in more ways than I can name – from the bottom of my heart, I thank you.

The research contained in this thesis was supported by an STFC studentship.

Contents

1	Introduction	8
2	Review	15
2.1	Scattering amplitudes of gluons	15
2.2	Tree-level amplitudes	22
2.3	Tree-level recursion relations	25
2.4	$\mathcal{N} = 4$ super Yang-Mills	29
2.5	Scaling dimension and the dilatation operator	40
2.6	Primary, descendant and half-BPS operators	44
2.7	Loop-level techniques	45
2.8	Two-loop remainder function	51
2.9	Form factors	56
3	The $SU(2 3)$ sector form factors	60
3.1	Introduction	60
3.2	One-loop minimal form factor $\langle \bar{X}\bar{Y}\bar{Z} \mathcal{O}_{\mathcal{B}} 0\rangle$	63
3.2.1	Two-particle cut of the one-loop form factor	64
3.2.2	Auxiliary one-loop form factors needed for two-loop cuts	67
3.3	Two-loop minimal form factor $\langle \bar{X}\bar{Y}\bar{Z} \mathcal{O}_{\mathcal{B}} 0\rangle$	69
3.3.1	Two-particle cuts of the two-loop form factor	69
3.3.2	Three-particle cuts of the two-loop form factor	73
3.3.3	Comparing the half-BPS form factors	79
3.3.4	Summary and integral reduction	82
3.4	Two-loop remainder function of $\langle \bar{X}\bar{Y}\bar{Z} \mathcal{O}_{\mathcal{B}} 0\rangle$	85
3.4.1	Connection to the remainder densities in the $SU(2)$ sector	88
3.5	One-loop non-minimal form factor $\langle \bar{X}\bar{Y}\bar{Z} \mathcal{O}_{\mathcal{F}} 0\rangle$	89
3.5.1	Two-particle cut in the q^2 -channel	89
3.5.2	Two-particle cut in the s_{23} -channel	90
3.5.3	Final result	94
3.6	Two-loop subminimal form factor $\langle \bar{\psi}\bar{\psi} \mathcal{O}_{\mathcal{B}} 0\rangle$	94

3.7	Two-loop dilatation operator in the $SU(2 3)$ sector	96
3.8	Summary	100
4	Form factors of $\text{Tr}(F^3)$ in $\mathcal{N}=4$ super Yang-Mills	101
4.1	Introduction	101
4.2	Operators and tree-level form factors	104
4.2.1	Supersymmetric form factors and mixing	105
4.2.2	Further tree-level form factors	107
4.3	One-loop minimal form factors	108
4.4	Two-loop minimal form factors in $\mathcal{N}=4$ SYM	110
4.4.1	Two-particle cuts	111
4.4.2	Three-particle cut in q^2 -channel	115
4.4.3	Three-particle cut in s_{23} -channel	117
4.4.4	Merging the cuts	125
4.4.5	Final result for the two-loop integrand in $\mathcal{N}=4$ SYM	127
4.4.6	Components vs. super-cut comparison	128
4.5	Remainder functions in $\mathcal{N}=4$ SYM	128
4.5.1	Definition of the BDS form factor remainder	129
4.5.2	The remainder and anomalous dimension of \mathcal{O}_S	129
4.5.3	The remainder of \mathcal{O}_C	132
4.6	Discussion	132
4.7	Summary	135
5	Form factors of $\text{Tr}(F^3)$ in $\mathcal{N}<4$ super Yang-Mills	137
5.1	Introduction	137
5.2	Operators and tree-level form factors in $\mathcal{N}<4$ SYM	139
5.3	One-loop minimal form factors	140
5.4	Two-loop minimal form factors in $\mathcal{N}<4$ SYM	141
5.4.1	An effective supersymmetric decomposition	141
5.4.2	Modifications to the two-particle cut	143
5.4.3	Modifications to the three-particle cut	144
5.5	Remainder functions in $\mathcal{N}<4$ SYM	146
5.5.1	Catani form factor remainder and renormalisation	146
5.5.2	$\mathcal{N}=2$ SYM	148
5.5.3	$\mathcal{N}=1$ SYM	152
5.6	Consistency checks	153
5.7	Summary	154

6	Conclusions	156
6.1	Summary of the key results	156
6.2	Pure Yang-Mills	157
6.3	Further work	158
A	Spinor conventions	160
A.1	Spinor manipulations	160
A.2	Spinor traces	161
A.3	Parity on spinors	162
B	Integral functions	163
B.1	One-loop scalar integrals	163
C	Integrands	166
C.1	Integrands for the form factor $\langle \bar{X}\bar{Y}\bar{Z} \mathcal{O}_{\mathcal{B}} 0\rangle$	166
C.2	Integrands for the form factor of $\langle g^+g^+g^+ \mathcal{O}_{\mathcal{C}} 0\rangle$	171
C.3	Scalar and fermion contributions to $\langle g^+g^+g^+ \mathcal{O}_{\mathcal{C}} 0\rangle$	174
D	Non-minimal form factors	177
D.1	Non-minimal form factors contributing to $\langle \bar{X}\bar{Y}\bar{Z} \mathcal{O}_{\mathcal{B}} 0\rangle$	177
D.2	Non-minimal form factors contributing to $\langle g^+g^+g^+ \mathcal{O}_{\mathcal{C}} 0\rangle$	181
E	Numerators	184
E.1	Two-loop integrand for $\langle g^+g^+g^+ \mathcal{O}_{\mathcal{S}} 0\rangle$ in $\mathcal{N}=4$ SYM	184
E.2	Two-loop integrand for $\langle g^+g^+g^+ \mathcal{O}_{\mathcal{C}} 0\rangle$ in $\mathcal{N}=4$ SYM	185
E.3	Two-loop integrand for $\langle g^+g^+g^+ \mathcal{O}_{\mathcal{S}} 0\rangle$ in $\mathcal{N}=2$ SYM	186
E.4	Two-loop integrand for $\langle g^+g^+g^+ \mathcal{O}_{\mathcal{C}} 0\rangle$ in $\mathcal{N}=2$ SYM	187
E.5	Two-loop integrand for $\langle g^+g^+g^+ \mathcal{O}_{\mathcal{S}} 0\rangle$ and $\langle g^+g^+g^+ \mathcal{O}_{\mathcal{C}} 0\rangle$ in $\mathcal{N}=1$ SYM	187
	Bibliography	188

Chapter 1

Introduction

4th of July 2012 marks the date of the announcement of one of the most iconic discoveries of our lifetime. A new particle with a mass of 126 GeV has been detected by both the CMS [5] and ATLAS [6] experiments at the Large Hadron Collider (LHC) at CERN and later confirmed by precise measurements to be the elusive Higgs boson [7–9]. The discovery, widely celebrated as a triumph of modern theoretical physics and leading to award of the 2013 Nobel Prize in Physics to Peter Higgs and François Englert, has cemented our confidence in the predictive power of the Standard Model of particle physics. Every discovery, however, opens a pathway to new investigation and our knowledge of fundamental physics is by no means complete. Many questions remain unanswered and as a result, research related to providing experimentally testable predictions from various theoretical models is as active as ever.

The most general observables for a given quantum field theory (QFT) are the correlation functions, defined as the vacuum expectation value of the time-ordered product of field operators. In this thesis we will be considering local, gauge invariant composite operators $\mathcal{O}_i(x_i)$ built out of fields of the theory evaluated at a common spacetime point x_i . The correlation function is then defined as

$$C_{\mathcal{O}_1, \dots, \mathcal{O}_n}(x_1, \dots, x_n) = \langle 0 | T \{ \mathcal{O}_1(x_1) \cdots \mathcal{O}_n(x_n) \} | 0 \rangle, \quad (1.0.1)$$

with $T\{\dots\}$ denoting time-ordering of the product of operators and $|0\rangle$ the ground, or vacuum state. For a D -dimensional theory with fundamental fields $\{\phi_1, \dots, \phi_n\}$, a Lagrangian $\mathcal{L}[\phi_1, \dots, \phi_n]$ and an action functional

$$S[\phi_1, \dots, \phi_n] = \int_{-T}^T d^D x \mathcal{L}[\phi_1, \dots, \phi_n], \quad (1.0.2)$$

it is possible to express the correlation function in the path integral formulation as

$$C_{\mathcal{O}_1, \dots, \mathcal{O}_n}(x_1, \dots, x_n) = \lim_{T \rightarrow \infty(1-i\epsilon)} \frac{\int \mathcal{D}\phi_1 \cdots \mathcal{D}\phi_n \mathcal{O}_1(x_1) \cdots \mathcal{O}_n(x_n) e^{iS[\phi_1, \dots, \phi_n]}}{\int \mathcal{D}\phi_1 \cdots \mathcal{D}\phi_n e^{iS[\phi_1, \dots, \phi_n]}}. \quad (1.0.3)$$

In the present work we will be studying quantities computed in perturbation theory. In order to do that, we decompose the Lagrangian of the quantum field theory under consideration into its free and interacting parts,

$$\mathcal{L} = \mathcal{L}_{\text{free}} + g \mathcal{L}_{\text{int}}, \quad (1.0.4)$$

where $\mathcal{L}_{\text{free}}$ describes the kinematics of the fields of the theory and \mathcal{L}_{int} the interactions between them. If the theory is weakly coupled, *i.e.* the coupling constant g is small, we can expand the exponentials in (1.0.3) and study the correlation function term by term as a power series in g . This approach proves very useful as, apart from the simplest of theories, the exact functional form of the correlator is often not known. As a result, as the types of interactions studied gain complexity it becomes increasingly difficult to make any meaningful predictions to be contrasted with the experimental results. Perturbative methods, however, allow us to compute the results with a certain level of precision, dictated by the order in g , and hence make testable predictions up to that accuracy.

By virtue of the Lehmann-Symanzik-Zimmermann (LSZ) reduction formula [10] one can relate the correlation function to the S -matrix element for n asymptotic initial $|i\rangle$ and final $\langle f|$ momentum eigenstates. This is achieved by Fourier-transforming the correlator (1.0.3) to momentum space and requiring that the fields in the initial and final states are momentum eigenstates. The S -matrix elements are found as the residues of the poles arising in the Fourier transform of the correlation function when the external momenta are put *on-shell*,

$$p_i^2 = m_i^2, \quad \forall i = 1, \dots, n. \quad (1.0.5)$$

The differential cross-section, which is directly relevant for scattering experiments, is then proportional to the modulus-squared of the S -matrix element, or the *scattering amplitude*:

$$\frac{d\sigma}{d\Omega} \sim |\langle f|S|i\rangle|^2 = |\mathcal{A}|^2. \quad (1.0.6)$$

The cross-section σ can then be obtained by integrating the above expression over all angles Ω . These quantities can be measured in a collider experiment and hence are crucial if one is to verify theoretical predictions of the given quantum field theory. The

important feature distinguishing between the correlation function and the scattering amplitude is the fact that for the latter the external momenta are constrained to be on-shell, for correlation functions no such restriction exists and we refer to them as being *off-shell*.

The traditional method of computing scattering amplitudes is through the machinery of Feynman diagrams. Developed in the late 1940s by Richard Feynman, the method has been extremely successful as it provides a convenient way of bookkeeping the mathematical expressions which sum to the amplitude. It is, unfortunately, also largely inefficient – while the individual diagrams are manifestly local, they also carry a large number of gauge redundancies and off-shell information. Simple calculations even at leading order in perturbation theory involve summation of a considerable number of diagrams and require significant amount of computing power for processes as complex as those occurring in the LHC. In the classic example [11], the number of Feynman diagrams contributing to the leading order scattering of gluons, $g + g \rightarrow ng$, increases rapidly with the number of particles involved, as outlined in Table 1.

n	2	3	4	5	6	7	8
Feynman diagrams	4	25	220	2485	34300	559405	10525900

Table 1: Number of Feynman diagrams contributing to the scattering $g + g \rightarrow ng$ at tree-level.

The theoretical interest in the subject of efficiently computing scattering amplitudes has been rekindled in the late 1980s when Parke and Taylor [12] made the observation that an amplitude of a particular configuration of *any number of gluons*, in principle resulting from summation of a huge number of complicated Feynman diagrams, can be brought to an extremely simple and compact form. The natural questions followed: is the underlying simplicity of the scattering amplitude obscured by the computational techniques we employ? What can we understand about the QFT through studying hidden structures of its amplitudes? And, most importantly for this thesis, can we extend our understanding to off-shell quantities?

Years of research activity followed as a result of Parke and Taylor’s discovery and much progress has been made in the past three decades. Amongst all the development one theory has emerged as particularly special in terms of the amount of properties it displays, namely the $\mathcal{N}=4$ *supersymmetric Yang-Mills* (SYM) theory. It is remarkable on many counts – it has the maximal amount of supersymmetry, lies in the heart of the famous AdS/CFT correspondence, is conformal in four dimensions and integrable in the planar limit. All of these features are reviewed in Chapter 2.

Conveniently, gluon amplitudes in $\mathcal{N} = 4$ SYM at tree level coincide with those

of pure Yang-Mills and as such the theory can be thought of as a testing ground for ideas potentially applicable to non-supersymmetric theories. Through application of powerful unitarity-based methods, reviewed in Chapter 2, and constraints resulting from collinear limits, one-loop $\mathcal{N}=4$ SYM amplitudes have been calculated by Bern, Dixon, Dunbar and Kosower in [13]. In [14] the study has been extended to a larger class of *cut-constructible* amplitudes and included less-than-maximally supersymmetric theories and contributions from loops of massive particles [15]. Higher loop order investigations followed, in particular in [16] two-loop *splitting amplitudes*, describing the limit where two gluon momenta become parallel, have been computed using generalised unitarity.

The second revolution in the subject area began in 2003 as a result of formulation of twistor string theory by Witten [17] and his discovery of a connection between scattering amplitudes in $\mathcal{N}=4$ SYM and the instanton expansion of a string theory with Penrose’s twistor space [18] as target space. As a result of this reformulation, significant progress in understanding properties of perturbative Yang-Mills theory has been made and powerful methods for evaluating scattering amplitudes have been developed. These are collectively referred to as *on-shell techniques* and include recursion relations of Britto, Cachazo, Feng and Witten (BCFW) [19] and Cachazo, Svrček and Witten expansion (CSW) [20], both reviewed in Chapter 2.

In parallel, one may ask to what extent on-shell techniques can be utilised in computing off-shell quantities. The simplest such objects are form factors, defined as an overlap of an on-shell n -particle state with an off-shell state created by an insertion of a local composite operator $\mathcal{O}(x)$ on the vacuum $|0\rangle$ and Fourier-transformed to momentum space,

$$\begin{aligned}
 F_{\mathcal{O}}(1, \dots, n; q) &= \int d^4x e^{-iqx} \langle 1, \dots, n | \mathcal{O}(x) | 0 \rangle \\
 &= (2\pi)^4 \delta^{(4)}\left(q - \sum_{i=1}^n p_i\right) \langle 1, \dots, n | \mathcal{O}(0) | 0 \rangle.
 \end{aligned}
 \tag{1.0.7}$$

These objects are interesting from both the theoretical and phenomenological point of view and appear in many contexts, which are reviewed in Chapter 2.

The study of form factors of composite operators is currently a very active area of research. After the pioneering paper [21], interest in the calculation of form factors in supersymmetric theories was rekindled first at strong coupling [22, 23]. Weak coupling investigation followed, where in particular it turned out that the powerful on-shell techniques find their applications also in the realm of partially off-shell quantities. In [24] form factors of protected operators in $\mathcal{N}=4$ SYM have been computed at tree-level and one loop. Interesting parallels have been found between the form factors with the external state of two scalars and $n-2$ positive helicity gluons and the Parke-Taylor amplitudes. Further investigations involving other operators [25–27],

higher loop-orders [28–30] and different theories [31–33] followed. The primary focus of this thesis are two-loop form factors of non-protected operators and we begin the investigation with simplest, scalar operators in $\mathcal{N}=4$ SYM in Chapter 3.

Interestingly from the phenomenological point of view, we may think of certain form factors as corrections to the scattering amplitude due to addition of a new, effective coupling into the action. If we write the n -point scattering amplitude of the theory as an overlap of an n -particle on-shell state and the vacuum,

$$\mathcal{A}_n = \langle 1, \dots, n | 0 \rangle, \quad (1.0.8)$$

and modify the action by addition of a new term,

$$\delta S = g_{\mathcal{O}} \int d^4x \mathcal{O}(x), \quad (1.0.9)$$

with $g_{\mathcal{O}}$ a new coupling, the scattering amplitude is modified by

$$\begin{aligned} \delta \mathcal{A}_n &= g_{\mathcal{O}} \int d^4x \langle 1, \dots, n | \mathcal{O}(x) | 0 \rangle + \mathcal{O}(g_{\mathcal{O}}^2) \\ &= g_{\mathcal{O}} F_{\mathcal{O}}(1, \dots, n; q=0) + \mathcal{O}(g_{\mathcal{O}}^2). \end{aligned} \quad (1.0.10)$$

We can therefore think of the scattering amplitude as a soft ($q \rightarrow 0$) limit of a form factor of an appropriate operator, see for instance [34–36] for examples of such effective amplitudes. As we will now see, this interpretation brings us back to our earlier discussion of production and detection of the Higgs boson at the LHC.

One of the leading mechanisms of such production is gluon fusion, a process which is mediated through a fermion loop. The leading-order contribution comes from the top quark running in the loop and in an approximation where the mass of the top quark, m_t , is much larger than the mass of the Higgs, m_H , an effective Lagrangian description can be used to compute scattering amplitudes, as presented in Figure 1.

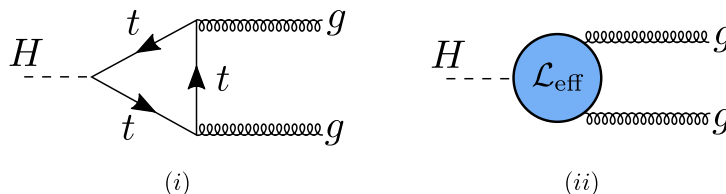


Figure 1: Higgs production (i): via top quark loop (ii): in an effective Lagrangian description, when m_t is large.

In this description, the quark loop is effectively replaced by a set of local interactions of increasing classical dimension. The expansion of the effective Lagrangian can be written as [37, 38]

$$\mathcal{L}_{\text{eff}} = \hat{C}_0 \mathcal{O}_0 + \frac{1}{m_t^2} \sum_{i=1}^4 \hat{C}_i \mathcal{O}_i + \mathcal{O}(m_t^{-4}) , \quad (1.0.11)$$

where the leading order term is a dimension-five operator $\mathcal{O}_0 \propto H \text{Tr}(F^2)$ with H representing the Higgs field and F the gluon field strength [39–41]. \hat{C}_0, \hat{C}_i are the matching coefficients and are proportional to $1/v$, where v is the Higgs field vacuum expectation value. Hence at leading order the scattering amplitude of the Higgs and a multi-gluon state $\langle g \dots g |$ in the infinite top-mass limit is nothing but a form factor of the operator $\text{Tr}(F^2(0))$ [42–47]. The terms subleading in $1/m_t$, denoted by \mathcal{O}_i , $i = 1, \dots, 4$, are dimension-seven operators of the type [37, 38, 48–50].

$$\mathcal{O}_1 \propto H \text{Tr}(F^3), \quad \mathcal{O}_j \propto H \text{Tr}(DFDF), \quad (1.0.12)$$

where $j = 1, \dots, 3$ schematically labels the three possible index contractions. We consider the two-loop form factors of these operators in $\mathcal{N}=4$ SYM with an external state of three gluons in Chapter 4.

Finally, a phenomenologically-minded reader may object to performing calculations in $\mathcal{N}=4$ SYM – after all, the real world seems to follow the rules of the Standard Model and gluon scattering in particular is governed by quantum chromodynamics (QCD). It may hence come as a surprise that one of the main findings of [30] is that the two-loop form factor of the lowest-weight operator in the stress-tensor multiplet in $\mathcal{N}=4$ SYM with the external state containing two scalars and one gluon shares a significant part with the form factor $\langle g^+ g^+ g^\pm | \text{Tr}(F^2) | 0 \rangle$ in QCD, computed in [51]. In particular, the so-called *maximally transcendental parts* of the two results are identical, for reasons currently not explainable via symmetries or other arguments. This led to the conjecture that the “most complicated” part of the Higgs plus multi gluon amplitude in infinite top mass limit in QCD can be computed using $\mathcal{N}=4$ SYM form factors. Following this initial remarkable discovery the theme of *universality*, central to the investigations presented throughout this thesis, began appearing in the literature, see for example [52]. In Chapter 5 we depart from $\mathcal{N}=4$ SYM and compute two-loop form factors in theories with less-than-maximal supersymmetry in order to quantify how much the results change when approaching pure Yang-Mills and eventually QCD.

The rest of the thesis is organised as follows. In Chapter 2 we introduce the recent most relevant concepts and tools in the field of study of scattering amplitudes and form factors at tree and loop level. In Chapter 3 we compute two-loop form factors of operators in the $SU(2|3)$ closed subsector of $\mathcal{N}=4$ SYM. In particular, we focus on the

non-protected, dimension-three operators for which we compute the four form factors needed to solve the mixing problem and the corresponding remainder functions. We show that the maximally transcendental part of the two-loop remainder of one of the operators turns out to be identical to that of the corresponding known quantity for the protected operator. We also find a surprising connection between the terms subleading in transcendentality and certain a priori unrelated remainder densities introduced in the study of the spin chain Hamiltonian in the $SU(2)$ sector. Finally, we use our calculation to resolve the mixing, recovering anomalous dimensions and eigenstates of the dilatation operator in the $SU(2|3)$ sector at two loops. In Chapter 4 we focus on the first finite top-mass correction to the Higgs effective Lagrangian (1.0.11) arising from the operator $\text{Tr}(F^3)$, up to two loops and three external gluons. Performing the calculation in $\mathcal{N} = 4$ SYM requires identification of an appropriate supersymmetric completion of $\text{Tr}(F^3)$, which we recognise as a descendant of the well-studied Konishi operator. We provide detailed computations for both this descendant operator and the component operator $\text{Tr}(F^3)$. Yet again, the results for both operators are expressed in terms of a few universal functions of transcendentality degree four and below, some of which we recognise from the calculation in Chapter 3. An important novel feature of the result is a delicate cancellation of unphysical poles appearing in the certain limits of the remainders, linking terms of different transcendentality. In Chapter 5 we extend our analysis of the first finite top-mass correction, arising from the operator $\text{Tr}(F^3)$, from $\mathcal{N} = 4$ SYM to theories with $\mathcal{N} < 4$, also for the case of three external gluons and up to two loops. We confirm our earlier result that the maximally transcendental part of the associated remainder is universal and equal to that of the form factor of a protected trilinear operator in the maximally supersymmetric theory. The terms with lower transcendentality deviate from the $\mathcal{N} = 4$ answer by a surprisingly small set of terms involving for example ζ_2 , ζ_3 and simple powers of logarithms. Finally, Chapter 6 reviews possible further research directions and contains conclusions of the work contained in the thesis.

Chapter 2

Review

In this chapter we review the background material and set up the conventions which will be used throughout the thesis. The review is largely based on references [17, 53, 54] unless explicitly indicated otherwise. We begin our discussion of scattering amplitudes by considering a simple yet very informative example involving n gluons in Yang-Mills theory with the gauge group $SU(N)$. From the point of view of Feynman-diagrammatic approach this may seem like an odd starting point since Feynman rules governing gluon scattering are one of the most complex and even at tree level the computation quickly becomes very involved. We will see however that this choice is in a way the most universal, in a sense that it essentially readily encapsulates most of the features applicable to simpler theories.

2.1 Scattering amplitudes of gluons

In perturbation theory we consider gluons to be asymptotic states described by the momentum four-vectors p_i^μ , the polarisation vectors ϵ_i^μ and the colours A_i where $i=1, \dots, n$ labels the particle in question. In the usual approach to calculating scattering amplitudes, as outlined in Chapter 1, we would first of all compute an appropriate correlation function in position space, Fourier-transform it to momentum space and using the LSZ reduction formula compute the multi-dimensional residue of the expression which has poles when the external particles go on-shell. The first thing to note is that the correlation function we would have computed to begin with has to be translation-invariant. As a result, after the Fourier transform, the amplitude, which we denote as \mathcal{A}_n , will involve a D -dimensional distribution of momenta:

$$\mathcal{A}_n(\{p_i^\mu, \epsilon_i^\mu, A_i\}) = (2\pi)^D \delta^{(D)}\left(\sum_{i=1}^n p_i^\mu\right) \times (\text{Sum over Feynman Diagrams}). \quad (2.1.1)$$

The delta function has support on the sum of momenta which obey the D -dimensional conservation.

Colour decomposition

For a theory of particles with colour charges such as QCD or Yang-Mills theory with a gauge group $SU(N)$, one can expect the scattering amplitude to depend on the colour structure. This can be understood as follows. The non-Abelian Yang-Mills Lagrangian describing purely gluonic interactions is

$$\mathcal{L}_{\text{YM}} = -\frac{1}{4} \text{Tr}(F^{\mu\nu} F_{\mu\nu}), \quad F_{\mu\nu} = \partial_\mu A_\nu - \partial_\nu A_\mu + \sqrt{2} g_{\text{YM}} [A_\mu, A_\nu], \quad (2.1.2)$$

with $A_\mu = A_\mu^a t^a$ and t^a the generators of the colour gauge group $SU(N)$ obeying the commutation relations of the underlying Lie algebra

$$[t^a, t^b] = i\sqrt{2} f^{abc} t^c, \quad (2.1.3)$$

and normalised such that

$$\text{Tr}(t^a t^b) = \delta^{ab}. \quad (2.1.4)$$

Using this interaction Lagrangian to construct the vertex Feynman rules, one can easily see that the dependence on the colour structure follows. Each three- and four-gluon vertex carries the colour dependence via associated structure constants as shown in Figure 2. This dependence, however, can be disentangled from the remaining variables

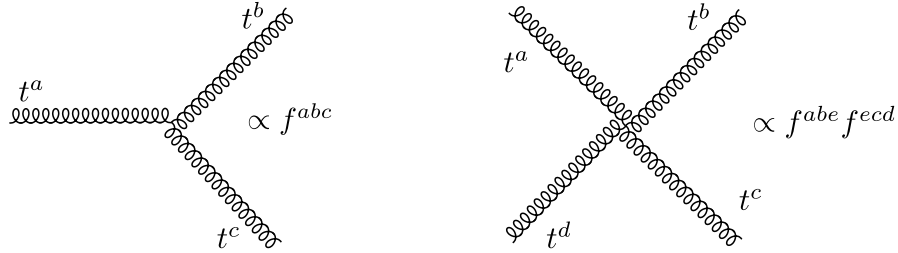


Figure 2: Colour structure carried by three- and four-gluon vertices.

of the scattering amplitude. To see that, let us use equations (2.1.3) and (2.1.4) to write the structure constants as¹

$$f^{abc} = -\frac{i}{\sqrt{2}} \text{Tr}(t^a [t^b, t^c]). \quad (2.1.5)$$

¹Note that in order to absorb the omnipresent factors of 2 we could redefine $t^a \rightarrow \sqrt{2}t^a$ and similarly $f^{abc} \rightarrow \sqrt{2}f^{abc}$, leading to $[t^a, t^b] = i f^{abc} t^c$.

Using the $SU(N)$ identity,

$$\sum_{a=1}^{N^2-1} (t^a)_j^i (t^a)_l^k = \delta_j^k \delta_l^i - \frac{1}{N} \delta_j^i \delta_l^k \quad (2.1.6)$$

we see that the products of generator traces arising from four-gluon vertices can be merged into single traces,

$$\begin{aligned} \sum_{e=1}^{N^2-1} f^{abe} f^{ecd} &= -\frac{1}{2} \sum_{e=1}^{N^2-1} \text{Tr}(t^a [t^b, t^e]) \text{Tr}(t^e [t^c, t^d]) \\ &= -\frac{1}{2} \left[\text{Tr}(t^a t^b t^c t^d) - \text{Tr}(t^a t^b t^d t^c) - \text{Tr}(t^b t^a t^c t^d) + \text{Tr}(t^b t^a t^d t^c) \right] \end{aligned} \quad (2.1.7)$$

as long as we consider N to be large, so that the second term of the Fierz identity (2.1.6) can be omitted. Going back to our schematic amplitude in (2.1.1), if instead of classifying the contributions coming from various Feynman diagrams by their topology or loop order we group them according to the colour trace structure in this *large N limit*, we can define a partial or *colour-ordered* amplitude A_n via

$$\mathcal{A}_n(\{p_i^\mu, \epsilon_i^\mu, A_i\}) = g_{\text{YM}}^{n-2} (2\pi)^D \delta^{(D)} \left(\sum_{i=1}^n p_i^\mu \right) \sum_{\sigma \in S_n / \mathbb{Z}_n} \text{Tr}(t^{a_{\sigma_1}} \dots t^{a_{\sigma_n}}) A_n(\sigma(1), \dots, \sigma(n)). \quad (2.1.8)$$

We note that the full amplitude of n particles will be a sum of $(n-1)!$ terms, each corresponding to one particular colour ordering, denoted here by σ . The colour trace, and hence the partial amplitude, are cyclic, thus we only sum over the non-cyclic permutations, *i.e.* $\sigma \in S_n / \mathbb{Z}_n$. Both the full and the partial amplitudes are gauge-invariant but since the colour dependence has been separated out, the colour-order amplitude depends only on the kinematical data of the incoming and outgoing particles.

A few words of explanation are required to account for the overall prefactor of g_{YM}^{n-2} in (2.1.8). Inspecting the form of the Yang-Mills Lagrangian in (2.1.2) we see that each three-gluon vertex comes with an associated factor of g_{YM} , while a four-gluon vertex carries a factor of g_{YM}^2 . Simple counting reveals that for n -points the Yang-Mills amplitude indeed scales with g_{YM}^{n-2} . Moreover, in what follows we will often be performing a perturbative expansion in powers of g_{YM}^2 , *i.e.* each loop order will carry additional two powers of the coupling. Keeping this scaling in mind for future discussion, we turn to inspect the dependence of the scattering amplitude on the external kinematic data.

Spinor-helicity formalism

We begin the discussion of the kinematic dependence with a review of the spinor-helicity formalism. It will shortly become apparent that it is a particularly useful framework for describing scattering amplitudes of massless particles, which are the main interest of this thesis.

Working in four spacetime dimensions and in the mostly-minus metric signature $\eta^{\mu\nu} = \text{diag}(+ - - -)$, given an on-shell four momentum vector $p^\mu = (p^0, p^i)$ we can rewrite it as a matrix, via

$$p^{\dot{\alpha}\alpha} = (\bar{\sigma}_\mu)^{\dot{\alpha}\alpha} p^\mu = \begin{pmatrix} p^0 + p^3 & p^1 - ip^2 \\ p^1 + ip^2 & p^0 - p^3 \end{pmatrix}, \quad (2.1.9)$$

where $(\bar{\sigma}_\mu)^{\dot{\alpha}\alpha} = (\mathbf{1}, \sigma_i)$, $\alpha, \dot{\alpha} = 1, 2$ and where the conventions for the Pauli sigma matrices are listed in Appendix A. In this particular representation, the on-shellness condition becomes manifest as a determinant condition:

$$\begin{aligned} \det(p^{\dot{\alpha}\alpha}) &= (p^0)^2 - (p^1)^2 - (p^2)^2 - (p^3)^2 = m^2 \\ m^2 = 0 &\Leftrightarrow \det(p^{\dot{\alpha}\alpha}) = 0. \end{aligned} \quad (2.1.10)$$

Any 2×2 matrix is at most of rank two.² If (and only if) additionally the determinant of such matrix vanishes, the rank is reduced to at most one and we can write the matrix in question, in our case the four momentum, as a product of two two-component spinors

$$p_i^{\dot{\alpha}\alpha} = \tilde{\lambda}_i^{\dot{\alpha}} \lambda_i^\alpha, \quad (2.1.11)$$

where again the index i runs over all in- and outgoing particles (often referred to as *legs*) of the scattering process.

The four-momentum p^μ transforms under finite representations of the Lorentz group $SO(1, 3)$. We recall that these representations can be described in terms of two copies of the $SU(2)$, often referred to as left and right, and correspondingly labelled by a pair of half-integers (p, q) . The four momentum $p_i^{\dot{\alpha}\alpha}$ transforms in the $(\frac{1}{2}, \frac{1}{2})$ representation of the Lorentz group. Consequently, we require for each of the two spinors in the decomposition (2.1.11) to transform as a doublet under one copy of the $SU(2)$ and singlet under the other. We are free to choose λ^α to transform in the $(0, \frac{1}{2})$ representation and $\tilde{\lambda}^{\dot{\alpha}}$ to transform in the $(\frac{1}{2}, 0)$ representation.

A massless momentum four-vector has only three independent components. Thus given a particular $p_i^{\dot{\alpha}\alpha}$ we are left with an ambiguity in defining the corresponding

²The rank of the matrix is defined as the dimension of the vector space spanned by its column vectors.

spinors λ_i^α and $\tilde{\lambda}_i^{\dot{\alpha}}$. These can only be defined modulo the rescaling

$$\lambda_i^\alpha \rightarrow t \lambda_i^\alpha, \quad \tilde{\lambda}_i^{\dot{\alpha}} \rightarrow t^{-1} \tilde{\lambda}_i^{\dot{\alpha}}, \quad t \in \mathbb{C}^*. \quad (2.1.12)$$

Clearly, the four-momentum is unchanged under such a transformation, which defines the *little group* of the Lorentz group.³ This freedom comes with an associated conserved charge, namely *helicity*, which we define as

$$H := \frac{1}{2} \sum_{i=1}^n \left(-\lambda_i^\alpha \frac{\partial}{\partial \lambda_i^\alpha} + \tilde{\lambda}_i^{\dot{\alpha}} \frac{\partial}{\partial \tilde{\lambda}_i^{\dot{\alpha}}} \right). \quad (2.1.13)$$

Using this definition, we immediately see that the spinor λ^α carries helicity $-\frac{1}{2}$ and $\tilde{\lambda}^{\dot{\alpha}}$ carries helicity $+\frac{1}{2}$. Furthermore, we will see that under the little group transformation of one of the momenta the scattering amplitude involving this momentum picks up an overall phase, which depends on the helicity of the rescaled particle,

$$\lambda_i^\alpha \rightarrow t \lambda_i^\alpha, \quad \tilde{\lambda}_i^{\dot{\alpha}} \rightarrow t^{-1} \tilde{\lambda}_i^{\dot{\alpha}} \quad \Rightarrow \quad \mathcal{A}_n \rightarrow t^{-2h_i} \mathcal{A}_n. \quad (2.1.14)$$

Given two spinors of negative helicity, λ_i^α and λ_j^β say, we can form a Lorentz invariant, antisymmetric bracket

$$\langle ij \rangle := \epsilon_{\alpha\beta} \lambda_i^\alpha \lambda_j^\beta = -\langle ji \rangle, \quad (2.1.15)$$

and similarly, for two positive helicity spinors, $\tilde{\lambda}_i^{\dot{\alpha}}$ and $\tilde{\lambda}_j^{\dot{\beta}}$ we define

$$[ij] := \epsilon^{\dot{\alpha}\dot{\beta}} \tilde{\lambda}_{i\dot{\alpha}} \tilde{\lambda}_{j\dot{\beta}} = -[ji], \quad (2.1.16)$$

where spinorial indices are raised and lowered using the antisymmetric invariant Levi-Civita tensors⁴

$$\epsilon_{\alpha\beta} = (i\sigma_2)_{\alpha\beta} = \begin{pmatrix} 0 & 1 \\ -1 & 0 \end{pmatrix}, \quad \epsilon^{\dot{\alpha}\dot{\beta}} = -(i\sigma_2)^{\dot{\alpha}\dot{\beta}} = \begin{pmatrix} 0 & -1 \\ 1 & 0 \end{pmatrix}. \quad (2.1.17)$$

For any two massless on-shell four-momenta p_i and p_j we can form a Mandelstam invariant

$$s_{ij} = (p_i + p_j)^2 = 2(p_i \cdot p_j) = \langle ij \rangle [ji]. \quad (2.1.18)$$

Few further important properties will be used frequently throughout this thesis.

³We define the little group as a subgroup of the Lorentz group which leaves the four-momentum invariant.

⁴Further spinor conventions used throughout this thesis are presented in Appendix A.

Firstly, it is often very useful to promote momenta to be complex, allowing us to use the powerful arsenal of complex analysis techniques in aid of our computations. So far, we have considered the four-momentum to be real in the usual $(+---)$ signature, which means that the positive- and negative-helicity spinors are related as $(\lambda_i^\alpha)^* = \pm \tilde{\lambda}_i^{\dot{\alpha}}$. For the complexified Lorentz group, $SL(2, \mathbb{C}) \times SL(2, \mathbb{C})$ the spinors λ^α and $\tilde{\lambda}^{\dot{\alpha}}$ are independent.⁵

Secondly, looking at expressions (2.1.15) and (2.1.16) it is straightforward to see that whenever $\lambda_i^\alpha \propto \lambda_j^\alpha$ we have $\langle ij \rangle = 0$ and correspondingly whenever $\tilde{\lambda}_i^{\dot{\alpha}} \propto \tilde{\lambda}_j^{\dot{\alpha}}$, $[ij] = 0$. The physical interpretation of vanishing of either of the angle or square bracket is that the momenta involved, p_i and p_j , are collinear.

Thirdly, it is often very useful to employ the following observation. On a plane, three vectors cannot all be linearly independent. As a result, if we consider three two-component vectors, λ_a , λ_b and λ_c , we can always write one as a linear combination of the other two:

$$\lambda_c = \alpha \lambda_a + \beta \lambda_b \quad \alpha, \beta \in \mathbb{R}. \quad (2.1.19)$$

By dotting (2.1.19) with λ_a and λ_b in turn, we can solve for coefficients α and β , such that the statement becomes

$$\langle ab \rangle \lambda_c + \langle bc \rangle \lambda_a + \langle ca \rangle \lambda_b = 0. \quad (2.1.20)$$

We are free to contract our expression with a fourth spinor, λ_d to cast it in its most usual form

$$\langle ab \rangle \langle cd \rangle + \langle ac \rangle \langle db \rangle + \langle ad \rangle \langle bc \rangle = 0. \quad (2.1.21)$$

This frequently-used identity and its counterpart in terms of square brackets,

$$[ab][cd] + [ac][db] + [ad][bc] = 0 \quad (2.1.22)$$

are referred to as the *Schouten identities*.

Polarisation

The final ingredient in the description of the scattering process we have not yet considered are the polarisation vectors. We discuss them separately for gluon and fermion fields, in turn.

⁵Alternatively, one could insist for the momenta to be real but change the metric signature in order for λ^α and $\tilde{\lambda}^{\dot{\alpha}}$ to be independent.

Gluon polarisation

Each gluon of helicity ± 1 in addition to its momentum carries a polarisation vector, $\epsilon^{(\pm)}$, satisfying

$$p_\mu(\epsilon^{(\pm)})^\mu = 0, \quad (\epsilon^{(\pm)})_\mu(\epsilon^{(\pm)})^\mu = 0, \quad (\epsilon^{(\pm)})_\mu(\epsilon^{(\mp)})^\mu = -1. \quad (2.1.23)$$

We can express the polarisation vectors in terms of the helicity spinors as

$$(\epsilon^{(+)})^{\dot{\alpha}\alpha} = \sqrt{2} \frac{\tilde{\lambda}^{\dot{\alpha}} \mu^\alpha}{\langle \mu \lambda \rangle}, \quad (\epsilon^{(-)})^{\dot{\alpha}\alpha} = \sqrt{2} \frac{\tilde{\mu}^{\dot{\alpha}} \lambda^\alpha}{[\lambda \mu]}, \quad (2.1.24)$$

with μ^α and $\tilde{\mu}^{\dot{\alpha}}$ arbitrary reference spinors. It is straightforward to verify that these expressions satisfy the properties (2.1.23) and when acted upon with the helicity generator (2.1.13) give the expected values, namely

$$H(\epsilon^{(+)})^{\dot{\alpha}\alpha} = (+1)(\epsilon^{(+)})^{\dot{\alpha}\alpha}, \quad H(\epsilon^{(-)})^{\dot{\alpha}\alpha} = (-1)(\epsilon^{(-)})^{\dot{\alpha}\alpha}. \quad (2.1.25)$$

It can also be easily seen that under the little group transformation (2.1.12) the gluon polarisation vectors scale as

$$\epsilon^{(+)} \rightarrow t^{-2} \epsilon^{(+)}, \quad \epsilon^{(-)} \rightarrow t^2 \epsilon^{(-)}. \quad (2.1.26)$$

Expressions (2.1.24) fix the polarisation vectors up to an overall gauge transformation. However it turns out that any change in the reference spinor is equivalent to changing the corresponding polarisation as

$$(\epsilon_i^{(+)})^{\dot{\alpha}\alpha} \rightarrow (\epsilon_i^{(+)})^{\dot{\alpha}\alpha} + c p_i^{\dot{\alpha}\alpha}, \quad (2.1.27)$$

where c is a constant. As a result of change in the reference spinor, the polarisation vector, and hence the amplitude, changes by an amount proportional to the momentum. This, however, is precisely the familiar local gauge invariance of the scattering amplitude, giving us confidence that representation (2.1.24) is a valid one and we are free to choose the reference spinors μ^α and $\tilde{\mu}^{\dot{\alpha}}$ at our convenience. We are now in a position to conclude that the partial colour-ordered amplitude of n massless gluons can be completely described using three pieces of data, $\{\lambda_i, \tilde{\lambda}_i, h_i\}$ for each particle $i = 1, \dots, n$.

Fermion polarisation

Despite the fact that so far we have been focusing our discussion on scattering amplitudes of massless gluons, everything that has been said follows for scalar and fermion fields. A distinction needs to be made however when it comes to discussion of po-

larisations. For Dirac fermions, the polarisation spinors are given by the particle and antiparticle solutions of the Dirac equation,

$$(\not{p} - m)u(p) = 0, \quad (\not{p} + m)v(p) = 0. \quad (2.1.28)$$

In the massless limit, these can be expressed in terms of helicity spinors as

$$u_+(p) = v_-(p) = \begin{pmatrix} \lambda_\alpha \\ 0 \end{pmatrix}, \quad u_-(p) = v_+(p) = \begin{pmatrix} 0 \\ \tilde{\lambda}^{\dot{\alpha}} \end{pmatrix}, \quad (2.1.29)$$

which explicitly satisfy the massless limit of (2.1.28). As a result, the polarisation spinors of massless Dirac fermions are given by

$$(\epsilon^{(-1/2)})^\alpha = \lambda^\alpha, \quad (\epsilon^{(+1/2)})^{\dot{\alpha}} = \tilde{\lambda}^{\dot{\alpha}}, \quad (2.1.30)$$

and, as expected,

$$H(\epsilon^{(\pm 1/2)}) = \pm \frac{1}{2}(\epsilon^{(\pm 1/2)}). \quad (2.1.31)$$

Under the little group transformation (2.1.12) the fermion polarisation vectors scale as

$$\epsilon^{(-1/2)} \rightarrow t \epsilon^{(-1/2)}, \quad \epsilon^{(+1/2)} \rightarrow t^{-1} \epsilon^{(+1/2)}. \quad (2.1.32)$$

We can now generalise the little group scaling to all possible polarisations – we see that for a field of helicity h_i , its polarisation tensor scales with t^{-2h_i} . The scattering amplitude inherits the scaling from that of the polarisation vectors of the external legs since neither vertices nor propagators can transform under the little group. As a result we confirm that the scattering amplitude transforms as anticipated in (2.1.14):

$$\lambda_i^\alpha \rightarrow t \lambda_i^\alpha, \quad \tilde{\lambda}_i^{\dot{\alpha}} \rightarrow t^{-1} \tilde{\lambda}_i^{\dot{\alpha}} \quad \Rightarrow \quad \mathcal{A}_n \rightarrow t^{-2h_i} \mathcal{A}_n.$$

This observation provides a useful consistency check. Whenever we write down an expression for a scattering amplitude, either as a result of a direct computation or using a recursive method which we introduce in Section 2.3, the little group scaling (2.1.14) must hold for each external leg.

2.2 Tree-level amplitudes

Having introduced the basic toolbox for dealing with momenta of massless particles, we proceed to discuss the kinematic dependence of the scattering amplitude. Let us first consider a few explicit examples and see how much we can infer about the form

of various scattering amplitudes just from the knowledge of the properties discussed in the previous sections.

First of all, let us consider amplitudes of $n \geq 4$ massless gluons in Yang-Mills theory of uniform, positive or negative, helicity. According to our previous discussion, this amplitude will depend on n polarisation vectors and it turns out that at least one pair of them will need to be contracted.⁶ As a result, if we consider an all-plus amplitude $A_n^{(0)}(1^+, 2^+, \dots, n^+)$, at least one $\epsilon_i^{(+)} \cdot \epsilon_j^{(+)}$ contraction arises. Using the expressions for polarisation vectors in (2.1.24) we can write this contraction as

$$\epsilon_i^{(+)} \cdot \epsilon_j^{(+)} = \frac{\langle \mu_i \mu_j \rangle [\lambda_j \lambda_i]}{\langle \lambda_i \mu_i \rangle \langle \lambda_j \mu_j \rangle}. \quad (2.2.1)$$

Since we are free to choose arbitrary reference spinors as long as $\mu_i^\alpha \neq \lambda_i^\alpha$ and $\mu_j^\alpha \neq \lambda_j^\alpha$ we can have $\mu_i^\alpha \propto \mu_j^\alpha$ so that $\epsilon_i^{(+)} \cdot \epsilon_j^{(+)} = 0$ and as a result, without performing any calculations we can conclude that

$$A_n^{(0)}(1^+, 2^+, \dots, n^+) = 0, \quad (2.2.2)$$

and a similar argument holds for the all-minus case. A careful choice of the reference spinors for an n -gluon amplitude with one particle of the opposite helicity to the rest, allows us to see that it vanishes as well, *i.e.*

$$A_n^{(0)}(1^+, 2^+, \dots, (i-1)^+, i^-, (i+1)^+, \dots, n^+) = 0, \quad (2.2.3)$$

and similarly for the opposite helicity assignment,

$$A_n^{(0)}(1^-, 2^-, \dots, (i-1)^-, i^+, (i+1)^-, \dots, n^-) = 0. \quad (2.2.4)$$

The results obtained so far are certainly striking – without a single line of calculation or considering any Feynman diagrams we have been able to deduce that an infinitely-large classes of scattering amplitudes vanish. The first non-vanishing amplitude is that of $(n-2)$ gluons of one helicity and 2 gluons of the opposite – we call such configuration *Maximally Helicity Violating* (MHV). The remarkable and initially surprising result for the tree-level gluon amplitude of the MHV type, known as the Parke-Taylor amplitude, conjectured by [12] and proven in [55] for gluons i and j of negative helicity in the form first given by [56] is

$$A_n^{(0)}(1^+, \dots, i^-, \dots, j^-, \dots, n^+) = i \frac{\langle ij \rangle^4}{\langle 12 \rangle \langle 23 \rangle \cdots \langle (n-1) n \rangle \langle n1 \rangle}, \quad (2.2.5)$$

⁶The scattering amplitude is Lorentz invariant, hence its numerator consists of a product of contractions $(\epsilon_i \cdot \epsilon_j)$, $(\epsilon_i \cdot p_j)$ and $(p_i \cdot p_j)$. The maximum power of momentum available for contractions in the numerator of an n -point gluonic amplitude is $n-2$, so at least one $(\epsilon_i \cdot \epsilon_j)$ must arise.

and the scattering amplitude for gluons i and j of positive helicity and the remaining gluons of negative helicity, referred to as an anti-MHV or $\overline{\text{MHV}}$, is

$$A_n^{(0)}(1^-, \dots, i^+, \dots, j^+, \dots, n^-) = i(-1)^n \frac{[ij]^4}{[12][23] \cdots [(n-1)n][n1]}. \quad (2.2.6)$$

Following the usual conventions, in future discussions we will refer to amplitudes with three negative helicity gluons as next-to-MHV (NMHV), four negative helicity gluons as next-to-next-to-MHV ($N^2\text{MHV}$) and so on, up to an amplitude with only three positive helicity gluons, referred to as next-to-anti-MHV ($\overline{\text{NMHV}}$). In general, an amplitude with $(k+2)$ negative helicity gluons and $(n-k-2)$ positive helicity gluons will be referred to as $N^k\text{MHV}$. The first non-trivial NMHV amplitude appears at six points, the first $N^2\text{MHV}$ at seven points and so on for higher MHV degrees.

As remarked in Chapter 1, the one-term expressions (2.2.5) and (2.2.6) are a result of summing a large number of individual Feynman diagrams – yet their general form is not affected by the number of legs in the process. Such astonishing simplicity served as a clue to existence of some underlying structures of scattering amplitudes. Before we introduce these, let us briefly review the special, three-particle amplitudes.

Three-point amplitudes

We have restricted our discussion so far to amplitudes of n gluons with special helicity configurations and where $n \geq 4$. Using the general formulas (2.2.5) and (2.2.6) let us now consider tree-level MHV amplitudes of three gluons. As we will see shortly, these will be used as fundamental building blocks for writing down higher point amplitudes. According to (2.2.5) we have, for example

$$A_3^{(0)}(1^+, 2^-, 3^-) = i \frac{\langle 23 \rangle^3}{\langle 12 \rangle \langle 31 \rangle}. \quad (2.2.7)$$

Three-point momentum conservation, namely $p_1 + p_2 + p_3 = 0$, together with the on-shell condition implies that

$$\langle 12 \rangle [21] = 0, \quad \langle 23 \rangle [32] = 0, \quad \langle 31 \rangle [13] = 0. \quad (2.2.8)$$

This is where our earlier assumption of momenta being complex becomes extremely useful. If momenta p_1 , p_2 and p_3 were to be real in Lorentz spacetime signature, we would have that $\tilde{\lambda}_i = \pm \lambda_i^*$ for all $i = 1, 2, 3$. In other words, both the angle and square brackets simultaneously vanish, there are no non-zero Mandelstam invariants the amplitude could depend on and as such the three-point amplitude in (2.2.7) is zero. If the momenta are complex however, the spinors λ_i and $\tilde{\lambda}_i$ are independent and the conditions in (2.2.8) can be solved either by $[12] = [23] = [13] = 0$ or by $\langle 12 \rangle = \langle 23 \rangle =$

$\langle 13 \rangle = 0$. The two cases correspond to MHV and anti-MHV three-point amplitudes respectively:

$$\begin{aligned} A_3^{\text{MHV}}(1^+, 2^-, 3^-) &= i \frac{\langle 23 \rangle^3}{\langle 12 \rangle \langle 31 \rangle}, & \tilde{\lambda}_1 \propto \tilde{\lambda}_2 \propto \tilde{\lambda}_3, \\ A_3^{\overline{\text{MHV}}}(1^-, 2^+, 3^+) &= -i \frac{[23]^3}{[12][31]}, & \lambda_1 \propto \lambda_2 \propto \lambda_3. \end{aligned} \quad (2.2.9)$$

These three-point amplitudes, despite being zero for real momenta, prove to constitute important building blocks in constructing higher-point amplitudes, as we review next.

2.3 Tree-level recursion relations

With the knowledge of the MHV amplitude (2.2.5) and the three-point amplitudes (2.2.9) we would like to be able to construct amplitudes of any MHV degree and with any number of external legs. There exist two powerful methods of obtaining this goal, which we introduce next.

BCFW recursion relation

The Britto, Cachazo, Feng, Witten (BCFW) [19, 57] recursion relations make use of the analytic properties of scattering amplitudes under complex deformations and allow us to evaluate higher point tree-level amplitudes as products of lower point ones. This simple technique proves to be extremely powerful - given three-point amplitudes as input, such as those in (2.2.9) for gluons, we are able to construct *all n -point tree-level gluon amplitudes*, regardless of the MHV degree.

In order to see that, we consider a partial scattering amplitude of n gluons and we perform a deformation of two of the spinors of chosen momenta p_i and p_j by a parameter $z \in \mathbb{C}$,

$$\lambda_i \rightarrow \hat{\lambda}_i(z) = \lambda_i + z\lambda_j, \quad \tilde{\lambda}_j \rightarrow \hat{\tilde{\lambda}}_j(z) = \tilde{\lambda}_j - z\tilde{\lambda}_i, \quad (2.3.1)$$

so that

$$\hat{p}_i(z) = (\lambda_i + z\lambda_j)\tilde{\lambda}_i, \quad \hat{p}_j(z) = \lambda_j(\tilde{\lambda}_j - z\tilde{\lambda}_i). \quad (2.3.2)$$

All the other momenta are left unchanged. We note that the shift is constructed such that it preserves the on-shellness of p_i and p_j as well as the overall momentum conservation. We can then define the z -deformed n -point on-shell partial amplitude as

$$\hat{A}_n(z) = A_n(p_1, \dots, p_{i-1}, \hat{p}_i(z), p_{i+1}, \dots, p_{j-1}, \hat{p}_j(z), p_{j+1}, \dots, p_n), \quad (2.3.3)$$

and we note that $\hat{A}_n(z)$ is a rational function of z which follows from the fact that A_n is a rational function of spinorial angle and square brackets. Moreover, we can show that $\hat{A}_n(z)$ exhibits only simple poles in z . We notice that momentum flowing through a propagator in a tree-level diagram is always a sum of a number of *adjacent* external momenta.⁷ For the two momenta p_i and p_j which we have singled out and a generic propagator $1/P_{k\ell}^2$, $P_{k\ell} = p_k + \dots + p_\ell$ for some $k < \ell$, we can have three distinct possibilities:

1. The propagator momentum $P_{k\ell}$ involves neither $\hat{p}_i(z)$ nor $\hat{p}_j(z)$, *i.e.* $i, j \notin \{k, \dots, \ell\}$ and as a result no pole in z occurs.
2. The propagator momentum involves either $\hat{p}_i(z)$ or $\hat{p}_j(z)$ and as such the propagator, $1/\hat{P}_{k\ell}^2(z)$ will have a pole in z . For concreteness, let $i \in \{k, \dots, \ell\}$ then

$$\begin{aligned}\hat{P}_{k\ell}(z) &= p_k + \dots + \hat{p}_i(z) + \dots + p_\ell \\ &= P_{k\ell} + z\lambda_j\tilde{\lambda}_i,\end{aligned}\tag{2.3.4}$$

and $\hat{P}_{k\ell}^2(z) = P_{k\ell}^2 - z\langle j|P_{k\ell}|i\rangle$. Clearly, a simple pole exists at

$$z_{k\ell} = \frac{P_{k\ell}^2}{\langle j|P_{k\ell}|i\rangle}.\tag{2.3.5}$$

3. The propagator momentum $P_{k\ell}$ involves both $\hat{p}_i(z)$ and $\hat{p}_j(z)$, *i.e.* $i, j \in \{k, \dots, \ell\}$, however in such case the z -dependence cancels between the two momenta and no pole in z occurs.

The aim of the discussion regarding the pole structure is to be able to reconstruct the “unshifted” amplitude $A_n = \hat{A}_n(0)$. We can achieve this by writing A_n as a contour integral

$$\hat{A}_n(0) = \frac{1}{2\pi i} \oint_{z=0} \frac{dz}{z} \hat{A}_n(z).\tag{2.3.6}$$

We can now use the Cauchy residue theorem to expand the right hand side of the expression (2.3.6) as a sum over the residues of all the poles at $z_{k\ell} \neq 0$,

$$\hat{A}_n(0) = - \sum_{k,\ell} \frac{1}{z_{k\ell}} \text{Res} \left[\hat{A}_n(z_{k\ell}) \right],\tag{2.3.7}$$

or in general

$$\hat{A}_n(z) = \sum_{k,\ell} \frac{1}{z - z_{k\ell}} \text{Res} \left[\hat{A}_n(z_{k\ell}) \right].\tag{2.3.8}$$

⁷Any propagator involving non-adjacent momenta would lead to a non-planar diagram. In the present discussion we are only dealing with planar interactions.

We have not yet considered the possibility of having a pole at $z_{k\ell} = \infty$. If we are able to show that the shifted amplitude $\hat{A}_n(z)$ scales with at least $1/z$ as $z \rightarrow \infty$ we would then have that the integral in (2.3.6) evaluated on a contour around infinity gives zero as the integrand scales as $1/z^2$. We can indeed show that this is the case provided that we choose the shifted legs i and j to be of appropriate helicity. It turns out that the three cases when $\hat{A}_n(z) \rightarrow 0$ for $z \rightarrow \infty$ are when the helicities are

$$(i, j) : (+, -), (+, +), (-, -). \quad (2.3.9)$$

For those three configurations the amplitude scales at least as $1/z$ if the two shifted legs are picked to be adjacent or as $1/z^2$ for non-adjacent i and j .⁸ In the remaining case, namely for the $(-, +)$ shift, the amplitude scales as z^3 and we cannot simply disregard the pole at infinity. While various attempts have been made at computing the form of the contribution from this unphysical pole [58–60], no general constructive method exists. In most calculations, like in the present discussion, one chooses a *valid shift*, for which $\hat{A}_n(z) \rightarrow 0$ for $z \rightarrow \infty$ and as a result the pole at infinity does not contribute.

We would like to now describe the residues of the poles we have detected. By the discussion above, the poles in z appear whenever a propagator containing one of the shifted momenta, $1/\hat{P}_{k\ell}^2(z)$, goes on shell. Such a propagator can be understood to connect two “clusters” of external momenta – one containing momenta in range from k to ℓ (left) and the other containing all other remaining external momenta (right), as presented in Figure 3.

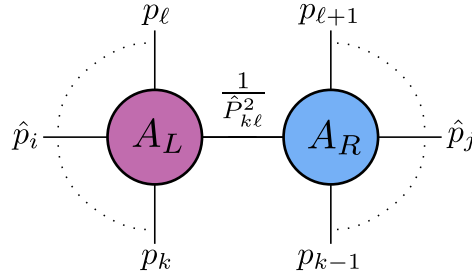


Figure 3: BCFW factorisation – n point amplitude factorises into lower-point “left” and “right” amplitudes connected by a propagator.

We sum over all possible helicity assignments on the propagator $1/\hat{P}_{k\ell}^2(z)$ and over all possible factorisation channels and write the shifted amplitude as

$$\hat{A}_n(z) = \sum_{k,\ell} \sum_h A_L^h(z_{k\ell}) \frac{1}{\hat{P}_{k\ell}^2(z)} A_R^{-h}(z_{k\ell}). \quad (2.3.10)$$

⁸The extra factor of $1/z$ comes from the fact that in the case of two shifted legs, i and j , being adjacent one of the spinorial brackets in the Parke-Taylor denominator, $\langle ij \rangle$, will be left unaffected by the shift. For non-adjacent i and j their bracket does not appear in the denominator, which introduces an extra factor of z .

In order to obtain the physical scattering amplitude, we set $z = 0$ in the denominator,

$$A_n = \sum_{k,\ell} \sum_h A_L^h(z_{k\ell}) \frac{1}{P_{k\ell}^2} A_R^{-h}(z_{k\ell}). \quad (2.3.11)$$

Thus we see that a higher point amplitude can be represented as a product of two lower-point amplitudes connected by a propagator. This factorisation can be recursively performed all the way to the smallest building blocks – three point MHV and anti-MHV amplitudes. As a result, from our knowledge of three-point amplitudes in (2.2.9), using the BCFW recursion procedure, we can build higher point amplitudes of a chosen MHV degree.

The $\mathcal{N}=4$ SYM generalisation of the BCFW recursion relations has been developed in [61] and the authors in [62] have extended the procedure to include all loop orders. There exists an alternative, equally successful method, which involves using only the MHV building blocks – we proceed to review it next.

MHV diagrams

Another way of obtaining higher-point amplitudes from lower-point ones recursively is through the method of *MHV diagrams*, also known as the Cachazo, Svrček and Witten (CSW) expansion, first introduced by these authors in [20]. The prescription involves decomposing scattering amplitudes as products of vertices which are off-shell continuations of MHV amplitudes and are connected by scalar propagators $1/P^2$, where the momentum P is off-shell. In order to continue the MHV amplitude off-shell we can decompose P as

$$P^{\dot{\alpha}\alpha} = p^{\dot{\alpha}\alpha} + z \xi^{\dot{\alpha}\alpha}, \quad (2.3.12)$$

where $\xi^{\dot{\alpha}\alpha} = \xi^{\dot{\alpha}} \xi^\alpha$ is a lightlike reference vector, $p^{\dot{\alpha}\alpha} = \tilde{\lambda}_{\dot{P}}^{\dot{\alpha}} \lambda_P^\alpha$ is a null momentum and z is a real parameter. From the Parke-Taylor formula (2.2.5) we see that the MHV amplitude is a function of the holomorphic spinors λ^α only and in particular does not involve the antiholomorphic $\tilde{\lambda}^{\dot{\alpha}}$. The CSW prescription is to use the holomorphic spinor λ_P^α to continue the internal leg off-shell. In particular, we can write it as

$$\lambda_P^\alpha = \frac{P^{\dot{\alpha}\alpha} \xi_{\dot{\alpha}}}{[p \xi]}, \quad (2.3.13)$$

and importantly gauge invariance of the scattering amplitude imposes the requirement that the final result of the calculation must be independent of the choice of the *reference spinor* $\xi_{\dot{\alpha}}$.

The method finds numerous applications, for example in the construction of N^k MHV amplitudes as a sum of tree-level diagrams with $(k + 1)$ MHV vertices evaluated using

the off-shell continuation (2.3.13). MHV diagrams have successfully been used in computations of amplitudes involving fermions [63] and in $\mathcal{N} = 4$ SYM [64, 65], including loop-level amplitudes [66]. Higgs plus multi-gluon QCD amplitudes at tree-level have been computed using a modification of the CSW method in [43] and at one-loop in [46]. The study has been extended to Higgs plus multi-parton tree-level amplitudes in [44].

2.4 $\mathcal{N} = 4$ super Yang-Mills

So far, we have avoided addressing in detail the exact theoretical setup we will be working in, focusing on the concepts which can be applied in all generality instead. In this section, we introduce $\mathcal{N} = 4$ SYM, the maximally supersymmetric theory which has been the subject of much interest in the recent years due to the discovery of several remarkable features.

The first of such properties relates to the *AdS/CFT correspondence* which provides a relation between a string theory on a background which contains an Anti-de-Sitter (AdS) spacetime and a conformal field theory (CFT) formulated on the boundary of that spacetime. The most famous example of this correspondence, which has been extensively studied since its postulation in [67], relates type IIB string theory on $AdS_5 \times S^5$ and $\mathcal{N} = 4$ SYM on the four dimensional boundary. As a result of this conjecture one is able to, using the so-called dictionary, relate calculations at strong and weak coupling, allowing insight into one model using the knowledge of the other, see *e.g.* [68].

Secondly, $\mathcal{N} = 4$ SYM turns out to be integrable in the *planar limit*, introduced by 't Hooft in [69]. The idea, alluded to in Section 2.1, consists of taking the rank of the $SU(N)$ gauge group to be large, $N \rightarrow \infty$ and introducing a new *'t Hooft coupling*,

$$a := \frac{g_{\text{YM}}^2 N}{(4\pi)^2}, \quad (2.4.1)$$

which is held fixed as $g_{\text{YM}} \rightarrow 0$. In this limit, scattering amplitudes which are of leading order when performing an expansion in $1/N$ are called planar – they can be drawn on a plane without crossing any lines. Subleading corrections can only be drawn on surfaces of higher genus, as illustrated in Figure 4.

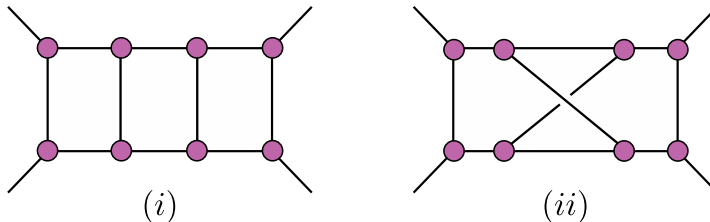


Figure 4: Example of (i): planar and (ii) non-planar topology. To distinguish between vertices and lines crossing without intersecting, the vertices have been coloured in.

$\mathcal{N} = 4$ SYM in the planar limit appears to be integrable and using techniques such as the Thermodynamic Bethe Ansatz (TBA) [70,71] one can successfully obtain the spectrum of the theory as well as many other observables. It is a remarkable statement by itself – integrability is a feature typically reserved for two-dimensional models. However, this property can be immediately understood in the context of the AdS/CFT correspondence as $\mathcal{N} = 4$ SYM is conjectured to be dual to an integrable string worldsheet model. In fact, appearance of integrability can serve in support of the duality conjecture. For an extensive review of AdS/CFT integrability see [72] and references within.

Thirdly, as we will discuss in the present section, the theory possesses remarkable amount of symmetry, some of which is hidden at first sight. This has an obvious benefit from the computational point of view, allowing us to calculate quantities even at higher loop orders with relative ease. The theory is said to be maximally supersymmetric – the symmetry group contains the largest possible number of generators (or *supercharges*) if the field content is to be restricted to particles of spin at most one, *i.e* no gravity is considered.⁹

The Lagrangian of the theory can be obtained from dimensional reduction of ten-dimensional $\mathcal{N} = 1$ SYM [73] and reads

$$\begin{aligned} \mathcal{L}_{\text{SYM}} = \text{Tr} \left(-\frac{1}{4} F_{\mu\nu} F^{\mu\nu} - (D_\mu \phi_{AB}) D^\mu \phi^{AB} + i \bar{\psi}_{\dot{\alpha}}^{ABC} (\bar{\sigma}_\mu)^{\dot{\alpha}\alpha} D^\mu \psi_{\alpha ABC} \right. \\ \left. - \frac{1}{2} [\phi^{AB}, \phi^{CD}] [\phi_{AB}, \phi_{CD}] - \frac{i}{2} \psi^{\alpha A} [\phi_{AB}, \psi_\alpha^B] - \frac{i}{2} \bar{\psi}_{\dot{\alpha} A} [\phi^{AB}, \bar{\psi}_{\dot{B}}^{\dot{\alpha}}] \right), \end{aligned} \quad (2.4.2)$$

where the field strength $F_{\mu\nu}$ has been introduced in (2.1.2) and $D_\mu = \partial_\mu - g_{\text{YM}} \sqrt{2}/2 [A_\mu, \cdot]$ is the $SU(N)$ gauge covariant derivative. A_μ is the spin-1 vector field while ϕ_{AB} denote three complex scalars with $A, B = 1, \dots, 4$ indices of the $SU(4)$ R -symmetry. The scalars are antisymmetric in $A \leftrightarrow B$ and related to each other by the reality condition,

$$\phi^{AB} = \bar{\phi}_{AB} = \frac{1}{2} \epsilon^{ABCD} \phi_{CD}. \quad (2.4.3)$$

Four chiral and four anti-chiral fermions, denoted by ψ and $\bar{\psi}$, transform in the fundamental and anti-fundamental representations of the $SU(4)$ and obey the relations

$$\psi_{\alpha ABC} = \epsilon_{ABCD} \psi_\alpha^D, \quad \bar{\psi}_{\dot{\alpha}}^{ABC} = \epsilon^{ABCD} \bar{\psi}_{\dot{\alpha} D}. \quad (2.4.4)$$

The field content of $\mathcal{N} = 4$ SYM and transformation properties under the Lorentz and the R -symmetry groups are summarised in Table 2.

The states are related to each other by the action of the $\mathcal{N} = 4$ supercharges, which

⁹Inclusion of higher spin fields leads to non-renormalisable coupling.

we denote by Q_A^α and $\bar{Q}^{\dot{\alpha}A}$. They obey the anticommutation relation

$$\{Q_A^\alpha, \bar{Q}^{\dot{\alpha}B}\} = \delta_A^B P^{\dot{\alpha}\alpha}, \quad (2.4.5)$$

where $P^{\dot{\alpha}\alpha}$ is the Lorentz generator of translations.

Symbol	Field	Multiplicity	$SU(2) \times SU(2)$	R -symmetry $SU(4)$
$g^{(+)}$	gluon	1	(1/2, 1/2)	singlet 1
ψ^A	gluino	4	(1/2, 0)	fundamental 4
ϕ^{AB}	scalar	6	(0, 0)	anti-symmetric 6
$\bar{\psi}^{ABC}$	anti-gluino	4	(0, 1/2)	anti-fundamental $\bar{\mathbf{4}}$
$g^{(-)}$	gluon	1	(1/2, 1/2)	singlet 1

Table 2: *Field content of $\mathcal{N} = 4$ SYM: multiplicities, transformation properties under the Lorentz and R -symmetry groups. We see that the numbers of fermionic and bosonic degrees of freedom agree, as expected.*

As always, we think of a quantum state as of an appropriate ladder operator acting on the vacuum. For instance $\langle 0 | \psi^A(p_1) \rangle$ is a state of a fermion with momentum p_1 and helicity $+\frac{1}{2}$, while $\langle 0 | \bar{\psi}^{ABC}(p_2) \rangle$ has momentum p_2 and helicity $-\frac{1}{2}$. In the following we will often use the shorthand notation $\langle \psi^A |$ and $\langle \bar{\psi}^{ABC} |$ to denote such states. Denoting by $\langle g^{(+)} |$ and $\langle g^{(-)} |$ the states of highest (+1) and lowest (-1) helicity respectively we have the following relations between the states:

$$\begin{aligned} \langle g^{(-) ABCD} | Q_A^\alpha &= \langle \bar{\psi}^{BCD} | \lambda^\alpha, & \langle g^{(-) ABCD} | \bar{Q}^{\dot{\epsilon}E} &= \langle 0 |, \\ \langle \bar{\psi}^{BCD} | Q_B^\beta &= \langle \phi^{CD} | \lambda^\beta, & \langle \bar{\psi}^{ABC} | \bar{Q}^{\dot{\delta}D} &= \langle g^{(-) ABCD} | \tilde{\lambda}^{\dot{\delta}}, \\ \langle \phi^{CD} | Q_C^\gamma &= \langle \psi^D | \lambda^\gamma, & \langle \phi^{AB} | \bar{Q}^{\dot{\gamma}C} &= \langle \bar{\psi}^{ABC} | \tilde{\lambda}^{\dot{\gamma}}, \\ \langle \psi^D | Q_D^\delta &= \langle g^{(+)} | \lambda^\delta, & \langle \psi^A | \bar{Q}^{\dot{\beta}B} &= \langle \phi^{AB} | \tilde{\lambda}^{\dot{\beta}}, \\ \langle g^{(+)} | Q_E^\epsilon &= \langle 0 |, & \langle g^{(+)} | \bar{Q}^{\dot{\alpha}A} &= \langle \psi^A | \tilde{\lambda}^{\dot{\alpha}}. \end{aligned} \quad (2.4.6)$$

The supercharge Q_A^α raises the helicity of the state by $\frac{1}{2}$ and contracts the R -symmetry index A , while $\bar{Q}^{\dot{\alpha}A}$ lowers the helicity by $\frac{1}{2}$ and adds index A to the state.

It is convenient to introduce the Nair super-annihilation operator [74], where all the individual annihilation operators for the fields of $\mathcal{N} = 4$ SYM are combined with the use of auxiliary Grassmannian variables η as

$$\Phi(p, \eta) = g^{(+)}(p) + \psi^A(p) \eta_A + \frac{1}{2} \phi^{AB}(p) \eta_A \eta_B + \frac{1}{3!} \bar{\psi}^{ABC}(p) \eta_A \eta_B \eta_C + g^{(-)}(p) \eta_1 \cdots \eta_4, \quad (2.4.7)$$

and where $g^{(+)}(p)$, $\psi^A(p)$, $\phi^{AB}(p)$, $\bar{\psi}^{ABC}(p)$ and $g^{(-)}(p)$, denote the ladder operators for the various particles. We assign helicity $+\frac{1}{2}$ to the newly-introduced variable η_A so that $\Phi(p, \eta)$ carries uniform helicity $+1$ and we can extend the definition of the helicity generator of (2.1.13) to the supersymmetric case as

$$H = \frac{1}{2} \sum_{i=1}^n \left[-\lambda_i^\alpha \frac{\partial}{\partial \lambda_i^\alpha} + \tilde{\lambda}_i^{\dot{\alpha}} \frac{\partial}{\partial \tilde{\lambda}_i^{\dot{\alpha}}} + \eta_{iA} \frac{\partial}{\partial \eta_{iA}} \right]. \quad (2.4.8)$$

By acting with $\Phi(p, \eta)$ on the vacuum, we create a super-state, which is an eigenstate of the Q_A^α and $\bar{Q}^{\dot{\alpha}A}$ supercharges,

$$\langle \Phi | Q_A^\alpha = \langle \Phi | \lambda^\alpha \eta_A, \quad \langle \Phi | \bar{Q}^{\dot{\alpha}A} = \langle \Phi | \tilde{\lambda}^{\dot{\alpha}} \frac{\partial}{\partial \eta_A}. \quad (2.4.9)$$

We refer to the eigenvalue of Q_A^α , $q_A^\alpha := \lambda^\alpha \eta_A$ as *super-momentum* carried by $\langle \Phi |$ and denote the eigenvalue of $\bar{Q}^{\dot{\alpha}A}$ as $\bar{q}^{\dot{\alpha}A}$. These eigenvalues satisfy the anti-commutation relation analogous to that of (2.4.5).

$\mathcal{N}=4$ SYM scattering amplitudes

Using the formalism of on-shell $\mathcal{N}=4$ supersymmetry, the MHV tree-level amplitude for $n \geq 4$ reads [74]

$$A_n^{(0)\text{MHV}}(\lambda_i, \tilde{\lambda}_i, \eta_i) = i \frac{\delta^{(4)}\left(\sum_{i=1}^n \lambda_i \tilde{\lambda}_i\right) \delta^{(8)}\left(\sum_{k=1}^n \lambda_k \eta_k\right)}{\langle 12 \rangle \langle 23 \rangle \cdots \langle n1 \rangle}, \quad (2.4.10)$$

where $\delta^{(4)}$ ensures the physical momentum conservation and we can think of $\delta^{(8)}$ as imposing super-momentum conservation. It is a Grassmann-odd delta function, since the variables η are Grassmannian and as such behaves differently to the usual $\delta^{(4)}$ we have dealt with so far. In particular, it has the explicit expression

$$\delta^{(8)}\left(\sum_{i=1}^n \lambda_i \eta_i\right) = \prod_{\alpha=1}^2 \prod_{A=1}^4 \left(\sum_{i=1}^n \lambda_i^\alpha \eta_{iA} \right), \quad (2.4.11)$$

and we see that both the $\delta^{(8)}$ as well as the entire the $\mathcal{N}=4$ SYM MHV amplitude are of degree 8 in η . The amplitude in (2.4.10) packages all of the MHV *component* amplitudes of n particles, meaning that it comprises of all the amplitudes of gluons, scalars and fermions as long as the helicity configuration is correct *i.e.* no more than two particles are of negative helicity.

The full n -point tree-level super-amplitude captures all possible component amplitudes of n particles with varying particle content and MHV degree. Overall momentum and super-momentum still need to be conserved and it is convenient to factor out the

entire MHV tree-level amplitude (2.4.10), including the Parke-Taylor denominator. We can hence express the most general $n \geq 4$ -point superamplitude of $\mathcal{N}=4$ SYM by

$$\begin{aligned} A_n^{(0)}(\lambda_i, \tilde{\lambda}_i, \eta_i) &= i \frac{\delta^{(4)}\left(\sum_{i=1}^n \lambda_i \tilde{\lambda}_i\right) \delta^{(8)}\left(\sum_{k=1}^n \lambda_k \eta_k\right)}{\langle 12 \rangle \langle 23 \rangle \cdots \langle n1 \rangle} \mathcal{P}_n(\lambda_i, \tilde{\lambda}_i, \eta_i) \\ &= A_n^{(0)\text{MHV}}(\lambda_i, \tilde{\lambda}_i, \eta_i) \mathcal{P}_n(\lambda_i, \tilde{\lambda}_i, \eta_i). \end{aligned} \quad (2.4.12)$$

In this definition we have introduced a function \mathcal{P}_n which is a Grassmann polynomial in η of the form

$$\mathcal{P}_n(\lambda_i, \tilde{\lambda}_i, \eta_i) = \mathcal{P}_n^{\text{MHV}} + \mathcal{P}_n^{\text{NMHV}} + \mathcal{P}_n^{\text{N}^2\text{MHV}} + \cdots + \overline{\mathcal{P}_n^{\text{MHV}}}. \quad (2.4.13)$$

Clearly $\mathcal{P}_n^{\text{MHV}} = 1$ in order to agree with (2.4.10) and the order in η increases in increments of 4,¹⁰ such that $\mathcal{P}_n^{\text{NMHV}}$ is of order 4 in η , $\mathcal{P}_n^{\text{N}^k\text{MHV}}$ is of order $4k$ and so on up to the highest-degree $4n-16$ of the anti-MHV amplitude. Each of the $\mathcal{P}_n^{\text{N}^k\text{MHV}}$ polynomials encodes all of the component amplitudes of the specified MHV degree k - purely gluonic, as well as those involving scalars and fermions. Using the integration rules for a Grassmann-odd variable η

$$\int d\eta \eta = 1, \quad \int d\eta 1 = 0, \quad (2.4.14)$$

we can extract component amplitudes by integrating (2.4.12) over the appropriate powers of η . For example, in order to extract an amplitude with a scalar ϕ^{AB} on one of the legs we need to integrate out η_C and η_D on that particular leg. The same reasoning follows for all the fields of $\mathcal{N} = 4$ SYM and we can summarise the extraction of component amplitudes as:

$$\begin{aligned} \int d^4\eta \eta_1 \eta_2 \eta_3 \eta_4 &\leftrightarrow \langle g^{(+)} |, \\ \int d^4\eta \eta_B \eta_C \eta_D &\leftrightarrow \langle \psi^A |, \\ \int d^4\eta \eta_C \eta_D &\leftrightarrow \langle \phi^{AB} |, \\ \int d^4\eta \eta_D &\leftrightarrow \langle \bar{\psi}^{ABC} |, \\ \int d^4\eta 1 &\leftrightarrow \langle g^{(-)} |, \end{aligned} \quad (2.4.15)$$

where we used the short-hand notation

$$\int d^4\eta := \int d\eta_1 d\eta_2 d\eta_3 d\eta_4. \quad (2.4.16)$$

¹⁰Otherwise the amplitude would not be R -symmetry invariant.

Using these rules, together with the definition (2.4.10), we can immediately understand our earlier claim regarding vanishing of the all-plus gluon amplitude. For $n \geq 3$ all-plus gluon legs, we would need to perform $4n$ Grassmann integrals. The delta function in the definition of the amplitude, however, has fermionic degree 8 and as such, following the property (2.4.14) the integral is forced to vanish. Many other component amplitudes can be immediately seen to vanish for the same reason.

Component amplitudes are related to each other by *supersymmetric Ward identities* [75, 76]. These linear relations are derived from the fact that the vacuum is supersymmetric, $Q|0\rangle = 0$, $\bar{Q}|0\rangle = 0$. As a consequence, if we write the n -point scattering amplitude as a matrix element $\langle 0|\Phi(1)\Phi(2)\cdots\Phi(n)|0\rangle$ where we use a shorthand notation $\Phi(i) := \Phi(p_i, \eta_i)$ then it follows that

$$\begin{aligned} 0 &= \langle 0|[Q, \Phi(1)\cdots\Phi(n)]|0\rangle \\ &= \sum_{i=1}^n \langle 0|\Phi(1)\cdots[Q, \Phi(i)]\cdots\Phi(n)|0\rangle, \end{aligned} \tag{2.4.17}$$

and similarly for \bar{Q} . Given the action of the supercharges on $\mathcal{N}=4$ SYM states in (2.4.6) we see that (2.4.17) relates component amplitudes with the same number of legs, but different external field content. As an example of one of such relations, we have that

$$A_n^{(0)}(g_1^+, g_2^+, \dots, g_i^-, \dots, g_j^-, \dots, g_n^+) = \frac{\langle ij \rangle^4}{\langle 12 \rangle^4} A_n^{(0)}(g_1^-, g_2^-, \dots, g_i^+, \dots, g_j^+, \dots, g_n^+). \tag{2.4.18}$$

This relation proves the Parke-Taylor gluon amplitude expression of (2.2.5) as a simple consequence of the supersymmetric Ward identities.

$\mathcal{N}=4$ superconformal symmetry

One of the features of Yang-Mills theory is the conformal symmetry, arising from the fact that the Yang-Mills coupling constant g_{YM} is dimensionless. As a result, the theory is invariant under scale transformations generated by the dilatation operator. Together with the other two symmetry groups of $\mathcal{N}=4$ SYM, the R -symmetry and supersymmetry, these can all be combined into one larger group, known as the $\mathcal{N}=4$ superconformal symmetry with the algebra $\mathfrak{psu}(2, 2|4)$. We review briefly the action of the generators of the superconformal symmetry on the superamplitudes in $\mathcal{N}=4$ SYM.

We begin first with the bosonic subalgebra, $\mathfrak{su}(2, 2) \times \mathfrak{su}(4)$. The $\mathfrak{su}(2, 2)$ is the four dimensional conformal algebra with 15 generators, realised here in the spinor-helicity representation, appropriate for massless particles [17]:

- 10 generators of the Poincaré algebra, which include

- four generators of the space-time translations

$$P^{\dot{\alpha}\alpha} = \tilde{\lambda}^{\dot{\alpha}} \lambda^{\alpha}, \quad (2.4.19)$$

- six generators of the Lorentz transformations

$$M_{\alpha\beta} = \frac{1}{2} \left(\lambda_{\alpha} \frac{\partial}{\partial \lambda^{\beta}} + \lambda_{\beta} \frac{\partial}{\partial \lambda^{\alpha}} \right), \quad \bar{M}_{\dot{\alpha}\dot{\beta}} = \frac{1}{2} \left(\tilde{\lambda}_{\dot{\alpha}} \frac{\partial}{\partial \tilde{\lambda}^{\dot{\beta}}} + \tilde{\lambda}_{\dot{\beta}} \frac{\partial}{\partial \tilde{\lambda}^{\dot{\alpha}}} \right), \quad (2.4.20)$$

• 4 generators of the special conformal transformations

$$K_{\alpha\dot{\alpha}} = \frac{\partial}{\partial \lambda^{\alpha}} \frac{\partial}{\partial \tilde{\lambda}^{\dot{\alpha}}}, \quad (2.4.21)$$

• 1 generator of the dilatations,

$$D = \frac{1}{2} \left(\lambda^{\alpha} \frac{\partial}{\partial \lambda^{\alpha}} + \tilde{\lambda}^{\dot{\alpha}} \frac{\partial}{\partial \tilde{\lambda}^{\dot{\alpha}}} + 2 \right). \quad (2.4.22)$$

The generators (2.4.19)-(2.4.22) obey the commutation relations of the conformal algebra $\mathfrak{su}(2,2)$:

$$\begin{aligned} [D, P^{\dot{\alpha}\alpha}] &= P^{\dot{\alpha}\alpha}, & [D, M_{\alpha\beta}] &= 0, & [D, \bar{M}_{\dot{\alpha}\dot{\beta}}] &= 0, & [D, K_{\alpha\dot{\alpha}}] &= -K_{\alpha\dot{\alpha}}, \\ [K_{\alpha\dot{\alpha}}, P^{\dot{\beta}\beta}] &= \delta_{\alpha}^{\beta} \delta_{\dot{\alpha}}^{\dot{\beta}} D + M_{\alpha}^{\beta} \delta_{\dot{\alpha}}^{\dot{\beta}} + \bar{M}_{\dot{\alpha}}^{\dot{\beta}} \delta_{\alpha}^{\beta}. \end{aligned} \quad (2.4.23)$$

All of the expressions for the $\mathfrak{su}(2,2)$ generators above can be generalised to their multi-particle action form by summing over the external particle labels, for example

$$P^{\dot{\alpha}\alpha} = \sum_{i=1}^n \tilde{\lambda}_i^{\dot{\alpha}} \lambda_i^{\alpha}, \quad (2.4.24)$$

reflecting the local nature of the symmetry. The $\mathfrak{su}(4)$ is the global $\mathcal{N}=4$ R -symmetry acting as an internal rotation in the η -space, with 15 traceless generators

$$R_A{}^B = \eta_A \frac{\partial}{\partial \eta_B} - \frac{1}{4} \delta_A^B \eta_C \frac{\partial}{\partial \eta_C}. \quad (2.4.25)$$

As far as the action of these bosonic generators on the tree-level MHV superamplitude (2.4.10) is concerned, the presence of the momentum-conserving delta function ensures invariance under the action of the generators of the space-time translations (2.4.19). Invariance under the Lorentz transformations (2.4.20) follows from the fact that the spinor brackets entering the superamplitude, *i.e.* $\langle ij \rangle$, are Lorentz-invariant. The proof of invariance under the special conformal transformations (2.4.21) is a little

more involved but using the chain rule one can show that

$$K_{\alpha\dot{\alpha}} \delta^{(4)}(P) = (n-4) \frac{\partial}{\partial P^{\dot{\alpha}\alpha}} \delta^{(4)}(P). \quad (2.4.26)$$

On the other hand, the Parke-Taylor denominator and the supermomentum-conserving $\delta^{(8)}$ are independent of $\tilde{\lambda}$ and hence

$$\begin{aligned} K_{\alpha\dot{\alpha}} A_n^{(0)\text{MHV}} &= (n-4) \left(\frac{\partial}{\partial P^{\dot{\alpha}\alpha}} \delta^{(4)}(P) \right) \frac{\delta^{(8)}(Q)}{\langle 12 \rangle \langle 23 \rangle \cdots \langle n1 \rangle} \\ &+ \left(\frac{\partial}{\partial P^{\dot{\alpha}\beta}} \delta^{(4)}(P) \right) \left(\sum_i \lambda_i^\beta \frac{\partial}{\partial \lambda_i^\alpha} \frac{\delta^{(8)}(Q)}{\langle 12 \rangle \langle 23 \rangle \cdots \langle n1 \rangle} \right) \\ &= (n-4) \left(\frac{\partial}{\partial P^{\dot{\alpha}\alpha}} \delta^{(4)}(P) \right) \frac{\delta^{(8)}(Q)}{\langle 12 \rangle \langle 23 \rangle \cdots \langle n1 \rangle} \\ &+ \left(\frac{\partial}{\partial P^{\dot{\alpha}\beta}} \delta^{(4)}(P) \right) \left(- (n-4) \delta_\alpha^\beta \frac{\delta^{(8)}(Q)}{\langle 12 \rangle \langle 23 \rangle \cdots \langle n1 \rangle} \right) = 0. \end{aligned} \quad (2.4.27)$$

Invariance under the dilatation generator (2.4.22) follows immediately from commutation relations (2.4.23). The only η -dependent part of the superamplitude is the supermomentum-conserving $\delta^{(8)}(Q)$ and from its definition (2.4.11) we see that it contains a simple product of the Grassmannian variables. The action of the R -charge generators (2.4.25) is a simple rotation of R -symmetry labels, leaving the superamplitude (2.4.10) invariant.

The fermionic part of the superconformal $\mathcal{N}=4$ algebra consists of 16 supercharges introduced in (2.4.5),

$$Q_A^\alpha = \lambda^\alpha \eta_A, \quad \bar{Q}^{\dot{\alpha}A} = \tilde{\lambda}^{\dot{\alpha}} \frac{\partial}{\partial \eta_A}, \quad (2.4.28)$$

and 16 fermionic superconformal charges,

$$S_\alpha^A = \frac{\partial}{\partial \lambda^\alpha} \frac{\partial}{\partial \eta_A}, \quad \bar{S}_{\dot{\alpha}A} = \eta_A \frac{\partial}{\partial \tilde{\lambda}^{\dot{\alpha}}}, \quad (2.4.29)$$

obtained by commuting supercharges with special conformal generators:

$$[K_{\alpha\dot{\alpha}}, Q_A^\beta] = \delta_\alpha^\beta \bar{S}_{\dot{\alpha}A}, \quad [K_{\alpha\dot{\alpha}}, \bar{Q}^{\dot{\beta}A}] = \delta_{\dot{\alpha}}^{\dot{\beta}} S_\alpha^A. \quad (2.4.30)$$

Presence of the supermomentum-conserving $\delta^{(8)}(Q)$ ensures immediate invariance under the action of the supercharges (2.4.28). For $\bar{S}_{\dot{\alpha}A}$ the invariance is straightforward to

verify, as

$$\bar{S}_{\dot{\alpha}}^A \delta^{(4)}(P) = \sum_i \eta_i^A \frac{\partial}{\partial \tilde{\lambda}_i^{\dot{\alpha}}} \delta^{(4)}(P) = \sum_i \eta_i^A \lambda_i^{\alpha} \frac{\partial}{\partial P^{\dot{\alpha}\alpha}} \delta^{(4)}(P) = Q^{\alpha A} \frac{\partial}{\partial P^{\dot{\alpha}\alpha}} \delta^{(4)}(P), \quad (2.4.31)$$

which vanishes on support of the supermomentum delta function $\delta^{(8)}(Q)$. Invariance under the action of the superconformal charge S_{α}^A can be inferred from relations (2.4.30).

The superconformal algebra $\mathfrak{psu}(2, 2|4)$ is a graded Lie algebra, combining the Poincaré and conformal generators with supercharges and superconformal charges by the way of commutation and anticommutation relations:

$$\begin{aligned} \{Q_A^{\alpha}, \bar{Q}^{\dot{\alpha}B}\} &= \delta_A^B P^{\dot{\alpha}\alpha}, & \{S_{\alpha}^A, \bar{S}_{\dot{\alpha}B}\} &= \delta_A^B K_{\alpha\dot{\alpha}}, \\ \{Q_A^{\alpha}, S_{\beta}^B\} &= M^{\alpha}_{\beta} \delta_A^B + \delta_{\beta}^{\alpha} R_A{}^B + \frac{1}{2} \delta_{\beta}^{\alpha} \delta_A^B D, \\ \{\bar{Q}^{\dot{\alpha}A}, \bar{S}_{\dot{\beta}B}\} &= \bar{M}^{\dot{\alpha}}_{\dot{\beta}} \delta_B^A - \delta_{\dot{\beta}}^{\dot{\alpha}} R_B{}^A + \frac{1}{2} \delta_{\dot{\beta}}^{\dot{\alpha}} \delta_B^A D, \\ [P^{\dot{\alpha}\alpha}, S_{\beta}^A] &= \delta_{\beta}^{\alpha} \bar{Q}^{\dot{\alpha}A}, & [P^{\dot{\alpha}\alpha}, \bar{S}_{\dot{\beta}A}] &= \delta_{\dot{\beta}}^{\dot{\alpha}} Q_A^{\alpha}. \end{aligned} \quad (2.4.32)$$

We can further extend the algebra $\mathfrak{psu}(2, 2|4)$ to $\mathfrak{su}(2, 2|4)$ by addition of the central charge C ,

$$C = 1 + \frac{1}{2} \left(\lambda^{\alpha} \frac{\partial}{\partial \lambda^{\alpha}} - \tilde{\lambda}^{\dot{\alpha}} \frac{\partial}{\partial \tilde{\lambda}^{\dot{\alpha}}} - \eta_A \frac{\partial}{\partial \eta_A} \right). \quad (2.4.33)$$

The central charge counts the degrees of freedom and commutes with all the generators of the superconformal algebra listed above. Comparing with the expression for the helicity generator in (2.4.8), we see that helicity and central charge are related via $C = 1 - H$. The central charge has the special feature of vanishing on the superamplitude locally for every leg,

$$C_i A_n = 0, \quad (2.4.34)$$

as a consequence of the fact that the on-shell superfield introduced in (2.4.7) is of uniform helicity +1, leading to

$$H_i A_n = A_n. \quad (2.4.35)$$

In addition to the astonishing amount of symmetry discussed in this section, planar scattering amplitudes in $\mathcal{N}=4$ SYM possess yet another, hidden symmetry referred to as the *dual superconformal symmetry*, which we review next.

Dual superconformal symmetry

Proposed in [77] and proven for all tree-level amplitudes in [61] the dual superconformal symmetry is revealed by introduction of the dual coordinate space, with new dual *region momenta* x_i related to the conventional momenta p_i by

$$p_i^{\dot{\alpha}\alpha} = (x_i - x_{i+1})^{\dot{\alpha}\alpha} \quad (2.4.36)$$

and illustrated in Figure 5.

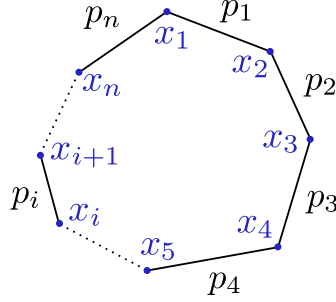


Figure 5: Pictorial realisation of momentum conservation. This polygon can be described in terms of its edges, corresponding to conventional momenta or its vertices, corresponding to dual momenta.

In order to consider the $\mathcal{N}=4$ SYM superamplitude in the dual description, we need to also introduce dual fermionic coordinates θ_{iA}^α as

$$\lambda_i^\alpha \eta_{iA} = (\theta_i - \theta_{i+1})_A^\alpha. \quad (2.4.37)$$

Naturally, in this description momentum is still conserved

$$p_1 + p_2 + \dots + p_n = (x_1 - x_2) + (x_2 - x_3) + \dots + (x_n - x_1) = 0, \quad (2.4.38)$$

and similarly for the supermomentum. Since we are dealing with massless particles, *i.e.* the momenta are null, we have additionally

$$(x_i - x_{i+1})^2 = 0, \quad (2.4.39)$$

and the differences of dual fermionic variables are constrained to be on-shell,

$$(\theta_i - \theta_{i+1})\lambda_i = 0. \quad (2.4.40)$$

In order to understand the action of the dual superconformal symmetry generators we need an expression for the conformal inversion, I , in terms of the dual momenta.

It turns out to be

$$\begin{aligned}
 I[x_i^{\dot{\alpha}\beta}] &:= x_i^{-1} = \frac{x_i^{\dot{\beta}\alpha}}{x_i^2}, & I[\theta_{iA}^\alpha] &= \theta_{i\beta A} \frac{x_i^{\dot{\alpha}\beta}}{x_i^2}, \\
 I[\lambda_i^\alpha] &= \lambda_{i\beta} \frac{x_i^{\dot{\alpha}\beta}}{x_i^2}, & I[\tilde{\lambda}_i^{\dot{\alpha}}] &= \frac{x_i^{\dot{\alpha}\beta}}{x_i^2} \tilde{\lambda}_{i\dot{\alpha}}, & I[\eta_{iA}] &= \frac{x_i^2}{x_{i+1}^2} \left(\eta_{iA} - \theta_{iA} x_i^{-1} \tilde{\lambda}_i \right).
 \end{aligned} \tag{2.4.41}$$

Under the dual conformal inversion, the MHV superamplitude (2.4.10) transforms covariantly,

$$I[A_n^{(0)\text{MHV}}] = A_n^{(0)\text{MHV}} \prod_{i=1}^n x_i^2. \tag{2.4.42}$$

Dual superconformal invariance follows immediately from this statement. Special conformal transformations are obtained as

$$K^{\dot{\alpha}\alpha} = IP^{\dot{\alpha}\alpha}I, \tag{2.4.43}$$

and combining these with supersymmetry transformations according to (2.4.30) we generate the superconformal transformations. Remarkably, the non-trivial transformation property (2.4.42) extends to all tree-level superamplitudes in $\mathcal{N} = 4$ SYM. The proof of the tree-level covariance required introduction of supersymmetric extension of the BCFW recursion relations discussed in Section 2.3 and as a result an introduction of $\mathcal{N} = 4$ SYM three-point anti-MHV superamplitude [61]¹¹

$$A^{\overline{\text{MHV}}}(1, 2, 3) = i \frac{\delta^{(4)}(p_1 + p_2 + p_3) \delta^{(4)}(\eta_1[23] + \eta_2[31] + \eta_3[12])}{[12][23][31]}. \tag{2.4.44}$$

Even more remarkably, the two symmetry groups of the $\mathcal{N} = 4$ SYM tree-level superamplitude, the superconformal and dual superconformal, can be combined to even larger symmetry known as *the Yangian*.

Yangian symmetry

The Yangian symmetry of the superamplitude [78] is realised by expressing the dual superconformal generators in terms of the variables entering the ordinary superconformal generators, $\{\lambda^\alpha, \tilde{\lambda}^{\dot{\alpha}}, \eta^A\}$, and subsequently finding the commutation relations between the two sets of generators. In doing so, we discover a certain degree of overlap between the two symmetries. The closure of the two symmetry algebras defines the *Yangian algebra*.

We define the Yangian level zero generators $J^{(0)}$ as the ordinary superconformal

¹¹The three-point MHV superamplitude is given by the usual Nair formula (2.4.10).

generators, satisfying

$$[J_a^{(0)}, J_b^{(0)}] = f_{ab}{}^c J_c^{(0)} \quad (2.4.45)$$

where $f_{ab}{}^c$ are the structure constants of the $\mathfrak{psu}(2, 2|4)$ algebra. The graded commutator is defined as

$$[\mathcal{O}_1, \mathcal{O}_2] := \mathcal{O}_1 \mathcal{O}_2 - (-1)^{\deg(\mathcal{O}_1)\deg(\mathcal{O}_2)} \mathcal{O}_2 \mathcal{O}_1, \quad (2.4.46)$$

where by $\deg(\mathcal{O})$ we mean the Grassmann degree of the operator \mathcal{O} . The level one generators $J^{(1)}$ are defined explicitly as

$$J_a^{(1)} = f_a{}^{cb} \sum_{i \leq 1 < j \leq n} J_{ib}^{(0)} J_{jc}^{(0)}, \quad (2.4.47)$$

and they satisfy the graded commutation relations

$$[J_a^{(1)}, J_b^{(0)}] = f_{ab}{}^c J_c^{(1)}, \quad (2.4.48)$$

as well as Serre relations. It turns out that level-one generators can be shown to be precisely the dual superconformal generators. As a result, the dual superconformal symmetry together with the conventional superconformal symmetry form a Yangian symmetry acting on the $\mathcal{N} = 4$ SYM superamplitude. This is an exciting discovery – the Yangian typically arises in the context of integrable two-dimensional quantum field theories. Yet again, we see hints of integrability of the four-dimensional interacting $\mathcal{N} = 4$ SYM, further evidence of which becomes apparent in studies of the dilatation operator of the theory.

2.5 Scaling dimension and the dilatation operator

One of the main problems of interest in study of any QFT is the prediction of the mass spectrum in terms of parameters of the theory in order to compare with experimental results. For a conformal theory such as $\mathcal{N} = 4$ SYM, however, there is no inherent mass scale to operate with as all of the fields are uniformly massless. Hence we have to focus on calculating an alternative characteristic quantity, which turns out to be *the scaling dimension*.

Let us consider a local scalar operator $\mathcal{O}(x)$. Acting with the dilatation operator we find

$$[D, \mathcal{O}(x)] = \left(\Delta + x \frac{\partial}{\partial x} \right) \mathcal{O}(x), \quad (2.5.1)$$

where the eigenvalue Δ is the *conformal dimension*, reflecting the fact that under the scaling $x \rightarrow \lambda x$, the operator scales as $\mathcal{O}(x) \rightarrow \lambda^{-\Delta} \mathcal{O}(\lambda x)$. The conformal dimension can be read off from the two point function of the operator \mathcal{O} and its conjugate $\bar{\mathcal{O}}$, whose form is fixed by the conformal symmetry as

$$\langle \mathcal{O}(x) \bar{\mathcal{O}}(y) \rangle \propto \frac{1}{|x - y|^{2\Delta}}. \quad (2.5.2)$$

We call the dimension at zero coupling, Δ_0 , the *bare dimension* and for a composite operator it is a sum of dimensions of its constituent fields, where we have

$$[\phi] = 1, \quad [\psi] = 3/2, \quad [F^{\mu\nu}] = 2. \quad (2.5.3)$$

In what follows we will be focusing on interacting theories where the scaling dimension gets renormalised. We will be interested in finding the quantum correction to the bare dimension of a given operator, known as the *anomalous dimension*, γ , where

$$\Delta = \Delta_0 + \gamma, \quad \gamma \ll \Delta_0. \quad (2.5.4)$$

In the case of an interacting theory, the two-point function (2.5.2) can therefore be expanded as

$$\langle \mathcal{O}(x) \bar{\mathcal{O}}(y) \rangle = \frac{1}{|x - y|^{2\Delta_0}} [1 - \gamma \log(|x - y|^2 \Lambda^2) + \dots], \quad (2.5.5)$$

where we have denoted the ultraviolet (UV) cutoff scale by Λ . We therefore see that in this simple case we can read off the one-loop anomalous dimension from the coefficient of the UV divergence of the two-point function.

However, the problem of finding the anomalous dimension is often further complicated by the issue of *operator mixing*. In this case the UV divergent term is not directly proportional to the tree-level correlator as in (2.5.5) but instead receives contributions from two-point functions of other operators. In such a case, one needs to find the *mixing matrix* of anomalous dimensions, diagonalise it and solve for the eigenvalues and eigenvectors, order by order in the coupling constant. If we expand the dilatation operator in the powers of 't Hooft coupling (2.4.1) as

$$D = \sum_{L=0}^{\infty} a^L D^{(2L)} \quad (2.5.6)$$

the eigenvalues of $D^{(0)}$ correspond to the bare dimensions and the eigenvalues of $D^{(2)}$ to the one-loop anomalous dimensions. Hence at one loop, solving the mixing problem consists of first finding the matrix $D^{(2)}$ then solving for its eigenvalues – the *spectrum*

of anomalous dimensions and its eigenvectors – operators with definite anomalous dimensions. A priori, finding the solution to the mixing problem is very difficult as we potentially have to consider a large number of operators. Fortunately, some simplifications are possible.

Firstly, there exist sets of operators which, at a certain loop order, only mix between themselves. The local composite operators are built out of the fundamental fields of the theory and we refer to such a set of fields, or *letters*, as a *sector*. We say a sector is *closed* if operators made out of the letters only mix between themselves. An example of a closed sector is the $SU(2|3)$ sector of $\mathcal{N} = 4$ SYM, which consists of three scalar fields and one fermion. The dilatation operator of this sector has been studied and determined up to three loops in [79,80] and we study it in detail in Chapter 3. Another example is the $SU(2)$ sector studied at two-loops in [52].

Secondly, in the seminal work of [81], Minahan and Zarembo showed that the one-loop dilatation operator in the $SO(6)$ sector can be related to a one-dimensional spin chain Hamiltonian with only nearest-neighbours interactions. Operators in this sector are made out of scalar fields, ϕ_{AB} , and we consider single-trace operators,¹²

$$\mathcal{O}_n(x) = \text{Tr}\left(\phi_{A_1 B_1}(x) \cdots \phi_{A_n B_n}(x)\right). \quad (2.5.7)$$

These operators can be thought of as a periodic one-dimensional spin chain, with every field in the operator mapped to a spin chain site carrying an $SO(6)$ vector index. Periodicity is imposed by the cyclicity of the trace and the mapping is schematically illustrated in Figure 6.

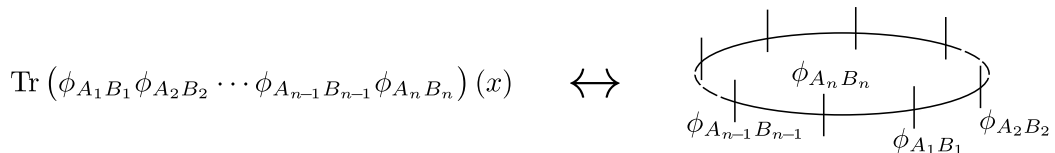


Figure 6: Single-trace scalar operator in the spin chain picture. Each site of the spin chain carries an associated $SO(6)$ vector index and the spin chain is closed and periodic since the trace is cyclic.

At one-loop order and in the planar limit only interactions between fields adjacent in the colour space are relevant, thus if we wish to find the one-loop anomalous dimension according to (2.5.5) in practice we only need to consider the two-point functions of the form

$$\langle \phi_{A_1 B_1} \phi_{C_1 D_1}(x) \phi_{A_2 B_2} \phi_{C_2 D_2}(y) \rangle. \quad (2.5.8)$$

As a result, the one-loop dilatation operator can be expanded in terms of operators

¹²Operators built out of products of traces are subleading in the large N limit, see discussion after (2.1.6).

acting only on two adjacent sites,

$$D^{1\text{-loop}} = a \sum_{i=1}^n D_{i\,i+1}^{(2)}, \quad (2.5.9)$$

where $D_{n\,n+1}^{(2)} = D_{n\,1}^{(2)}$. There exist only three distinct ways to contract the R -symmetry indices between the two sets of scalar fields at this loop order, as presented in Figure 7.

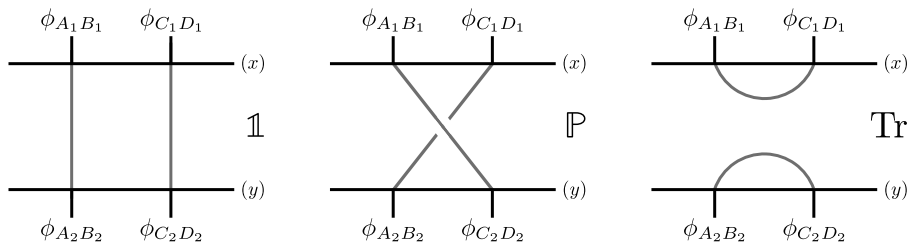


Figure 7: Three possible ways of contracting the $SO(6)$ R -symmetry indices between two sets of scalar fields: identity, permutation and trace.

The result found in [81] for the one-loop dilatation operator in the $SO(6)$ sector reads

$$D^{1\text{-loop}} = a \sum_{i=1}^n (2\mathbb{1} - 2\mathbb{P} + \text{Tr})_{i\,i+1}. \quad (2.5.10)$$

The remarkable feature of this result is that (2.5.10) is a Hamiltonian belonging to a family of integrable spin chains with $SO(n)$ symmetry. Integrability for such Hamiltonians requires the ratio between the coefficients of the permutation and trace operator to be delicately balanced and equal to $-(n/2 - 1)$. For $SO(6)$ this ratio is -2 , precisely as obtained in (2.5.10).

The discovery of connection between the one-loop dilatation operator and integrable spin chain has allowed for use of an array of techniques, such as the Bethe ansatz, previously reserved to lower-dimensional problems, to be utilised in diagonalising the dilatation operator and finding its eigenvalues. The one-loop dilatation operator of $\mathcal{N} = 4$ SYM has been since extensively studied and is known completely at one loop [79, 82]. At higher loop orders the $SO(6)$ sector is not closed and calculations without the aid of integrability have been performed up to four loops [83–88].

The final simplification useful in solving the mixing problem comes from the fact that the superconformal symmetry of $\mathcal{N} = 4$ SYM relates certain operators, which we review next.

2.6 Primary, descendant and half-BPS operators

Let us consider the action of the dilatation generator D on the commutator $[K_{\alpha\dot{\alpha}}, \mathcal{O}(0)]$ where $K_{\alpha\dot{\alpha}}$ is the generator of special conformal transformations, introduced in (2.4.21). We find that, using the relations in (2.4.23)

$$\begin{aligned} [D, [K_{\alpha\dot{\alpha}}, \mathcal{O}(0)]] &= [[D, K_{\alpha\dot{\alpha}}], \mathcal{O}(0)] + [K_{\alpha\dot{\alpha}}, [D, \mathcal{O}(0)]] \\ &= -[K_{\alpha\dot{\alpha}}, \mathcal{O}(0)] + \Delta[K_{\alpha\dot{\alpha}}, \mathcal{O}(0)] \\ &= (\Delta - 1)[K_{\alpha\dot{\alpha}}, \mathcal{O}(0)]. \end{aligned} \tag{2.6.1}$$

Hence we see that the action of $K_{\alpha\dot{\alpha}}$ on $\mathcal{O}(0)$ leads to a new operator with dimension lowered by one. Apart from the identity operator, the requirement for local operators in a unitary field theory is to have a positive scaling dimension, therefore the chain we create by considering further commutators of the type above must at some point terminate. We call the operator $\tilde{\mathcal{O}}(x)$ of the lowest dimension in the chain, such that

$$[K_{\alpha\dot{\alpha}}, \tilde{\mathcal{O}}(0)] = 0, \tag{2.6.2}$$

the *primary* and we call higher dimensional operators the *descendants* of $\tilde{\mathcal{O}}(x)$, which in turn we obtain by acting with the momentum generator $P^{\dot{\alpha}\alpha}$ as

$$[D, [P^{\dot{\alpha}\alpha}, \mathcal{O}(0)]] = (\Delta + 1)[P^{\dot{\alpha}\alpha}, \mathcal{O}(0)]. \tag{2.6.3}$$

The primary operator and its descendants make up an irreducible representation of the $\mathfrak{psu}(2, 2|4)$, with the primary as the highest weight. Since $\mathfrak{psu}(2, 2|4)$ is non-compact, the representation is infinite-dimensional. Indeed, we do not have an upper bound on the dimension of the operator and we can carry on acting with the momentum generator to create higher-dimensional operators. An important observation arises as a result of this discussion. The anomalous dimensions of a primary operator and its descendants is the same since relations (2.6.1) and (2.6.3) only affect the bare dimension. As a result, it is often interesting to study operators which are known descendants of a well-studied primary operator. Since they have a definite, known anomalous dimension or in other words are eigenstates of the dilatation operator, the discussion of the mixing simplifies. If, in addition to (2.6.2), a primary operator is annihilated by a number of supersymmetry generators Q_A^α ,

$$[Q_A^\alpha, \tilde{\mathcal{O}}(0)] = 0, \tag{2.6.4}$$

a further simplification occurs. Using the definitions of the superconformal charges in (2.4.29) and the dilatation generator in (2.4.22) we can immediately see that the

following commutation relations hold

$$[D, S_\alpha^A] = -\frac{1}{2}S_\alpha^A, \quad [D, \bar{S}_{\dot{\alpha}A}] = -\frac{1}{2}\bar{S}_{\dot{\alpha}A}. \quad (2.6.5)$$

As a result, in analogy to (2.6.1), the action of S_α^A or $\bar{S}_{\dot{\alpha}A}$ on an operator lowers the dimension by a half and the action on the lowest dimension primary operator $\tilde{\mathcal{O}}(0)$ annihilates it,

$$[S_\alpha^A, \tilde{\mathcal{O}}(0)] = 0, \quad [\bar{S}_{\dot{\alpha}A}, \tilde{\mathcal{O}}(0)] = 0. \quad (2.6.6)$$

Let us now consider the action of the anticommutator $\{Q_A^\alpha, S_\beta^B\}$ on the primary operator. We have, using (2.6.4) and (2.6.6)

$$[\{Q_A^\alpha, S_\beta^B\}, \tilde{\mathcal{O}}(0)] = 0, \quad (2.6.7)$$

but also using the second relation in (2.4.32):

$$[\{Q_A^\alpha, S_\beta^B\}, \tilde{\mathcal{O}}(0)] = \delta_A^B [M^\alpha{}_\beta, \tilde{\mathcal{O}}(0)] + \delta_\beta^\alpha [R_A{}^B, \tilde{\mathcal{O}}(0)] + \frac{1}{2} \delta_\beta^\alpha \delta_A^B [D, \tilde{\mathcal{O}}(0)]. \quad (2.6.8)$$

For scalar operators, which will be the subject of discussion in Chapter 3, the first commutator vanishes and we have that

$$\delta_\beta^\alpha [R_A{}^B, \tilde{\mathcal{O}}(0)] + \frac{1}{2} \delta_\beta^\alpha \delta_A^B [D, \tilde{\mathcal{O}}(0)] = 0, \quad (2.6.9)$$

i.e. the conformal dimension and the R -charge are related. The R -charge, however, is an integer while the anomalous dimension γ is a smooth function of the coupling constant. For the relation (2.6.9) to hold, the anomalous dimension must be zero for all values of the coupling, *i.e.* $\Delta = \Delta_0$ and it receives no quantum corrections. We call operators which satisfy the supercharge annihilation condition (2.6.4) the BPS, or *protected* operators. If the operator is annihilated by half of the total amount of supercharges of the theory¹³ we call it *half-BPS*, with analogous definitions for $\frac{1}{4}$ -BPS and even $\frac{1}{8}$ -BPS operators. The area of study of properties of half-BPS operators is by itself very extensive. As we will see in the present work, they play very special role in computations of two-loop form factors of other, a priori unrelated operators.

2.7 Loop-level techniques

Up until this point in the discussion we have focused solely on tree-level objects, for which we have successfully used the understanding of the pole structure in order to

¹³Equal to 8 in the case of $\mathcal{N}=4$ SYM.

construct higher point amplitudes from lower point ones. Moving on to the next order in perturbation theory we encounter loop diagrams, which require integration over loop momenta and give rise to more complicated structures involving logarithms, dilogarithms and other special functions. As a result, in addition to simple poles in sums of adjacent momenta, loop amplitudes will exhibit branch cut singularities.

It is often useful to separate the discussion of the loop *integrand* from that of loop *integral*. In order to perform the latter, we first need to construct the former – here we focus our discussion on obtaining the loop integrand using the method of generalised unitarity. Once a well defined integrand has been obtained one can proceed to evaluation, where an appropriate method of regulating divergences needs to be employed.

Generalised unitarity

The physical requirement of conservation of probability implies unitarity of the S -matrix, $S^\dagger S = \mathbb{1}$. This seemingly very simple statement has remarkable consequences and leads to powerful computational techniques, as outlined next, based on the review in [89].

The S -matrix consists of a trivial part, where no scattering takes place and the so-called transfer matrix, $S = \mathbb{1} + iT$. The unitarity requirement implies a non-linear relation for the transfer matrix,

$$-i(T - T^\dagger) = TT^\dagger. \quad (2.7.1)$$

Expanding T order by order in perturbation theory,

$$T = gT^{(0)} + g^2 T^{(1)} + g^3 T^{(2)} + \mathcal{O}(g^4), \quad (2.7.2)$$

we notice that (2.7.1) leads to a non-trivial relationship between contributions at different loop orders. At first order in g we have $T^{(0)} = T^{(0)\dagger}$ and at the second order, using the first order relation we see that

$$-i(T^{(1)} - T^{(1)\dagger}) = T^{(0)}T^{(0)}. \quad (2.7.3)$$

Evaluating between incoming $|i\rangle$ and outgoing $\langle f|$ asymptotic states we see that (2.7.3) becomes

$$2\text{Im}\left(\langle f|T^{(1)}|i\rangle\right) = \int d\mu \langle f|T^{(0)}|\mu\rangle\langle\mu|T^{(0)}|i\rangle \quad (2.7.4)$$

where on the left hand side we have used the fact that $\langle f|T^{(1)\dagger}|i\rangle = \langle i|T^{(1)}|f\rangle^*$ and applied time reversal while on the right hand side we have inserted a complete set of states. Relation (2.7.4) is known as the *optical theorem*.

We will now see that in order to find the imaginary part of the loop amplitude on the left-hand side of (2.7.4) we require the intermediate particles on the right-hand side of the expression to go on shell. Since a loop amplitude is nothing else but a product of propagators integrated over a Lorentz-invariant phase space, let us start by evaluating an imaginary part of a generic propagator. Using Sochocki-Plemelj theorem,

$$\frac{1}{x + i\epsilon} = \mathcal{P}\left(\frac{1}{x}\right) - i\pi\delta(x), \quad (2.7.5)$$

where $\mathcal{P}(f(x))$ denotes the Cauchy principal value of a function $f(x)$, we have that

$$\text{Im}\left(\frac{1}{p^2 + i\epsilon}\right) = -\pi\delta(p^2). \quad (2.7.6)$$

This vanishes for $\epsilon \rightarrow 0$ except near $p^2 = 0$, *i.e.* the propagator is real except for when the particle goes on shell. In other words, the imaginary part of the amplitude arises from the intermediate particles going on shell. The discontinuity of the loop amplitude across a branch cut, defined as a difference

$$\text{Disc}[i\mathcal{A}(p^0)] := i\mathcal{A}(p^0 + i\epsilon) - i\mathcal{A}(p^0 - i\epsilon) = -2\text{Im}[\mathcal{A}(p^0)] \quad (2.7.7)$$

can be hence computed by replacing or *cutting* the propagators as

$$\frac{1}{p^2} \rightarrow \delta^{(+)}(p^2) := \Theta(p^0)\delta(p^2), \quad (2.7.8)$$

where the Heaviside function $\Theta(p^0)$ restricts to positive on-shell energies of the physical states. This is known as the Cutkosky's rule [90], graphically represented for one loop amplitude in Figure 8.

Figure 8: Cutkosky's rule. The discontinuity of a one-loop amplitude is given by the product of two lower-order amplitudes with the intermediate propagators sent on-shell.

The term *generalised unitarity* refers to the procedure of replacing any number of propagators as per relation (2.7.8). We refer to such replacements as higher-order cuts – for example, a *triple* (or *three-particle*) cut involves setting three loop propagators on shell. The cut where the greatest possible number of propagators is put on shell without violating momentum conservation is referred to as the *maximal cut*.

In order to evaluate a given one-loop amplitude, one starts from the decomposition

of a generic one-loop integral I_n in terms of a basis of one-loop scalar integrals [91],

$$I_n = \sum_i c_{\text{Box}_i} \text{Box}_i + \sum_i c_{\text{Tri}_i} \text{Tri}_i + \sum_i c_{\text{Bub}_i} \text{Bub}_i + \sum_i c_{\text{Tad}_i} \text{Tad}_i + R, \quad (2.7.9)$$

where the individual contributions to this expression are detailed in Figure 9 and the index i enumerates different ways of distributing external momenta on the legs of each integral topology. The explicit expressions for the one-loop master integrals can be found in Appendix B.1.

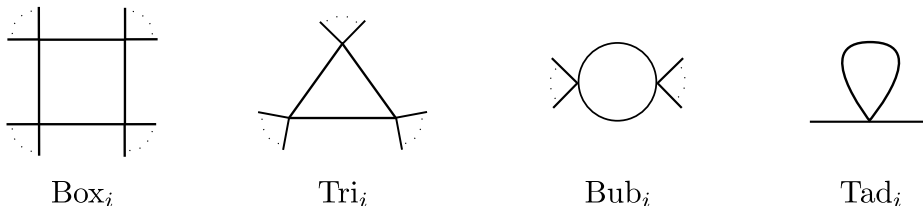


Figure 9: One loop master integrals.

It is worth stressing that I_n is the most generic one-loop integral and can involve non-trivial numerators build out of powers of loop momenta. The final term in expression (2.7.9) denotes rational terms. These, however, cannot be detected by unitarity cuts (as they contain no propagators) and need to be found by alternative methods, some of which we will discuss later in the section. We refer to the part of the quantity where the rational terms have been omitted as *cut constructible*. Hence we have that the cut constructible part of a general n -point one loop amplitude is given by¹⁴

$$\mathcal{A}_n^{(1)} = \sum_i c_{\text{Box}_i} \text{Box}_i + \sum_i c_{\text{Tri}_i} \text{Tri}_i + \sum_i c_{\text{Bub}_i} \text{Bub}_i + \sum_i c_{\text{Tad}_i} \text{Tad}_i. \quad (2.7.10)$$

The generalised unitarity procedure of finding the one-loop integrand is as follows. We first employ the maximal cut, which in this case involves four particles. The only integral topology on the right hand side of (2.7.10) which has enough propagators and hence has a non-vanishing quadruple cut is the box and as such we can isolate and compute its coefficient directly from this cut. Next, we move on to a three-particle cut, which will affect both the box and the triangle – we need to be mindful of possible double counting here and subtract the contribution already known from the higher order cut. Finally we move on to two-particle cut and determine the bubble coefficient, hence fixing the one-loop integrand completely.

¹⁴Note that tadpole integrals can only be defined for massive theories and in our usual case of $\mathcal{N}=4$ SYM do not contribute.

Divergences and regularisation

Once we construct the loop integrand using the generalised unitarity technique, we would like to proceed to evaluation of the integral. For a generic loop integral one may face two types of divergences, referred to as ultraviolet (UV) and infrared (IR) and corresponding to large and small momentum values, respectively.

Formula (2.7.9) tells us that any one-loop integral can be decomposed as a sum of boxes, triangles, bubbles, tadpoles and rational terms. A four-dimensional integral

$$\int d^4l \frac{l^m}{l^n} \quad (2.7.11)$$

is divergent as $l \rightarrow \infty$ if $4+m \geq n$. For scalar integrals $m = 0$ while $n = 2$ for a tadpole and $n = 4$ for a bubble integral. Hence we see that only these two types of scalar integrals are UV-divergent.

IR divergences arise in massless theories for integrals where too many of the propagators go on-shell simultaneously, introducing singularities which cannot be counter-balanced by the integration measure. To see that, let us consider the following one-loop triangle integral in four dimensions:

$$I_3^{1m}(p_1 + p_2) = \int \frac{d^4l}{(2\pi)^4} \frac{1}{l^2(l-p_1)^2(l+p_2)^2}. \quad (2.7.12)$$

In the region where $l^\mu \rightarrow 0$ the integral diverges – we call it the *soft* limit, corresponding to the physical inability to, in case of a massless theory, distinguish a single particle state and the state where it emits many particles with small, undetectable momenta. Moreover, such an integral also diverges in the region where $l^\mu \propto p_1$ *i.e.* the loop momentum becomes parallel to one of the external momenta. We call it the *collinear* limit, again corresponding to the fact that for massless particles it is impossible to distinguish between one and many particles with collinear momenta.

In order to deal with the divergences arising we choose one of the ways to regulate loop integrals, known as *dimensional regularisation* [92].¹⁵ In this scheme we perform integrals in $D = 4 - 2\epsilon$ dimensions, an infinitesimal parameter ϵ away from $D = 4$. The result of the integral is a Laurent series in ϵ and we aim to take the physical limit of $\epsilon \rightarrow 0$ at the end of the calculation, once all of the divergences, corresponding to poles in ϵ , have been cancelled. In our scheme we switch to D dimensions right at the beginning of the calculation but we keep the external states in four dimensions in order to be able to use the powerful spinor-helicity techniques. We refer to this prescription as *four-dimensional helicity scheme* (FDH). We need to be careful not to miss any terms as a result of this replacement, as discussed later on in the section.

¹⁵Other choices, less convenient for the present discussion, include Pauli-Villars regularisation [93] and the method of unitary regulators [94].

Explicit example

Let us briefly illustrate an application of the method of generalised unitarity and our knowledge of divergences on an explicit example of a one-loop amplitude in $\mathcal{N}=4$ SYM. For massless theories, as the ones we are focusing on in the present work, and in dimensional regularisation tadpole integrals do not contribute. Thus we can expand the cut-constructible part of a one-loop amplitude in a massless theory as

$$\mathcal{A}_n^{(1)} = \sum_i c_{\text{Box}_i} \text{Box}_i + \sum_i c_{\text{Tri}_i} \text{Tri}_i + \sum_i c_{\text{Bub}_i} \text{Bub}_i. \quad (2.7.13)$$

The following method has been applied in order to find the integrand of the n -point one-loop MHV amplitude in $\mathcal{N}=4$ SYM in [13, 14]. The first observation is that the theory is UV-finite (since the beta function vanishes to all orders) and therefore the UV-divergent bubbles must be absent from the integrand. Moreover, it has been argued, using string-based method in [13] and unitarity¹⁶ in [95] that triangle integrals do not contribute to the one-loop integrand. This statement is known as *no-triangle* property of $\mathcal{N}=4$ SYM.¹⁷ As a result, the one-loop MHV n -point amplitude can be written simply in terms of scalar box integrals

$$\mathcal{A}_n^{(1)\mathcal{N}=4\text{MHV}} = \sum_i c_{\text{Box}_i} \text{Box}_i. \quad (2.7.14)$$

Explicit evaluation of the maximal cuts with the help of collinear constraints leads to the following MHV result

$$\mathcal{A}_n^{(1)\mathcal{N}=4\text{MHV}} = c_\Gamma \mathcal{A}_n^{(0)\mathcal{N}=4\text{MHV}} \sum_{\text{channels}} F^{2\text{me}}, \quad (2.7.15)$$

where c_Γ is a constant defined in (B.1.5) and $F^{2\text{me}}$ are the so called two-mass easy box functions defined in (B.1.8).

Rational terms

To complete our discussion on generalised unitarity, let us return to the issue of finding possible rational terms, denoted as R in (2.7.9). As already alluded to, the unitarity technique is blind to such terms as they contain no propagators which could be cut as a part of the procedure. In other words, the method can only detect terms in the amplitude which possess discontinuities, such as logarithms, and as a result rational terms, with no discontinuities, are not visible in the procedure.

¹⁶Also for the case of $\mathcal{N}=8$ supergravity.

¹⁷Alternatively, one can show the requirement for triangles to vanish by considering the dual conformal invariance of $\mathcal{N}=4$ SYM. Triangle integrals are not dual conformally invariant and as such cannot contribute.

In all generality, finding rational terms is a difficult problem. Supersymmetry, however, comes to the rescue – it turns out that supersymmetric loop amplitudes contain no rational terms and as such are completely cut constructible [13, 14].

Perhaps more surprisingly, even for pure Yang-Mills theory supersymmetry can lend us an important simplification when it comes to finding the rational terms of certain loop amplitudes. For one-loop amplitude of gluons one makes use of the *supersymmetric decomposition* to write it as

$$\mathcal{A}_{\text{gluon}}^{(1)} = (\mathcal{A}_{\text{gluon}}^{(1)} + 4\mathcal{A}_{\text{fermion}}^{(1)} + 3\mathcal{A}_{\text{scalar}}^{(1)}) - 4(\mathcal{A}_{\text{fermion}}^{(1)} + \mathcal{A}_{\text{scalar}}^{(1)}) + \mathcal{A}_{\text{scalar}}^{(1)}, \quad (2.7.16)$$

where $\mathcal{A}_{\text{fermion}}^{(1)}$ is a one-loop amplitude with the same external states as $\mathcal{A}_{\text{gluon}}^{(1)}$ but with a Weyl fermion running in the loop and similarly for $\mathcal{A}_{\text{scalar}}^{(1)}$, where a complex scalar runs in the loop. The benefit of such seemingly trivial decomposition is that the first term on the right hand side of (2.7.16) corresponds to a complete $\mathcal{N}=4$ SYM multiplet and as a result contains no rational terms. Similarly, the second term is equal to the contribution of (minus four times) a chiral $\mathcal{N}=1$ SYM multiplet¹⁸ and also contains no rational terms as a result. The problem of finding the rational terms localises hence to a single contribution of $\mathcal{A}_{\text{scalar}}^{(1)}$.

The further remarkable simplification arises from the fact that a massless scalar in $D = 4 - 2\epsilon$ dimensions can be described as a massive scalar in four dimensions, which we see by decomposing the $(4 - 2\epsilon)$ -dimensional loop momentum as

$$L^2 = \ell_{(4)}^2 + \ell_{(-2\epsilon)}^2 = \ell_{(4)}^2 - \mu^2, \quad (2.7.17)$$

with the mass μ to be integrated over. Terms involving a power of such “mass” in the integral, in turn, can be mapped to higher-dimensional loop integrals involving a massless scalar. For a mass term of the form $(\mu^2)^m$ the corresponding higher dimension is $4 + 2m - 2\epsilon$. Under such rewriting, and carefully keeping track of all orders of the dimensional regulator ϵ , one finds that it is possible to find the rational terms as they too develop discontinuities [15]. An alternative method, using generalised unitarity modified to $D=4 - 2\epsilon$ dimensions, has been shown to lead to same results for a range of amplitudes [96].

2.8 Two-loop remainder function

The method of generalised unitarity described in Section 2.7 can be applied at higher loop orders. In fact, the main results of this thesis are quantities calculated at two loops with the use of generalised unitarity. As one would expect, things turn considerably

¹⁸Supersymmetric Yang-Mills theories with $\mathcal{N} < 4$ are discussed in detail in Chapter 5.

more complicated with an increase in loop order. For instance, there is no universal basis of two-loop scalar integrals as the one-loop one in (2.7.9) that one can perform unitarity cuts on. Instead, and as we will see in Chapter 4 one constructs an ansatz consisting of integrals suggested by properties such as power-counting of momenta and then uses various cuts to determine the coefficients.

At higher loop orders, in order to strip out as much complexity as possible, it becomes convenient to study a helicity-blind *ratio function* which can be defined for amplitudes at L loops as

$$\mathcal{M}_n^{(L)} = \frac{A_n^{(L)}}{A_n^{(0)}}. \quad (2.8.1)$$

Study of the two-loop four-gluon amplitudes, first calculated in [97], have lead Anastasiou, Bern, Dixon and Kosower (ABDK) [98] to an observation of a possible underlying structure for loop objects. It turns out that the two-loop result can be expressed in terms of the one-loop result, namely

$$\mathcal{M}_4^{(2)\text{MHV}}(\epsilon) = \frac{1}{2} \left(\mathcal{M}_4^{(1)\text{MHV}}(\epsilon) \right)^2 + \mathcal{M}_4^{(1)\text{MHV}}(2\epsilon) f^{(2)}(\epsilon) + C^{(2)} + \mathcal{O}(\epsilon), \quad (2.8.2)$$

where

$$f^{(2)}(\epsilon) = -2 (\zeta_2 + \epsilon \zeta_3 + \epsilon^2 \zeta_4), \quad C^{(2)} = -\zeta_2^2, \quad (2.8.3)$$

and $\zeta_n := \zeta(n)$ is a particular value of the Riemann zeta function. Further study, involving the three-loop four-point superamplitude by Bern, Dixon and Smirnov (BDS) [99] has led to discovery of a similar iterative structure and formulation of the *ABDK/BDS Ansatz* for the full MHV $\mathcal{N}=4$ SYM superamplitude ratio function

$$\mathcal{M}_n^{\text{MHV}}(\epsilon) = \exp \left[\sum_{L=1}^{\infty} \tilde{a}^L \left(f^{(L)}(\epsilon) \mathcal{M}_n^{(1)\text{MHV}}(L\epsilon) + C^{(L)} + \mathcal{O}(\epsilon) \right) \right], \quad (2.8.4)$$

where the function $f^{(L)}(\epsilon)$ is of the form

$$f^{(L)}(\epsilon) = f_0^{(L)} + \epsilon f_1^{(L)} + \epsilon^2 f_2^{(L)}, \quad (2.8.5)$$

and we call the constant $f_0^{(L)}$ the L -loop *cusp anomalous dimension* and $f_1^{(L)}$ the *collinear anomalous dimension*. $C^{(L)}$ is a constant independent of the number of external particles and of ϵ . Finally, \tilde{a} is a function of the 't Hooft coupling defined in (2.4.1),

$$\tilde{a} = \frac{g_{\text{YM}}^2 N e^{-\epsilon \gamma_E}}{(4\pi)^{2-\epsilon}} = a(4\pi e^{-\gamma_E})^\epsilon, \quad (2.8.6)$$

and $\gamma_E \approx 0.577$ is the Euler-Mascheroni constant, grouped here together with the coupling in order to absorb factors arising in the loop integration.

Despite the early success and further verification for two-loop five-point amplitude [100,101], the ABDK/BDS ansatz begins to fail at six points. The discrepancy, however, is by itself very interesting. It turns out that the ansatz reproduces the IR-divergent parts of the six point amplitude correctly and the difference is a finite function of the dual conformal cross-ratios,

$$u_{ijkl} = \frac{x_{ij}^2 x_{kl}^2}{x_{ik}^2 x_{jl}^2}, \quad x_{ab} = x_a - x_b, \quad (2.8.7)$$

where x_a are the region momenta defined in (2.4.36). The explanation for the exact matching between the ABDK/BDS ansatz and four and five point analytic result is credited to the fact that we need at least six momenta to create a non-vanishing dual conformal cross-ratio. In fact, the number of such cross-ratios for n -particle scattering process is $3n-15$,¹⁹ which is non-zero only for $n \geq 6$. It is hence interesting to study the difference between the actual loop amplitude and the ABDK/BDS ansatz prediction – this quantity is referred to as the *remainder function*. At two-loops, which is the order relevant for this thesis, we define the BDS remainder as

$$\mathcal{R}_n^{(2)} := \mathcal{M}_n^{(2)}(\epsilon) - \frac{1}{2}(\mathcal{M}_n^{(1)}(\epsilon))^2 - f^{(2)}(\epsilon) \mathcal{M}_n^{(1)}(2\epsilon) - C^{(2)} + \mathcal{O}(\epsilon), \quad (2.8.8)$$

with $f^{(2)}(\epsilon)$ and $C^{(2)}$ defined in (2.8.5).

The study of the remainder functions is the central topic of this thesis. These are IR finite quantities but nevertheless can be very complicated and involve transcendental functions, which we consider next.

Transcendentality and symbol

The most intuitive notion of a transcendental function is via its “negative” definition: we call a function $F_{(m)}$ *transcendental* if it is not algebraic, *i.e.* it does not satisfy a polynomial equation, meaning it cannot be expressed as a finite sequence of the algebraic operations - addition, multiplication, extraction of a root. Examples include the logarithm to any non-trivial base and the trigonometric functions, defined in terms of an infinite series of their arguments.

More formally, we define a function $F_{(m)}$ of transcendentality degree m as one which can be expressed as a linear combination of m -fold *iterated integrals*:

$$F_{(m)} = \int_a^b d \log f_1 \circ \cdots \circ d \log f_m. \quad (2.8.9)$$

¹⁹15 is the dimension of the conformal group in four dimensions.

Here a and b are rational numbers, f_i are algebraic functions with rational coefficients and we iterate the integrals as follows:

$$\int_a^b d \log f_1 \circ \cdots \circ d \log f_m = \int_t^b \left(\int_a^t d \log f_1 \circ \cdots \circ d \log f_{m-1} \right) d \log f_m(t). \quad (2.8.10)$$

From the definition (2.8.9) it is evident that the logarithm is a transcendental function of degree one but we can quote several further examples. For instance, we define the classical polylogarithm of transcendentality m as

$$\operatorname{Li}_1(x) := -\log(1-x), \quad \operatorname{Li}_m(x) := -\int_0^x d \log(1-t) \circ \underbrace{d \log(t) \circ \cdots \circ d \log(t)}_{m-1 \text{ times}}, \quad (2.8.11)$$

and a more general class of Goncharov polylogarithms [102], also recursively, as

$$G(z) := 1, \quad G(a_k, a_{k-1}, \dots; z) := \int_0^z G(a_{k-1}, \dots; t) d \log(a_1 - t). \quad (2.8.12)$$

In our discussion, apart from the transcendental functions, we will encounter the notion of *transcendental numbers*, defined analogously as numbers which are not algebraic, *i.e.* cannot be found as roots of a non-zero polynomial equation with rational coefficients. Examples of such numbers include π and particular roots of the Riemann zeta function, such as ζ_2 and ζ_4 .

Despite their complicated appearance, polylogarithms enjoy many relations between themselves which get increasingly complex with the degree of transcendentality. For instance, at the simplest transcendentality one we have the very simple relation

$$\log(xy) = \log(x) + \log(y). \quad (2.8.13)$$

Moving on to transcendentality two, we have many identities relating several classical polylogarithms (dilogarithms), such as the famous relation due to Euler

$$\operatorname{Li}_2(z) = -\operatorname{Li}_2(1-z) - \log(1-z) \log(z) + \frac{\pi^2}{6}, \quad (2.8.14)$$

or the more general version of it, known as the “five-term” identity

$$\sum_{n=1}^5 \left[\operatorname{Li}_2(a_n) + \log(a_{n-1}) \log(a_n) \right] = \frac{\pi^2}{6}, \quad (2.8.15)$$

$$a_1 = x, \quad a_2 = \frac{1-x}{1-xy}, \quad a_3 = \frac{1-y}{1-xy}, \quad a_4 = y, \quad a_5 = 1-xy.$$

At higher degree of transcendentality similar, increasingly complex relations appear. We

would like to make use of existence of these complicated relations, possibly without having to resort to huge computational power. This is where the *symbol* of a transcendental function becomes an essential tool.

Given an iterated integral of a form (2.8.9) we define its symbol [103, 104] as an element of an m -fold tensor product of the group of algebraic functions under multiplication, modulo constants:

$$\mathcal{S}(F_{(m)}) = f_1 \otimes \cdots \otimes f_m. \quad (2.8.16)$$

As a consequence of the multiplicative group properties for algebraic functions, the symbol satisfies the following properties:

$$\begin{aligned} f_1 \otimes \cdots \otimes (f_a f_b) \otimes \cdots \otimes f_m &= f_1 \otimes \cdots \otimes f_a \otimes \cdots \otimes f_m + f_1 \otimes \cdots \otimes f_b \otimes \cdots \otimes f_m, \\ f_1 \otimes \cdots \otimes (c f_a) \otimes \cdots \otimes f_m &= f_1 \otimes \cdots \otimes f_a \otimes \cdots \otimes f_m, \end{aligned} \quad (2.8.17)$$

where c is a constant, which in turn implies

$$\begin{aligned} \mathcal{S}(f_a f_b) &= \mathcal{S}(f_a) + \mathcal{S}(f_b), \\ \mathcal{S}(f_a^n) &= n \mathcal{S}(f_a), \\ \mathcal{S}(c f_a) &= \mathcal{S}(f_a). \end{aligned} \quad (2.8.18)$$

A few examples of symbols of functions mentioned earlier on, using definitions (2.8.9) and (2.8.16), are

$$\begin{aligned} \mathcal{S}(\log(x)) &= x, \\ \mathcal{S}(\text{Li}_2(x)) &= -(1-x) \otimes x, \\ \mathcal{S}(\text{Li}_m(x)) &= -(1-x) \underbrace{\otimes x \otimes \cdots \otimes x}_{m-1 \text{ times}}. \end{aligned} \quad (2.8.19)$$

We can immediately see the benefit of taking the symbol of a transcendental function – let us for example consider the identity in (2.8.14) and take the symbol on both sides. We arrive at a rather trivial statement:

$$-(1-z) \otimes z = z \otimes (1-z) - (1-z) \otimes z - z \otimes (1-z). \quad (2.8.20)$$

Hence we see that the complicated-looking identities involving logarithms and polylogarithms can be turned into simple algebraic relations between the terms of the symbol.

A few comments are in order. Firstly, the symbol is blind to some information, specifically constants, such as π . Hence, if we wish to go back and reconstruct the transcendental function from its symbol, we can only do it up to a constant and we may need to use numerical methods in order to fix the “beyond the symbol terms”, depending

on the problem in question. Furthermore, as a result of the aforementioned relations and simplifications, while the symbol of a function is unique, infinitely many functions can lead to the same symbol. In other words, the symbol is an injective, but not a surjective operation. We can think of the symbol as a “fingerprint” of a transcendental function, allowing us to capture its key features but obscuring some of the details.

Nonetheless, the concept of symbol has proved to be of great use in calculations of scattering amplitudes, where the higher-loop results often come in the form of several pages filled with linear combinations of generalised polylogarithms. Most famously, in the pioneering paper [105], Goncharov, Spradlin, Vergu and Volovich turn the seventeen page long result of Del Duca, Duhr and Smirnov [106, 107] for the two-loop six-point MHV amplitude remainder into a one line expression, consisting only of classical polylogarithms. Recent interesting applications of the symbol to the construction of various remainder functions in $\mathcal{N} = 4$ SYM were presented in [108–113]. In this thesis we will use the machinery of the symbol extensively in the proceeding chapters, where we apply it to calculations of two-loop form factors.

2.9 Form factors

In the discussion so far we have mainly focused on the scattering amplitudes of massless particles, *i.e.* purely on-shell quantities. In this section we would like to introduce in more detail the objects that allow us to move one step towards the realm of off-shell objects, such as correlation functions. These are *form factors*, defined in (1.0.7) as an overlap of a on-shell n -particle state with an off-shell state created by an insertion of a local composite operator $\mathcal{O}(x)$ on the vacuum $|0\rangle$,

$$\begin{aligned} F_{\mathcal{O}}(1, \dots, n; q) &= \int d^4x e^{-iqx} \langle 1, \dots, n | \mathcal{O}(x) | 0 \rangle \\ &= \int d^4x e^{-iqx} \langle 1, \dots, n | e^{i\hat{P}\cdot x} \mathcal{O}(0) e^{-i\hat{P}\cdot x} | 0 \rangle \\ &= (2\pi)^4 \delta^{(4)}\left(q - \sum_{i=1}^n p_i\right) \langle 1, \dots, n | \mathcal{O}(0) | 0 \rangle, \end{aligned} \tag{2.9.1}$$

where \hat{P} is the momentum operator, whose eigenstate $\langle 1, \dots, n |$ has eigenvalue $\sum_{i=1}^n p_i$. We call a form factor *minimal* when the number of particles in the external state, n , is the same as the number of fields in the operator. *Subminimal* form factors have less external particles than operator fields and any form factor with more external particles than fields in the operator is referred to as *non-minimal*. Form factors interpolate between on- and off-shell quantities and as such are often referred to as a “bridge” between scattering amplitudes and correlation functions. Apart from the theoretical appeal, form factors are objects of interest from the experimental point of view. One

of such processes is the *Mott scattering*, which describes the probing of the hadronic sub-structure with electrons. Figure 10 shows a schematic representation of a process where the form factor is used to describe the charge distribution within the hadronic structure.

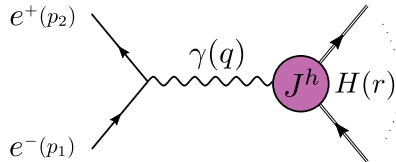


Figure 10: Tree-level Mott scattering probes the hadronic charge distribution.

The operator used to compute the form factor is the hadronic electromagnetic current J_ν^h , and the whole diagram can be calculated as

$$\bar{v}(p_2)(ie\gamma_\mu)u(p_1)\frac{\eta^{\mu\nu}}{q^2}\langle r|J_\nu^h(0)|0\rangle, \quad (2.9.2)$$

where $\langle r|$ is the external hadronic state. Other examples of processes where form factors are measured experimentally include deep inelastic scattering of quarks and the anomalous magnetic moment of the electron. The latter has been calculated at three loops [114, 115] where the authors had to compute and sum over 70 individual complicated three-loop Feynman diagrams. While the numerical values of each of the individual diagrams oscillate heavily, after summation the result turns out to be of $\mathcal{O}(1)$, suggesting, similarly as for the amplitudes, simplicity and existence of underlying structures obstructed by computational inefficiency.

Indeed, all of the techniques reviewed for scattering amplitudes in Sections 2.1-2.8 can be successfully applied to calculations involving form factors. In [24] form factors of the half-BPS operator $\text{Tr}(\phi_{12}^2)$ in $\mathcal{N}=4$ SYM at tree-level and one loop have been calculated using generalised unitarity and extension of BCFW recursion relations to form factors. There it has been found that the expressions for the form factors of this operator with two scalars and an arbitrary number of positive-helicity gluons in the external state share many features with MHV scattering amplitudes. In particular, the tree-level expression is resemblant of the Parke-Taylor amplitude (2.2.5) and reads

$$F_{\text{Tr}(\phi_{12}^2)}^{(0)}(1^+, \dots, i^{\phi^{12}}, \dots, j^{\phi^{12}}, \dots, n^+; q) = g_{\text{YM}}^{n-2}(2\pi)^4\delta^{(4)}\left(\sum_{k=1}^n \lambda_k \tilde{\lambda}_k - q\right) \frac{\langle ij \rangle^2}{\langle 12 \rangle \dots \langle n1 \rangle}. \quad (2.9.3)$$

The one-loop result is equally simple and given by

$$F_{\text{Tr}(\phi_{12}^2)}^{(1)}(1^+, \dots, n^+; q) = F_{\text{Tr}(\phi_{12}^2)}^{(0)}(1^+, \dots, n^+; q) \left[-\sum_{l=1}^n \frac{(-s_{ll+1})^{-\epsilon}}{\epsilon^2} + \sum_{\text{channels}} F^{2\text{me}} \right], \quad (2.9.4)$$

which can be immediately contrasted with the expression for the one-loop MHV amplitude (2.7.15). The novel feature here is the presence of the sum of IR-divergent terms containing two-particle kinematic invariants.

In [25] the investigation into applying on-shell techniques to form factor has been continued and included extension of the method of MHV diagrams as well as recursion relations. Using these methods, the NMHV form factors of $\text{Tr}(\phi_{12}^2)$ have been found. In the same work, the super form factor of the chiral part of the stress-tensor multiplet \mathcal{T}_2 has been studied. It is the simplest composite operator in the $\mathcal{N}=4$ SYM theory which is protected from quantum corrections, does not mix with any other operators and whose form factors hence have only IR divergences. Two components of \mathcal{T}_2 are particularly relevant for the present work: the chiral on-shell Lagrangian [25, 116], $\mathcal{L}_{\text{on-shell}}$, which contains $\text{Tr}(F^2)$, and $\text{Tr}(\phi_{12}^2)$. The extension of supersymmetric Ward identities has been used to constrain the expressions of these form factor, which also turn out to be very simple.

In [30] the authors have extended the study of the form factor of $\text{Tr}(\phi_{12}^2)$ to two loops with the external state $\langle 1^{\phi^{12}}, 2^{\phi^{12}}, 3^+ |$. In QCD, similar quantities have been calculated at one [117] and two loops [51] using Feynman diagrams. As described in Chapter 1, these form factors are phenomenologically important since they are related to the scattering of $H \rightarrow 3$ jets. In order to present the two-loop result efficiently, the two-loop remainder function for the form factor of a generic operator \mathcal{O} was introduced similarly to the amplitude remainder function in (2.8.8)²⁰

$$\mathcal{R}_{\mathcal{O}}^{(2)} := \mathcal{F}_{\mathcal{O}}^{(2)}(\epsilon) - \frac{1}{2}(\mathcal{F}_{\mathcal{O}}^{(1)}(\epsilon))^2 - f^{(2)}(\epsilon) \mathcal{F}_{\mathcal{O}}^{(1)}(2\epsilon) - C^{(2)} + \mathcal{O}(\epsilon), \quad (2.9.5)$$

where, in analogy to definition (2.8.1) we define a helicity-blind ratio function for form factors as $\mathcal{F}_{\mathcal{O}}^{(L)} = F_{\mathcal{O}}^{(L)} / F_{\mathcal{O}}^{(0)}$. The function $f^{(2)}(\epsilon)$ is the same as for amplitudes and the procedure removes the universal IR divergences of the result. In the case of protected operators this gives a finite remainder while in the case of bare, unprotected operators, we are still left with UV divergences. The remainder is constructed such that it has the correct collinear limits, namely $\mathcal{R}_2^{(2)} = 0$ and in the collinear limit $\mathcal{R}_n^{(2)} \rightarrow \mathcal{R}_{n-1}^{(2)}$.

²⁰Form factor remainder is defined for $n \geq 3$ legs. Only Lorentz symmetry and dilatations remain unbroken for form factors, leaving $3n-7$ cross-ratios on which the remainder may depend, compared to $3n-15$ for the amplitude remainder function (2.8.8).

One of the findings of [30] was that the two-loop form factor $\langle 1^{\phi^{12}}, 2^{\phi^{12}}, 3^+ | \text{Tr}(\phi_{12}^2) | 0 \rangle$ is equal to the form factor $\langle 1^-, 2^-, 3^+ | \mathcal{L}_{\text{on-shell}}(0) | 0 \rangle$, up to a universal, helicity-dependent prefactor. The later, however, displays a surprising connection to the quantity calculated in [51] in QCD. In that paper, the two-loop amplitudes for $H \rightarrow ggg$ and $H \rightarrow q\bar{q}g$ were computed in the large top mass limit. As discussed in the introduction, the calculation is equivalent to that of a two-loop form factor of the operator $\text{Tr}(F^2)$, which in turn in $\mathcal{N} = 4$ SYM is contained in the on-shell Lagrangian, $\mathcal{L}_{\text{on-shell}}$. While the full QCD result is very complicated, the remarkable observation is that the maximally transcendental part of the QCD remainder function²¹ is equal to the full two-loop form factor of $\text{Tr}(\phi_{12}^2)$, which by itself is of uniform transcendentality four. This coincidence seems to suggest an appearance of the principle of maximal transcendentality [119, 120] in the context of quantities with non-trivial kinematic dependence. In its original formulation, the principle relates the anomalous dimensions of twist-two operators in $\mathcal{N} = 4$ SYM to those calculated in QCD [121, 122] by simply deleting all terms of less-than-maximal transcendentality degree.

Two-loop form factors of half-BPS operators were further studied in [123] where in particular the minimal form factor of $\text{Tr}(\phi_{12}^3)$ has been found. As we shall see in the forthcoming chapters, this quantity plays a central role in the investigations in this thesis and its very simple remainder function reads

$$\begin{aligned} \mathcal{R}_{\text{BPS}}^{(2)} = & -\frac{3}{2} \text{Li}_4(u) + \frac{3}{4} \text{Li}_4\left(-\frac{uv}{w}\right) - \frac{3}{2} \log(w) \text{Li}_3\left(-\frac{u}{v}\right) + \frac{1}{16} \log^2(u) \log^2(v) \\ & + \frac{\log^2(u)}{32} \left[\log^2(u) - 4 \log(v) \log(w) \right] + \frac{\zeta_2}{8} \log(u) \left[5 \log(u) - 2 \log(v) \right] \\ & + \frac{\zeta_3}{2} \log(u) + \frac{7}{16} \zeta_4 + \text{perms}(u, v, w), \end{aligned} \tag{2.9.6}$$

where $u = s_{12}/q^2$, $v = s_{23}/q^2$, $w = s_{13}/q^2$. The hope is that in analogy with $\text{Tr}(\phi_{12}^2)$ and its appropriate supersymmetric completion \mathcal{T}_2 , form factors of $\text{Tr}(\phi_{12}^3)$ and \mathcal{T}_3 will play a role in computing related quantities in QCD. We invite the reader to explore this possibility in Chapters 3, 4 and 5.

²¹Appropriately translated from the formalism of [118] to the BDS formulation of (2.9.5).

Chapter 3

The $SU(2|3)$ sector form factors

3.1 Introduction

In this chapter we present the results of a preliminary study which has been completed as a prelude to computation of the two-loop form factor of the operator $\text{Tr}(F^3)$ in $\mathcal{N}=4$ SYM. Before embarking on the rather involved calculation of the form factor of $\text{Tr}(F^3)$ with three gluons in the external state we focus on a technically simpler, but equally interesting problem and seek to consider operators which may provide insights into the computation we later perform in Chapter 4. Several length-three operators immediately come to mind as possible candidates, for example the half-BPS operator

$$\mathcal{O}_{\text{BPS}} = \text{Tr}(\phi_{12}^3), \quad (3.1.1)$$

whose form factors have been studied at one and two loops in [26, 123]. However this operator a priori appears to be too simple to draw parallels with our intended calculation of $\text{Tr}(F^3)$. The most important difference is that unlike $\text{Tr}(F^3)$ in QCD, half-BPS operators are protected from quantum corrections as discussed in Section 2.6. The preferred building blocks for our “toy model” operator are scalar fields, as their form factors are the simplest possible. In order to build a non-protected, trilinear operator we need to consider three complex scalar fields, which we choose to be

$$X := \phi_{12}, \quad Y := \phi_{23}, \quad Z := \phi_{31}. \quad (3.1.2)$$

As a first attempt, one can construct and consider the following two operators built out of the three fields

$$\tilde{\mathcal{O}}_{\text{BPS}} := \text{Tr}(X\{Y, Z\}), \quad (3.1.3)$$

$$\mathcal{O}_{\mathcal{B}} := \text{Tr}(X[Y, Z]). \quad (3.1.4)$$

While the first operator is another half-BPS combination,²² it is not the case for the second one as quantum corrections lead to mixing between $\mathcal{O}_{\mathcal{B}}$ and the dimension-three operator,

$$\mathcal{O}_{\mathcal{F}} := \frac{1}{2} \text{Tr}(\psi^\alpha \psi_\alpha), \quad (3.1.5)$$

where we have defined

$$\psi_\alpha := \psi_{123,\alpha}. \quad (3.1.6)$$

The fields $\{X, Y, Z; \psi_\alpha\}$ are the letters of the $SU(2|3)$ sector of $\mathcal{N} = 4$ SYM, which is closed under operator mixing discussed in Section 2.5. Apart from the possible connections to phenomenologically relevant quantities in QCD as described in Chapter 1, there exist several additional reasons to study form factors of operators such as $\mathcal{O}_{\mathcal{B}}$ and $\mathcal{O}_{\mathcal{F}}$.

Firstly, it is very interesting to scan the possible remainders of form factors of wider classes of non-protected operators and compare to results obtained for protected operators and operators belonging to different sectors, such as that presented in (2.9.6) for two-loop minimal form factor remainder function of the operator $\text{Tr}(X^3)$. A key motivation here is to search for regularities and determine universal building blocks in the results that are common to form factors of different operators.

Calculation of the two-loop remainder of the form factor $\langle \bar{X}\bar{Y}\bar{Z} | \mathcal{O}_{\mathcal{B}} | 0 \rangle$ is very instructive with regards to searching for such universality. Indeed, we will show that the remainder function is given by a sum of terms of decreasing transcendentality, where the leading, transcendentality-four term turns out to be identical to the remainder (2.9.6) computed in [123]. Furthermore, the terms of transcendentality ranging from three to zero turn out to be related to certain finite remainder densities introduced in [52] in the study of the dilatation operator in the $SU(2)$ sector.

Secondly, computing loop corrections to form factors of non-protected operators allows us to find the dilatation operator of the sector, as we briefly review next. Complementary approaches based on two-point functions were recently explored in [124–126].

Dilatation operator from form factors

In this chapter we focus on the non-protected, dimension-three operators, the *Bosonic* $\mathcal{O}_{\mathcal{B}}$ defined in (3.1.4) and *Fermionic* $\mathcal{O}_{\mathcal{F}}$ in (3.1.5). All other dimension-three operators in the $SU(2|3)$ sector such as $\text{Tr}(X^3)$, $\text{Tr}(X^2Y)$ and $\tilde{\mathcal{O}}_{\text{BPS}}$ in (3.1.3) are half-BPS and hence do not mix. Therefore $\mathcal{O}_{\mathcal{B}}$ and $\mathcal{O}_{\mathcal{F}}$ are the only two operators which will mix

²²It is symmetric and traceless once written in $SO(6)$ indices, which is sufficient to conclude that it is protected.

under renormalisation in this sector and the bare and renormalised operators can be related as

$$\begin{pmatrix} \mathcal{O}_{\mathcal{F}}^{\text{ren}} \\ \mathcal{O}_{\mathcal{B}}^{\text{ren}} \end{pmatrix} = \begin{pmatrix} \mathcal{Z}_F^F & \mathcal{Z}_F^B \\ \mathcal{Z}_B^F & \mathcal{Z}_B^B \end{pmatrix} \begin{pmatrix} \mathcal{O}_{\mathcal{F}} \\ \mathcal{O}_{\mathcal{B}} \end{pmatrix}. \quad (3.1.7)$$

$\mathcal{O}_{\mathcal{F}}$ and $\mathcal{O}_{\mathcal{B}}$ are the bare operators which we use to compute form factors. The matrix of renormalisation constants \mathcal{Z} , also called the mixing matrix, is universal for the given operators and it has to cancel the UV divergences associated with any gauge-invariant correlation functions, in particular those defining the form factors. As a result, \mathcal{Z} can be determined by requiring the UV-finiteness of the form factors of the renormalised operators $\mathcal{O}_{\mathcal{F}}^{\text{ren}}$ and $\mathcal{O}_{\mathcal{B}}^{\text{ren}}$ with the external states $\langle \bar{\psi}\bar{\psi} |$ and $\langle \bar{X}\bar{Y}\bar{Z} |$. The form factors can be packaged into a matrix, *i.e.*

$$\begin{pmatrix} \langle \bar{\psi}\bar{\psi} | \mathcal{O}_{\mathcal{F}} | 0 \rangle & \langle \bar{X}\bar{Y}\bar{Z} | \mathcal{O}_{\mathcal{F}} | 0 \rangle \\ \langle \bar{\psi}\bar{\psi} | \mathcal{O}_{\mathcal{B}} | 0 \rangle & \langle \bar{X}\bar{Y}\bar{Z} | \mathcal{O}_{\mathcal{B}} | 0 \rangle \end{pmatrix}, \quad (3.1.8)$$

and we determine the entries of the mixing matrix as the UV counterterms, for example

$$\mathcal{Z}_F^F = - \langle \bar{\psi}\bar{\psi} | \mathcal{O}_{\mathcal{F}} | 0 \rangle \Big|_{\text{UV}}. \quad (3.1.9)$$

Note that the four form factors are different in nature: while $\langle \bar{X}\bar{Y}\bar{Z} | \mathcal{O}_{\mathcal{B}} | 0 \rangle$ and $\langle \bar{\psi}\bar{\psi} | \mathcal{O}_{\mathcal{F}} | 0 \rangle$ are minimal, $\langle \bar{\psi}\bar{\psi} | \mathcal{O}_{\mathcal{B}} | 0 \rangle$ is subminimal, and $\langle \bar{X}\bar{Y}\bar{Z} | \mathcal{O}_{\mathcal{F}} | 0 \rangle$ is non-minimal. Furthermore, at loop order up to which we are working the latter two are free from IR divergences as the corresponding tree-level form factors vanish.²³

We can expand the mixing matrix perturbatively as

$$\mathcal{Z} = \mathbb{1} + \delta\mathcal{Z} = \mathbb{1} + \sum_{L=1}^{\infty} \mathcal{Z}^{(L)} := \mathbb{1} + \sum_{L=1}^{\infty} a(\mu_R)^L z^{(L)}, \quad (3.1.10)$$

where $a(\mu_R)$ is the running 't Hooft coupling,

$$a(\mu_R) := \frac{g_{\text{YM}}^2 N e^{-\epsilon\gamma_E}}{(4\pi)^{2-\epsilon}} \left(\frac{\mu_R}{\mu} \right)^{-2\epsilon}, \quad (3.1.11)$$

μ is the dimensional regularisation mass parameter, μ_R is the renormalisation scale, and consider its logarithm, understood as a formal series in powers of $\delta\mathcal{Z}$. Then the quantum correction to the dilatation operator D , denoted by δD , is related to the

²³Discontinuities of subminimal form factors at two loops were computed in [127] in complete generality.

mixing matrix \mathcal{Z} as

$$\delta D = \lim_{\epsilon \rightarrow 0} \left[-\mu_R \frac{\partial}{\partial \mu_R} \log(\mathcal{Z}) \right]. \quad (3.1.12)$$

Hence, computing loop corrections to minimal form factors of non-protected operators will allow us to find the dilatation operator in the $SU(2|3)$ sector, which potentially holds promise for gaining further insights into the integrability of $\mathcal{N} = 4$ SYM. The complete dilatation operator at one loop has recently been computed in [128] and at two loops in the $SU(2)$ sector in [52].

The rest of this chapter is organised as follows. In Sections 3.2 and 3.3 we will derive the form factor $\langle \bar{X}\bar{Y}\bar{Z} | \mathcal{O}_{\mathcal{B}} | 0 \rangle$ at one and two loops, respectively. The two-loop IR-finite (but still UV-divergent) remainder function is then derived in Section 3.4. There we also establish relations of our result to those of [123] and [52] for the maximally and subleading transcendental pieces of the remainder, respectively. In Section 3.5 we compute the subminimal form factor $\langle \bar{X}\bar{Y}\bar{Z} | \mathcal{O}_{\mathcal{F}} | 0 \rangle$ up to one loop, which is sufficient for the computation of the two-loop dilatation operator performed later. Section 3.6 is devoted to computing the subminimal form factor $\langle \bar{\psi}\bar{\psi} | \mathcal{O}_{\mathcal{B}} | 0 \rangle$ at two loops. Using the UV-divergent parts of these form factors, in Section 3.7 we compute the two-loop dilatation operator in the $SU(2|3)$ sector, finding its eigenvectors and corresponding anomalous dimensions up to two loops.

3.2 One-loop minimal form factor $\langle \bar{X}\bar{Y}\bar{Z} | \mathcal{O}_{\mathcal{B}} | 0 \rangle$

In this section we consider form factors of the operator introduced in (3.1.4),

$$\mathcal{O}_{\mathcal{B}} = \text{Tr}(X[Y, Z]),$$

at one loop. We recall that the fields ϕ_{AB} satisfy the reality condition (2.4.3) and therefore

$$\bar{X} = \phi_{34} = \phi^{12}, \quad \bar{Y} = \phi_{14} = \phi^{23}, \quad \bar{Z} = \phi_{24} = \phi^{31}. \quad (3.2.1)$$

Often we will also use the following shorthand notation $\langle \bar{X}\bar{Y}\bar{Z} | := \langle 1^{\phi^{12}} 2^{\phi^{23}} 3^{\phi^{31}} |$ and $\langle \bar{\psi}\bar{\psi} | := \langle 1^{\bar{\psi}^{123}} 2^{\bar{\psi}^{123}} |$. In order to compute the form factor $\langle \bar{X}\bar{Y}\bar{Z} | \mathcal{O}_{\mathcal{B}} | 0 \rangle$ we will make use of the trivial decomposition

$$\mathcal{O}_{\mathcal{B}} = \tilde{\mathcal{O}}_{\text{BPS}} + \mathcal{O}_{\text{offset}}, \quad (3.2.2)$$

where $\tilde{\mathcal{O}}_{\text{BPS}}$ is the half-BPS operator defined in (3.1.3) and

$$\mathcal{O}_{\text{offset}} := -2\text{Tr}(XZY). \quad (3.2.3)$$

This decomposition turns out to be particularly useful as it separates out the contribution of the half-BPS operator $\tilde{\mathcal{O}}_{\text{BPS}}$. Its form factor is identical to that of the half-BPS operator $\text{Tr}(X^3)$ obtained in [26, 123] up to two loops and does not need to be computed again.²⁴ Therefore in what follows we mainly focus on the form factors of the offset operator (3.2.3), from which the result for $\mathcal{O}_{\mathcal{B}}$ can be easily obtained.

3.2.1 Two-particle cut of the one-loop form factor

In the following we denote the L -loop contribution to the form factor $\langle \bar{X}\bar{Y}\bar{Z} | \mathcal{O}_{\text{offset}}(0) | 0 \rangle$ by $F_{\mathcal{O}_{\text{offset}}}^{(L)}(1^{\phi^{12}}, 2^{\phi^{23}}, 3^{\phi^{31}}; q)$. We begin by computing $F_{\mathcal{O}_{\text{offset}}}^{(1)}(1^{\phi^{12}}, 2^{\phi^{23}}, 3^{\phi^{31}}; q)$ using a two-particle cut in the s_{23} -channel as shown in Figure 11. This, plus two cyclic permutations of the external legs, are the only cuts contributing to this form factor.

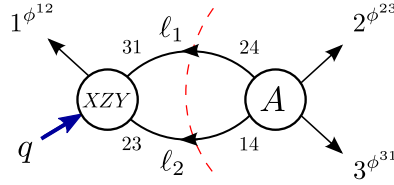


Figure 11: Two-particle cut of the one-loop form factor $F_{\mathcal{O}_{\text{offset}}}^{(1)}(1^{\phi^{12}}, 2^{\phi^{23}}, 3^{\phi^{31}}; q)$. Two more cuts are obtained by cyclically permuting the external legs.

The tree-level amplitude entering the cut is, trivially,²⁵

$$A^{(0)}(2^{\phi^{23}}, 3^{\phi^{31}}, \ell_2^{\phi^{14}}, \ell_1^{\phi^{24}}) = i, \quad (3.2.4)$$

where according to (2.1.8) we have stripped out the factors of the coupling, $(2\pi)^D$ and momentum-conserving $\delta^{(4)}$ and we only keep track of the kinematics and factors of i . The required tree-level form factor is equally simple,

$$F_{\mathcal{O}_{\text{offset}}}^{(0)}(1^{\phi^{12}}, -\ell_1^{\phi^{31}}, -\ell_2^{\phi^{23}}; q) = -2. \quad (3.2.5)$$

As a result, uplifting from the two-particle cut we simply get bubble integrals.²⁶

$$F_{\mathcal{O}_{\text{offset}}}^{(1)}(1^{\phi^{12}}, 2^{\phi^{23}}, 3^{\phi^{31}}; q) = 2i \times \begin{array}{c} q \\ \swarrow \quad \searrow \\ \circ \\ \nwarrow \quad \nearrow \\ 1 \quad 2 \\ \quad 3 \end{array} + \text{cyclic}(1, 2, 3). \quad (3.2.6)$$

²⁴See Section 3.3.3 for a detailed comparison.

²⁵Whenever explicit expressions for tree-level amplitudes are given, these have been obtained with help of the `bcfw.m` `Mathematica` package [129].

²⁶Note that in the pictorial notation we employ in this thesis each line represents a propagator stripped of the factor of i . Such factors of i arising from (cut) propagators are collected separately.

A similar calculation shows that, as anticipated, the one-loop form factor of the operator $\tilde{\mathcal{O}}_{\text{BPS}}$ introduced in (3.1.3) is identical to that of the operator $\text{Tr}(X^3)$ computed in [26]. In order to see that, let us consider the cut diagram for the one-loop form factor $\langle \bar{X}\bar{Y}\bar{Z} | \text{Tr}(XYZ) | 0 \rangle$ in Figure 12.

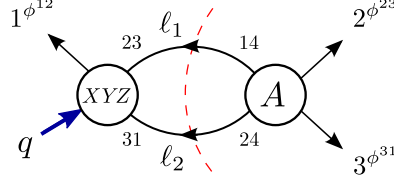


Figure 12: Two-particle cut of the one-loop form factor $F_{\text{Tr}(XYZ)}^{(1)}(1^{\phi^{12}}, 2^{\phi^{23}}, 3^{\phi^{31}}; q)$.

The tree-level amplitude entering the cut is now

$$A^{(0)}(2^{\phi^{23}}, 3^{\phi^{31}}, \ell_2^{\phi^{24}}, \ell_1^{\phi^{14}}) = i \frac{\langle 2\ell_2 \rangle \langle 3\ell_1 \rangle}{\langle 3\ell_2 \rangle \langle \ell_1 2 \rangle} = -i \left(\frac{\langle 23 \rangle \langle \ell_1 \ell_2 \rangle}{\langle 3\ell_2 \rangle \langle \ell_1 2 \rangle} + 1 \right), \quad (3.2.7)$$

where we have made use of the Schouten identity (2.1.21). The required tree-level form factor is again simply

$$F_{\text{Tr}(XYZ)}^{(0)}(1^{\phi^{12}}, -\ell_1^{\phi^{23}}, -\ell_2^{\phi^{31}}; q) = 1, \quad (3.2.8)$$

and hence, if we denote the m -particle cut of an L -loop form factor of an operator \mathcal{O} in a generic P^2 -channel by

$$F_{\mathcal{O}}^{(L)}(\dots; q) \Big|_{m, P^2}, \quad (3.2.9)$$

the one-loop integrand is

$$F_{\text{Tr}(XYZ)}^{(1)}(1^{\phi^{12}}, 2^{\phi^{23}}, 3^{\phi^{31}}; q) \Big|_{2, s_{23}} = -i \left(\frac{\langle 23 \rangle \langle \ell_1 \ell_2 \rangle [\ell_2 3]}{2(p_3 \cdot \ell_2) \langle \ell_1 2 \rangle} + 1 \right) = -i \left(\frac{s_{23}}{2(p_3 \cdot \ell_2)} + 1 \right). \quad (3.2.10)$$

In the second line we have used the overall momentum conservation implying that $\langle \ell_1 \ell_2 \rangle [\ell_2 3] = -\langle \ell_1 2 \rangle [23]$ and as usual we denote $s_{ij} = (p_i + p_j)^2$. Thus, the one-loop form factor of $\text{Tr}(XYZ)$, after uplift from the cut, is

$$F_{\text{Tr}(XYZ)}^{(1)}(1^{\phi^{12}}, 2^{\phi^{23}}, 3^{\phi^{31}}; q) = i \times \text{circle diagram} + i s_{23} \times \text{triangle diagram} + \text{cyclic}(1, 2, 3). \quad (3.2.11)$$

Hence we see that the one-loop form factor of $\tilde{\mathcal{O}}_{\text{BPS}}$, given by the difference of (3.2.11)

and a half of (3.2.6) according to definition (3.1.3) is given by

$$F_{\tilde{\mathcal{O}}_{\text{BPS}}}^{(1)}(1^{\phi^{12}}, 2^{\phi^{23}}, 3^{\phi^{31}}; q) = i s_{23} \times \begin{array}{c} q \nearrow 1 \\ \triangle \\ \searrow 2 \\ \downarrow 3 \end{array} + \text{cyclic}(1, 2, 3), \quad (3.2.12)$$

which precisely agrees with the result in (6.4) of [26], while the one-loop form factor of $\mathcal{O}_{\mathcal{B}}$, given by the sum of form factors of $\tilde{\mathcal{O}}_{\text{BPS}}$ (3.2.12) and $\mathcal{O}_{\text{offset}}$ (3.2.6) is given by

$$F_{\mathcal{O}_{\mathcal{B}}}^{(1)}(1^{\phi^{12}}, 2^{\phi^{23}}, 3^{\phi^{31}}; q) = 2i \times \begin{array}{c} q \nearrow \\ \bigcirc \\ \searrow 2 \\ \downarrow 3 \\ \leftarrow 1 \end{array} + i s_{23} \times \begin{array}{c} q \nearrow 1 \\ \triangle \\ \searrow 2 \\ \downarrow 3 \end{array} + \text{cyclic}(1, 2, 3). \quad (3.2.13)$$

From (3.2.13) we can easily extract the one-loop anomalous dimension of $\mathcal{O}_{\mathcal{B}}$. In order to extract and read off the coefficient of the UV divergence in (3.2.13) we have to remove the IR divergences. This is achieved by simply dropping the purely IR-divergent triangle integrals. Using the expressions for one-loop master integrals in Appendix B.1, we find the UV divergence at the renormalisation scale μ_R to be

$$F_{\mathcal{O}_{\mathcal{B}}}^{(1)} \Big|_{\mu_R, \text{UV}} = -\frac{6}{\epsilon} a(\mu_R). \quad (3.2.14)$$

We can read off the one-loop anomalous dimension using the relation (3.1.12) as

$$\gamma_{\mathcal{O}} = -\mu_R \frac{\partial}{\partial \mu_R} \log(1 + a(\mu_R) z_{\mathcal{O}}^{(1)} + \dots) \Big|_{\epsilon \rightarrow 0},$$

so that at one-loop order

$$\gamma_{\mathcal{O}}^{(1)} = \lim_{\epsilon \rightarrow 0} \left(2\epsilon a(\mu_R) z_{\mathcal{O}}^{(1)} \right) = \lim_{\epsilon \rightarrow 0} \left(2\epsilon \mathcal{Z}_{\mathcal{O}}^{(1)} \right). \quad (3.2.15)$$

where $\mathcal{Z}_{\mathcal{O}}^{(1)} = -F_{\mathcal{O}_{\mathcal{B}}}^{(1)} \Big|_{\mu_R, \text{UV}}$ is the UV counterterm leading to

$$\gamma_{\mathcal{O}}^{(1)} = 12 a, \quad (3.2.16)$$

with a the four-dimensional 't Hooft coupling introduced in (2.4.1). The one-loop anomalous dimension (3.2.16) is in agreement with the known result for the Konishi multiplet [130, 131], where the Konishi operator is defined as

$$\mathcal{O}_{\mathcal{K}} \sim \epsilon_{ABCD} \text{Tr}(\phi^{AB} \phi^{CD}). \quad (3.2.17)$$

This multiplet has been extensively studied in many context [132–134], most recently due to the fact that in the AdS/CFT conjecture it corresponds to the first string level in the spectrum of excitations of type IIB theory around the $AdS_5 \times S^5$ background [135–137]²⁷. In Section 3.7 we will see that once the operator mixing has been resolved, the matching of the one-loop anomalous dimension (3.2.16) with that of the Konishi multiplet turns out to be more than just a simple coincidence.

3.2.2 Auxiliary one-loop form factors needed for two-loop cuts

In this section we discuss two additional one-loop form factors that will be needed as building blocks for the two-particle cuts of the two-loop form factor of $\mathcal{O}_{\text{offset}}$ (and thus \mathcal{O}_B) in Section 3.3.1.

The first form factor we consider is $F_{\mathcal{O}_{\text{offset}}}^{(1)}(1^{\phi^{12}}, 2^{\phi^{31}}, 3^{\phi^{23}}; q)$, where now the ordering of the particles in the state parallels that of the fields in the operator, *i.e.* $-2 \langle \bar{X} \bar{Z} \bar{Y} | \text{Tr}(XZY) | 0 \rangle$. Again a simple two-particle cut is sufficient to determine it, as presented in Figure 13.

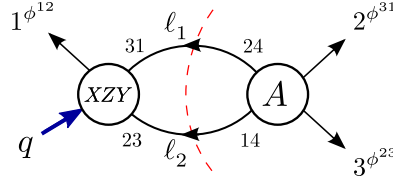


Figure 13: Two-particle cut of the one-loop form factor $F_{\mathcal{O}_{\text{offset}}}^{(1)}(1^{\phi^{12}}, 2^{\phi^{31}}, 3^{\phi^{23}}; q)$.

The amplitude entering the cut is, just as in the case of (3.2.7)

$$A^{(0)}(2^{\phi^{31}}, 3^{\phi^{23}}, \ell_2^{\phi^{14}}, \ell_1^{\phi^{24}}) = i \frac{\langle 2\ell_2 \rangle \langle 3\ell_1 \rangle}{\langle 3\ell_2 \rangle \langle \ell_1 2 \rangle}, \quad (3.2.18)$$

and after similar manipulations, noting that the tree-level form factor is that of (3.2.5) we get

$$F_{\mathcal{O}_{\text{offset}}}^{(1)}(1^{\phi^{12}}, 2^{\phi^{31}}, 3^{\phi^{23}}; q) = -2i \times \text{[circle diagram]} - 2i s_{23} \times \text{[triangle diagram]} + \text{cyclic}(1, 2, 3). \quad (3.2.19)$$

Next we consider the form factors of $\mathcal{O}_{\text{offset}}$ but with a fermionic external state made of excitations ψ^3 and $\bar{\psi}^{123}$, as shown in Figure 14.

²⁷See also [138] for a study of properties of the Konishi multiplet.

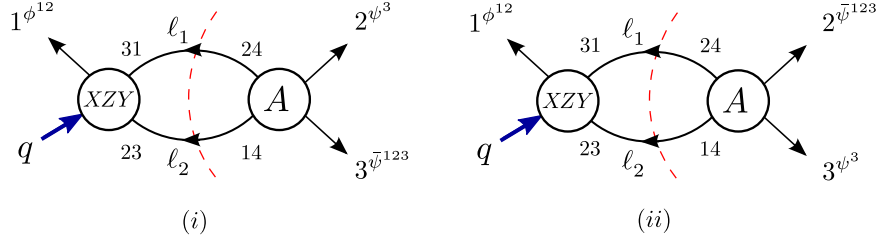


Figure 14: Two-particle cuts of one-loop form factors $F_{\mathcal{O}_{\text{offset}}}^{(1)}(1^{\phi^{12}}, 2^{\psi^3}, 3^{\bar{\psi}^{123}}; q)$ and $F_{\mathcal{O}_{\text{offset}}}^{(1)}(1^{\phi^{12}}, 2^{\bar{\psi}^{123}}, 3^{\psi^3}; q)$.

For the cut presented in Figure 14(i), we have the tree level form factor (3.2.5) and the tree-level amplitude

$$A(2^{\psi^3}, 3^{\bar{\psi}^{123}}, \ell_2^{\phi^{14}}, \ell_1^{\phi^{24}}) = i \frac{\langle 3\ell_1 \rangle}{\langle \ell_1 2 \rangle} = -i \frac{\langle 3|\ell_1|2 \rangle}{2(\ell_1 \cdot p_2)}. \quad (3.2.20)$$

The result for the two-particle cut of this one-loop form factor is then

$$F_{\mathcal{O}_{\text{offset}}}^{(1)}(1^{\phi^{12}}, 2^{\psi^3}, 3^{\bar{\psi}^{123}}; q) \Big|_{2, s_{23}}^{(i)} = -2i [2|\ell_1|3] \times \text{triangle diagram} \quad (3.2.21)$$

For the cut presented in Figure 14(ii), we again have the tree level form factor (3.2.5) and the tree-level amplitude

$$A(2^{\bar{\psi}^{123}}, 3^{\psi^3}, \ell_2^{\phi^{14}}, \ell_1^{\phi^{24}}) = -i \frac{\langle 2\ell_2 \rangle}{\langle 3\ell_2 \rangle} = -i \frac{\langle 2|\ell_2|3 \rangle}{2(\ell_2 \cdot p_3)}. \quad (3.2.22)$$

The result for the two-particle cut of this one-loop form factor is then

$$F_{\mathcal{O}_{\text{offset}}}^{(1)}(1^{\phi^{12}}, 2^{\bar{\psi}^{123}}, 3^{\psi^3}; q) \Big|_{2, s_{23}}^{(ii)} = -2i \langle 2|\ell_2|3 \rangle \times \text{triangle diagram} \quad (3.2.23)$$

Both form factors are expressed in terms of a linear triangle which we refrain from reducing to scalar integrals or uplifting since in later sections we will use this result directly, working at the integrand level. Furthermore, both expressions as they are would vanish upon performing the loop integration. Indeed by Lorentz invariance, after PV reduction one would have *e.g.* for the first form factor $\ell_1 \rightarrow ap_2 + bp_3$, thus $[2|\ell_1|3] \rightarrow 0$ after the reduction. Instead of reducing straight away, we will plug these expressions directly into the two-particle cuts of the two-loop form factors discussed in Section 3.3.1 .

3.3 Two-loop minimal form factor $\langle \bar{X}\bar{Y}\bar{Z} | \mathcal{O}_{\mathcal{B}} | 0 \rangle$

We proceed to compute the minimal form factor of $\mathcal{O}_{\mathcal{B}} = \text{Tr}(X[Y, Z])$ at two loops with the external state $\langle \bar{X}\bar{Y}\bar{Z} |$ following the strategy outlined below:

1. Thanks to the decomposition (3.2.2), we only need to compute the form factor of the operator $\mathcal{O}_{\text{offset}} = -2 \text{Tr}(XZY)$. This will be done using generalised unitarity cuts in Sections 3.3.1 and 3.3.2.
2. We then obtain the form factor of $\mathcal{O}_{\mathcal{B}}$ by adding to the result for $\mathcal{O}_{\text{offset}}$ that of the half-BPS operator $\tilde{\mathcal{O}}_{\text{BPS}} = \text{Tr}(X\{Y, Z\})$. This is identical to the form factor $\langle \bar{X}\bar{X}\bar{X} | \text{Tr}(X^3) | 0 \rangle$ computed in [123] and quoted here for the reader's convenience:

$$\begin{aligned}
 F_{\tilde{\mathcal{O}}_{\text{BPS}}}^{(2)}(1^{\phi^{12}}, 2^{\phi^{23}}, 3^{\phi^{31}}; q) = & -s_{12}s_{3\ell} \text{ (diagram 1)} - s_{23}s_{1\ell} \text{ (diagram 2)} \\
 & - s_{12}^2 \text{ (diagram 3)} - s_{23} \text{ (diagram 4)} + s_{123} \text{ (diagram 5)} + \text{cyclic}(1, 2, 3). \quad (3.3.1)
 \end{aligned}$$

The equivalence of the two-loop form factors of $\tilde{\mathcal{O}}_{\text{BPS}}$ and $\text{Tr}(X^3)$ is verified in Section 3.3.3.

3. In Section 3.3.4 we summarise the complete result for the form factor integrand and perform integral reduction. In doing so, we can proceed to evaluate the integrand using known expressions for two-loop integral functions.

3.3.1 Two-particle cuts of the two-loop form factor

We begin by considering the possible two-particle cuts of the two-loop form factor. There are two types of cuts to consider, which are of the form $F^{(0)} \times A^{(1)}$ and $F^{(1)} \times A^{(0)}$.

Tree-level form factor \times one-loop amplitude

The first two-particle cut we consider is of the form $F^{(0)} \times A^{(1)}$ and we will focus on the s_{23} -channel. The other cuts are obtained by cyclically permuting the external legs.

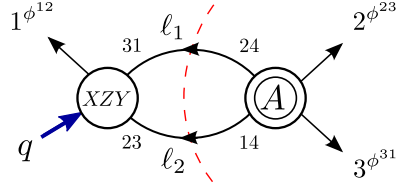


Figure 15: Two-particle cut in the s_{23} -channel contributing to the two-loop form factor $F_{\mathcal{O}_{\text{offset}}}(1^{\phi^{12}}, 2^{\phi^{23}}, 3^{\phi^{31}}; q)$.

In this case the one-loop amplitude is

$$\begin{aligned}
 A^{(1)}(2^{\phi^{23}}, 3^{\phi^{31}}, \ell_2^{\phi^{14}}, \ell_1^{\phi^{24}}) &= A^{(0)}(2^{\phi^{23}}, 3^{\phi^{31}}, \ell_2^{\phi^{14}}, \ell_1^{\phi^{24}}) \left(-s_{2\ell_1} s_{23} \times \begin{array}{c} \ell_1 \rightarrow \quad \rightarrow 2 \\ \square \\ \ell_2 \rightarrow \quad \rightarrow 3 \end{array} \right) \\
 &= -s_{2\ell_1} s_{23} \times \begin{array}{c} \ell_1 \rightarrow \quad \rightarrow 2 \\ \square \\ \ell_2 \rightarrow \quad \rightarrow 3 \end{array}, \quad (3.3.2)
 \end{aligned}$$

hence, after appropriately attaching the tree-level form factor we get the following result for the two-particle cut:

$$F_{\mathcal{O}_{\text{offset}}}^{(2)}(1^{\phi^{12}}, 2^{\phi^{23}}, 3^{\phi^{31}}; q) \Big|_{2, s_{23}} = -2 s_{23} s_{2\ell_1} \times \begin{array}{c} 1 \quad q \\ \diagdown \quad \diagup \\ \ell_2 \quad \ell_1 \\ \square \\ 3 \quad 2 \end{array}. \quad (3.3.3)$$

One-loop form factor \times tree-level amplitude

Next, we consider two-particle cuts of the form $F^{(1)} \times A^{(0)}$. There are two options for the states running in the loop: these can either be scalars, as shown in Figure 16, or fermions, as in Figure 17. We consider these two types of contributions in turn.

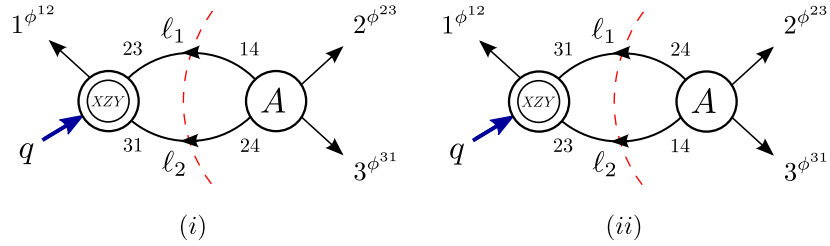


Figure 16: Contribution to the two-loop form factor from scalars running in the loop.

Scalars in the loop

This case is illustrated in Figure 16. The relevant one-loop form factors were calculated in Section 3.2.1 and are given by (3.2.6) for Figure 16(i) and by (3.2.19) for Figure 16(ii), while the tree-level amplitudes entering the cuts are

$$(i) : A^{(0)}(2^{\phi^{23}}, 3^{\phi^{31}}, \ell_2^{\phi^{24}}, \ell_1^{\phi^{14}}) = i \frac{\langle 2\ell_2 \rangle \langle 3\ell_1 \rangle}{\langle 3\ell_2 \rangle \langle \ell_1 2 \rangle} = -i \left(1 + \frac{s_{23}}{2(\ell_1 \cdot p_2)} \right), \quad (3.3.4)$$

$$(ii) : A^{(0)}(2^{\phi^{23}}, 3^{\phi^{31}}, \ell_2^{\phi^{14}}, \ell_1^{\phi^{24}}) = i.$$

This results in the following two-loop form factor cut in the s_{23} -channel:

$$F_{\mathcal{O}_{\text{offset}}}^{(2)}(1^{\phi^{12}}, 2^{\phi^{23}}, 3^{\phi^{31}}; q) \Big|_{2, s_{23}}^{\text{scalars}} = -4 \times \left[\begin{array}{c} \text{Diagram 1} \\ \text{Diagram 2} \end{array} \right] + \left[\begin{array}{c} \text{Diagram 3} \\ \text{Diagram 4} \end{array} \right] - 2 \times \left[\begin{array}{c} \text{Diagram 5} \\ \text{Diagram 6} \end{array} \right] - 2 s_{23} \times \left[\begin{array}{c} \text{Diagram 7} \\ \text{Diagram 8} \\ \text{Diagram 9} \\ \text{Diagram 10} \end{array} \right]. \quad (3.3.5)$$

For a detailed derivation of this integrand see Appendix C.1. Note that all the topologies which have a one-loop sub-amplitude containing triangles or bubbles will have to cancel as a consequence of the amplitude no-triangle theorem as discussed in Section 2.7 – these are the third, sixth and seventh integral in (3.3.5). This cancellation occurs after adding the contribution from fermions running in the loop, which we compute next.

Fermions in the loop

The contribution from fermions in the loop are shown in Figure 17. We use the expres-

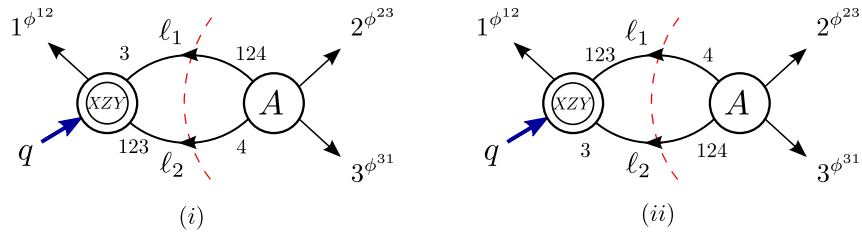


Figure 17: Two-loop form factors with internal fermions. The one-loop form factors on the left-hand-side of the cuts were computed in (3.2.21).

sions for the one-loop form factors given in (3.2.21). The tree-level amplitudes can be graphically represented as:

$$\begin{aligned}
 (i) : A^{(0)}(2^{\phi^{23}}, 3^{\phi^{31}}, \ell_2^{\psi^4}, \ell_1^{\bar{\psi}^{124}}) &= i \frac{\langle \ell_1 3 \rangle}{\langle 3 \ell_2 \rangle} = i \frac{\langle \ell_1 | 3 | \ell_2 \rangle}{2(p_3 \cdot \ell_2)} = i \langle \ell_1 | 3 | \ell_2 \rangle \times \begin{array}{c} \ell_2 \quad \ell_1 \\ \downarrow \quad \downarrow \\ 3 \quad 2 \\ \hline \ell_2 \quad \ell_1 \\ \downarrow \quad \downarrow \\ 3 \quad 2 \end{array}, \\
 (ii) : A^{(0)}(2^{\phi^{23}}, 3^{\phi^{31}}, \ell_2^{\bar{\psi}^{124}}, \ell_1^{\psi^4}) &= i \frac{\langle 2 \ell_2 \rangle}{\langle \ell_1 2 \rangle} = i \frac{[\ell_1 | 2 | \ell_2 \rangle}{2(p_2 \cdot \ell_1)} = i [\ell_1 | 2 | \ell_2 \rangle \times \begin{array}{c} \ell_2 \quad \ell_1 \\ \downarrow \quad \downarrow \\ 3 \quad 2 \\ \hline \ell_2 \quad \ell_1 \\ \downarrow \quad \downarrow \\ 3 \quad 2 \end{array}.
 \end{aligned} \tag{3.3.6}$$

The derivation of the integrand is detailed in Appendix C.1 where we arrive at the result

$$\begin{aligned}
 F_{\mathcal{O}_{\text{offset}}}^{(2)}(1^{\phi^{12}}, 2^{\phi^{23}}, 3^{\phi^{31}}; q) \Big|_{2, s_{23}}^{\text{fermions}} &= 2s_{23} \times \left[\begin{array}{c} q \\ \swarrow \quad \searrow \\ \ell_1 \quad \ell_2 \\ \downarrow \quad \downarrow \\ 2 \quad 3 \end{array} + \begin{array}{c} q \\ \swarrow \quad \searrow \\ \ell_1 \quad \ell_2 \\ \downarrow \quad \downarrow \\ 2 \quad 3 \end{array} \right] \\
 -2s_{23}s_{3l} \times \begin{array}{c} 1 \quad q \\ \swarrow \quad \searrow \\ \ell \quad \ell \\ \downarrow \quad \downarrow \\ \ell_2 \quad \ell_1 \\ \downarrow \quad \downarrow \\ 3 \quad 2 \end{array} - 2 \times \left[\begin{array}{c} q \\ \swarrow \quad \searrow \\ \ell_1 \quad \ell_2 \\ \downarrow \quad \downarrow \\ 2 \quad 3 \end{array} + \begin{array}{c} q \\ \swarrow \quad \searrow \\ \ell_1 \quad \ell_2 \\ \downarrow \quad \downarrow \\ 2 \quad 3 \end{array} \right] + 4 \times \begin{array}{c} q \\ \swarrow \quad \searrow \\ \ell_1 \quad \ell_2 \\ \downarrow \quad \downarrow \\ 2 \quad 3 \end{array}.
 \end{aligned} \tag{3.3.7}$$

It remains to sum up the scalar and fermion contributions to the cut in question, given in (3.3.5) and (3.3.7), respectively.

Result of two-particle cuts

The result of combining the contributions (3.3.5) and (3.3.7) is:

$$\begin{aligned}
 F_{\mathcal{O}_{\text{offset}}}^{(2)}(1^{\phi^{12}}, 2^{\phi^{23}}, 3^{\phi^{31}}; q) \Big|_{2, s_{23}} &= -2s_{23}s_{3l} \times \begin{array}{c} 1 \quad q \\ \swarrow \quad \searrow \\ \ell \quad \ell \\ \downarrow \quad \downarrow \\ \ell_2 \quad \ell_1 \\ \downarrow \quad \downarrow \\ 3 \quad 2 \end{array} + 2s_{1l_2} \times \begin{array}{c} q \\ \swarrow \quad \searrow \\ \ell_1 \quad \ell_2 \\ \downarrow \quad \downarrow \\ 2 \quad 3 \end{array} \\
 + 2s_{1l_1} \times \begin{array}{c} q \\ \swarrow \quad \searrow \\ \ell_1 \quad \ell_2 \\ \downarrow \quad \downarrow \\ 2 \quad 3 \end{array} - 2s_{23} \times \left[\begin{array}{c} 1 \quad q \\ \swarrow \quad \searrow \\ \ell_2 \quad \ell_1 \\ \downarrow \quad \downarrow \\ 3 \quad 2 \end{array} + \begin{array}{c} q \\ \swarrow \quad \searrow \\ \ell_2 \quad \ell_1 \\ \downarrow \quad \downarrow \\ 3 \quad 2 \end{array} \right] \\
 - 2 \times \left[\begin{array}{c} q \\ \swarrow \quad \searrow \\ \ell_1 \quad \ell_2 \\ \downarrow \quad \downarrow \\ 2 \quad 3 \end{array} + \begin{array}{c} q \\ \swarrow \quad \searrow \\ \ell_1 \quad \ell_2 \\ \downarrow \quad \downarrow \\ 2 \quad 3 \end{array} \right] - 4 \times \left[\begin{array}{c} 1 \quad q \\ \swarrow \quad \searrow \\ \ell_2 \quad \ell_1 \\ \downarrow \quad \downarrow \\ 3 \quad 2 \end{array} + \begin{array}{c} q \\ \swarrow \quad \searrow \\ \ell_2 \quad \ell_1 \\ \downarrow \quad \downarrow \\ 3 \quad 2 \end{array} \right].
 \end{aligned} \tag{3.3.8}$$

We observe that the first, second and last integral in (3.3.7) precisely cancel the unwanted contributions in (3.3.5), leaving the result in agreement with the no-triangle property of $\mathcal{N}=4$ SYM, as expected.

Some of the numerators in (3.3.8) are “ambiguous” due to the cut conditions and will need to be confirmed by three-particle cuts. By ambiguity we mean here the fact that for two cut momenta, p_i and p_j , it is impossible to distinguish between their Mandelstam invariant $(p_i + p_j)^2$ and their scalar product $2(p_i \cdot p_j)$. This is due to the fact that the cutting procedure puts the two momenta on shell, $p_{i,j}^2 = 0$. As a result, if a dot product involving these momenta features in the numerator of an integral detected by a cut involving p_i and p_j we must use further cuts, which do not involve simultaneously both momenta p_i and p_j , in order to resolve the ambiguity. In particular, for the second and third integral of (3.3.8), the numerators involve one of the cut legs. We will use further channels where ℓ_2 is not involved in the cut in order to resolve these ambiguities.

3.3.2 Three-particle cuts of the two-loop form factor

In this section we study the three-particle cuts of the form factor of the operator $\mathcal{O}_{\text{offset}}$ defined in (3.2.3) at two loops. This computation will allow us to fix ambiguities of the numerators of integrals obtained from two-particle cuts in (3.3.8) and, in addition, provide additional integrals which have not been detected by two-particle cuts. We consider three-particle cuts in the q^2 -channel first and then proceed to the s_{23} -channel.

Three-particle cuts in the q^2 -channel

We begin by studying the three-particle cuts in the q^2 -channel shown in Figure 18. There are three distinct cuts in this channel, differentiated by the R -symmetry index

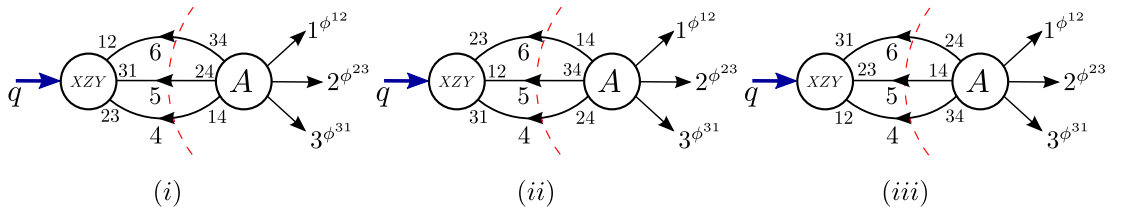


Figure 18: Three-particle cuts of the two-loop form factor of $\mathcal{O}_{\text{offset}}$ in the q^2 -channel.

assignment on the internal legs. The corresponding six-point scalar amplitudes are:

$$\begin{aligned}
 (i) : A^{(0)}(1^{\phi^{12}}, 2^{\phi^{23}}, 3^{\phi^{31}}, 4^{\phi^{14}}, 5^{\phi^{24}}, 6^{\phi^{34}}) &= i \left[\frac{1}{s_{126}} + \frac{1}{s_{234}} - \frac{1}{s_{16}} + \frac{s_{12}}{s_{16}s_{126}} + \frac{s_{56}}{s_{16}s_{234}} \right], \\
 (ii) : A^{(0)}(1^{\phi^{12}}, 2^{\phi^{23}}, 3^{\phi^{31}}, 4^{\phi^{24}}, 5^{\phi^{34}}, 6^{\phi^{14}}) &= i \left[\frac{1}{s_{126}} + \frac{1}{s_{234}} - \frac{1}{s_{34}} + \frac{s_{23}}{s_{34}s_{234}} + \frac{s_{45}}{s_{34}s_{126}} \right], \\
 (iii) : A^{(0)}(1^{\phi^{12}}, 2^{\phi^{23}}, 3^{\phi^{31}}, 4^{\phi^{34}}, 5^{\phi^{14}}, 6^{\phi^{24}}) &= 0,
 \end{aligned} \tag{3.3.9}$$

where to simplify the notation we have denoted the cut legs p_4 , p_5 and p_6 . We can now immediately read off the contribution of the three-particle cut since the tree-level form factor is given by (3.2.5):

$$\begin{aligned}
 F_{\mathcal{O}_{\text{offset}}}^{(2)}(1\phi^{12}, 2\phi^{23}, 3\phi^{31}; q) \Big|_{3, q^2} &= -4 \times \left[\text{Diagram 1} + \text{Diagram 2} \right] \\
 &+ 2 \times \left[\text{Diagram 3} + \text{Diagram 4} \right] - 2s_{23} \times \text{Diagram 5} - 2s_{12} \times \text{Diagram 6} \\
 &- 2s_{1\ell} \times \text{Diagram 7} - 2s_{3\ell} \times \text{Diagram 8} . \tag{3.3.10}
 \end{aligned}$$

Two observations are in order. Firstly, new topologies have appeared, which do not have a two-particle cut - these are the third and fourth integral of (3.3.10). Furthermore, the ambiguities we had found in some of the numerators of topologies identified using two-particle cuts have now been resolved. Namely, in the last two integrals of expression (3.3.10) the previously ambiguous numerator now involves an off-shell leg ℓ .

As a final set of consistency checks and in order to detect any potential topologies the previous cuts might have missed, we now perform additional three-particle cuts in the s_{23} -channel.

Three-particle cuts in the s_{23} -channel

In this cut, the R -symmetry allows for two possibilities for the particles running in the loop, namely two scalars and a gluon, or two fermions and a scalar. Moreover, there are two further distinct cases to consider, namely

$$F^{\overline{\text{MHV}}} \times A^{\text{MHV}} \quad \text{and} \quad F^{\text{MHV}} \times A^{\overline{\text{MHV}}} . \tag{3.3.11}$$

We now study the first case in detail, while the second can be obtained by interchanging $\langle ab \rangle \leftrightarrow -[ab]$ and simply doubles up the contribution from the first case.²⁸ As before, we focus our attention on the operator $\mathcal{O}_{\text{offset}}$ introduced in (3.2.3).

²⁸See Appendix A.3 for action of parity on spinor brackets.

Gluons in the loop

The gluon can be exchanged on any of the three loop legs, as shown in Figure 19.

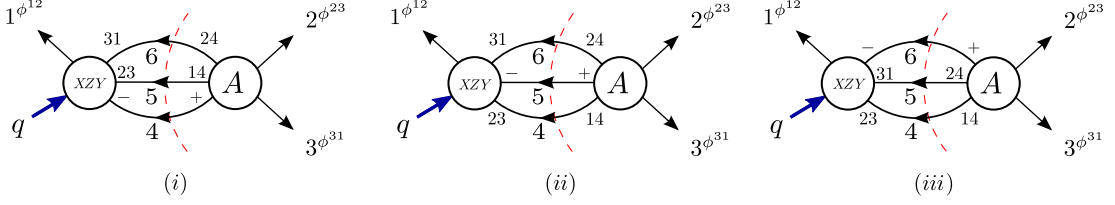


Figure 19: Three cut diagrams for the case of a single gluon running on one of the internal loop legs. There are three more diagrams where the internal gluon has the opposite helicity. These are obtained by parity conjugation of the diagrams in this Figure.

In order to consider such diagrams, we need expressions for the anti-MHV form factors involving both scalars and gluons. We calculate these using the method of MHV diagrams, as introduced in Section 2.3. Details of the computation are presented in Appendix D, where we show that the tree-level non-minimal form factors we need are given by

$$\begin{aligned}
 (i) : F_{\mathcal{O}_{\text{offset}}}^{(0)}(1^{\phi^{12}}, -6^{\phi^{31}}, -5^{\phi^{23}}, -4^-; q) &= 2 \frac{[51]}{[54][41]}, \\
 (ii) : F_{\mathcal{O}_{\text{offset}}}^{(0)}(1^{\phi^{12}}, -6^{\phi^{31}}, -5^-, -4^{\phi^{23}}; q) &= 2 \frac{[64]}{[65][54]}, \\
 (iii) : F_{\mathcal{O}_{\text{offset}}}^{(0)}(1^{\phi^{12}}, -6^-, -5^{\phi^{31}}, -4^{\phi^{23}}; q) &= 2 \frac{[15]}{[16][65]}.
 \end{aligned} \tag{3.3.12}$$

The tree-level amplitudes required for the computation of the cut are given by

$$\begin{aligned}
 (i) : A^{(0)}(2^{\phi^{23}}, 3^{\phi^{31}}, 4^+, 5^{\phi^{14}}, 6^{\phi^{24}}) &= i \frac{\langle 35 \rangle}{\langle 34 \rangle \langle 45 \rangle}, \\
 (ii) : A^{(0)}(2^{\phi^{23}}, 3^{\phi^{31}}, 4^{\phi^{14}}, 5^+, 6^{\phi^{24}}) &= i \frac{\langle 46 \rangle}{\langle 45 \rangle \langle 56 \rangle}, \\
 (iii) : A^{(0)}(2^{\phi^{23}}, 3^{\phi^{31}}, 4^{\phi^{14}}, 5^{\phi^{24}}, 6^+) &= i \frac{\langle 52 \rangle}{\langle 56 \rangle \langle 62 \rangle},
 \end{aligned} \tag{3.3.13}$$

so that multiplying by the form factors (3.3.12) the corresponding integrands are

$$F_{\mathcal{O}_{\text{offset}}}^{(2)}(1^{\phi^{12}}, 2^{\phi^{23}}, 3^{\phi^{31}}; q) \Big|_{3, s_{23}}^{\text{gluons } (i)} = \frac{2 \langle 35 \rangle [51]}{\langle 34 \rangle \langle 45 \rangle [54] [41]}, \tag{3.3.14}$$

$$F_{\mathcal{O}_{\text{offset}}}^{(2)}(1^{\phi^{12}}, 2^{\phi^{23}}, 3^{\phi^{31}}; q) \Big|_{3, s_{23}}^{\text{gluons } (ii)} = \frac{2 \langle 46 \rangle [64]}{\langle 45 \rangle \langle 56 \rangle [65] [54]}, \tag{3.3.15}$$

$$F_{\mathcal{O}_{\text{offset}}}^{(2)}(1^{\phi^{12}}, 2^{\phi^{23}}, 3^{\phi^{31}}; q) \Big|_{3, s_{23}}^{\text{gluons } (iii)} = \frac{2 \langle 25 \rangle [51]}{\langle 56 \rangle \langle 62 \rangle [16] [65]}. \tag{3.3.16}$$

As explained earlier, the other three cases corresponding to the opposite helicity assign-

ment of the gluon with $F^{\text{MHV}} \times A^{\overline{\text{MHV}}}$ are related to those discussed above, $F^{\overline{\text{MHV}}} \times A^{\text{MHV}}$, by simply interchanging $\langle ab \rangle \leftrightarrow -[ab]$.

Fermions in the loop

Next we consider the cut where two of the loop legs are fermionic. There are four diagrams corresponding to the $F^{\overline{\text{MHV}}} \times A^{\text{MHV}}$ case, as shown in Figures 20 and 21.

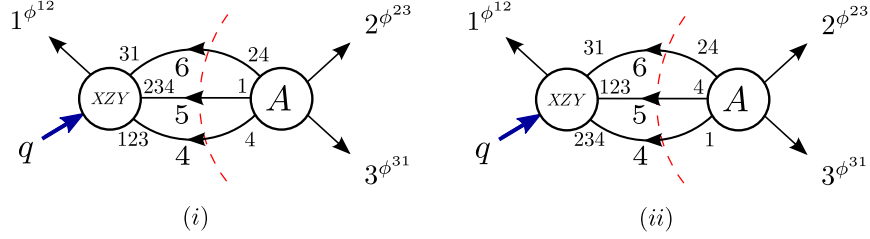


Figure 20: The first two diagrams with fermions in the loop. In our conventions, the Yukawa couplings are of the form, schematically, $\text{Tr}(\psi^A \phi_{AB} \psi^B)$ and $\text{Tr}(\bar{\psi}_A \phi^{AB} \bar{\psi}_B)$, where ϕ_{AB} is related to ϕ^{AB} via (2.4.3).

As before, we use MHV diagrams to find the tree-level form factors and provide details of the computation in Appendix D. These are given by

$$\begin{aligned}
 (i) : F_{\mathcal{O}_{\text{offset}}}^{(0)}(1^{\phi^{12}}, -6^{\phi^{31}}, -5^{\bar{\psi}^{234}}, -4^{\bar{\psi}^{123}}; q) &= \frac{2}{[45]}, \\
 (ii) : F_{\mathcal{O}_{\text{offset}}}^{(0)}(1^{\phi^{12}}, -6^{\phi^{31}}, -5^{\bar{\psi}^{123}}, -4^{\bar{\psi}^{234}}; q) &= \frac{2}{[54]},
 \end{aligned} \tag{3.3.17}$$

while the required amplitudes are

$$\begin{aligned}
 (i) : A^{(0)}(2^{\phi^{23}}, 3^{\phi^{31}}, 4^{\psi^4}, 5^{\psi^1}, 6^{\phi^{24}}) &= i \frac{\langle 35 \rangle \langle 64 \rangle}{\langle 34 \rangle \langle 45 \rangle \langle 56 \rangle}, \\
 (ii) : A^{(0)}(2^{\phi^{23}}, 3^{\phi^{31}}, 4^{\psi^1}, 5^{\psi^4}, 6^{\phi^{24}}) &= i \frac{1}{\langle 45 \rangle},
 \end{aligned} \tag{3.3.18}$$

so that the integrands corresponding to the cuts in Figure 20, taking into account the usual fermion loop minus sign, are

$$F_{\mathcal{O}_{\text{offset}}}^{(2)}(1^{\phi^{12}}, 2^{\phi^{23}}, 3^{\phi^{31}}; q) \Big|_{3, s_{23}}^{\text{fermions } (i)} = \frac{2}{s_{45}} \frac{\langle 35 \rangle \langle 64 \rangle}{\langle 34 \rangle \langle 56 \rangle}, \tag{3.3.19}$$

$$F_{\mathcal{O}_{\text{offset}}}^{(2)}(1^{\phi^{12}}, 2^{\phi^{23}}, 3^{\phi^{31}}; q) \Big|_{3, s_{23}}^{\text{fermions } (ii)} = -\frac{2}{s_{45}}. \tag{3.3.20}$$

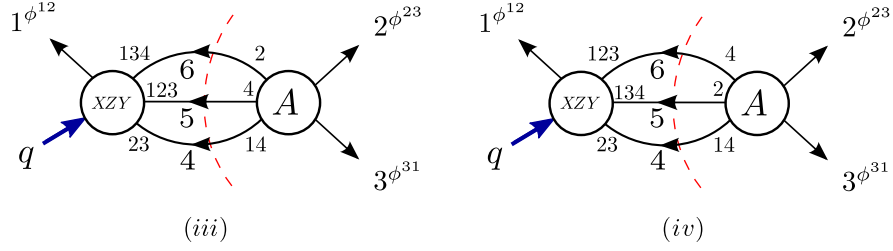


Figure 21: The remaining two diagrams with fermions in the loop.

For the cuts in Figure 21 we have the tree-level form factors

$$\begin{aligned}
 (iii) : F_{\mathcal{O}_{\text{offset}}}^{(0)}(1^{\phi^{12}}, -6^{\bar{\psi}^{134}}, -5^{\bar{\psi}^{123}}, -4^{\phi^{23}}; q) &= \frac{2}{[65]}, \\
 (iv) : F_{\mathcal{O}_{\text{offset}}}^{(0)}(1^{\phi^{12}}, -6^{\bar{\psi}^{123}}, -5^{\bar{\psi}^{134}}, -4^{\phi^{23}}; q) &= \frac{2}{[56]},
 \end{aligned} \tag{3.3.21}$$

and the tree-level amplitudes

$$\begin{aligned}
 (iii) : A^{(0)}(2^{\phi^{23}}, 3^{\phi^{31}}, 4^{\phi^{14}}, 5^{\psi^4}, 6^{\psi^2}) &= i \frac{1}{\langle 56 \rangle}, \\
 (iv) : A^{(0)}(2^{\phi^{23}}, 3^{\phi^{31}}, 4^{\phi^{14}}, 5^{\psi^2}, 6^{\psi^4}) &= i \frac{\langle 25 \rangle \langle 46 \rangle}{\langle 45 \rangle \langle 56 \rangle \langle 62 \rangle},
 \end{aligned} \tag{3.3.22}$$

so that the integrands are

$$F_{\mathcal{O}_{\text{offset}}}^{(2)}(1^{\phi^{12}}, 2^{\phi^{23}}, 3^{\phi^{31}}; q) \Big|_{3, s_{23}}^{\text{fermions (iii)}} = -\frac{2}{s_{56}}, \tag{3.3.23}$$

$$F_{\mathcal{O}_{\text{offset}}}^{(2)}(1^{\phi^{12}}, 2^{\phi^{23}}, 3^{\phi^{31}}; q) \Big|_{3, s_{23}}^{\text{fermions (iv)}} = \frac{2}{s_{56}} \frac{\langle 25 \rangle \langle 46 \rangle}{\langle 45 \rangle \langle 62 \rangle}. \tag{3.3.24}$$

Again, there are four more diagrams corresponding to $F^{\text{MHV}} \times A^{\overline{\text{MHV}}}$ which can be obtained by interchanging $\langle ab \rangle \leftrightarrow -[ab]$.

Combining the terms

We can now convert the integrands into traces and expand them into dot products. In doing so, it is useful to notice that the following combination of integrands is particularly simple:

$$(3.3.14) + (3.3.19) + (3.3.20) + \frac{1}{2}(3.3.15) = \frac{s_{1\ell}}{s_{45}s_{14}} + \frac{s_{13}}{s_{34}s_{14}} - \frac{1}{s_{45}} - \frac{s_{23}s_{26}}{s_{34}s_{45}s_{56}} - \frac{1}{s_{14}}, \tag{3.3.25}$$

where we denote $\ell = -p_4 - p_5$. The corresponding integrals are shown in (3.3.26) below. In uplifting the cut expression, we have to pay close attention to the momentum flow: for example, in the expression above $1/s_{14} = 1/[2(p_1 \cdot p_4)]$ should be uplifted to the prop-

agator $-1/(p_1 - p_4)^2$ since p_1 and p_4 flow in the same direction (see Figure 20). Keeping these additional signs in mind we arrive at the the following combination of integrals:

$$-s_{1l} \times \text{triangle}(l) - s_{13} \times \text{bubble}(q) - s_{23}s_{26} \times \text{bubble}(q) - s_{23}s_{26} \times \text{triangle}(q) + \text{triangle}(q) \quad (3.3.26)$$

Similarly, we can single out the following combination

$$(3.3.16) + (3.3.23) + (3.3.24) + \frac{1}{2}(3.3.15) = \frac{s_{1l}}{s_{56}s_{16}} + \frac{s_{12}}{s_{16}s_{26}} - \frac{1}{s_{56}} - \frac{s_{23}s_{34}}{s_{45}s_{56}s_{26}} - \frac{1}{s_{16}}, \quad (3.3.27)$$

where now we denote $\ell = -p_5 - p_6$. This leads to the combination of integrals shown below,

$$-s_{1l} \times \text{triangle}(l) - s_{12} \times \text{bubble}(q) - s_{23}s_{34} \times \text{bubble}(q) - s_{23}s_{34} \times \text{triangle}(q) + 4s_{23}s_{34} \times \text{triangle}(q) \quad (3.3.28)$$

The complete contribution of the three-particle cut in the s_{23} -channel is then obtained by adding (3.3.26) and (3.3.28) and multiplying the result by two to take into account the second helicity configuration corresponding to $F^{\text{MHV}} \times A^{\overline{\text{MHV}}}$. Before we proceed to presenting the full two-loop integrand and evaluating the remainder function, we remind the reader that so far we have only been considering the operator $\mathcal{O}_{\text{offset}}$ and that according to (3.2.2),

$$\mathcal{O}_{\mathcal{B}} = \tilde{\mathcal{O}}_{\text{BPS}} + \mathcal{O}_{\text{offset}}.$$

In the next section, we turn our attention on $\tilde{\mathcal{O}}_{\text{BPS}}$ and show with explicit computation that the minimal two-loop form factor of this half-BPS operator indeed has the same integrand as that of the minimal form factor of $\text{Tr}(X^3)$ considered in [123].

3.3.3 Comparing the half-BPS form factors

We proceed to find the integrand for the two-loop form factor of $\tilde{\mathcal{O}}_{\text{BPS}}$, where we will again use the trivial decomposition of (3.2.2) in order to write

$$\tilde{\mathcal{O}}_{\text{BPS}} = \text{Tr}(XYZ) - \frac{1}{2}\mathcal{O}_{\text{offset}}. \quad (3.3.29)$$

Since we already know the integrand for $\mathcal{O}_{\text{offset}}$, we begin by considering the three diagrams in the gluonic contribution to the s_{23} -channel, presented in Figure 22 below and corresponding to the $\text{Tr}(XYZ)$ operator.

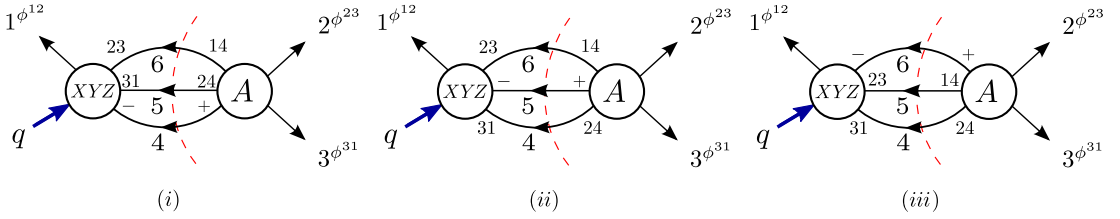


Figure 22: Three possibilities for a single gluon running on one of the internal loop legs for the s_{23} -channel cut of the two-loop form factor of the $\text{Tr}(XYZ)$ operator.

The tree-level amplitudes required for the computation of the cut are given by

$$\begin{aligned} (i) : \quad & A^{(0)}(2^{\phi^{23}}, 3^{\phi^{31}}, 4^+, 5^{\phi^{24}}, 6^{\phi^{14}}) = -i \frac{\langle 25 \rangle \langle 36 \rangle}{\langle 34 \rangle \langle 45 \rangle \langle 62 \rangle}, \\ (ii) : \quad & A^{(0)}(2^{\phi^{23}}, 3^{\phi^{31}}, 4^{\phi^{24}}, 5^+, 6^{\phi^{14}}) = -i \frac{\langle 24 \rangle \langle 36 \rangle \langle 46 \rangle}{\langle 34 \rangle \langle 45 \rangle \langle 56 \rangle \langle 62 \rangle}, \\ (iii) : \quad & A^{(0)}(2^{\phi^{23}}, 3^{\phi^{31}}, 4^{\phi^{24}}, 5^{\phi^{14}}, 6^+) = -i \frac{\langle 24 \rangle \langle 35 \rangle}{\langle 34 \rangle \langle 56 \rangle \langle 62 \rangle}, \end{aligned} \quad (3.3.30)$$

and the non-minimal tree-level form factors, derived in detail in Appendix D,²⁹ are

$$\begin{aligned} (i) : \quad & F_{\text{Tr}(XYZ)}^{(0)}(1^{\phi^{12}}, -6^{\phi^{23}}, -5^{\phi^{31}}, -4^-; q) = \frac{[51]}{[54][41]}, \\ (ii) : \quad & F_{\text{Tr}(XYZ)}^{(0)}(1^{\phi^{12}}, -6^{\phi^{23}}, -5^-, -4^{\phi^{31}}; q) = \frac{[64]}{[54][65]}, \\ (iii) : \quad & F_{\text{Tr}(XYZ)}^{(0)}(1^{\phi^{12}}, -6^-, -5^{\phi^{23}}, -4^{\phi^{33}}; q) = \frac{[15]}{[16][65]}. \end{aligned} \quad (3.3.31)$$

such that the corresponding integrands are

$$F_{\text{Tr}(XYZ)}^{(2)}(1^{\phi^{12}}, 2^{\phi^{23}}, 3^{\phi^{31}}; q) \Big|_{3, s_{23}}^{\text{gluons } (i)} = \frac{\langle 25 \rangle \langle 36 \rangle [15]}{\langle 34 \rangle \langle 45 \rangle \langle 62 \rangle [54][41]}, \quad (3.3.32)$$

$$F_{\text{Tr}(XYZ)}^{(2)}(1^{\phi^{12}}, 2^{\phi^{23}}, 3^{\phi^{31}}; q) \Big|_{3, s_{23}}^{\text{gluons } (ii)} = \frac{\langle 24 \rangle \langle 36 \rangle \langle 46 \rangle [46]}{\langle 34 \rangle \langle 45 \rangle \langle 56 \rangle \langle 62 \rangle [54][65]}, \quad (3.3.33)$$

²⁹Note that these are the same as the tree-level non-minimal form factors of $\mathcal{O}_{\text{offset}}$ in (3.3.39) except for the numerical constant arising from the definition of the operator.

$$F_{\text{Tr}(XYZ)}^{(2)}(1^{\phi^{12}}, 2^{\phi^{23}}, 3^{\phi^{31}}; q) \Big|_{3, s_{23}}^{\text{gluons}(iii)} = \frac{\langle 24 \rangle \langle 35 \rangle [51]}{\langle 34 \rangle \langle 56 \rangle \langle 62 \rangle [16] [65]}. \quad (3.3.34)$$

We refrain from manipulating these integrands further and instead combine them into “anti-commutator” pieces according to (3.3.29) by appropriately adding to them $-1/2$ of the terms that appear in expressions (3.3.14)–(3.3.16), corresponding to the $\text{Tr}(XZY)$ operator. We then find for the diagrams in Figure 19(i) and 22(i),

$$AC_1 := (3.3.32) - \frac{1}{2}(3.3.14) = -\frac{(\langle 25 \rangle \langle 36 \rangle + \langle 35 \rangle \langle 62 \rangle) [51]}{\langle 34 \rangle \langle 45 \rangle \langle 62 \rangle [54] [41]} = -\frac{\langle 23 \rangle \langle 56 \rangle [51]}{\langle 34 \rangle \langle 45 \rangle \langle 62 \rangle [54] [41]}, \quad (3.3.35)$$

where we have used the Schouten identity (2.1.21). Similarly, we find for the diagrams in Figure 19(ii) and 22(ii),

$$AC_2 := (3.3.33) - \frac{1}{2}(3.3.15) = -\frac{\langle 23 \rangle \langle 46 \rangle^2 [64]}{\langle 34 \rangle \langle 45 \rangle \langle 56 \rangle \langle 62 \rangle [54] [65]}, \quad (3.3.36)$$

and finally, for the integrands of Figure 19(iii) and 22(iii),

$$AC_3 := (3.3.34) - \frac{1}{2}(3.3.16) = -\frac{\langle 23 \rangle \langle 45 \rangle [15]}{\langle 34 \rangle \langle 56 \rangle \langle 62 \rangle [16] [65]}. \quad (3.3.37)$$

Next we consider the fermionic contributions to this cut for the operator $\text{Tr}(XYZ)$. These are presented in Figure 23 below.

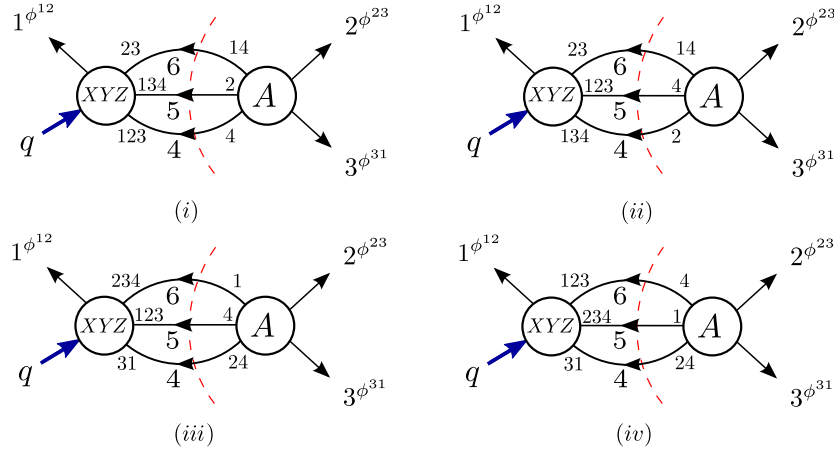


Figure 23: Four possibilities for fermions running on the internal loop legs for the $\text{Tr}(XYZ)$ operator.

The tree-level amplitudes are given by

$$\begin{aligned}
 (i) : A^{(0)}(2^{\phi^{23}}, 3^{\phi^{31}}, 4^{\psi^4}, 5^{\psi^2}, 6^{\phi^{14}}) &= -i \frac{\langle 25 \rangle \langle 46 \rangle \langle 36 \rangle}{\langle 34 \rangle \langle 45 \rangle \langle 56 \rangle \langle 62 \rangle}, \\
 (ii) : A^{(0)}(2^{\phi^{23}}, 3^{\phi^{31}}, 4^{\psi^2}, 5^{\psi^4}, 6^{\phi^{14}}) &= -i \frac{\langle 24 \rangle \langle 63 \rangle}{\langle 34 \rangle \langle 45 \rangle \langle 62 \rangle}, \\
 (iii) : A^{(0)}(2^{\phi^{23}}, 3^{\phi^{31}}, 4^{\phi^{24}}, 5^{\psi^4}, 6^{\psi^1}) &= -i \frac{\langle 24 \rangle \langle 63 \rangle}{\langle 34 \rangle \langle 56 \rangle \langle 62 \rangle}, \\
 (iv) : A^{(0)}(2^{\phi^{23}}, 3^{\phi^{31}}, 4^{\phi^{24}}, 5^{\psi^1}, 6^{\psi^4}) &= -i \frac{\langle 24 \rangle \langle 35 \rangle \langle 46 \rangle}{\langle 34 \rangle \langle 45 \rangle \langle 56 \rangle \langle 62 \rangle},
 \end{aligned} \tag{3.3.38}$$

and the non-minimal tree-level form factors are

$$\begin{aligned}
 (i) : F_{\text{Tr}(XYZ)}^{(0)}(1^{\phi^{12}}, -6^{\phi^{23}}, -5^{\bar{\psi}^{134}}, -4^{\bar{\psi}^{123}}; q) &= \frac{1}{[54]}, \\
 (ii) : F_{\text{Tr}(XYZ)}^{(0)}(1^{\phi^{12}}, -6^{\phi^{23}}, -5^{\bar{\psi}^{123}}, -4^{\bar{\psi}^{134}}; q) &= \frac{1}{[45]}, \\
 (iii) : F_{\text{Tr}(XYZ)}^{(0)}(1^{\phi^{12}}, -6^{\bar{\psi}^{234}}, -5^{\bar{\psi}^{123}}, -4^{\phi^{31}}; q) &= \frac{1}{[56]}, \\
 (iv) : F_{\text{Tr}(XYZ)}^{(0)}(1^{\phi^{12}}, -6^{\bar{\psi}^{123}}, -5^{\bar{\psi}^{234}}, -4^{\phi^{31}}; q) &= \frac{1}{[65]},
 \end{aligned} \tag{3.3.39}$$

such that the corresponding integrands are

$$F_{\text{Tr}(XYZ)}^{(2)}(1^{\phi^{12}}, 2^{\phi^{23}}, 3^{\phi^{31}}; q) \Big|_{3, s_{23}}^{\text{fermions}^{(i)}} = \frac{\langle 25 \rangle \langle 46 \rangle \langle 36 \rangle}{\langle 34 \rangle \langle 56 \rangle \langle 62 \rangle s_{45}}, \tag{3.3.40}$$

$$F_{\text{Tr}(XYZ)}^{(2)}(1^{\phi^{12}}, 2^{\phi^{23}}, 3^{\phi^{31}}; q) \Big|_{3, s_{23}}^{\text{fermions}^{(ii)}} = \frac{\langle 24 \rangle \langle 36 \rangle}{\langle 34 \rangle \langle 62 \rangle s_{45}}, \tag{3.3.41}$$

$$F_{\text{Tr}(XYZ)}^{(2)}(1^{\phi^{12}}, 2^{\phi^{23}}, 3^{\phi^{31}}; q) \Big|_{3, s_{23}}^{\text{fermions}^{(iii)}} = \frac{\langle 36 \rangle \langle 24 \rangle}{\langle 34 \rangle \langle 62 \rangle s_{56}}, \tag{3.3.42}$$

$$F_{\text{Tr}(XYZ)}^{(2)}(1^{\phi^{12}}, 2^{\phi^{23}}, 3^{\phi^{31}}; q) \Big|_{3, s_{23}}^{\text{fermions}^{(iv)}} = \frac{\langle 24 \rangle \langle 35 \rangle \langle 46 \rangle}{\langle 34 \rangle \langle 62 \rangle \langle 45 \rangle s_{56}}. \tag{3.3.43}$$

We combine them similarly to the gluonic case and after some algebra we find, for Figure 20 plus Figure 23(i) and (ii),

$$\begin{aligned}
 AC_4 &:= (3.3.40) + (3.3.41) - \frac{1}{2}(3.3.19) - \frac{1}{2}(3.3.20) \\
 &= \frac{1}{\langle 34 \rangle \langle 56 \rangle \langle 62 \rangle s_{45}} \left(\langle 25 \rangle \langle 36 \rangle \langle 46 \rangle - \langle 36 \rangle \langle 42 \rangle \langle 56 \rangle - \langle 26 \rangle \langle 35 \rangle \langle 46 \rangle + \langle 34 \rangle \langle 56 \rangle \langle 62 \rangle \right) \\
 &= -\frac{\langle 23 \rangle}{\langle 34 \rangle \langle 45 \rangle \langle 56 \rangle \langle 62 \rangle} \frac{2 \langle 46 \rangle \langle 65 \rangle}{[54]},
 \end{aligned} \tag{3.3.44}$$

and for Figure 21 plus Figure 23(*iii*) and (*iv*),

$$\begin{aligned}
 AC_5 &:= (3.3.42) + (3.3.43) - \frac{1}{2}(3.3.23) - \frac{1}{2}(3.3.24) \\
 &= -\frac{1}{\langle 34 \rangle \langle 45 \rangle \langle 62 \rangle_{s_{56}}} \left(\langle 36 \rangle \langle 42 \rangle \langle 45 \rangle - \langle 24 \rangle \langle 35 \rangle \langle 46 \rangle + \langle 25 \rangle \langle 46 \rangle \langle 34 \rangle - \langle 34 \rangle \langle 45 \rangle \langle 62 \rangle \right) \\
 &= -\frac{\langle 23 \rangle}{\langle 34 \rangle \langle 45 \rangle \langle 56 \rangle \langle 62 \rangle} \frac{2 \langle 45 \rangle \langle 64 \rangle}{[65]}. \tag{3.3.45}
 \end{aligned}$$

Finally we combine all the “anti-commutator” terms to get

$$\begin{aligned}
 \sum_{i=1}^5 AC_i &= \frac{\langle 23 \rangle}{\langle 34 \rangle \langle 45 \rangle \langle 56 \rangle \langle 62 \rangle} \left(\frac{[51] \langle 54 \rangle^2}{[65][16]} - 2 \frac{\langle 54 \rangle \langle 64 \rangle}{[65]} + \frac{[16] \langle 64 \rangle^2}{[65][51]} \right. \\
 &\quad \left. - \frac{[14] \langle 46 \rangle^2}{[45][51]} + 2 \frac{\langle 46 \rangle \langle 56 \rangle}{[45]} - \frac{[51] \langle 56 \rangle^2}{[45][14]} \right), \tag{3.3.46}
 \end{aligned}$$

where again we have used the Schouten identity (2.1.21) to recast

$$-\frac{\langle 46 \rangle^2 [64]}{[54][65]} = \frac{[16] \langle 46 \rangle^2}{[65][51]} - \frac{[14] \langle 46 \rangle^2}{[45][51]}. \tag{3.3.47}$$

(3.3.46) is precisely the result of the s_{23} -channel cut of the two-loop form factor of the operator $\text{Tr}(X^3)$, as presented in (3.16) of [123]. The integrand, corresponding to this result (plus its parity conjugate) has been quoted in (3.3.1) and hence we can add it directly for our answer for the form factor of $\mathcal{O}_{\mathcal{B}}$, in agreement with decomposition (3.2.2). We proceed to do so in the next section, where we present the full two-loop integrand and perform the integration.

3.3.4 Summary and integral reduction

We now summarise the result of our calculation and present the result for the two-loop form factor integrand of $\mathcal{O}_{\mathcal{B}} = \text{Tr}(X[Y, Z])$ which includes the half-BPS contribution from $\tilde{\mathcal{O}}_{\text{BPS}} = \text{Tr}(X\{Y, Z\})$ computed in [123] and quoted in (3.3.1). The list of integrals needed for the result is shown in Table 6.

The two-loop minimal form factor of $\mathcal{O}_{\mathcal{B}}$ is given by

$$\begin{aligned}
 F_{\mathcal{O}_{\mathcal{B}}}^{(2)}(1^{\phi^{12}}, 2^{\phi^{23}}, 3^{\phi^{31}}; q) &= -s_{12}s_{3\ell} I_1 - s_{23}s_{1\ell} I_2 - s_{12}^2 I_3 - s_{23} I_4 + s_{123} I_5 \\
 &\quad - 2 \times \left[s_{12}s_{2\ell} I_6 + s_{23} I_7 + s_{12} I_8 + s_{3\ell} I_9 + s_{1\ell} I_{10} \right. \\
 &\quad \left. - I_{11} - I_{12} + I_{13} + I_{14} \right] - 4 \times \left[I_{15} + I_{16} \right] + \text{cyclic}(1, 2, 3), \tag{3.3.48}
 \end{aligned}$$

Some of the integrals appearing in (3.3.48), in particular I_i for $i = \{3, 5, 7, 8, 15, 16\}$,

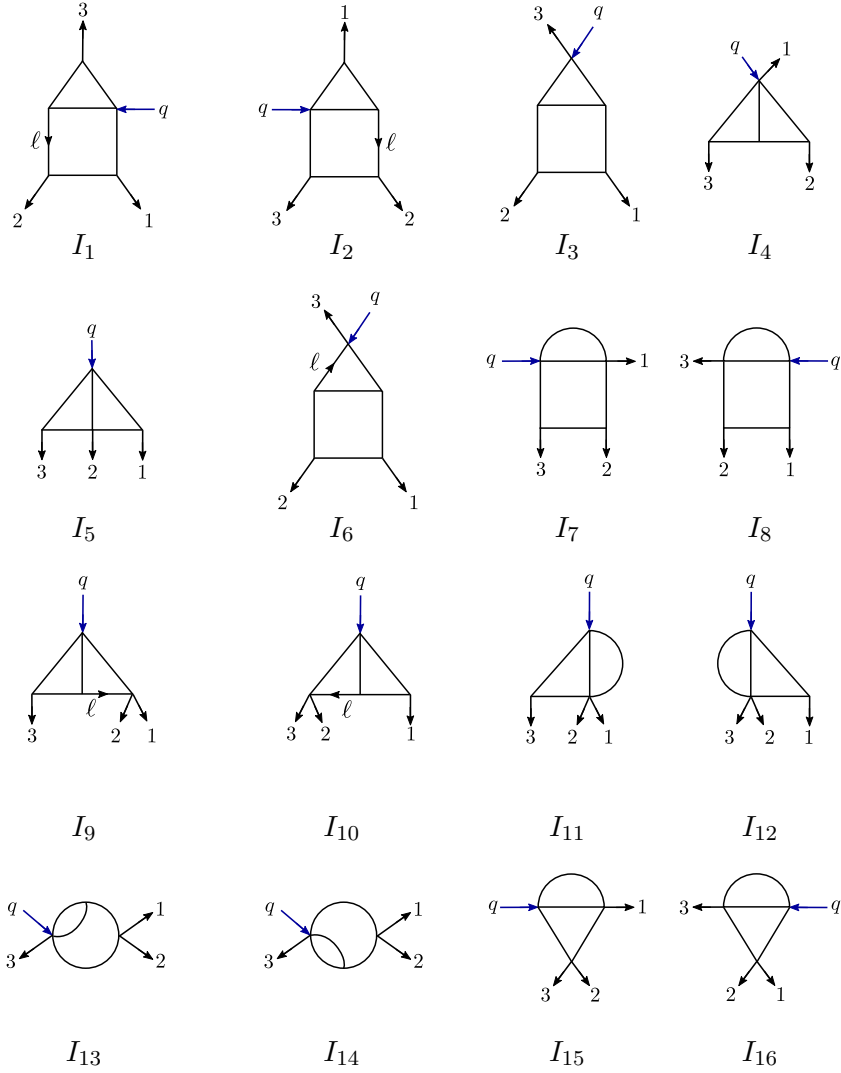


Table 3: Integrals for the two-loop form factor $F_{\mathbb{C}\mathbb{P}^2}^{(2)}(1^{\phi^{12}}, 2^{\phi^{23}}, 3^{\phi^{31}}; q)$. Note that the integrals $\{I_1, \dots, I_5\}$ correspond precisely to the BPS case, shown in Eq. (3.25) of [123].

are two-loop master integrals and we can proceed to substitute their expressions from [139, 140]. The remaining ones will be reduced using an integration-by-parts procedure implemented in the `Mathematica` package `LiteRed` [141, 142].

Integral reduction with LiteRed

The package is an extremely efficient tool for fast reduction of multi-loop integrals to a basis of master integral topologies, using integration-by-parts (IBP) identities. It is not strictly a reduction algorithm, in a sense that unlike the approach taken by alternative popular packages, *e.g.* `FIRE` [143] or `Reduze` [144], it does not rely on the very successful but computationally inefficient Laporta algorithm [145]. Instead, the heuristic approach is taken where symbolic reduction rules are generated at the initial

stages of computation, thus drastically decreasing the processing time but not always guaranteeing a successful outcome. For our practical purposes, the package worked extremely well – this is partially due to the fact that for a two-loop integral depending on three external momenta there exists a very limited number of multi-particle invariants we can build numerators out of. In particular, for an L -loop integral with E independent external momenta there are $N = L(L + 1)/2 + LE$ invariants involving loop momentum (nine in our case). Out of those, $M = E + 3L - 2$ (seven for our case) are inverse propagators, which, if present in the numerator, lead to a cancellation of a propagator and a smaller integral topology. The remaining $N - M$ (two) invariants are the so-called irreducible numerators. Since any multi-particle invariant can be rewritten as a linear combination of the N invariants (plus three involving external momenta only), the problem centres around integral topologies with irreducible numerators. For those, all IBPs are generated, any resultant scaleless integrals are rejected and further symmetry relations are utilised until the result is given in terms of known master integrals.

For the integrals listed in (3.3.48), using `LiteRed` we find the following reductions:

$$\begin{aligned}
 s_{12}s_{2\ell} \int \text{diagram} &= \frac{4(\epsilon - 1)(3\epsilon - 2)(3\epsilon - 1)}{s_{12} \epsilon^2 (2\epsilon - 1)} \int \text{diagram} \\
 &\quad - \frac{2(3\epsilon - 1)}{\epsilon} \int \text{diagram} - \frac{2(\epsilon - 1)}{\epsilon} \int \text{diagram}, \\
 s_{1\ell} \int \text{diagram} &= \frac{(3\epsilon - 2)[s_{12}\epsilon + (2\epsilon - 1)(s_{13} + s_{23})]}{(s_{13} + s_{23})s_{12} \epsilon^2} \int \text{diagram} \\
 &\quad - \frac{2\epsilon - 1}{\epsilon} \int \text{diagram} - \frac{3\epsilon - 2}{(s_{13} + s_{23})\epsilon} \int \text{diagram}, \\
 \int \text{diagram} &= \frac{3\epsilon - 2}{2(s_{13} + s_{23})\epsilon} \left(\int \text{diagram} - \int \text{diagram} \right), \\
 \int \text{diagram} &= \frac{3\epsilon - 2}{2s_{12}\epsilon} \int \text{diagram}.
 \end{aligned}$$

These reduced integrals, with expressions for the master topologies known from [139, 140], can then be plugged into (3.3.48) to give the final result of the two-loop form factor $F_{\mathcal{O}_B}^{(2)}(1^{\phi^{12}}, 2^{\phi^{23}}, 3^{\phi^{31}}; q)$. We refrain from writing the full expression here due to its significant length. Instead, we consider next a much simpler quantity obtained from a standard subtraction of the IR singularities and introduced in Section 2.8 – the two-loop remainder function.

3.4 Two-loop remainder function of $\langle \bar{X}\bar{Y}\bar{Z} | \mathcal{O}_B | 0 \rangle$

Two-loop remainder function for the form factor of a generic operator \mathcal{O} was introduced in (2.9.5) and reads

$$\mathcal{R}_{\mathcal{O}}^{(2)} = F_{\mathcal{O}}^{(2)}(\epsilon) - \frac{1}{2}(F_{\mathcal{O}}^{(1)}(\epsilon))^2 - f^{(2)}(\epsilon) F_{\mathcal{O}}^{(1)}(2\epsilon) - C^{(2)} + \mathcal{O}(\epsilon),$$

where $f^{(2)}(\epsilon) = -2(\zeta_2 + \epsilon\zeta_3 + \epsilon^2\zeta_4)$. In general we would define the remainder for the helicity-blind ratio $F_{\mathcal{O}}^{(2)}/F_{\mathcal{O}}^{(0)}$ but in the particular case of a scalar operator this is not necessary since the tree-level form factor is equal to one. We note here that following [123], for two-loop form factor remainder we choose $C^{(2)} = 0$. In order to fix its value exactly we would need to study the remainder of the two-loop non-minimal form factor (*i.e.* with four external legs) and impose that in the collinear limit, when two adjacent momenta become parallel, $\mathcal{R}_{4\text{-point}}^{(2)} \rightarrow \mathcal{R}_{3\text{-point}}^{(2)}$ without any additional constant.

The procedure of computing the remainder removes the universal IR divergences of the result but since in the present case we are considering a bare, unprotected operator, we are still left with UV divergences. In Section 3.7 we will determine the appropriate renormalised operators and form factors that have a UV- and IR-finite remainder function. Here however we wish to take a first look at the IR-finite, but UV-divergent remainder function of the form factor $\langle \bar{X}\bar{Y}\bar{Z} | \mathcal{O}_B | 0 \rangle$.

Using the decomposition (3.2.2), the remainder function splits into a term arising solely from the form factor of $\tilde{\mathcal{O}}_{\text{BPS}}$ and a piece which contains terms involving $\tilde{\mathcal{O}}_{\text{BPS}}$ and $\mathcal{O}_{\text{offset}}$, which we denote by $\mathcal{R}_{\text{non-BPS}}^{(2)}$:

$$\mathcal{R}_{\mathcal{O}_B}^{(2)} = \mathcal{R}_{\text{BPS}}^{(2)} + \mathcal{R}_{\text{non-BPS}}^{(2)}, \quad (3.4.1)$$

where

$$\mathcal{R}_{\text{BPS}}^{(2)} = F_{\tilde{\mathcal{O}}_{\text{BPS}}}^{(2)}(\epsilon) - \frac{1}{2}(F_{\tilde{\mathcal{O}}_{\text{BPS}}}^{(1)}(\epsilon))^2 - f^{(2)}(\epsilon) F_{\tilde{\mathcal{O}}_{\text{BPS}}}^{(1)}(2\epsilon), \quad (3.4.2)$$

$$\mathcal{R}_{\text{non-BPS}}^{(2)} = F_{\mathcal{O}_{\text{offset}}}^{(2)}(\epsilon) - F_{\mathcal{O}_{\text{offset}}}^{(1)}\left(\frac{1}{2}F_{\mathcal{O}_{\text{offset}}}^{(1)} + F_{\tilde{\mathcal{O}}_{\text{BPS}}}^{(1)}\right)(\epsilon) - f^{(2)}(\epsilon) F_{\mathcal{O}_{\text{offset}}}^{(1)}(2\epsilon). \quad (3.4.3)$$

The remainder of the half-BPS operator $\text{Tr}(X^3)$ was computed in (4.21) of [123] and is identical to the BPS remainder appearing here, as discussed in Section 3.3.3. It is given by a function of uniform transcendentality equal to four, written in terms of classical polylogarithms only. Explicitly, its expression has been quoted in (2.9.6) and reads

$$\begin{aligned} \mathcal{R}_{\text{BPS}}^{(2)} = & -\frac{3}{2} \text{Li}_4(u) + \frac{3}{4} \text{Li}_4\left(-\frac{uv}{w}\right) - \frac{3}{2} \log(w) \text{Li}_3\left(-\frac{u}{v}\right) + \frac{1}{16} \log^2(u) \log^2(v) \\ & + \frac{\log^2(u)}{32} \left[\log^2(u) - 4 \log(v) \log(w) \right] + \frac{\zeta_2}{8} \log(u) \left[5 \log(u) - 2 \log(v) \right] \\ & + \frac{\zeta_3}{2} \log(u) + \frac{7}{16} \zeta_4 + \text{perms}(u, v, w), \end{aligned}$$

where

$$u = \frac{s_{12}}{q^2}, \quad v = \frac{s_{23}}{q^2}, \quad w = \frac{s_{31}}{q^2}, \quad u + v + w = 1. \quad (3.4.4)$$

The new contribution is the non-BPS remainder defined in (3.4.3), which is IR finite, but still has UV divergences. Interestingly, it is given by a sum of functions of transcendentality ranging from three to zero, with no term of maximal transcendentality:

$$\mathcal{R}_{\text{non-BPS}}^{(2)} = \frac{c}{\epsilon} + \sum_{i=0}^3 \mathcal{R}_{\text{non-BPS};3-i}^{(2)}, \quad (3.4.5)$$

where the subscript m in $\mathcal{R}_{\text{non-BPS};m}^{(2)}$ denotes the degree of transcendentality of the corresponding term. For the coefficient of the UV pole we find

$$c = 18 - \pi^2. \quad (3.4.6)$$

The expression arising from replacing the integral functions appearing in the two-loop form factor with the explicit results of [139, 140] can be considerably simplified using the concept of the symbol of a transcendental function discussed in Section 2.8, while beyond-the-symbol terms can be fixed numerically and/or analytically. At transcendentality three, we are guaranteed that the whole result can be written in terms of classical polylogarithms only,³⁰ and hence this procedure is very simple to carry out. We find that the symbol of $\mathcal{R}_{\text{non-BPS};3}^{(2)}$ is

$$\begin{aligned} \mathcal{S}_3^{(2)}(u, v, w) = & -2 \left[u \otimes (1-u) \otimes \frac{u}{1-u} + u \otimes u \otimes \frac{v}{1-u} + u \otimes v \otimes \frac{uv}{w^2} \right] \\ & + \text{perms}(u, v, w), \end{aligned} \quad (3.4.7)$$

³⁰The lowest transcendentality degree for a Goncharov polylogarithm is four.

while for the integrated expression, including beyond-the-symbol terms, we obtain

$$\begin{aligned} \mathcal{R}_{\text{non-BPS};3}^{(2)} &= 2 \left[\text{Li}_3(u) + \text{Li}_3(1-u) \right] - \frac{1}{2} \log^2(u) \log \frac{vw}{(1-u)^2} + \frac{2}{3} \log(u) \log(v) \log(w) \\ &\quad + \frac{2}{3} \zeta_3 + 2 \zeta_2 \log(-q^2) + \text{perms}(u, v, w). \end{aligned} \quad (3.4.8)$$

The transcendentality-two part of the remainder can also be simplified slightly. A short calculation leads to the expression

$$\mathcal{R}_{\text{non-BPS};2}^{(2)} = -12 \left[\text{Li}_2(1-u) + \text{Li}_2(1-v) + \text{Li}_2(1-w) \right] - 2 \log^2(uvw) + 36 \zeta_2. \quad (3.4.9)$$

Finally, for the transcendentality-one and zero terms we have

$$\mathcal{R}_{\text{non-BPS};1}^{(2)} = -12 \log(uvw) - 36 \log(-q^2), \quad (3.4.10)$$

$$\mathcal{R}_{\text{non-BPS};0}^{(2)} = 126. \quad (3.4.11)$$

We would like to make two observations on the results we have derived here.

Firstly, we observe that the $-\pi^2$ term in (3.4.6) comes from the last term on the right-hand side of (3.4.3). It amounts to introducing a spurious UV divergence in the remainder arising when the bubbles contained in the term $F_{\mathcal{O}_{\text{offset}}}^{(1)}(2\epsilon)$ are multiplied by $-2\zeta_2$ inside $f^{(2)}(\epsilon)$. For the sake of extracting the correct UV divergences and studying the mixing, this term must be omitted, see Section 3.7 for this discussion.

Secondly, we stress the usefulness of the decomposition (3.2.2) and (3.4.1), which has the great advantage of separating out completely the terms of maximal transcendentality from the rest. This agrees with the findings of [52], where it was observed in the $SU(2)$ sector that the finite remainder densities, corresponding to different “shuffling” of the R -symmetry field flavours, have the highest degree of transcendentality equal to $4-s$ with s equal to the shuffling in that remainder density, see Figure 24 for illustration of the “shuffling”.

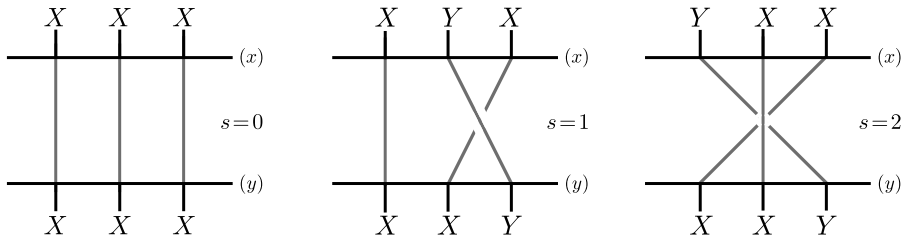


Figure 24: “Shuffling” in the spin-chain picture. In the first case, field configuration on two sites is identical and the shuffling number $s=0$. In the second, fields are shuffled by one site, $s=1$, and in the third case the position is changed by two sites, $s=2$.

In the present case of the $SU(2|3)$ sector we have the operator $\text{Tr}(XZY)$ acting on an external state $\langle \bar{X}\bar{Y}\bar{Z} |$, which corresponds to $s = 1$. Indeed in (3.4.5) we find that the corresponding remainder is composed of terms with transcendentality ranging from three to zero. We explore this connection to the findings in the $SU(2)$ sector in more detail in the next section.

3.4.1 Connection to the remainder densities in the $SU(2)$ sector

We now establish a connection between the UV-finite part of the non-BPS remainder $\mathcal{R}_{\text{non-BPS}}^{(2)}$ and the remainder densities which have appeared in [52] in the context of the calculation of the dilatation operator in the $SU(2)$ sector. $SU(2)$ is a closed subsector of $SU(2|3)$ and operators are built out of the complex scalars, X and Y , as defined in (3.1.2).

In [52] it was found that there are only three independent finite remainder densities, denoted as $(R_i^{(2)})_{XXX}^{XXX}$, $(R_i^{(2)})_{XXY}^{XYX}$, $(R_i^{(2)})_{XXY}^{YXX}$ and illustrated in Figure 24. The first density, $(R_i^{(2)})_{XXX}^{XXX}$, has uniform transcendentality equal to four and is identical to the half-BPS remainder computed in [123], which we also see in our present computation. $(R_i^{(2)})_{XXY}^{XYX}$ contains terms of transcendentality ranging from three to zero, while $(R_i^{(2)})_{XXY}^{YXX}$ contains terms of transcendentality two, one and zero, in agreement with the “shuffling” statement we mentioned in the previous section. The index i denotes the spin chain site, and the remainder densities depend on the three variables

$$u_i = \frac{s_{ii+1}}{s_{i+1i+2}}, \quad v_i = \frac{s_{i+1i+2}}{s_{ii+1i+2}}, \quad w_i = \frac{s_{ii+2}}{s_{i+1i+2}}, \quad (3.4.12)$$

as well as on s_{ii+1} , s_{i+2i+2} , s_{ii+2} and s_{i+1i+2} separately.

We have observed an interesting connection between these remainder densities and our non-BPS remainder, namely

$$\begin{aligned} \frac{1}{2}\mathcal{R}_{\text{non-BPS};3}^{(2)} &= - \sum_{S_3} (R_i^{(2)})_{XXY}^{XYX} \Big|_3 + 6\zeta_3, \\ \frac{1}{2}\mathcal{R}_{\text{non-BPS};2}^{(2)} &= - \sum_{S_3} \left[(R_i^{(2)})_{XXY}^{XYX} - (R_i^{(2)})_{XXY}^{YXX} \right] \Big|_2 + 5\pi^2, \\ \frac{1}{2}\mathcal{R}_{\text{non-BPS};1}^{(2)} &= - \sum_{S_3} \left[(R_i^{(2)})_{XXY}^{XYX} - (R_i^{(2)})_{XXY}^{YXX} \right] \Big|_1, \\ \frac{1}{2}\mathcal{R}_{\text{non-BPS};0}^{(2)} &= - \sum_{S_3} \left[(R_i^{(2)})_{XXY}^{XYX} - (R_i^{(2)})_{XXY}^{YXX} \right] \Big|_0, \end{aligned} \quad (3.4.13)$$

where $f|_m$ denotes the transcendentality- m part of the function f , the remainder densities are evaluated with the replacements $(u_i, v_i, w_i) \rightarrow (u, v, w)$, and S_3 denotes permutations of (u, v, w) .

This is a surprising statement as a priori we should not expect to find connections between remainders of operators belonging to different sectors. The differences between these objects are not insignificant – firstly, the remainder densities studied in [52] correspond to operators which are products of fields without taking the trace. Moreover, the operators we are considering here belong to the larger $SU(2|3)$ sector, hence we should not expect to find similarities with results obtained in smaller sectors. In particular, in the $SU(2|3)$ sector the spin chain becomes *dynamic i.e.* the number of spin sites can fluctuate due to length-changing interactions, something which cannot occur in the $SU(2)$ sector. It is hence intriguing that these quantities seem to be related. As we continue our investigation into the realm of more complicated operators and less supersymmetric theories, we hope to uncover similar connections, hinting at an underlying regularity in the structure of two-loop form factors.

3.5 One-loop non-minimal form factor $\langle \bar{X}\bar{Y}\bar{Z} | \mathcal{O}_{\mathcal{F}} | 0 \rangle$

In this section we compute one of the off-diagonal entries of the matrix of form factors (3.1.8), namely $F_{\mathcal{O}_{\mathcal{F}}}^{(1)}(1^{\phi^{12}}, 2^{\phi^{23}}, 3^{\phi^{31}}; q)$, where $\mathcal{O}_{\mathcal{F}} = (1/2)\text{Tr}(\psi^\alpha \psi_\alpha)$. Note that $\mathcal{O}_{\mathcal{F}}$ is defined in a way that its minimal tree-level form factor

$$F_{\mathcal{O}_{\mathcal{F}}}^{(0)}(1^{\bar{\psi}^{123}}, 2^{\bar{\psi}^{123}}; q) = \langle 21 \rangle. \quad (3.5.1)$$

We construct the one-loop integrand by considering two-particle cuts in the q^2 and s_{23} channels. We will find that the result is IR finite as it should be since this non-minimal form factor does not exist at tree level.³¹ However, UV divergences are expected to appear reflecting the mixing between $\mathcal{O}_{\mathcal{B}}$ and $\mathcal{O}_{\mathcal{F}}$. This will be studied in detail in Section 3.7.

3.5.1 Two-particle cut in the q^2 -channel

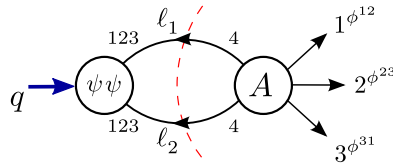


Figure 25: Two-particle cut of the non-minimal form factor $F_{\mathcal{O}_{\mathcal{F}}}^{(1)}(1^{\phi^{12}}, 2^{\phi^{23}}, 3^{\phi^{31}}; q)$.

We start by computing the q^2 -channel cut of the form factor $F_{\mathcal{O}_{\mathcal{F}}}^{(1)}(1^{\phi^{12}}, 2^{\phi^{23}}, 3^{\phi^{31}}; q)$.

³¹ IR-divergent piece of a one-loop form factor must be proportional to its tree-level counterpart in order to ensure correct exponentiation of divergences [26].

This is shown in Figure 25 and is given by

$$\begin{aligned}
 F_{\mathcal{O}_{\mathcal{F}}}^{(1)}(1^{\phi^{12}}, 2^{\phi^{23}}, 3^{\phi^{31}}; q) \Big|_{2, q^2} &= i^2 F_{\mathcal{O}_{\mathcal{F}}}^{(0)}(-\ell_1^{\bar{\psi}^{123}}, -\ell_2^{\bar{\psi}^{123}}; q) \times A(1^{\phi^{12}}, 2^{\phi^{23}}, 3^{\phi^{31}}, \ell_2^{\psi^4}, \ell_1^{\psi^4}) \\
 &= -i \langle \ell_2 \ell_1 \rangle \times \frac{\langle 13 \rangle}{\langle 3 \ell_2 \rangle \langle \ell_1 1 \rangle} = i \frac{\langle \ell_1 \ell_2 \rangle \langle 13 \rangle [\ell_2 3] [1 \ell_1]}{s_{3 \ell_2} s_{1 \ell_1}} = -i \frac{\text{Tr}_-(\ell_1 \ell_2 3 1)}{s_{3 \ell_2} s_{1 \ell_1}} \\
 &= -\frac{i}{2} \left(\frac{s_{3 \ell_2} s_{1 \ell_1} + s_{\ell_1 \ell_2} s_{13} - s_{1 \ell_4} s_{3 \ell_1}}{s_{3 \ell_2} s_{1 \ell_1}} \right).
 \end{aligned} \tag{3.5.2}$$

The corresponding topology is the box shown in Figure 26.

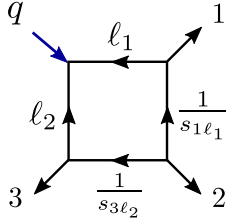


Figure 26: The integral topology that appears in the q^2 -channel two-particle cut. For future convenience we indicate explicitly the uncut propagators.

We now rewrite the numerators in (3.5.2) using

$$s_{\ell_1 \ell_2} = s_{123}, \quad s_{1 \ell_2} = -(s_{12} + s_{13} + s_{1 \ell_1}), \quad s_{3 \ell_1} = -(s_{13} + s_{23} + s_{3 \ell_2}), \tag{3.5.3}$$

which follows from momentum conservation $\sum_{i=1}^3 p_i + \ell_1 + \ell_2 = 0$ and the cut conditions $\ell_1^2 = \ell_2^2 = 0$. Doing so, (3.5.2) becomes

$$\begin{aligned}
 F_{\mathcal{O}_{\mathcal{F}}}^{(1)}(1^{\phi^{12}}, 2^{\phi^{23}}, 3^{\phi^{31}}; q) \Big|_{2, q^2} &= \frac{i}{2} \left(\frac{s_{12} s_{23}}{s_{3 \ell_2} s_{1 \ell_1}} + \frac{s_{13} + s_{23}}{s_{3 \ell_2}} + \frac{s_{12} + s_{13}}{s_{1 \ell_1}} \right) \\
 &= \frac{i}{2} \left[s_{12} s_{23} \times \text{[Box Diagram]} + (s_{13} + s_{23}) \times \text{[Triangle Diagram 1]} + (s_{12} + s_{13}) \times \text{[Triangle Diagram 2]} \right].
 \end{aligned} \tag{3.5.4}$$

Note that in this cut no UV-divergent integrals have appeared and that, as always, we have to add two additional contributions from cyclic permutations of the external particles.

3.5.2 Two-particle cut in the s_{23} -channel

We now compute the two-particle cut of $F_{\mathcal{O}_{\mathcal{F}}}^{(1)}(1^{\phi^{12}}, 2^{\phi^{23}}, 3^{\phi^{31}}; q)$ in the s_{23} -channel. There are two possible diagrams to consider, shown in Figure 27.

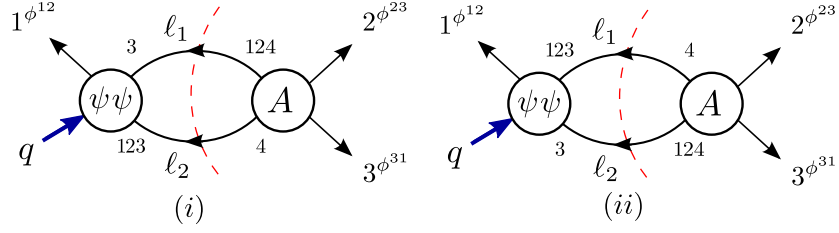


Figure 27: Two diagrams entering the two-particle cut in the s_{23} -channel.

These two diagrams give rise to the master topologies shown in Figure 28, with corresponding numerators determined by the cuts.

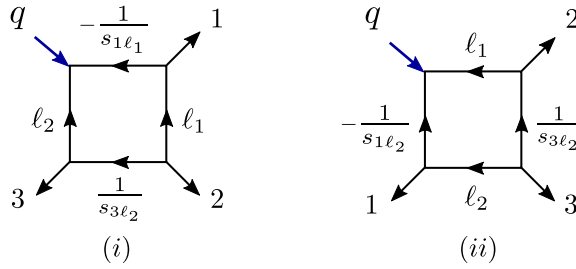


Figure 28: Master topologies generated by the two diagrams of Figure 27, respectively. The uncut propagators are explicitly shown in order to bookkeep their sign reflecting the momentum flow. For the coefficient of the box integral, only the diagram on the left can be compared with the box detected in the q^2 -cut of Figure 25 due to the ordering of external legs.

In the cuts we need the tree-level non-minimal form factors $F_{\mathcal{O}_{\mathcal{F}}}^{(0)}(1^{\phi^{12}}, 2^{\psi^3}, 3^{\bar{\psi}^{123}}; q)$ and $F_{\mathcal{O}_{\mathcal{F}}}^{(0)}(1^{\phi^{12}}, 2^{\psi^{123}}, 3^{\bar{\psi}^3}; q)$, which we compute using factorisation. The first form factor has only one possible factorisation diagram corresponding to a fermion splitting into an anti-fermion and a scalar, as shown in Figure 29.

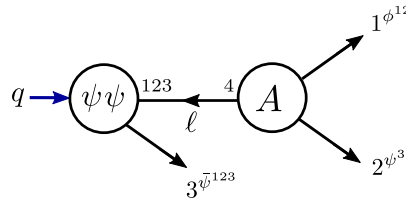


Figure 29: A factorisation diagram of the non-minimal form factor $F_{\mathcal{O}_{\mathcal{F}}}^{(0)}(1^{\phi^{12}}, 2^{\psi^3}, 3^{\bar{\psi}^{123}}; q)$ featuring in the two-particle cut of $F_{\mathcal{O}_{\mathcal{F}}}^{(1)}(1^{\phi^{12}}, 2^{\phi^{23}}, 3^{\phi^{31}}; q)$ in the s_{23} -channel.

From this factorisation diagram we can infer the expression for the tree-level form factor, which is given by

$$F_{\mathcal{O}_{\mathcal{F}}}^{(0)}(1^{\phi^{12}}, 2^{\psi^3}, 3^{\bar{\psi}^{123}}; q) = F_{\mathcal{O}_{\mathcal{F}}}^{(0)}(-\ell^{\bar{\psi}^{123}}, 3^{\bar{\psi}^{123}}; q) \times \frac{i}{s_{12}} \times A^{\overline{\text{MHV}}}(1^{\phi^{12}}, 2^{\psi^3}, \ell^{\psi^4}). \quad (3.5.5)$$

The anti-MHV amplitude can be easily determined using parity, as

$$A^{\overline{\text{MHV}}}(1^{\phi^{12}}, 2^{\psi^3}, \ell^{\psi^4}) = -[A^{\text{MHV}}(1^{\phi^{34}}, 2^{\bar{\psi}^{124}}, \ell^{\bar{\psi}^{123}})]^* = i[2\ell]. \quad (3.5.6)$$

Using $\ell = -(p_1 + p_2)$ we obtain the result

$$F_{\mathcal{O}_{\mathcal{F}}}^{(0)}(1^{\phi^{12}}, 2^{\psi^3}, 3^{\bar{\psi}^{123}}; q) = \frac{[21]\langle 13 \rangle}{s_{12}}. \quad (3.5.7)$$

We now compute the two diagrams of Figure 27 separately.

Diagram (i)

This diagram is given by

$$\begin{aligned} F_{\mathcal{O}_{\mathcal{F}}}^{(1)}(1^{\phi^{12}}, 2^{\phi^{23}}, 3^{\phi^{31}}; q) \Big|_{2, s_{23}}^{(i)} &= F_{\mathcal{O}_{\mathcal{F}}}^{(0)}(1^{\phi^{12}}, -\ell_1^{\psi^3}, -\ell_2^{\bar{\psi}^{123}}; q) \times A^{\text{MHV}}(2^{\phi^{23}}, 3^{\phi^{31}}, \ell_2^{\psi^4}, \ell_1^{\bar{\psi}^{124}}) \\ &= -\frac{i}{2} \left(\frac{s_{1\ell_2} s_{3\ell_1} + s_{3\ell_2} s_{1\ell_1} - s_{13} s_{\ell_1 \ell_2}}{s_{1\ell_1} s_{3\ell_2}} \right). \end{aligned} \quad (3.5.8)$$

Using $p_2 + p_3 + \ell_1 + \ell_2 = 0$ and $\ell_1^2 = \ell_2^2 = 0$ on the cut, we can substitute

$$s_{\ell_1 \ell_2} = s_{23}, \quad s_{3\ell_1} = -(s_{3\ell_2} + s_{32}), \quad s_{1\ell_2} = -(s_{12} + s_{13} + s_{1\ell_1}), \quad (3.5.9)$$

so that (3.5.8) becomes

$$\begin{aligned} F_{\mathcal{O}_{\mathcal{F}}}^{(1)}(1^{\phi^{12}}, 2^{\phi^{23}}, 3^{\phi^{31}}; q) \Big|_{2, s_{23}}^{(i)} &= -\frac{i}{2} \left[2 + \frac{s_{12} + s_{13}}{s_{1\ell_1}} + \frac{s_{23}}{s_{3\ell_2}} + \frac{s_{12} s_{23}}{s_{1\ell_1} s_{3\ell_2}} \right] \\ &= \frac{i}{2} \left[-2 \times \text{Diagram 1} + (s_{12} + s_{13}) \times \text{Diagram 2} - s_{23} \times \text{Diagram 3} + s_{12} s_{23} \times \text{Diagram 4} \right]. \end{aligned} \quad (3.5.10)$$

Note that when the cut-integrals are uplifted to full Feynman integrals $1/s_{1\ell_1}$, has to be replaced by $-1/(p_1 - \ell_1)^2$ due to the momentum flow, according to Figure 28(i).

Diagram (ii)

For diagram (ii) we need the form factor

$$F_{\mathcal{O}_{\mathcal{F}}}^{(0)}(1^{\phi^{12}}, -\ell_1^{\bar{\psi}^{123}}, -\ell_2^{\psi^3}; q) = F_{\mathcal{O}_{\mathcal{F}}}^{(0)}(1^{\phi^{12}}, -\ell_2^{\psi^3}, -\ell_1^{\bar{\psi}^{123}}; q) = \frac{[\ell_2 1]\langle 1\ell_1 \rangle}{s_{1\ell_2}}. \quad (3.5.11)$$

The one-loop expression is hence given by

$$\begin{aligned}
 F_{\mathcal{O}_{\mathcal{F}}}^{(1)}(1^{\phi^{12}}, 2^{\phi^{23}}, 3^{\phi^{31}}; q) \Big|_{2, s_{23}}^{(ii)} &= F_{\mathcal{O}_{\mathcal{F}}}^{(0)}(1^{\phi^{12}}, -\ell_1^{\bar{\psi}^{123}}, -\ell_2^{\psi^3}; q) \times A^{\text{MHV}}(2^{\phi^{23}}, 3^{\phi^{31}}, \ell_2^{\bar{\psi}^{124}}, \ell_1^{\psi^4}) \\
 &= i \frac{[\ell_2 1] \langle 1 \ell_1 \rangle}{s_{1\ell_2}} \times \frac{\langle 2 \ell_2 \rangle}{\langle \ell_1 2 \rangle} = -i \frac{[1 \ell_2] \langle 1 \ell_1 \rangle \langle 2 \ell_2 \rangle [2 \ell_1]}{s_{1\ell_2} s_{2\ell_1}} \\
 &= -i \frac{\text{Tr}_-(1 \ell_1 2 \ell_2)}{s_{1\ell_2} s_{2\ell_1}} = i \frac{\text{Tr}_-(1 \ell_1 3 \ell_2)}{s_{1\ell_2} s_{3\ell_2}}, \tag{3.5.12}
 \end{aligned}$$

where we used momentum conservation in the last step. Expanding the trace and using a set of replacements similar to (3.5.9),

$$s_{\ell_1 \ell_2} = s_{23}, \quad s_{3\ell_1} = -(s_{3\ell_2} + s_{32}), \quad s_{1\ell_1} = -(s_{12} + s_{13} + s_{1\ell_2}), \tag{3.5.13}$$

we arrive at the result

$$\begin{aligned}
 F_{\mathcal{O}_{\mathcal{F}}}^{(1)}(1^{\phi^{12}}, 2^{\phi^{23}}, 3^{\phi^{31}}; q) \Big|_{2, s_{23}}^{(ii)} &= -\frac{i}{2} \left[2 + \frac{s_{12} + s_{13}}{s_{1\ell_2}} + \frac{s_{23}}{s_{3\ell_2}} + \frac{s_{13} s_{23}}{s_{1\ell_2} s_{3\ell_2}} \right] \tag{3.5.14} \\
 &= \frac{i}{2} \left[-2 \times \text{Diagram (i)} + (s_{12} + s_{13}) \times \text{Diagram (ii)} - s_{23} \times \text{Diagram (iii)} + s_{13} s_{23} \times \text{Diagram (iv)} \right],
 \end{aligned}$$

which is identical to (3.5.10) – apart from the box. Note that in the sum over cyclic permutations of these two cuts three different one-mass boxes appear, each with their two possible two-particle cuts. The cuts of the same boxes in the q^2 -channel are already accounted for in (3.5.4).

Diagram (i) + Diagram (ii)

Combining the results (3.5.10) and (3.5.14) and noting that the coefficients of the integrals are consistent with those obtained from the q^2 -channel cut in (3.5.4), we find

$$\begin{aligned}
 F_{\mathcal{O}_{\mathcal{F}}}^{(1)}(1^{\phi^{12}}, 2^{\phi^{23}}, 3^{\phi^{31}}; q) \Big|_{2, s_{23}} &= F_{\mathcal{O}_{\mathcal{F}}}^{(1)}(1^{\phi^{12}}, 2^{\phi^{23}}, 3^{\phi^{31}}; q) \Big|_{2, s_{23}}^{(i)} + F_{\mathcal{O}_{\mathcal{F}}}^{(1)}(1^{\phi^{12}}, 2^{\phi^{23}}, 3^{\phi^{31}}; q) \Big|_{2, s_{23}}^{(ii)} \\
 &= \frac{i}{2} \left[-4 \times \text{Diagram (i)} + 2(s_{12} + s_{13}) \times \text{Diagram (ii)} - 2s_{23} \times \text{Diagram (iii)} \right. \\
 &\quad \left. + s_{12} s_{23} \times \text{Diagram (iv)} + s_{13} s_{23} \times \text{Diagram (v)} \right]. \tag{3.5.15}
 \end{aligned}$$

Note that the coefficient of the box integral with q inserted between p_1 and p_3 matches that obtained in the q^2 -channel (3.5.4), namely $(i/2)(s_{12}s_{23})$. Moreover, the second box appearing in (3.5.15) is detected in the q^2 -cut with cyclically shifted external momenta: $1 \rightarrow 2 \rightarrow 3 \rightarrow 1$.

3.5.3 Final result

Performing the cyclic sum we get the final result for the one-loop form factor:

$$\begin{aligned}
 F_{\mathcal{O}_{\mathcal{F}}}^{(1)}(1^{\phi^{12}}, 2^{\phi^{23}}, 3^{\phi^{31}}; q) = & \frac{i}{2} \left[-4 \times \begin{array}{c} q \\ \swarrow \quad \searrow \\ \text{circle} \\ \swarrow \quad \searrow \\ 1 \quad 2 \quad 3 \end{array} + 2(s_{13} + s_{23}) \times \begin{array}{c} q \\ \downarrow \\ \triangle \\ \swarrow \quad \searrow \\ 3 \quad 2 \quad 1 \end{array} \right. \\
 & \left. - 2s_{23} \times \begin{array}{c} q \\ \swarrow \quad \searrow \\ \triangle \\ \swarrow \quad \searrow \\ 3 \quad 2 \quad 1 \end{array} + s_{12}s_{23} \times \begin{array}{c} q \\ \swarrow \quad \searrow \\ \square \\ \swarrow \quad \searrow \\ 3 \quad 2 \quad 1 \end{array} + \text{cyclic}(1, 2, 3) \right]. \quad (3.5.16)
 \end{aligned}$$

Expanding the result up to $\mathcal{O}(1)$ we get

$$\begin{aligned}
 F_{\mathcal{O}_{\mathcal{F}}}^{(1)}(1^{\phi^{12}}, 2^{\phi^{23}}, 3^{\phi^{31}}; q) = & \frac{6}{\epsilon} + 12 + \frac{\pi^2}{2} - \left[2 \log(-s_{12}) - \frac{1}{2} \log^2 \left(\frac{s_{12}}{s_{23}} \right) \right. \\
 & \left. - 2 \text{Li}_2 \left(1 - \frac{q^2}{s_{12}} \right) + \text{cyclic}(1, 2, 3) \right] + \mathcal{O}(\epsilon). \quad (3.5.17)
 \end{aligned}$$

Importantly, the infrared $1/\epsilon^2$ poles have cancelled in the final result, which is expected since the corresponding tree-level form factor does not exist. We can also rewrite the result using the variables u, v and w introduced in (3.4.4), getting

$$F_{\mathcal{O}_{\mathcal{F}}}^{(1)}(1^{\phi^{12}}, 2^{\phi^{23}}, 3^{\phi^{31}}; q) = 2 \frac{(-s_{12})^{-\epsilon}}{\epsilon(1-2\epsilon)} - \left[2 \text{Li}_2(1-u) + \log u \log v \right] + \zeta_2 + \text{cyclic}(1, 2, 3), \quad (3.5.18)$$

where the first term corresponds to the bubble integral exact to all orders in ϵ , according to the expression in Appendix B.1 and where we have made use of the dilogarithm identity

$$\text{Li}_2(1-x) + \text{Li}_2(1-x^{-1}) = -\frac{1}{2} \log^2 x. \quad (3.5.19)$$

3.6 Two-loop subminimal form factor $\langle \bar{\psi} \bar{\psi} | \mathcal{O}_{\mathcal{B}} | 0 \rangle$

Here we consider the second off-diagonal form factor in the matrix (3.1.8), namely the subminimal form factor $\langle \bar{\psi} \bar{\psi} | \mathcal{O}_{\mathcal{B}} | 0 \rangle$ with $\mathcal{O}_{\mathcal{B}} = \text{Tr}(X[Y, Z])$ and $\langle \bar{\psi} \bar{\psi} |$ being a shorthand

notation for $\langle 1^{\bar{\psi}^{123}} 2^{\bar{\psi}^{123}} |$. As it is clear from Figure 30, this object exists only at two loops or more, hence we only need to consider the two three-particle cuts presented here.

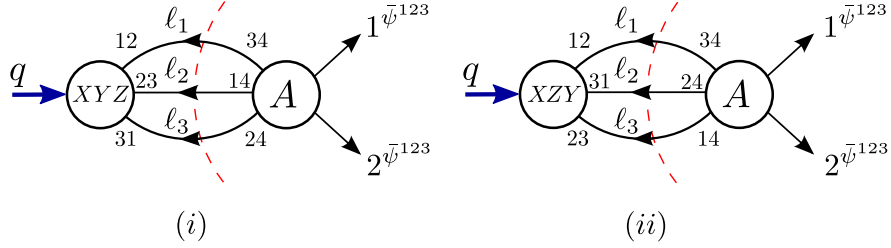


Figure 30: Triple cut of the two-loop subminimal form factor $\langle \bar{\psi}\bar{\psi} | \mathcal{O}_B | 0 \rangle$. The second set of identical diagrams, but with external legs 1 and 2 swapped has to be added, corresponding to the fact that it leads to the same colour-ordering.

For the first diagram, the relevant amplitude (and hence the integrand, since the tree-level form factor is equal to 1 according to (3.2.8)) is

$$(i) : A^{(0)}(1^{\bar{\psi}^{123}}, 2^{\bar{\psi}^{123}}, \ell_3^{\phi^{24}}, \ell_2^{\phi^{14}}, \ell_1^{\phi^{34}}) = -i \frac{[\ell_1 \ell_3]}{[2\ell_3][\ell_1 1]}. \quad (3.6.1)$$

For the second diagram, the relevant amplitude is

$$(ii) : A^{(0)}(1^{\bar{\psi}^{123}}, 2^{\bar{\psi}^{123}}, \ell_3^{\phi^{14}}, \ell_2^{\phi^{24}}, \ell_1^{\phi^{34}}) = i \frac{[\ell_1 \ell_3]}{[2\ell_3][\ell_1 1]}, \quad (3.6.2)$$

which differs from (i) only by a sign, corresponding to interchange of helicities on legs ℓ_2 and ℓ_3 . Taking into account the relative minus sign between the two diagrams coming from the commutator and converting to momentum invariants we get

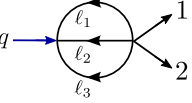
$$\begin{aligned} (i) - (ii) : & -2 \frac{[\ell_1 \ell_3]}{[2\ell_3][\ell_1 1]} = 2 \frac{1}{[12]} \frac{[\ell_1 \ell_3] \langle \ell_3 2 \rangle [21] \langle 1 \ell_1 \rangle}{s_{2\ell_3} s_{1\ell_1}} = \frac{2}{[12]} \frac{\text{Tr}_+(\ell_1 \ell_3 2 1)}{s_{2\ell_3} s_{1\ell_1}} \\ & = \frac{1}{[12]} \frac{s_{\ell_1 \ell_3} s_{12} - s_{2\ell_1} s_{1\ell_3} + s_{1\ell_1} s_{2\ell_3}}{s_{2\ell_3} s_{1\ell_1}}, \end{aligned} \quad (3.6.3)$$

where we have taken into account the factor of i^3 coming from the cut propagators. We note that for the half-BPS case of $\tilde{\mathcal{O}}_{\text{BPS}} = \text{Tr}(X \{Y, Z\})$ the two contributions would cancel out exactly, which is consistent with the fact that the operator is protected.

The cut integrand corresponding to the expression in (3.6.3) is given by

$$F_{\mathcal{O}_B}^{(2)}(1^{\bar{\psi}^{123}}, 2^{\bar{\psi}^{123}}; q) \Big|_{3, q^2} = \frac{1}{[12]} (s_{\ell_1 \ell_3} s_{12} - s_{2\ell_1} s_{1\ell_3} + s_{1\ell_1} s_{2\ell_3}) \times \text{triangle diagram} \quad (3.6.4)$$

Lifting the cut momenta off-shell and performing the integral reductions using the LiteRed package gives

$$F_{\mathcal{O}_B}^{(2)}(1^{\bar{\psi}^{123}}, 2^{\bar{\psi}^{123}}; q) = \frac{1}{[12]} \frac{2(3\epsilon - 2)}{2\epsilon - 1} \times q \rightarrow \text{Diagram} \cdot \quad (3.6.5)$$


Note that any ambiguity associated with factors of ℓ_i^2 , $i = 1, 2, 3$ in the numerator of (3.6.4) would lead to a vanishing scaleless integral.

Finally, we proceed to substitute the expression for the master integral, which can be found in [139]. We also perform a summation over the cyclic permutations of the internal legs and note that having done so, the value of the five-point amplitude entering the cut does not change and so the result picks up an overall factor of three. Finally, a further factor of two is included corresponding to the two possible orderings of the external legs.

We proceed by expanding the results in powers of ϵ up to $\mathcal{O}(1)$ and get

$$\begin{aligned} F_{\mathcal{O}_B}^{(2)}(1^{\bar{\psi}^{123}}, 2^{\bar{\psi}^{123}}; q) &= \frac{6}{[12]} \frac{\epsilon^2}{(1 - 2\epsilon)^2} \frac{\Gamma(1 + 2\epsilon)\Gamma(-\epsilon)^3}{\Gamma(2 - 3\epsilon)} (e^{\gamma_E \epsilon})^2 (-q^2)^{1-2\epsilon} \\ &= -6\langle 12 \rangle \left[\frac{1}{\epsilon} + 7 - 2 \log(-q^2) \right] + \mathcal{O}(\epsilon). \end{aligned} \quad (3.6.6)$$

Note that this subminimal two-loop form factor has no lower-loop counterparts and therefore it has only a $1/\epsilon$ UV divergence and no IR divergences.

3.7 Two-loop dilatation operator in the $SU(2|3)$ sector

In this section we resolve the mixing between the operators $\mathcal{O}_B = \text{Tr}(X[Y, Z])$ and $\mathcal{O}_F = (1/2)\text{Tr}(\psi^\alpha \psi_\alpha)$ at two loops. The schematic form of the perturbative expansions of the relevant form factors from which we extract the renormalisation constants can be written as:

$$\langle \bar{\psi} \bar{\psi} | \mathcal{O}_F | 0 \rangle \Big|_{\text{UV}} := \langle 21 \rangle \left[f^{(1)} a(\mu_R) + f^{(2)} a^2(\mu_R) + \dots \right], \quad (3.7.1)$$

$$\langle \bar{X} \bar{Y} \bar{Z} | \mathcal{O}_F | 0 \rangle \Big|_{\text{UV}} := a(\mu_R) [g_{\text{YM}} d^{(1)}] + \dots, \quad (3.7.2)$$

$$\langle \bar{\psi} \bar{\psi} | \mathcal{O}_B | 0 \rangle \Big|_{\text{UV}} := \langle 21 \rangle a^2(\mu_R) \left[\frac{c^{(2)}}{g_{\text{YM}}} \right] + \dots, \quad (3.7.3)$$

$$\langle \bar{X} \bar{Y} \bar{Z} | \mathcal{O}_B | 0 \rangle \Big|_{\text{UV}} := b^{(1)} a(\mu_R) + b^{(2)} a^2(\mu_R) + \dots, \quad (3.7.4)$$

where the coefficients carrying the UV divergences are

$$\begin{aligned}
 f^{(1)} &= \frac{f_1^{(1)}}{\epsilon}, & f^{(2)} &= \frac{f_2^{(2)}}{\epsilon^2} + \frac{f_1^{(2)}}{\epsilon}, \\
 b^{(1)} &= \frac{b_1^{(1)}}{\epsilon}, & b^{(2)} &= \frac{b_2^{(2)}}{\epsilon^2} + \frac{b_1^{(2)}}{\epsilon}, \\
 d^{(1)} &= \frac{d_1^{(1)}}{\epsilon}, & c^{(2)} &= \frac{c_1^{(2)}}{\epsilon}.
 \end{aligned} \tag{3.7.5}$$

These schematic forms can be explained as follows. The running 't Hooft coupling $a(\mu_R)$ defined in (3.1.11) counts the number of loops and contains the factor of g_{YM}^2 . We have been careful in distinguishing the coupling constant g_{YM} from $a(\mu_R)$ on the right-hand side of (3.7.1)–(3.7.4). This is necessary in case of the non-minimal form factors (3.7.2) and (3.7.3) where a five-point amplitude enters the cut, contributing the factor of g_{YM}^3 , see discussion in Section 2.1. We can still factor out the appropriate power of $a(\mu_R)$ according to the loop order of these form factors but we need to compensate the power of g_{YM} by appropriately multiplying or dividing in order to obtain an overall factor of g_{YM}^3 . In particular, (3.7.2) is the result of a one-loop calculation and hence carries a single power of $a(\mu_R)$. The calculation also involves a five-point amplitude, which is $\mathcal{O}(g_{\text{YM}}^3)$ and hence the extra power of g_{YM} . In turn (3.7.3) is the result of a two-loop calculation, again involving a five-point amplitude. This is proportional to $a(\mu_R)^2/g_{\text{YM}}$, which is $\mathcal{O}(g_{\text{YM}}^3)$ just like (3.7.2). Note that in (3.7.1) and (3.7.3) we have factored out the tree-level form factor $\langle 1\bar{\psi}2\bar{\psi}|\mathcal{O}_{\mathcal{F}}|0\rangle^{(0)} = \langle 21\rangle$.

Expanding the mixing matrix \mathcal{Z} according to (3.1.10) as

$$\mathcal{Z} = \mathbb{1} + \mathcal{Z}^{(1)} + \mathcal{Z}^{(2)} + \dots = \mathbb{1} + a(\mu_R)z^{(1)} + a(\mu_R)^2z^{(2)} + \dots, \tag{3.7.6}$$

and requiring the finiteness of the renormalised form factors we arrive at

$$\begin{aligned}
 (z^{(1)})_F^F &= -\frac{f_1^{(1)}}{\epsilon}, & (z^{(2)})_F^F &= -\frac{f_2^{(2)} - (f_1^{(1)})^2}{\epsilon^2} - \frac{f_1^{(2)}}{\epsilon}, \\
 (z^{(1)})_B^B &= -\frac{b_1^{(1)}}{\epsilon}, & (z^{(2)})_B^B &= -\frac{b_2^{(2)} - (b_1^{(1)})^2}{\epsilon^2} - \frac{b_1^{(2)}}{\epsilon}, \\
 (z^{(1)})_F^B &= -g_{\text{YM}} \frac{d_1^{(1)}}{\epsilon}, & (z^{(2)})_B^F &= -\frac{1}{g_{\text{YM}}} \frac{c_1^{(2)}}{\epsilon}.
 \end{aligned} \tag{3.7.7}$$

Using the definition in (3.1.10) the $\log(\mathcal{Z})$ matrix has the form, up to $\mathcal{O}(a(\mu_R)^2)$,

$$\begin{aligned} \log(\mathcal{Z}) &\sim \begin{pmatrix} (\mathcal{Z}^{(1)})_F^F + [(\mathcal{Z}^{(2)})_F^F - \frac{1}{2}((\mathcal{Z}^{(1)})_F^F)^2] & (\mathcal{Z}^{(1)})_F^B - \frac{1}{2}(\mathcal{Z}^{(1)})_F^B [(\mathcal{Z}^{(1)})_F^F + (\mathcal{Z}^{(1)})_B^B] \\ (\mathcal{Z}^{(2)})_B^F & (\mathcal{Z}^{(1)})_B^B + [(\mathcal{Z}^{(2)})_B^B - \frac{1}{2}((\mathcal{Z}^{(1)})_B^B)^2] \end{pmatrix} \\ &= \begin{pmatrix} -a(\mu_R) \frac{f_1^{(1)}}{\epsilon} - a^2(\mu_R) \left[\frac{f_2^{(2)} - \frac{1}{2}(f_1^{(1)})^2}{\epsilon^2} + \frac{f_1^{(2)}}{\epsilon} \right] & -g_{\text{YM}} a(\mu_R) \cdot \frac{d_1^{(1)}}{\epsilon} \left[1 + \frac{1}{2} a(\mu_R) \frac{f_1^{(1)} + b_1^{(1)}}{\epsilon} \right] \\ -\frac{a^2(\mu_R)}{g_{\text{YM}}} \frac{c_1^{(2)}}{\epsilon} & -a(\mu_R) \frac{b_1^{(1)}}{\epsilon} - a^2(\mu_R) \left[\frac{b_2^{(2)} - \frac{1}{2}(b_1^{(1)})^2}{\epsilon^2} + \frac{b_1^{(2)}}{\epsilon} \right] \end{pmatrix}. \end{aligned} \quad (3.7.8)$$

We now move on to determine the various matrix elements. From (3.2.11) we read off that $b_1^{(1)} = -6$, and hence

$$(z^{(1)})_B^B = \frac{6}{\epsilon}. \quad (3.7.9)$$

Next we compute $(z^{(2)})_B^B - (1/2)((z^{(1)})_B^B)^2$. This quantity has already been calculated in Section 3.4, and we remark that we should drop the π^2 term in (3.4.6), which is not of UV origin. Doing so we find $b_1^{(2)} = 18$, and therefore

$$(z^{(2)})_B^B - \frac{1}{2}((z^{(1)})_B^B)^2 = -\frac{18}{\epsilon}. \quad (3.7.10)$$

Next, from the two-loop result of (3.6.6) we obtain

$$(z^{(2)})_B^F = -\frac{6}{\epsilon} \frac{1}{g_{\text{YM}}}, \quad (3.7.11)$$

while from (3.5.17) we find

$$(z^{(1)})_F^B = -\frac{6}{\epsilon} g_{\text{YM}}. \quad (3.7.12)$$

Finally, we need to determine $(z^{(1)})_F^F$ and $(z^{(2)})_F^F$. In order to do so, we recall that $\mathcal{O}_{\mathcal{F}}$ appears as a component of the chiral part of the stress tensor multiplet operator (see (3.3) of [146]). The components of this multiplet can be obtained by acting with four of the eight supercharges $Q^{\alpha A}$ on the bottom component $\text{Tr}(X^2) = \text{Tr}(\phi_{12}^2)$, leading to the following half-BPS descendant:

$$\mathcal{O}_{\text{BPS}'} := \frac{1}{2} \text{Tr}(\psi^\alpha \psi_\alpha) + g_{\text{YM}} \text{Tr}(X[Y, Z]) = \mathcal{O}_{\mathcal{F}} + g_{\text{YM}} \mathcal{O}_B. \quad (3.7.13)$$

Since this operator is half-BPS the corresponding form factors are UV finite. Therefore,

we can infer that

$$F_{\mathcal{O}_{\mathcal{F}}}(1^{\bar{\psi}^{123}}, 2^{\bar{\psi}^{123}}; q) \Big|_{\text{UV}} = -g_{\text{YM}} F_{\mathcal{O}_{\mathcal{B}}}(1^{\bar{\psi}^{123}}, 2^{\bar{\psi}^{123}}; q) \Big|_{\text{UV}}, \quad (3.7.14)$$

from which we get

$$(z^{(1)})_F^F = -g_{\text{YM}}(z^{(1)})_B^F = 0, \quad (z^{(2)})_F^F = -g_{\text{YM}}(z^{(2)})_B^F = \frac{6}{\epsilon}. \quad (3.7.15)$$

Therefore we have

$$(z^{(2)})_F^F - \frac{1}{2}((z^{(1)})_F^F)^2 = \frac{6}{\epsilon}. \quad (3.7.16)$$

We can now write down the matrix (3.7.8), with the result

$$\log(\mathcal{Z}) = \begin{pmatrix} a^2(\mu_R) \frac{6}{\epsilon} & -a(\mu_R) g_{\text{YM}} \frac{6}{\epsilon} \\ -\frac{a^2(\mu_R)}{g_{\text{YM}}} \frac{6}{\epsilon} & a(\mu_R) \frac{6}{\epsilon} - a^2(\mu_R) \frac{18}{\epsilon} \end{pmatrix} + \mathcal{O}(a(\mu_R)^3). \quad (3.7.17)$$

Finally, we obtain the dilatation operator up to two loops as

$$\delta D = \lim_{\epsilon \rightarrow 0} \left[-\mu_R \frac{\partial}{\partial \mu_R} \log(\mathcal{Z}) \right] = 12 \times \begin{pmatrix} 2a^2 & -a g_{\text{YM}} \\ -2 \frac{a^2}{g_{\text{YM}}} & a - 6a^2 \end{pmatrix}, \quad (3.7.18)$$

where we recall that our 't Hooft coupling is defined in (2.4.1). The eigenvalues of this matrix are the anomalous dimensions of the eigenstates of the dilatation operator. One of the eigenvalues vanishes indicating the presence of a non-trivial additional protected operator. The second one is

$$\gamma_{\mathcal{K}} = 12a - 48a^2 + \mathcal{O}(a^3), \quad (3.7.19)$$

in precise agreement with the one- and two-loop anomalous dimensions for the Konishi supermultiplet [147]. We can also write the corresponding eigenstates by diagonalising the transpose of δD .³² One arrives at the two operators [138, 148–150]

$$\mathcal{O}_{\text{BPS}'}^{\text{ren}} = \mathcal{O}_{\mathcal{F}}^{\text{ren}} + g_{\text{YM}} \mathcal{O}_{\mathcal{B}}^{\text{ren}}, \quad (3.7.20)$$

$$\mathcal{O}_{\mathcal{K}}^{\text{ren}} = \mathcal{O}_{\mathcal{B}}^{\text{ren}} - \frac{g_{\text{YM}} N}{8\pi^2} \mathcal{O}_{\mathcal{F}}^{\text{ren}}. \quad (3.7.21)$$

³²Note that in this sector δD is not symmetric. A generic combination of the two operators $\mathcal{O}_{\mathcal{F}}$ and $\mathcal{O}_{\mathcal{B}}$ can be written as $v_f \mathcal{O}_{\mathcal{F}} + v_b \mathcal{O}_{\mathcal{B}} := (\mathbf{v}, \mathbf{O})$, with $\mathbf{v}^T := (v_f, v_b)$ and $\mathbf{O}^T := (\mathcal{O}_{\mathcal{F}}, \mathcal{O}_{\mathcal{B}})$. Under the action of the dilatation operator we have $(\mathbf{v}, \mathbf{O}) \rightarrow (\mathbf{v}, \delta D \mathbf{O}) = ((\delta D)^T \mathbf{v}, \mathbf{O})$.

The first one is the protected operator introduced in (3.7.13) above, while the second combination is a descendant of the Konishi operator.

3.8 Summary

In this chapter we have considered two-loop form factors of operators belonging to the closed $SU(2|3)$ sector of $\mathcal{N} = 4$ SYM. Here we wish to briefly summarise the main findings so far:

1. The one-loop minimal form factor of $\mathcal{O}_{\mathcal{B}} = \text{Tr}(X[Y, Z])$ has been found in (3.2.13), leading to the result for the one-loop anomalous dimension $\gamma_{\mathcal{O}_{\mathcal{B}}}^{(1)} = 12a$, the same as the one-loop anomalous dimension of the Konishi operator $\mathcal{O}_{\mathcal{K}}$.
2. Generalised unitarity, applied to form factors, has been used to find the two-loop integrand for the minimal form factor of $\mathcal{O}_{\mathcal{B}}$. For this particular operator, a useful decomposition (3.2.2) meant that we could separately consider the two-loop minimal form factors of $\tilde{\mathcal{O}}_{\text{BPS}} = \text{Tr}(X\{Y, Z\})$, shown in Section 3.3.3 to be equivalent to the known result for $\mathcal{O}_{\text{BPS}} = \text{Tr}(X^3)$, and $\mathcal{O}_{\text{offset}} = -2\text{Tr}(XZY)$. The two-loop integrand for the minimal form factor of $\mathcal{O}_{\mathcal{B}}$ has been then obtained by combining the two in (3.3.48).
3. After the integration has been performed, the two-loop remainder function of the form factor of $\mathcal{O}_{\mathcal{B}}$ has been computed in Section 3.4. It contains terms of transcendentality ranging from four to zero and is IR finite but UV divergent since the operator is not protected. The maximally transcendental part is equal to the two-loop remainder of \mathcal{O}_{BPS} while the terms of lower transcendentality display interesting connections to the remainder densities in the smaller $SU(2)$ sector.
4. In order to solve the mixing problem with the operator $\mathcal{O}_{\mathcal{F}} = 1/2 \text{Tr}(\psi^\alpha \psi_\alpha)$ three further form factors have been calculated. In particular, the non-minimal $\langle \bar{X}\bar{Y}\bar{Z} | \mathcal{O}_{\mathcal{F}} | 0 \rangle$ has been considered in Section 3.5 and the subminimal $\langle \bar{\psi}\bar{\psi} | \mathcal{O}_{\mathcal{B}} | 0 \rangle$ has been discussed in Section 3.6.
5. Mixing has been resolved in Section 3.7, leading to the expression for the two-loop dilatation operator in the $SU(2|3)$ sector in (3.7.18). Diagonalising it leads to two operators with a definite anomalous dimension, another BPS combination (3.7.20) and a descendant of $\mathcal{O}_{\mathcal{K}}$ (3.7.21).

In the next chapter we study form factors of $\text{Tr}(F^3)$ and its $\mathcal{N} = 4$ supersymmetric completion up to two-loop order and find surprising connections between quantities discussed in these two chapters.

Chapter 4

Form factors of $\text{Tr}(F^3)$ in $\mathcal{N}=4$ super Yang-Mills

4.1 Introduction

As reviewed briefly in Chapter 1, one of the main channels of production of the Higgs boson at the LHC is gluon fusion. Since gluons are massless, they do not couple to the Higgs directly but instead the interaction is mediated by loops of colour-charged quarks. In particular, only the loops of heavy quarks – the top ($m_t \sim 178$ GeV) and to a lesser extent the bottom quark ($m_b \sim 5$ GeV) contribute. Even though such fusion is a loop-induced process, the fact that gluon-dense protons are the primary particles collided at the LHC means that it is the most important Higgs production channel there. Indeed, all the other channels, *e.g.* the vector boson fusion $qq \rightarrow Hqq$ or Higgs production $q\bar{q} \rightarrow HW$ are suppressed by about an order of magnitude [151].

An efficient method of computing the contribution of this channel to the fusion cross-section is through effective field theory (EFT), where the heavy top quark is integrated out and the quark loop is replaced by a set of local interactions, reducing the order of the computation by one loop. The effective Lagrangian in the limit where $m_t \gg m_H$ is given by (1.0.11),

$$\mathcal{L}_{\text{eff}} = \hat{C}_0 \mathcal{O}_0 + \frac{1}{m_t^2} \sum_{i=1}^4 \hat{C}_i \mathcal{O}_i + \mathcal{O}(m_t^{-4}) ,$$

where

$$\begin{aligned} \mathcal{O}_0 &\propto H \text{Tr}(F^{\mu\nu} F_{\mu\nu}), & \mathcal{O}_1 &\propto H \text{Tr}(F_\nu{}^\mu F_\mu{}^\sigma F_\sigma{}^\nu), \\ \mathcal{O}_2 &\propto H \text{Tr}(D_\alpha F_{\mu\nu} D^\alpha F^{\mu\nu}), & \mathcal{O}_3 &\propto H \text{Tr}(D^\alpha F_{\alpha\nu} D_\beta F^{\beta\nu}), \\ \mathcal{O}_4 &\propto H \text{Tr}(F_{\alpha\nu} D^\nu D^\beta F_{\beta\alpha}), \end{aligned} \tag{4.1.1}$$

and where H denotes the Higgs. The matching coefficients are inversely proportional to the Higgs vacuum expectation value; at two-loop order, relevant to the present discussion, \hat{C}_0 has been found in [41, 152], and \hat{C}_i for $i = 1, \dots, 4$ have been computed in [37].

In this chapter we focus on the non-protected operator denoted in the effective Lagrangian (1.0.11) as \mathcal{O}_1 , namely $\text{Tr}(F^3)$. In four dimensions it can be rewritten as a sum of selfdual and anti-selfdual terms

$$\text{Tr}(F^3) = \text{Tr}(F_{\text{ASD}}^3) + \text{Tr}(F_{\text{SD}}^3) \propto \mathcal{O}_C + \bar{\mathcal{O}}_C, \quad (4.1.2)$$

where the subscript \mathcal{C} stands for \mathcal{C} omponent. In the spirit of the discussion in Chapter 1, we compute its form factors at two loops in $\mathcal{N}=4$ SYM and for three external gluons, hoping to observe, just as in the case of $\text{Tr}(F^2)$ [30], an overlap between the maximally transcendental parts of the supersymmetric and QCD calculations.

Validity of the effective field theory approximation

One may wonder whether the EFT description provides a good approximation of the full result for Higgs production through a quark loop. The discrepancy between the full amplitude for $H \rightarrow gg$ at leading order and the EFT result is presented in Figure 31 [153].

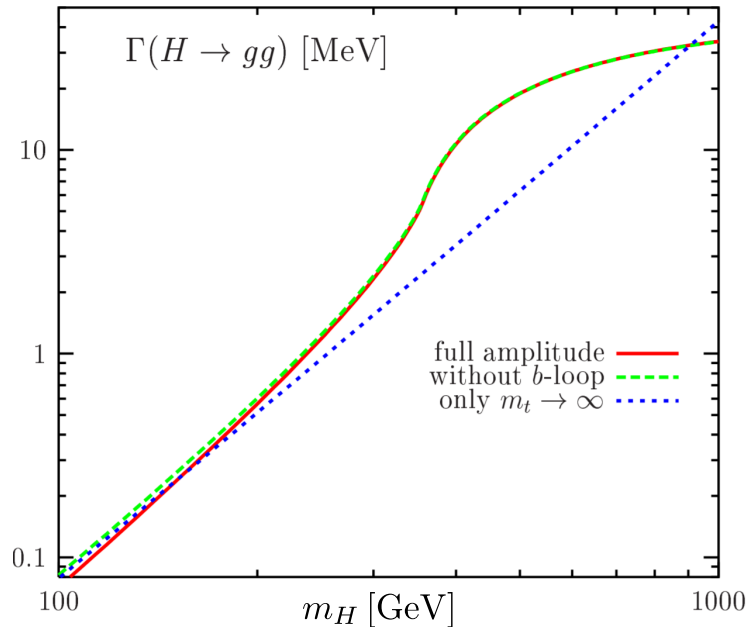


Figure 31: The gluonic decay width as a function of the Higgs mass. The full amplitude (red solid line), top quark loop contribution only (green dashed line) and the $m_t \rightarrow \infty$ limit result (blue dotted line). Figure reprinted with permission from [153].

First of all, comparing the full result for the partial decay width $\Gamma(H \rightarrow gg)$ (red line) with the contribution of the top quark loop only (green line), we see that the results practically coincide, with error below the order of 10%. Compared to the full result, the approximation where the top quark mass is sent to infinity (blue line) and hence contributions from operators other than \mathcal{O}_0 are suppressed, is very accurate, especially below the $m_H = 2m_t$ threshold.³³

As far as the next-to-leading order (NLO) contribution is concerned, the EFT still proves to be a useful approximation. Figure 32 [153] shows the difference between the full and effective QCD correction factor E_H for the partial width $\Gamma(H \rightarrow gg)$ defined via

$$\Gamma(H \rightarrow gg(g), gq\bar{q}) = \Gamma_{\text{LO}}(H \rightarrow gg) \left(1 + \frac{\alpha_s}{\pi} E_H \right), \quad (4.1.3)$$

where the NLO QCD correction width $\Gamma(H \rightarrow gg(g), gq\bar{q})$ includes virtual corrections with gluons are attached to quark loop lines as well as real corrections with three gluons in the final state. The full correction (blue line) and the EFT $m_t \rightarrow \infty$ limit result (red line) agree up to a few percent for $m_H \leq 300$ GeV.

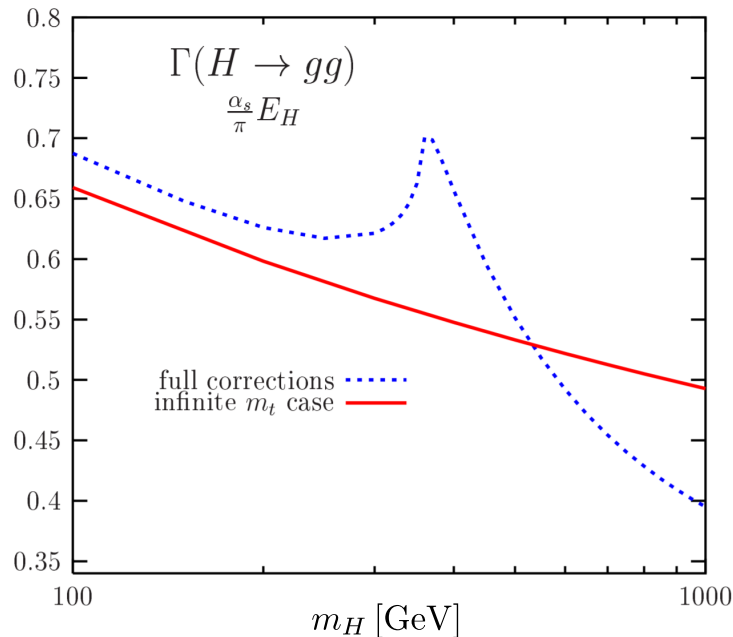


Figure 32: The QCD correction factor for the partial width $\Gamma(H \rightarrow gg)$ as a function of the Higgs mass. The full correction (blue dotted line) and the $m_t \rightarrow \infty$ limit result (red solid line), $\alpha_s = 0.118$. Figure reprinted with permission from [153].

Further checks of validity of the effective expansion in the $m_t \gg m_H$ limit and hence including the higher-dimensional operators have been performed in [38, 154].

³³Above this limit, the amplitude develops an imaginary part.

The rest of this chapter is organised as follows. In Section 4.2 we consider the operators relevant for the present discussion – \mathcal{O}_C and its appropriate supersymmetric completion denoted as \mathcal{O}_S and list their tree-level form factors. Section 4.3 details the computation of the one-loop correction to the minimal form factor of these operators and their one-loop anomalous dimension. In Section 4.4 we find the two-loop minimal form factors using unitarity cuts and present the final result for the two-loop integrands in Section 4.4.5. The two-loop remainder functions of the form factors are found in Section 4.5 and finally in Section 4.6 we make some observations regarding their properties.

4.2 Operators and tree-level form factors

The precise normalisation of $\mathcal{O}_C \propto \text{Tr}(F_{\text{ASD}}^3)$ and $\overline{\mathcal{O}}_C$ is fixed in such a way that the minimal tree-level form factor of \mathcal{O}_C with three positive helicity gluons in the external state is given by

$$F_{\mathcal{O}_C}^{(0)}(1^+, 2^+, 3^+; q) = -[12][23][31], \quad (4.2.1)$$

and hence the minimal form factor of $\overline{\mathcal{O}}_C \propto \text{Tr}(F_{\text{SD}}^3)$ is

$$F_{\overline{\mathcal{O}}_C}^{(0)}(1^-, 2^-, 3^-; q) = \langle 12 \rangle \langle 23 \rangle \langle 31 \rangle. \quad (4.2.2)$$

For computations in later sections we need several non-minimal tree-level form factors of \mathcal{O}_C . Examples of those include members of an infinite family of $\overline{\text{MHV}}$ form factors with three positive helicity gluons and an arbitrary number of negative helicity gluons in the external state,

$$F_{\mathcal{O}_C}^{(0)}(1^-, \dots, i^+, \dots, j^+, \dots, k^+, \dots, n^-; q) = (-1)^n \frac{([ij][jk][ki])^2}{[12][23] \cdots [n1]}. \quad (4.2.3)$$

Note that form factors belonging to this family but with different number of negative helicity gluons are related by soft factors³⁴

$$-\frac{[(s-1)(s+1)]}{[(s-1)s^-][s^-(s+1)]}, \quad (4.2.4)$$

where s denotes a negative-helicity gluon. The expression for these form factors at zero-momentum transfer, *i.e.* with $q=0$, was first given for four and five legs in [34], and later

³⁴Tree-level gluon amplitudes exhibit universal soft behaviour. An n -point amplitude with a soft gluon leg s factorises into a product of $(n-1)$ -point amplitude and a soft factor of the form (4.2.4) if s is of negative helicity, or its counterpart in terms of angle brackets if s has positive helicity [55].

extended to a generic number of particles in [43]. A particular member of this family is

$$F_{\mathcal{O}_c}^{(0)}(1^+, 2^+, 3^+, 4^-; q) = \frac{([12][23][31])^2}{[12][23][34][41]}, \quad (4.2.5)$$

which can be obtained from (4.2.1) by multiplying by the soft factor $-\frac{[31]}{[34][41]}$. A different non-minimal tree-level form factor which we use in the later sections has four positive-helicity gluons in the external state:

$$F_{\mathcal{O}_c}^{(0)}(1^+, 2^+, 3^+, 4^+; q) = \frac{[12][23][34][41]}{s_{12}} \left(1 + \frac{[31][4|q|3]}{s_{23}[41]} \right) + \text{cyclic}(1, 2, 3, 4). \quad (4.2.6)$$

This all-plus form factor has been calculated using Feynman diagrams and MHV diagrams in [38]. Its expression is confirmed by an independent calculation in Appendix D.2.

4.2.1 Supersymmetric form factors and mixing

As reviewed in Section 2.5, the operator \mathcal{O}_c can mix with other operators under renormalisation and hence here we briefly address the mixing before embarking on concrete calculations. An important observation is that in $\mathcal{N}=4$ SYM \mathcal{O}_c is contained within a certain descendant of the Konishi operator generated by acting with tree-level supercharges Q_A^α and $\bar{Q}^{\dot{\alpha}A}$ on the lowest-dimensional operator introduced in (3.2.17)

$$\mathcal{O}_K \sim \epsilon_{ABCD} \text{Tr}(\phi^{AB} \phi^{CD}).$$

Importantly, acting with eight tree-level supercharges $\bar{Q}^{\dot{\alpha}A}$ on \mathcal{O}_K we generate an operator \mathcal{O}_S such that

$$\mathcal{O}_S = \mathcal{O}_c + \mathcal{O}(g_{\text{YM}}), \quad (4.2.7)$$

where the subscript \mathcal{S} stands for \mathcal{S} upersymmetric and the additional $\mathcal{O}(g_{\text{YM}})$ terms are of length four or more in fields and include, for example and schematically $g_{\text{YM}} \text{Tr}(F\psi\psi\phi)$, $g_{\text{YM}} \text{Tr}(\psi^4)$ or $g_{\text{YM}}^3 \text{Tr}(\phi^6)$.³⁵ These corrections can only affect tree-level non-minimal form factors with more than three external lines while at loop level, the mixing can affect also the minimal form factors. Importantly, \mathcal{O}_S solves the mixing problem at one loop, thus any further corrections to \mathcal{O}_S due to mixing can only appear at two-loop order or higher.

Fortunately, the explicit expression for the supersymmetric completion terms are not required for our computations. Indeed, the tree-level MHV form factors of the full

³⁵A simpler situation was addressed in Chapter 3 in the $SU(2|3)$ sector, where two operators mix at dimension three, see Section 3.7 for a detailed discussion.

Konishi multiplet in $\mathcal{N}=4$ SYM have been constructed and expressed in a compact formula [155],

$$\begin{aligned} \langle 1, 2, \dots, n | \mathcal{K}(\theta, \bar{\theta}) | 0 \rangle_{\text{MHV}}^{(0)} &= \\ &= \frac{e^{\sum_{l=1}^n [l\bar{\theta}\theta^l] + \eta_l \langle \theta l \rangle}}{\langle 12 \rangle \cdots \langle n1 \rangle} \sum_{i \leq j < k \leq l} (2 - \delta_{ij})(2 - \delta_{kl}) \epsilon^{ABCD} \hat{\eta}_{iA} \hat{\eta}_{jB} \hat{\eta}_{kC} \hat{\eta}_{lD} \langle jk \rangle \langle li \rangle, \end{aligned} \quad (4.2.8)$$

where $\hat{\eta}_A := \eta_A + 2[\tilde{\lambda} \bar{\theta}_A]$ and η_A are the usual on-shell superspace coordinates labelling the external on-shell states as reviewed in Section 2.4, with $A = 1, \dots, 4$. The θ_α^A and $\bar{\theta}_{A\dot{\alpha}}$ label the components of the Konishi multiplet.

The MHV form factors of $\mathcal{O}_{\mathcal{K}}$ are obtained by setting $\theta = \bar{\theta} = 0$, while the form factors of $\bar{\mathcal{O}}_{\mathcal{S}}$ are obtained by setting $\bar{\theta} = 0$ and extracting the θ^8 -term:

$$\begin{aligned} F_{\bar{\mathcal{O}}_{\mathcal{S}}, \text{MHV}}^{(0)}(1, 2, \dots, n; q) &= \\ &= \frac{1}{144} \frac{\delta^{(8)}(\sum_{i=1}^n \eta_i \lambda_i)}{\langle 12 \rangle \cdots \langle n1 \rangle} \sum_{i \leq j < k \leq l} (2 - \delta_{ij})(2 - \delta_{kl}) \epsilon^{ABCD} \eta_{iA} \eta_{jB} \eta_{kC} \eta_{lD} \langle jk \rangle \langle li \rangle. \end{aligned} \quad (4.2.9)$$

For this particular component we recover the supermomentum-conserving $\delta^{(8)}$ -function for the external on-shell particles, which simplifies the calculations of supersymmetric unitarity cuts such as the ones we employ in Section 4.4.

In this chapter we are interested in two-loop form factors with an external state of three gluons with positive helicities. Taking into account these constraints, there are several further gluonic operators which will appear in the mixing at two loops and need to be considered, namely \mathcal{O}_2 , \mathcal{O}_3 and \mathcal{O}_4 in (4.1.1). The equations of motion relate these to $\mathcal{O}_{\mathcal{C}}$, the operator \mathcal{O}_0 in (4.1.1), and further operators containing fermions and scalars,³⁶ which are irrelevant for the present discussion given the gluonic external state [49]. As a result, the only other operator which we expect to participate in the two-loop mixing is

$$\mathcal{O}_{\mathcal{M}} \propto q^2 \text{Tr}(F^2). \quad (4.2.10)$$

We choose a specific normalisation for this operator in such a way that its tree-level form factor is given by

$$F_{\mathcal{O}_{\mathcal{M}}}^{(0)}(1^+, 2^+, 3^+; q) = \frac{q^6}{\langle 12 \rangle \langle 23 \rangle \langle 31 \rangle} = \frac{F_{\mathcal{O}_{\mathcal{C}}}^{(0)}(1^+, 2^+, 3^+; q)}{uvw}. \quad (4.2.11)$$

³⁶See [38] for a discussion of operator bases in QCD.

4.2.2 Further tree-level form factors

It is interesting to consider further examples of tree-level MHV form factors of \mathcal{O}_S with up to four external legs and contrast them with the corresponding form factors of \mathcal{O}_C . We will make use of these results in our explicit two-loop calculations in Section 4.4 and we list them here together for reader's convenience.

Firstly, from (4.2.9) and its appropriately chosen prefactor, we find that the minimal tree-level form factors are independent of the choice of operator:

$$F_{\overline{\mathcal{O}}_S, \overline{\mathcal{O}}_C}^{(0)}(1^-, 2^-, 3^-; q) = \langle 12 \rangle \langle 23 \rangle \langle 31 \rangle, \quad (4.2.12)$$

and correspondingly

$$F_{\mathcal{O}_S, \mathcal{O}_C}^{(0)}(1^+, 2^+, 3^+; q) = -[12][23][31]. \quad (4.2.13)$$

The situation for four external particles is more involved, and the tree-level form factors depend in general on which of the two operators is studied. However, for purely gluonic external lines there is no difference and from (4.2.9) we recover

$$F_{\mathcal{O}_S, \mathcal{O}_C}^{(0)}(1^+, 2^+, 3^+, 4^-; q) = \frac{[12][23][31]^2}{[34][41]}, \quad (4.2.14)$$

in agreement with (4.2.5). Similarly, if two adjacent external lines are fermionic, the result does not depend on the operator:

$$F_{\mathcal{O}_S, \mathcal{O}_C}^{(0)}(1^+, 2^+, 3^{\psi^4}, 4^{\bar{\psi}^{123}}; q) = \frac{[12][23][31]}{[34]}, \quad (4.2.15)$$

$$F_{\mathcal{O}_S, \mathcal{O}_C}^{(0)}(1^+, 2^+, 3^{\bar{\psi}^{123}}, 4^{\psi^4}; q) = -\frac{[12][24][41]}{[34]}, \quad (4.2.16)$$

where we have explicitly indicated the fermion R -symmetry indices. If in turn two scalars are included in the external state, we need to distinguish between the two cases,

$$F_{\mathcal{O}_C}^{(0)}(1^+, 2^+, 3^{\phi^{12}}, 4^{\phi^{34}}; q) = -\frac{1}{2} \frac{[12]}{[34]} ([13][24] + [14][23]), \quad (4.2.17)$$

and

$$F_{\mathcal{O}_S}^{(0)}(1^+, 2^+, 3^{\phi^{12}}, 4^{\phi^{34}}; q) = F_{\mathcal{O}_C}^{(0)}(1^+, 2^+, 3^{\phi^{12}}, 4^{\phi^{34}}; q) + \frac{1}{6} [12]^2, \quad (4.2.18)$$

where the extra term arises due to a correction of the form, schematically, $\text{Tr}(F^2 \phi \bar{\phi})$ in \mathcal{O}_S . If, on the other hand, the two scalars are not adjacent we find

$$F_{\mathcal{O}_C}^{(0)}(1^+, 2^{\phi^{12}}, 3^+, 4^{\phi^{34}}; q) = 0, \quad (4.2.19)$$

$$F_{\mathcal{O}_S}^{(0)}(1^+, 2^{\phi^{12}}, 3^+, 4^{\phi^{34}}; q) = -\frac{1}{3} [13]^2. \quad (4.2.20)$$

Finally we present a few examples involving fermions in the external state where the form factor vanishes for the operator \mathcal{O}_C but is non-vanishing for \mathcal{O}_S :

$$\begin{aligned} F_{\mathcal{O}_S}^{(0)}(1^+, 2^{\psi^4}, 3^{\phi^{23}}, 4^{\psi^1}; q) &= -\frac{2}{3} [12][14], \\ F_{\mathcal{O}_S}^{(0)}(1^+, 2^{\psi^4}, 3^{\psi^1}, 4^{\phi^{23}}; q) &= \frac{1}{3} [12][13], \\ F_{\mathcal{O}_S}^{(0)}(1^{\psi^4}, 2^{\psi^3}, 3^{\psi^2}, 4^{\psi^1}; q) &= \frac{1}{3} ([12][34] - [14][23]). \end{aligned} \quad (4.2.21)$$

The examples in (4.2.20) and (4.2.21) have no kinematic poles and are produced by the contact terms inside \mathcal{O}_S .

We could equivalently repeat the entire discussion and consider form factors of the conjugate operator $\overline{\mathcal{O}}_C$, with all helicities of external particles flipped. These are obtained from the form factors of \mathcal{O}_C by the replacement $\langle ab \rangle \leftrightarrow -[ab]$, according to (A.3.2). In terms of states, this corresponds to performing the transformation

$$\phi^{AB} \rightarrow \frac{1}{2} \epsilon_{ABCD} \phi^{CD}, \quad \psi^{ABC} \rightarrow \epsilon_{ABCD} \psi^D, \quad \psi^D \rightarrow \frac{1}{3!} \epsilon_{ABCD} \psi^{ABC}. \quad (4.2.22)$$

We also note that the $\overline{\text{MHV}}$ form factors of \mathcal{O}_S were found using the helicity-flip rule $\langle ab \rangle \leftrightarrow -[ab]$ on (4.2.9).

4.3 One-loop minimal form factors

An important ingredient needed to compute two-loop form factors using generalised unitarity cuts is the one-loop correction to the minimal form factor of the operators \mathcal{O}_S and \mathcal{O}_C . In both cases the only non-vanishing result is obtained for an external state of three positive-helicity gluons and is completely determined by the two-particle cut shown in Figure 33 together with its cyclic permutations.

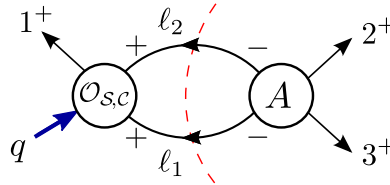


Figure 33: A two-particle cut of the one-loop minimal form factor of \mathcal{O}_S or \mathcal{O}_C .

The tree-level MHV gluon amplitude entering this cut is

$$A^{(0)}(\ell_1^-, \ell_2^-, 2^+, 3^+) = i \frac{\langle \ell_1 \ell_2 \rangle^3}{\langle \ell_2 2 \rangle \langle 23 \rangle \langle 3 \ell_1 \rangle}, \quad (4.3.1)$$

whereas the tree-level form factor is given in (4.2.13) so that the two-particle cut of the one-loop form factor is given by

$$F_{\mathcal{O}_S, \mathcal{O}_C}^{(1)}(1^+, 2^+, 3^+; q) \Big|_{2, s_{23}} = i [1\ell_2][\ell_2\ell_1][\ell_11] \frac{\langle \ell_1\ell_2 \rangle^3}{\langle \ell_22 \rangle \langle 23 \rangle \langle 3\ell_1 \rangle}. \quad (4.3.2)$$

Multiplying and dividing the integrand by $[\ell_2\ell_1]$ and using the fact that due to momentum conservation $\ell_1 + \ell_2 = -p_2 - p_3$ we can manipulate the expression by noting that on the cut

$$[\ell_2\ell_1]\langle \ell_1\ell_2 \rangle = (\ell_1 + \ell_2)^2 = s_{23}, \quad -[\ell_1\ell_2]\langle \ell_22 \rangle = \langle 23 \rangle [3\ell_1]. \quad (4.3.3)$$

Upon such simplification, the integrand becomes

$$\begin{aligned} F_{\mathcal{O}_S, \mathcal{O}_C}^{(1)}(1^+, 2^+, 3^+; q) \Big|_{2, s_{23}} &= -i \left(\frac{s_{23}}{\langle 23 \rangle} \right)^2 \frac{[1\ell_2]\langle \ell_2\ell_1 \rangle [\ell_11]}{2(p_3 \cdot \ell_1)} \\ &= i [23]^2 \frac{[1|\ell_1\ell_2|1]}{2(p_2 \cdot \ell_1)}. \end{aligned} \quad (4.3.4)$$

The cuts in the s_{12} - and s_{31} -channels are obtained by relabelling this expression. Factoring out the tree-level object (4.2.13) and performing a standard PV reduction we arrive at an expression where the cut integrals can be lifted off shell unambiguously. We obtain

$$F_{\mathcal{O}_S, \mathcal{O}_C}^{(1)}(1^+, 2^+, 3^+; q) \quad (4.3.5)$$

$$= i F_{\mathcal{O}_S, \mathcal{O}_C}^{(0)}(1^+, 2^+, 3^+; q) \left(2 \times \begin{array}{c} q \\ \swarrow \quad \searrow \\ \text{circle} \\ \swarrow \quad \searrow \\ 1 \quad 2 \\ \quad \quad 3 \end{array} + s_{23} \times \begin{array}{c} q \\ \swarrow \quad \searrow \\ \text{triangle} \\ \swarrow \quad \searrow \\ 3 \quad 2 \end{array} + \text{cyclic}(1, 2, 3) \right).$$

Note that this formula should be multiplied by a factor of the 't Hooft coupling (2.4.1). Due to the normalisation of the tree-level form factor (4.2.1) the one-loop correction (4.3.5) is universal for both operators \mathcal{O}_S and \mathcal{O}_C . Moreover, comparing (4.3.5) with the expression for the one-loop form factor of \mathcal{O}_B in (3.2.13) we see that the one-loop form factors coincide, up to factoring out the corresponding tree-level form factor. Using (4.3.5) we can extract the one-loop anomalous dimensions of \mathcal{O}_S and \mathcal{O}_C at one loop from the coefficient of the UV-divergent bubble integral, as discussed in detail for \mathcal{O}_B in Section 3.2.1. It turns out that at this order these operators are eigenstates of the dilatation operator with anomalous dimension

$$\gamma_{\mathcal{O}_S, \mathcal{O}_C}^{(1)} = 12a, \quad (4.3.6)$$

which is the same as the one-loop anomalous dimension of $\mathcal{O}_{\mathcal{B}}$ found in (3.2.16). This observation, together with the fact that at zero coupling $\mathcal{O}_{\mathcal{B}}$ and $\mathcal{O}_{\mathcal{S}}$ are related by supersymmetry transformations, was the original motivation for the study of the two-loop form factor of $\mathcal{O}_{\mathcal{B}}$ presented in Chapter 3.

4.4 Two-loop minimal form factors in $\mathcal{N}=4$ SYM

In this section we determine the two-loop form factors of the operators $\mathcal{O}_{\mathcal{S}}$ and $\mathcal{O}_{\mathcal{C}}$ introduced in Section 4.2 using the strategy analogous to that employed in calculation of the two-loop form factor of $\mathcal{O}_{\mathcal{B}}$ presented in Chapter 3:

1. First, we consider two-particle cuts in one of the possible kinematic channels, for example the s_{23} -channel. There are two cuts to consider, shown in Figure 34(i) and 34(ii).
2. We then move on to the three-particle cut in the q^2 -channel, presented in Figure 34(iii), which we use to fix potential ambiguities of the previous result and to detect integral topologies which do not have a two-particle cut.
3. Finally we turn to the more involved three-particle cut in the s_{23} -channel, presented in Figure 34(iv), where we fix all remaining ambiguities of the integrand.
4. By consistently merging the results of all the cuts, we construct the complete four-dimensional integrand at two loops.

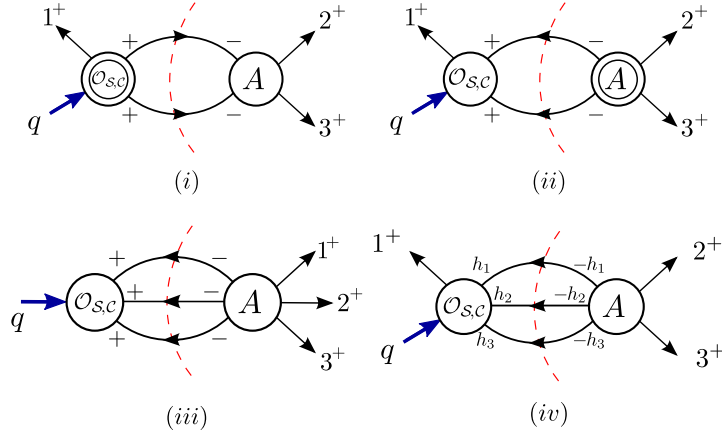


Figure 34: Four different cuts of the two-loop form factors which will be used to construct the two-loop integrand.

4.4.1 Two-particle cuts

We begin by calculating the two-particle cuts of the two-loop form factor. These can only be considered in the s_{23} -channel since in the q^2 -channel the two-particle cut would lead to a sub-minimal tree-level form factor, which does not exist at this loop order. We proceed to consider the following two-particle cuts in the s_{23} -channel: the case with $F^{(0)} \times A^{(1)}$ and that with $F^{(1)} \times A^{(0)}$.

Tree-level form factor \times one-loop amplitude

We consider the two-particle cut presented in Figure 35, whose ingredients are a tree-level form factor and a one-loop amplitude. Similarly to the one-loop case in Figure 33, this cut is universal for the two operators, \mathcal{O}_S and \mathcal{O}_C , due to the equality of the tree-level minimal form factors (4.2.13).

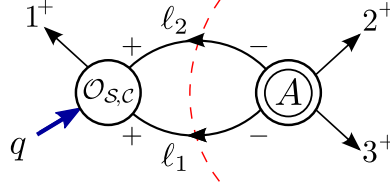


Figure 35: A double cut of the two-loop minimal form factor of $\mathcal{O}_S, \mathcal{O}_C$: the case of a tree-level form factor joined to a one-loop amplitude.

The four-point one-loop amplitude in $\mathcal{N}=4$ SYM on the right-hand-side of the cut has a very simple form,

$$A^{(1)}(\ell_1^-, \ell_2^-, 2^+, 3^+) = A^{(0)}(\ell_1^-, \ell_2^-, 2^+, 3^+) \left[-s_{23}s_2\ell_2 \times \begin{array}{c} \ell_1 \swarrow \quad \searrow 2 \\ \square \\ \ell_2 \swarrow \quad \searrow 3 \end{array} \right]. \quad (4.4.1)$$

Combining the amplitude (4.4.1) and the form factor (4.2.13) we see that the algebra of the one-loop calculation in Section 4.3 iterates. Reinstating the cut propagators we arrive at the following result for this two-particle cut:

$$F_{\mathcal{O}_S, \mathcal{O}_C}^{(2)}(1^+, 2^+, 3^+; q) \Big|_{2, s_{23}} = F_{\mathcal{O}_S, \mathcal{O}_C}^{(0)}(1^+, 2^+, 3^+; q) s_{23}^2 \frac{[1|q\ell_1|1]}{[12]\langle 23\rangle[31]} \times \begin{array}{c} 1 \swarrow \quad \searrow q \\ \ell_1 \swarrow \quad \searrow \ell_2 \\ \square \\ 3 \swarrow \quad \searrow 2 \end{array} + \text{cyclic}(1, 2, 3). \quad (4.4.2)$$

One-loop form factor \times tree-level amplitude

Next we turn our attention to the second of the two-particle cuts, shown in Figure 36, in which we glue a one-loop minimal form factor and a tree-level amplitude. As discussed in Section 4.3 the one loop form factor (4.3.5) is the same for \mathcal{O}_S and \mathcal{O}_C and as a result this cut is identical for the two operators.

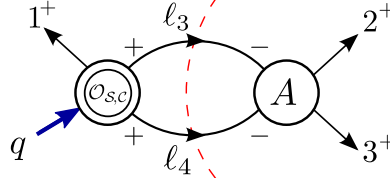


Figure 36: A double cut of the two-loop minimal form factor of $\mathcal{O}_S, \mathcal{O}_C$ – the case of a one-loop form factor joined to a tree-level amplitude.

In order to construct the integrand, it is important that we use the expression for the one-loop form factor (4.3.5) prior to PV reduction, as given in (4.3.4). The reason is that the reduction procedure discards certain integrals that vanish in dimensional regularisation, *e.g.* scaleless bubbles. Such integrals may however appear as subtopologies inside a two-loop integral and therefore should not be discarded at an earlier stage of the calculation. Thus, in order to obtain the complete result for the two-particle cut we use the expression for the one-loop form factor *before* the PV reduction, namely:

$$F_{\mathcal{O}_S, \mathcal{O}_C}^{(1)}(1^+, 2^+, 3^+; q) = i \left(\frac{s_{23}}{\langle 23 \rangle} \right)^2 [1|q \ell|1] \times \begin{array}{c} q \nearrow 1 \\ \ell \nearrow \\ \searrow \\ 3 \quad 2 \end{array} + \text{cyclic}(1, 2, 3).$$

Using the tree-level four-gluon amplitude in (4.3.1) and rewriting it in the pictorial notation as

$$A^{(0)}(\ell_4^-, \ell_3^-, 2^+, 3^+) = -i \frac{\langle \ell_3 \ell_4 \rangle^2}{\langle 23 \rangle^2} \frac{s_{23}}{2(p_2 \cdot \ell_3)} = -i s_{23} \left(\frac{\langle \ell_3 \ell_4 \rangle}{\langle 23 \rangle} \right)^2 \times \begin{array}{c} \ell_4 \quad \ell_3 \\ \downarrow \quad \downarrow \\ 3 \quad 2 \end{array}, \quad (4.4.3)$$

where we recall that each line represents a propagator stripped of the factor of i and factors of i arising from propagators are collected separately, we arrive at the following

expression for the two-particle cut:

$$\begin{aligned}
 F_{\mathcal{O}_S, \mathcal{O}_C}^{(2)}(1^+, 2^+, 3^+; q) \Big|_{2, s_{23}} &= -s_{23} \left(\frac{\langle \ell_3 \ell_4 \rangle}{\langle 23 \rangle} \right)^2 \times \left[\left(\frac{s_{\ell_3 \ell_4}}{\langle \ell_3 \ell_4 \rangle} \right)^2 [1|q \cdot \ell|1] \times \right. \\
 &+ \left. \left(\frac{s_{\ell_4 1}}{\langle \ell_4 1 \rangle} \right)^2 [\ell_3 | q \cdot \ell | \ell_3] \times \right. \\
 &+ \left. \left(\frac{s_{1 \ell_3}}{\langle 1 \ell_3 \rangle} \right)^2 [\ell_4 | \ell \cdot q | \ell_4] \times q \right] \times \text{Diagram}
 \end{aligned}
 \tag{4.4.4}$$

The first integral in (4.4.4) with its numerator can be simplified to

$$-\frac{s_{23}^3}{\langle 23 \rangle^2} [1|q \cdot \ell|1] \times \text{Diagram} = F_{\mathcal{O}_S, \mathcal{O}_C}^{(0)}(1^+, 2^+, 3^+; q) s_{23}^2 \frac{[1|q \ell|1]}{[12] \langle 23 \rangle [31]} \times \text{Diagram}$$

We immediately see that this is identical to the result of the two-particle cut (4.4.2), where we have computed the case of $F^{(0)} \times A^{(1)}$. This would lead to the conclusion that the correct answer is obtained by simply lifting (4.4.5) off shell. However, an important subtlety arises here. Any term proportional to ℓ^2 (or $(\ell + p_2 + p_3)^2$) would cancel one of the propagators and generate the integral topology in Figure 37 (or its mirror).

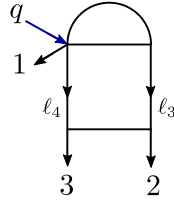


Figure 37: Integral topology that cannot be detected by the two-particle s_{23} -channel cut.

When ℓ_3 and ℓ_4 are cut a scale-free bubble on the form factor side is isolated, which vanishes in dimensional regularisation. As a result, we cannot make any meaningful statement about the presence of this topology given the information provided only by this pair of two-particle cuts, and we must defer the verdict until three-particle cuts

have been considered. This will be discussed in detail in Section 4.4.4.

In order to perform an integral reduction using `LiteRed`, it is useful to rewrite the numerator of (4.4.5) in terms of scalar products of momenta:

$$\begin{aligned} s_{23}^2 \frac{[1|q\ell|1]}{[12]\langle 23\rangle[31]} &= \frac{s_{23}^2}{s_{12}s_{23}s_{31}} \text{Tr}_+(1q\ell 132) \\ &= \frac{s_{23}}{2s_{13}} (s_{23}s_{\ell 1} - s_{\ell 3}s_{12} + s_{13}s_{\ell 2}) - \frac{s_{23}}{2s_{12}} (s_{23}s_{\ell 1} - s_{\ell 2}s_{13} + s_{12}s_{\ell 3}). \end{aligned} \quad (4.4.6)$$

We now perform a PV reduction on the terms which contain the invariant $s_{1\ell}$ since any dependence on p_1 is unphysical and only the combination $q-p_1$ is relevant. Following the standard steps we find that

$$s_{1\ell} \times \begin{array}{c} \begin{array}{c} 1 \quad q \\ \diagdown \quad \diagup \\ \ell \\ \diagup \quad \diagdown \\ \square \\ \diagdown \quad \diagup \\ 3 \quad 2 \end{array} \end{array} = \frac{1}{s_{23}} [s_{12}s_{3\ell} + s_{13}s_{2\ell}] \times \begin{array}{c} \begin{array}{c} 1 \quad q \\ \diagdown \quad \diagup \\ \ell \\ \diagup \quad \diagdown \\ \square \\ \diagdown \quad \diagup \\ 3 \quad 2 \end{array} \end{array}. \quad (4.4.7)$$

Inserting this result into (4.4.6), we find that (4.4.5) becomes

$$-\frac{s_{23}^3}{\langle 23\rangle^2} [1|q\ell|1] \times \begin{array}{c} \begin{array}{c} 1 \quad q \\ \diagdown \quad \diagup \\ \ell \\ \diagup \quad \diagdown \\ \square \\ \diagdown \quad \diagup \\ 3 \quad 2 \end{array} \end{array} = F_{\mathcal{O}_S, \mathcal{O}_C}^{(0)}(1^+, 2^+, 3^+; q) s_{23} (s_{2\ell} - s_{3\ell}) \times \begin{array}{c} \begin{array}{c} 1 \quad q \\ \diagdown \quad \diagup \\ \ell \\ \diagup \quad \diagdown \\ \square \\ \diagdown \quad \diagup \\ 3 \quad 2 \end{array} \end{array}. \quad (4.4.8)$$

Note that p_1 no longer appears in the numerator, as desired. Inspecting the result of the two-particle cut in (4.4.8) we see that, because of the form of the numerator factor $(s_{2\ell} - s_{3\ell})$ it is impossible to say at this stage whether $s_{2\ell}$ and $s_{3\ell}$ stand for a full invariant or just a scalar product of two momenta – the ℓ^2 -terms which would arise from the full invariants cancel in the difference. This is a manifestation of the ambiguity mentioned earlier, leading to topologies of the type depicted in Figure 37. This matter will be settled in Section 4.4.4 by means of a three-particle cut.

We now move to the second term of (4.4.4). After factoring out the the tree-level

form factor, it can be rewritten as

$$F_{\mathcal{O}_S, \mathcal{O}_C}^{(0)}(1^+, 2^+, 3^+; q) \frac{\text{Tr}_+(1 q \ell_3 q \ell \ell_3 q 1 3 2)}{s_{12}s_{23}s_{13}} \times \text{Diagram} \quad (4.4.9)$$

while the numerator of the third integral of (4.4.4) can be obtained from (4.4.9) upon relabelling ($\ell_3 \leftrightarrow \ell_4, 2 \leftrightarrow 3$)

$$F_{\mathcal{O}_S, \mathcal{O}_C}^{(0)}(1^+, 2^+, 3^+; q) \frac{\text{Tr}_+(1 q \ell_4 q \ell \ell_4 q 1 2 3)}{s_{12}s_{23}s_{13}} \times q \text{Diagram} \quad (4.4.10)$$

Summary of results after two-particle cuts

For the reader's convenience, in Table 4 we summarise the results of the cuts we have performed so far. We have presented each distinct integral topology with the corresponding numerator we have detected. The result after the two particle cuts consists of the three topologies with their numerators and the two remaining cyclic shifts of the external momentum labels.

4.4.2 Three-particle cut in q^2 -channel

In this section we consider the three-particle cut of the two-loop form factor in the q^2 -channel, as presented in Figure 50. We note that for this channel there exists only one possible helicity assignment for the momenta running in the loop – all gluons.

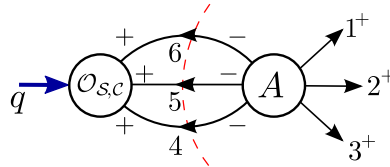


Figure 38: Triple-cut of the two-loop form factor in the q^2 -channel. Only one possible helicity assignment exists.

Integral topology			
Numerator	$s_{23}(s_{2\ell} - s_{3\ell})$	$\frac{\text{Tr}_+(1 q \ell_3 q \ell \ell_3 q 1 3 2)}{s_{12}s_{23}s_{13}}$	$\frac{\text{Tr}_+(1 q \ell_4 q \ell \ell_4 q 1 2 3)}{s_{12}s_{23}s_{13}}$
Ambiguity	ℓ	ℓ_3, ℓ_4	ℓ_3, ℓ_4

Table 4: Summary of the results of the two-particle cuts considered so far. All numerators have the tree-level form factor (4.2.1) factored out. The propagators which appear cut are still ambiguous given the cuts performed so far.

For the six-point tree-level gluon amplitude, we use the expression of [11], which reads

$$\begin{aligned}
 A^{(0)}(1^+, 2^+, 3^+, 4^-, 5^-, 6^-) = i \left[\frac{\overbrace{([23]\langle 56 \rangle [1|p_2 + p_3|4])^2}^{\beta^2}}{s_{234}s_{23}s_{34}s_{56}s_{61}} + \frac{\overbrace{([12]\langle 45 \rangle [3|p_1 + p_2|6])^2}^{\gamma^2}}{s_{345}s_{34}s_{45}s_{61}s_{12}} \right. \\
 \left. + \frac{\overbrace{s_{123}[23]\langle 56 \rangle [1|p_2 + p_3|4][12]\langle 45 \rangle [3|p_1 + p_2|6]}^{\beta\gamma}}{s_{12}s_{23}s_{34}s_{45}s_{56}s_{61}} \right], \quad (4.4.11)
 \end{aligned}$$

and for the tree-level form factor, as before, we use (4.2.13). We now consider the contribution of each term in (4.4.11) separately - for detailed derivation of the integrand in this cut channel, see Appendix C.2.

β^2 -term: The first term in (4.4.11) gives rise to a previously-detected topology, namely

$$F_{\mathcal{O}_S, \mathcal{O}_C}^{(2)}(1^+, 2^+, 3^+; q) \Big|_{3, q^2}^{\beta^2} = F_{\mathcal{O}_S, \mathcal{O}_C}^{(0)}(1^+, 2^+, 3^+; q) \frac{\text{Tr}_+(1 q 4 5 6 4 q 1 2 3)}{s_{12}s_{23}s_{13}} \times q \cdot \text{Diagram} \quad (4.4.12)$$

After an appropriate relabelling, it is easy to see that the numerator becomes identical to that of (4.4.10), obtained from a two-particle cut. In particular in order to compare (4.4.10) to (4.4.12) we simply relabel $\ell_4 \rightarrow -p_4$ and $\ell \rightarrow p_5$ to immediately see that the

two numerators are identical after using $q = -p_4 - p_5 - p_6$.

γ^2 -term: Considering the second term in (4.4.11) we detect a similarly familiar topology, namely

$$F_{\mathcal{O}_S, \mathcal{O}_C}^{(2)}(1^+, 2^+, 3^+; q) \Big|_{3, q^2}^{\gamma^2} = F_{\mathcal{O}_S, \mathcal{O}_C}^{(0)}(1^+, 2^+, 3^+; q) \frac{\text{Tr}_+(3 q 6 5 4 6 q 3 2 1)}{s_{12}s_{23}s_{13}} \times \text{Diagram} \quad (4.4.13)$$

Once again, after an appropriate relabelling we observe that the numerator (4.4.13) is the same as in (4.4.9). In particular, under $\ell_3 \rightarrow -p_6$ and $\ell \rightarrow p_4$ and with $q = -p_4 - p_5 - p_6$ the two traces become identical. This shows that the results for this topology obtained from two- and three- particle cuts are mutually consistent.

$\beta\gamma$ -term: Finally, we consider the third term in (4.4.11), for which we obtain

$$F_{\mathcal{O}_S, \mathcal{O}_C}^{(2)}(1^+, 2^+, 3^+; q) \Big|_{3, q^2}^{\beta\gamma} = F_{\mathcal{O}_S, \mathcal{O}_C}^{(0)}(1^+, 2^+, 3^+; q) \frac{s_{123}}{s_{12}s_{23}s_{13}} \text{Tr}_+(1 q 6 4 q 3) \times \text{Diagram} \quad (4.4.14)$$

This is a new topology which could not have been detected by any of the two-particle cuts. As such, we add it to our result for the integrand. The numerator of this last integral will be confirmed by a different three-particle cut considered in the next section but we can note that p_5 does not appear in the numerator and as such is not ambiguous. Table 5 summarises the integrand as found by the two- and three-particle cuts studied up to this point.

4.4.3 Three-particle cut in s_{23} -channel

In this section we compute the last three-particle cut of the two-loop form factor we need to consider: the s_{23} -channel cut presented in Figure 39. This is the most intricate cut, as it involves a non-minimal tree-level form factor, and we will see that it provides the necessary final constraints to fix the two-loop integrand completely. The motivation to consider this cut is two-fold: first, we would like to fix potential ambiguities in the numerators of the other previously detected topologies as shown in Table 5, since they

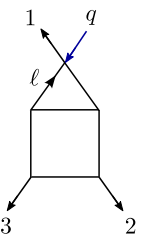
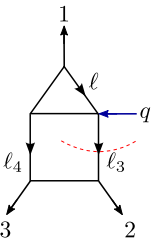
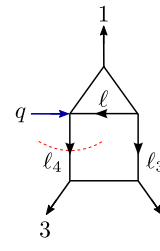
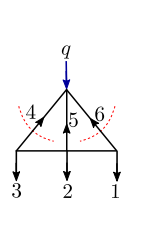
Integral topology				
Numerator	$s_{23} (s_{2\ell} - s_{3\ell})$	$\frac{\text{Tr}_+(1 q \ell_3 q \ell \ell_3 q 1 3 2)}{s_{12}s_{23}s_{13}}$	$\frac{\text{Tr}_+(1 q \ell_4 q \ell \ell_4 q 1 2 3)}{s_{12}s_{23}s_{13}}$	$\frac{s_{123} \text{Tr}_+(1 q 6 4 q 3)}{s_{12}s_{23}s_{13}}$
Ambiguity	ℓ	ℓ_3	ℓ_4	p_4, p_6

Table 5: Summary of the result after the two-particle cuts and the three-particle cut in the q^2 -channel. All numerators have the tree-level form factor (4.2.1) factored out. The propagators which are cut are still ambiguous given the cuts performed so far.

all have a non-vanishing three-particle cut in the s_{23} -channel. Moreover, we expect to observe new integrals which have non-vanishing cuts only in this channel.

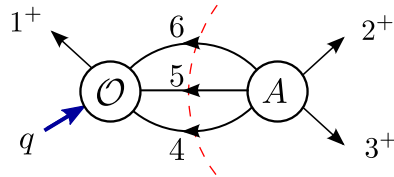


Figure 39: Triple cut of the two-loop form factor in the s_{23} -channel.

This cut also carries important information which distinguishes the two-loop form factors of the operators \mathcal{O}_S and \mathcal{O}_C . Since it features a non-minimal tree-level form factor, fermions and scalars can run in the loops, unlike the case of the triple cut in the q^2 -channel where only gluons could appear. As a result, the non-minimal form factor is sensitive to the choice of the operator, as confirmed by the expressions for tree-level form factors in Section 4.2.2. In what follows, we will work first with the operator \mathcal{O}_C , and then move on to consider the operator \mathcal{O}_S . We begin by presenting the ingredients of the computation and subsequently discuss the methodology and results.

Component calculation

Working in components, the triple cut in the s_{23} -channel requires us to consider separately all possible configurations of gluons, fermions and scalars for the particles running in the loop. Below we discuss each case in turn.

Gluons in the loop: First, we consider diagrams where only gluons are running in the loop. There are two possible cases, involving either an MHV or $\overline{\text{MHV}}$ amplitude and respectively an $\overline{\text{MHV}}$ or next-to- $\overline{\text{MHV}}$ form factor. The case with an $\overline{\text{MHV}}$ amplitude is presented in Figure 40, and there is only one possible helicity configuration for the internal particles.

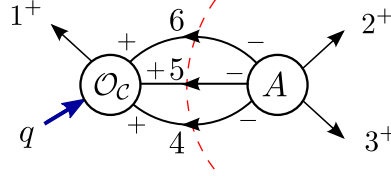


Figure 40: Triple cut of the two-loop form factor in the s_{23} -channel with only gluons running in the loop involving an $\overline{\text{MHV}}$ amplitude.

We have computed the the tree-level form factor entering the cut using MHV diagrams applied to form factors. The result was quoted in (4.2.6) and derived in Appendix D.2; we write it here for the choice of loop momenta directions as indicated in Figure 40:

$$\begin{aligned}
 F_{\mathcal{O}_c}^{(0)}(1^+, -6^+, -5^+, -4^+; q) &= -[16][65][54][41] \left[\frac{1}{s_{16}} \left(1 - \frac{[51][4|q|5]}{s_{56}[41]} \right) \right. \\
 &\quad \left. - \frac{1}{s_{56}} \left(1 - \frac{[46][1|q|4]}{s_{45}[16]} \right) - \frac{1}{s_{54}} \left(1 - \frac{[15][6|q|1]}{s_{14}[65]} \right) + \frac{1}{s_{14}} \left(1 + \frac{[64][5|q|6]}{s_{16}[54]} \right) \right].
 \end{aligned} \tag{4.4.15}$$

The five-point tree-level $\overline{\text{MHV}}$ amplitude is given by

$$A^{(0)}(2^+, 3^+, 4^-, 5^-, 6^-) = -i \frac{[23]^3}{[34][45][56][62]}. \tag{4.4.16}$$

The second possible internal helicity assignment involves an MHV amplitude. In this case, there are three configurations depending on the position of the internal positive-helicity gluon. These are indicated in Figure 41.

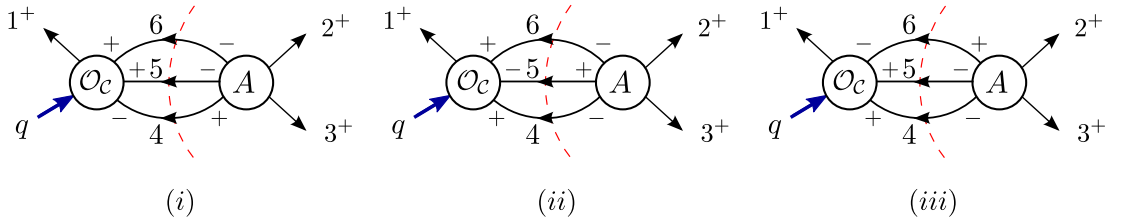


Figure 41: Triple cut of the two-loop form factor in the s_{23} -channel with only gluons running in the loop: the case of $F^{\overline{\text{MHV}}} \times A^{\text{MHV}}$.

The form factors entering the cuts above are a part of an $\overline{\text{MHV}}$ family (4.2.3), whose

expression is known for any number of legs, and in particular

$$\begin{aligned}
 F_{\mathcal{O}_c}^{(0)}(1^+, -6^+, -5^+, -4^-; q) &= \frac{[16][65][51]^2}{[54][41]}, \\
 F_{\mathcal{O}_c}^{(0)}(1^+, -6^+, -5^-, -4^+; q) &= \frac{[16][64]^2[41]}{[65][54]}, \\
 F_{\mathcal{O}_c}^{(0)}(1^+, -6^-, -5^+, -4^+; q) &= \frac{[15]^2[54][41]}{[16][65]}.
 \end{aligned} \tag{4.4.17}$$

For the tree-level MHV amplitudes entering the cut we have

$$\begin{aligned}
 A^{(0)}(2^+, 3^+, 4^+, 5^-, 6^-) &= i \frac{\langle 56 \rangle^3}{\langle 23 \rangle \langle 34 \rangle \langle 45 \rangle \langle 62 \rangle}, \\
 A^{(0)}(2^+, 3^+, 4^-, 5^+, 6^-) &= i \frac{\langle 46 \rangle^4}{\langle 23 \rangle \langle 34 \rangle \langle 45 \rangle \langle 56 \rangle \langle 62 \rangle}, \\
 A^{(0)}(2^+, 3^+, 4^-, 5^-, 6^+) &= i \frac{\langle 45 \rangle^3}{\langle 23 \rangle \langle 34 \rangle \langle 56 \rangle \langle 62 \rangle}.
 \end{aligned} \tag{4.4.18}$$

Scalars in the loop: We now consider the case where we allow scalars to run in the loop in addition to gluons, as presented in Figure 42.

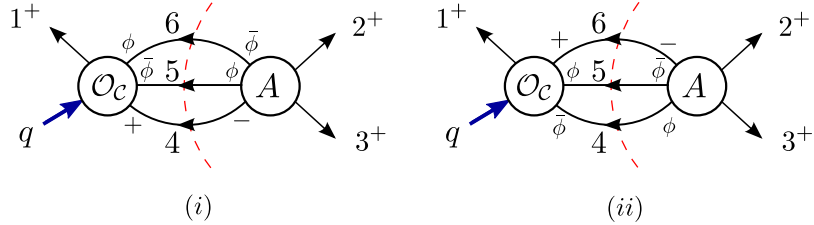


Figure 42: Triple cut of the two-loop form factor in the s_{23} -channel with two scalars and a gluon running in the loop.

The non-minimal tree-level form factor for the configuration in Figure 42(i) is

$$F_{\mathcal{O}_c}^{(0)}(1^+, -6^\phi, -5^{\bar{\phi}}, -4^+; q) = -\frac{1}{2} \frac{[14]}{[65]} ([54][16] + [51][46]), \tag{4.4.19}$$

while the tree-level amplitude is given by

$$A^{(0)}(2^+, 3^+, 4^-, 5^\phi, 6^{\bar{\phi}}) = i \frac{\langle 45 \rangle \langle 46 \rangle^2}{\langle 23 \rangle \langle 34 \rangle \langle 56 \rangle \langle 62 \rangle}. \tag{4.4.20}$$

We note that the result of this diagram needs to be multiplied by a factor of three to account for the distinct complex scalar/anti-scalar pairs arising from the splitting of the gluon in $\mathcal{N}=4$ SYM. One could also imagine diagrams where we assign the scalars in the opposite way, with $\bar{\phi}$ incoming into the form factor on leg p_6 and ϕ on leg p_5 .

However, the form factor and amplitude turn out to be identical to those of the previous case, hence such diagram would lead to the same result as that in Figure 42(i). We multiply our result by a further factor of two to account for this.

The second configuration of scalars we need to consider is presented in Figure 42(ii) – note that the two scalars can only be adjacent as they arise from the splitting of a gluon into a scalar/anti-scalar pair. In this case, the tree-level form factor and amplitude read

$$F_{\mathcal{O}_c}^{(0)}(1^+, -6^+, -5^\phi, -4^{\bar{\phi}}; q) = -\frac{1}{2} \frac{[16]}{[54]} ([46][51] + [41][56]), \quad (4.4.21)$$

$$A^{(0)}(2^+, 3^+, 4^\phi, 5^{\bar{\phi}}, 6^-) = i \frac{\langle 56 \rangle \langle 46 \rangle^2}{\langle 23 \rangle \langle 34 \rangle \langle 45 \rangle \langle 62 \rangle}.$$

Similarly to the case discussed above, we need to multiply this result by six in order to account for the helicity state sum and the opposite assignment of scalar/anti-scalar pair for the internal legs.

Fermions in the loop: Finally, we consider the case with fermions running in the loop, as shown in Figure 43.

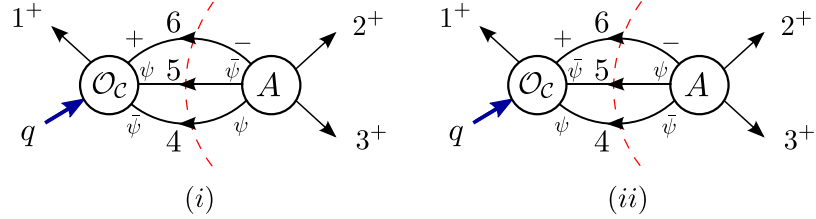


Figure 43: Triple cut of the two-loop form factor in the s_{23} -channel – fermions and a gluon running in the loop, the first possible configuration.

The non-minimal tree-level form factors are given by

$$F_{\mathcal{O}_c}^{(0)}(1^+, -6^+, -5^\psi, -4^{\bar{\psi}}; q) = -\frac{[51][56][16]}{[54]}, \quad (4.4.22)$$

$$F_{\mathcal{O}_c}^{(0)}(1^+, -6^+, -5^{\bar{\psi}}, -4^\psi; q) = \frac{[41][46][16]}{[54]},$$

while the tree-level amplitudes entering the cuts are

$$A^{(0)}(2^+, 3^+, 4^\psi, 5^{\bar{\psi}}, 6^-) = i \frac{\langle 56 \rangle^2 \langle 46 \rangle}{\langle 23 \rangle \langle 34 \rangle \langle 45 \rangle \langle 62 \rangle}, \quad (4.4.23)$$

$$A^{(0)}(2^+, 3^+, 4^{\bar{\psi}}, 5^\psi, 6^-) = -i \frac{\langle 46 \rangle^3}{\langle 23 \rangle \langle 34 \rangle \langle 45 \rangle \langle 62 \rangle}.$$

The second possible helicity configuration is that presented in Figure 44.

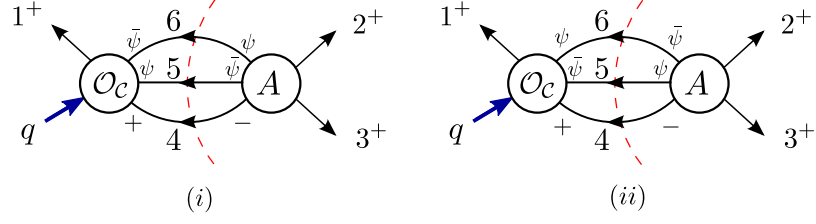


Figure 44: Triple cut of the two-loop form factor in the s_{23} -channel - fermions and a gluon running in the loop, the second possible configuration.

In this case, the tree-level form factors are

$$\begin{aligned}
 F_{\mathcal{O}_C}^{(0)}(1^+, -6^{\bar{\psi}}, -5^{\psi}, -4^+; q) &= \frac{[54][51][41]}{[65]}, \\
 F_{\mathcal{O}_C}^{(0)}(1^+, -6^{\psi}, -5^{\bar{\psi}}, -4^+; q) &= -\frac{[64][61][41]}{[65]},
 \end{aligned}
 \tag{4.4.24}$$

and the tree-level amplitudes are

$$\begin{aligned}
 A^{(0)}(2^+, 3^+, 4^-, 5^{\bar{\psi}}, 6^{\psi}) &= -i \frac{\langle 45 \rangle^2 \langle 46 \rangle}{\langle 23 \rangle \langle 34 \rangle \langle 56 \rangle \langle 62 \rangle}, \\
 A^{(0)}(2^+, 3^+, 4^-, 5^{\psi}, 6^{\bar{\psi}}) &= i \frac{\langle 46 \rangle^3}{\langle 23 \rangle \langle 34 \rangle \langle 56 \rangle \langle 62 \rangle}.
 \end{aligned}
 \tag{4.4.25}$$

We note that each of the results of the calculation of a cut involving fermions should be multiplied by a factor of four in order to account for the possible R -symmetry index assignments.

As mentioned earlier, this three-particle cut carries most of the information distinguishing between the operators \mathcal{O}_C and \mathcal{O}_S . Having collected all of the ingredients necessary for the calculation of the two-loop form factor of the component operator \mathcal{O}_C , we move on to do the same for the supersymmetric descendant of the Konishi, \mathcal{O}_S . The method of solving this cut is the same for both operators.

Supersymmetric calculation

The operator \mathcal{O}_S introduced in Section 4.2 is a tree-level descendant of the Konishi operator, whose MHV form-factors can be extracted from (4.2.8). Once an appropriate component of the (parity conjugate of) super form factor (4.2.8) has been extracted, it captures all of the helicity assignments discussed in the previous section. The only exception is the all-plus gluon case (4.4.15) as this form factor is not $\overline{\text{MHV}}$. As a result, the way to compute this cut is to multiply the appropriate $\overline{\text{MHV}}$ component of the (parity conjugate of) tree-level super-form factor (4.2.8) by the corresponding

five-point MHV tree-level $\mathcal{N}=4$ super-amplitude (2.4.10),

$$A_5^{(0)\text{MHV}}(\lambda_i, \tilde{\lambda}_i, \eta_i) = i \frac{\delta^{(8)}\left(\sum_{i=1}^5 \lambda_i^\alpha \eta_i^A\right)}{\langle 12 \rangle \langle 23 \rangle \langle 34 \rangle \langle 45 \rangle \langle 51 \rangle}, \quad (4.4.26)$$

and integrate over the internal fermionic variables η . To this result we then add the all-plus gluon form factor of (4.4.15) multiplied by the corresponding amplitude (4.4.16). The individual expressions are lengthy and we refrain from presenting them here in full. We discuss the result of this calculation and contrast it with that of the component operator in Section 4.4.5.

Solving for the three-particle cuts

Having collected all the ingredients for the evaluation of the triple cut in the s_{23} -channel, we proceed to discuss the methodology for finding the correct two-loop integrand for the form factors. Due to the complexity of the terms to be summed in this channel, each depending on high powers of loop momenta, instead of manipulating the expressions directly we generate an ansatz with all possible integrand topologies and fix their precise combination by demanding consistency with the previous cuts. The procedure is as follows, explained here for the component operator \mathcal{O}_C and equivalent for the supersymmetric operator \mathcal{O}_S :

1. We combine the cut integrand expression, consisting of the sum of tree-level form factors (4.4.15)–(4.4.24) multiplied by the corresponding tree-level amplitudes (4.4.16)–(4.4.25), taking into account appropriate multiplicities arising from R -symmetry assignment.
2. The integrated form factor does not contain parity-odd terms, but its integrand does. In order to work with a parity even integrand ansatz, we add to the cut expression its parity conjugate and divide the whole result by 2.
3. We construct an ansatz for the integrand in terms of integrals with non-trivial numerators in the following way. All possible two-loop topologies are obtained from the two maximal ones presented in Figure 45.

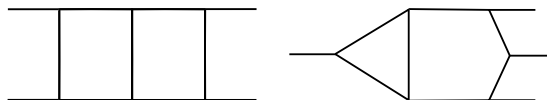


Figure 45: *Maximal two-loop topologies.*

We begin by multiplying those topologies by inverse propagators in such a way that a three-point tree-level form factor appears as one of the vertices. Each topology produced in this way must then be cut in the s_{23} -channel in all possible

ways, thereby generating the ansatz. The steps of this procedure are schematically illustrated in Figure 46.

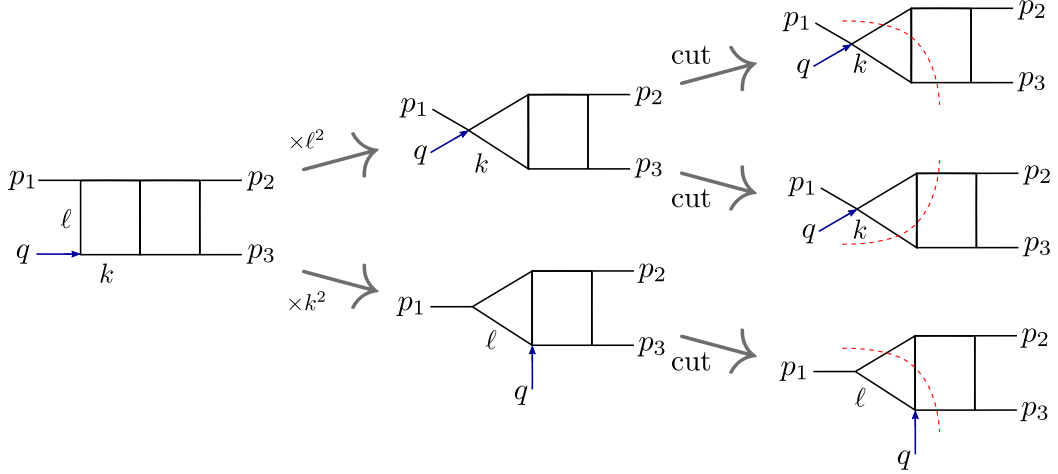


Figure 46: Generating integrand ansatz from maximal two-loop topologies. First, multiply by inverse propagators in a way such that a three-legged form factor appears as one of the vertices. Then cut in the s_{23} -channel in all possible ways.

4. Each of these cut topologies can be described using a basis of irreducible scalar products of the two loop momenta and the three external momenta. There are nine irreducible scalar products involving the loop momenta [141] and three further scalar products involving only the external legs, resulting in twelve irreducible scalar products from which we build numerators.
5. After choosing a basis of irreducible scalar products for the maximal topologies, we generate all possible numerators, up to a maximum power of loop momenta restricted by a theory-specific power counting. For example, for a Yang-Mills theory, a three-point minimal form factor carries three powers of momenta and each three-point Yang-Mills vertex carries one power of momentum. In the case of $\mathcal{N}=4$ SYM we impose a further constraint as a result of the no-triangle property, namely that multiplication by inverse propagators cannot lead to triangles appearing on the amplitude side of the two-loop topology.
6. We then write down a general linear combination of the integral topologies generated above and solve for the coefficients of each integral. Schematically, we have:

$$\text{Cut integrand} = \sum_{i,j} c_{ij} \text{Numerator}_{ij} \times \text{Cut Topology}_j, \quad (4.4.27)$$

where i runs over all possible numerators appearing for a certain topology j . The result of the computation in this channel consists of hundreds of terms which we need to merge

with the integrals obtained in the other cuts (see Table 5) to solve for the ambiguities and detect new integrals. In some cases, the comparison is immediate. In others, as discussed next, important subtleties arise.

4.4.4 Merging the cuts

In this section we combine the results of all generalised unitarity cuts of the two-loop form factor to finally obtain the loop integrand. Having obtained the triple cut in the s_{23} -channel as described in Section 4.4.3 we proceed to gather and reconcile the information obtained from different cuts in order to remove any ambiguities in the numerators of integral topologies.

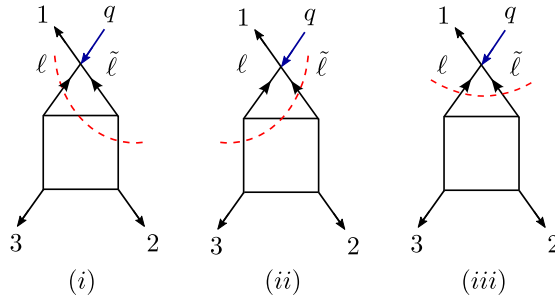


Figure 47: Three cuts of one of the integral topologies.

We illustrate this procedure using a specific example. Figure 47 presents three different cuts of one of the integral topologies contributing to the result for the two-loop form factor. After PV reduction, the three numerators detected by the cuts are:

$$N_i = -s_{23} [s_{23} + 4(\ell \cdot p_3)] , \quad (4.4.28)$$

$$N_{ii} = -s_{23} [s_{23} + 4(\tilde{\ell} \cdot p_2)] , \quad (4.4.29)$$

$$N_{iii} = s_{23}(s_{2\ell} - s_{3\ell}) , \quad (4.4.30)$$

and we recall from the discussion in Section 4.4.1 that on the basis of two particle cuts alone we were unable to conclusively tell whether the $s_{2\ell}$ and $s_{3\ell}$ in (4.4.30) denote the scalar products $2(p_{2,3} \cdot \ell)$, or the full Mandelstam invariants $(p_{2,3} + \ell)^2$. With additional information from the three-particle cut in the s_{23} -channel we are now able to merge the three numerators into an unambiguous expression for the integrand.

The merging between (4.4.28) and (4.4.29) is straightforward. We can rewrite the two numerators as

$$N_i = -s_{23} [s_{23} + 2(\ell + p_3)^2] , \quad N_{ii} = -s_{23} [s_{23} + 2(\tilde{\ell} + p_2)^2] , \quad (4.4.31)$$

which on the cut, with $\ell^2 = 0$ and $\tilde{\ell}^2 = 0$, respectively reduce to (4.4.28) and (4.4.29).

Momentum conservation $\ell + \tilde{\ell} + p_2 + p_3 = 0$ implies that $(\ell + p_3)^2 = (\tilde{\ell} + p_2)^2$ and we see immediately that the two numerators are equivalent.

The merging between these two numerators and (4.4.30) is more subtle. We rewrite

$$\begin{aligned} 2(\ell + p_3)^2 &= (\ell + p_3)^2 + (\tilde{\ell} + p_2)^2 \\ &= \ell^2 + 2(\ell \cdot p_3) + \tilde{\ell}^2 - 2(\ell \cdot p_2) - 2(p_2 \cdot p_3) \\ &= \ell^2 + \tilde{\ell}^2 + s_{3\ell} \Big|_{\ell^2=0} - s_{2\ell} \Big|_{\ell^2=0} - s_{23}, \end{aligned} \quad (4.4.32)$$

where in the second line we made use of momentum conservation. As a result, we have

$$\begin{aligned} N_i &= -s_{23} [s_{23} + 2(\ell + p_3)^2] \\ &= -s_{23} (s_{23} + \ell^2 + \tilde{\ell}^2 + s_{3\ell} \Big|_{\ell^2=0} - s_{2\ell} \Big|_{\ell^2=0} - s_{23}) \\ &= N_{iii} - s_{23}(\ell^2 + \tilde{\ell}^2). \end{aligned} \quad (4.4.33)$$

The last term in (4.4.33) constitutes precisely the kind of ambiguity which could not have been detected by any two-particle cut. Using the information obtained from the three-particle cut, we add this term to the numerator, which now becomes:

$$N = 2s_{23} [(\ell \cdot p_2) - (\ell \cdot p_3)] - s_{23}(\ell^2 + \tilde{\ell}^2). \quad (4.4.34)$$

We note that the merging procedure could have been carried out using numerators before the PV reduction. We refrain from presenting such discussion here as the numerators involved are more complicated but the outcome is, upon PV reduction, equivalent to (4.4.34).

The result of the computation described in Section 4.4.3 contains several topologies with *only* an s_{23} -channel three-particle cut, some of which are presented in Figure 48. Since we cannot obtain any other information about numerators of these topologies, we take them directly from the s_{23} -channel cut expression, which we then lift off shell. These topologies also do not carry any numerator ambiguities as any terms proportional to the cut propagators would lead to a vanishing integral in dimensional regularisation. We are now ready to present the results for the two-loop form factors of \mathcal{O}_S and \mathcal{O}_C .

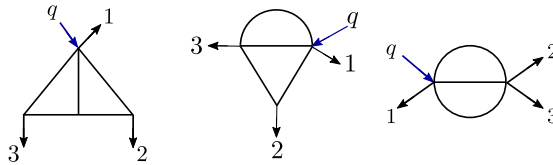


Figure 48: Examples of topologies with only one valid cut, namely the three-particle cut in the kinematic s_{23} -channel.

4.4.5 Final result for the two-loop integrand in $\mathcal{N}=4$ SYM

We begin by presenting the answer for the two-loop form factor of the supersymmetric operator \mathcal{O}_S as discussed in Section 4.4.3. We then move on to present the result of the component calculation for \mathcal{O}_C but we note that the sole difference between the two form factors lies in topologies which can only be detected in the s_{23} -channel triple cut. We list the integrals contributing to the result in Table 6 and the corresponding numerators are detailed in Appendix E.

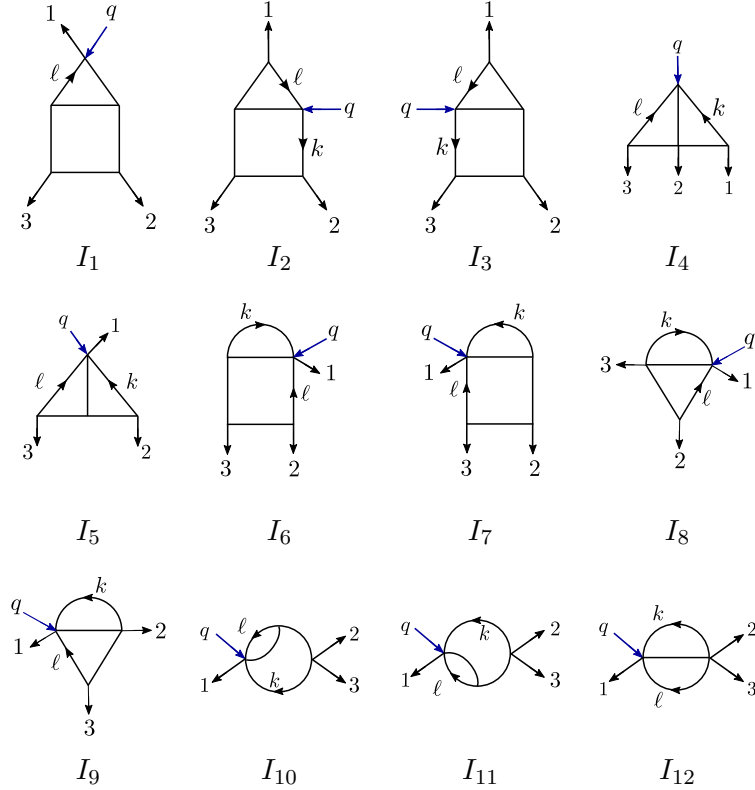


Table 6: Integrals for the two-loop form factor $F_{\mathcal{O}_S, \mathcal{O}_C}^{(2)}(1^+, 2^+, 3^+; q)$ in $\mathcal{N}=4$ SYM.

The two-loop integrand of the minimal form factor of the Konishi descendant \mathcal{O}_S is given by

$$F_{\mathcal{O}_S}^{(2)}(1^+, 2^+, 3^+; q) = F_{\mathcal{O}_S, \mathcal{O}_C}^{(0)}(1^+, 2^+, 3^+; q) \sum_{i=1}^{12} N_i \times I_i + \text{cyclic}(1, 2, 3). \quad (4.4.35)$$

The expressions for the complete numerators are somewhat involved, and we present them in Appendix E.1.

In order not to repeat lengthy expressions, we present the result for the two-loop form factor of the component operator \mathcal{O}_C in terms of a difference when compared to

the two-loop form factor of the supersymmetric operator \mathcal{O}_S . Specifically, we have

$$F_{\mathcal{O}_c}^{(2)}(1^+, 2^+, 3^+; q) = F_{\mathcal{O}_S}^{(2)}(1^+, 2^+, 3^+; q) + \Delta_{\mathcal{N}=4}, \quad (4.4.36)$$

$$\Delta_{\mathcal{N}=4} = F_{\mathcal{O}_S, \mathcal{O}_c}^{(0)}(1^+, 2^+, 3^+; q) \sum_{i=5}^{12} \tilde{N}_i \times I_i + \text{cyclic}(1, 2, 3),$$

i.e. the difference between the two form factors consists solely of topologies which have only a two-particle channel triple cut, denoted by I_5 to I_{12} in Table 6. The numerators are listed in Appendix E.2.

4.4.6 Components vs. super-cut comparison

Having obtained the results for the two-loop form factors of supersymmetric operator \mathcal{O}_S and component operator \mathcal{O}_c we can make a few observations resulting from the comparison of the two results.

As previously noted, the difference between the two-loop form factors of \mathcal{O}_S and \mathcal{O}_c consists of topologies which are only present in the two-particle channel triple cut. These topologies, denoted by I_5 to I_{12} in Table 6, have five propagators or fewer and are of sub-maximal transcendental weight. As a result, we observe that the maximally-transcendental part of the form factor is universal for the two operators.

Moreover, explicit evaluation of the difference between the two form factors reveals terms of order $1/\epsilon$ and constant. Therefore, we conclude that the cancellation of IR poles in the remainder function works exactly in the same way for the two operators. The difference between the remainders of the operators lies in the $1/\epsilon$ terms which are associated to UV renormalisation of the operators. With these observations in mind, we now discuss the remainder function of the two-loop form factor of the supersymmetric operator \mathcal{O}_S .

4.5 Remainder functions in $\mathcal{N}=4$ SYM

In the previous section we have outlined the computation of the two-loop minimal form factors of the supersymmetric operator \mathcal{O}_S and of the component operator \mathcal{O}_c with a final state consisting of three gluons of positive helicity. In this section, we present the result for the two-loop remainder function of the form factor of \mathcal{O}_S , obtained through an appropriate subtraction of the IR divergences. We then move on to discuss the remainder function of the two-loop form factor of \mathcal{O}_c .

4.5.1 Definition of the BDS form factor remainder

The remainder function for form factors is defined through the subtraction of the BDS ansatz, as introduced in (2.9.5) for a generic operator \mathcal{O} ,

$$\mathcal{R}_{\mathcal{O}}^{(2)} = \mathcal{F}_{\mathcal{O}}^{(2)}(\epsilon) - \frac{1}{2}(\mathcal{F}_{\mathcal{O}}^{(1)}(\epsilon))^2 - f^{(2)}(\epsilon) \mathcal{F}_{\mathcal{O}}^{(1)}(2\epsilon) + \mathcal{O}(\epsilon),$$

where $\mathcal{F}_{\mathcal{O}}^{(L)} = F_{\mathcal{O}}^{(L)}/F_{\mathcal{O}}^{(0)}$ and $f^{(2)}(\epsilon) = -2(\zeta_2 + \epsilon \zeta_3 + \epsilon^2 \zeta_4)$. In dimensional regularisation, the definition (2.9.5) allows for the cancellation of all IR poles as well as the $1/\epsilon^2$ pole of UV origin, leaving behind a $1/\epsilon$ pole.

4.5.2 The remainder and anomalous dimension of $\mathcal{O}_{\mathcal{S}}$

Our result for the remainder of the form factor of $\mathcal{O}_{\mathcal{S}}$ has the following properties:

1. All poles of the form $1/\epsilon^k$ vanish for $k > 1$, as expected.
2. The $1/\epsilon$ pole has a coefficient

$$\mathcal{R}_{\mathcal{O}_{\mathcal{S}}}^{(2)} \Big|_{\frac{1}{\epsilon}} = 12 - \pi^2 + \frac{1}{uvw}. \quad (4.5.1)$$

The constant π^2 is an artefact of the subtraction scheme and is not part of the anomalous dimension, see the discussion after (3.4.11). On the other hand, the kinematic-dependent term $1/(uvw)$ indicates mixing with an operator of the form $\mathcal{O}_{\mathcal{M}} \propto q^2 \text{Tr}(F^2)$. This is consistent with the observation in Section 4.2.1 that there is only one other possible form factor structure, denoted as $F_{\mathcal{O}_{\mathcal{M}}}^{(0)}(1^+, 2^+, 3^+; q)$ in (4.2.11), appearing in the mixing at two loops. More precisely, in (4.2.11) we have normalised the operator $\mathcal{O}_{\mathcal{M}}$ such that its tree-level form factor

$$F_{\mathcal{O}_{\mathcal{M}}}^{(0)}(1^+, 2^+, 3^+; q) = \frac{F_{\mathcal{O}_{\mathcal{S}}}^{(0)}(1^+, 2^+, 3^+; q)}{uvw}, \quad (4.5.2)$$

explaining the presence of the $1/(uvw)$ term in (4.5.1).

3. From (4.5.1) we can infer the expression of the operator with definite anomalous dimension at two loops. It requires a one-loop correction of the form

$$\tilde{\mathcal{O}}_{\mathcal{S}} = \mathcal{O}_{\mathcal{S}} + C a \mathcal{O}_{\mathcal{M}}. \quad (4.5.3)$$

The coefficient C is determined by requiring that the $1/\epsilon$ pole of the two-loop form factor of $\tilde{\mathcal{O}}_{\mathcal{S}}$ has no $1/(uvw)$ contribution. This fixes $C = 1/6$, and correspondingly

$$\mathcal{R}_{\tilde{\mathcal{O}}_{\mathcal{S}}}^{(2)} \Big|_{\frac{1}{\epsilon}} = 12 - \pi^2. \quad (4.5.4)$$

From (4.5.4) we can obtain the two-loop anomalous dimension of $\tilde{\mathcal{O}}_{\mathcal{S}}$ using the relation (3.1.12) expanded to second order in $a(\mu_R)$,

$$\gamma_{\mathcal{O}} = -\mu_R \frac{\partial}{\partial \mu_R} \log(1 + a(\mu_R) z_{\mathcal{O}}^{(1)} + a^2(\mu_R) z_{\mathcal{O}}^{(2)} + \dots) \Big|_{\epsilon \rightarrow 0},$$

leading to

$$\gamma_{\mathcal{O}}^{(2)} = \lim_{\epsilon \rightarrow 0} \left(4\epsilon a^2(\mu_R) z_{\mathcal{O}}^{(2)} \right) = \lim_{\epsilon \rightarrow 0} \left(4\epsilon \mathcal{Z}_{\mathcal{O}}^{(2)} \right), \quad (4.5.5)$$

such that

$$\gamma_{\tilde{\mathcal{O}}_{\mathcal{S}}}^{(2)} = -48 a^2, \quad (4.5.6)$$

in agreement with the anomalous dimension of the Konishi multiplet at this loop order [147]. This is an important consistency check of our calculation.

4. The finite part of the remainder function is surprisingly simple for an operator as intricate as $\mathcal{O}_{\mathcal{S}}$. It is comprised of classical polylogarithms and zeta functions only. It can be split into slices of fixed transcendentality ranging from zero to four.

In the following, we present and discuss each transcendentality slice of the remainder function in turn.

Transcendentality four: We find that the maximally transcendental part of the remainder function is the same as that of the BPS operator $\text{Tr}(X^3)$ in (2.9.6), already recognised as a universal building block in Chapter 3

$$\begin{aligned} \mathcal{R}_{\mathcal{O}_{\mathcal{S};4}}^{(2)} = \mathcal{R}_{\text{BPS}}^{(2)} &= -\frac{3}{2} \text{Li}_4(u) + \frac{3}{4} \text{Li}_4\left(-\frac{uv}{w}\right) - \frac{3}{2} \log(w) \text{Li}_3\left(-\frac{u}{v}\right) + \frac{1}{16} \log^2(u) \log^2(v) \\ &+ \frac{\log^2(u)}{32} \left[\log^2(u) - 4 \log(v) \log(w) \right] + \frac{\zeta_2}{8} \log(u) \left[5 \log(u) - 2 \log(v) \right] \\ &+ \frac{\zeta_3}{2} \log(u) + \frac{7}{16} \zeta_4 + \text{perms}(u, v, w). \end{aligned}$$

Transcendentality three: The transcendentality-three piece has a feature which was also observed in the $SL(2)$ sector in [156]: it contains terms with kinematic-dependent prefactors taken from the list

$$\left\{ \frac{u}{v}, \frac{v}{u}, \frac{v}{w}, \frac{w}{v}, \frac{u}{w}, \frac{w}{u} \right\} \quad (4.5.7)$$

in addition to terms without any kinematic-dependent prefactor – which we refer to as

“pure”. The pure part of the degree-three slice is

$$\begin{aligned} \mathcal{R}_{\mathcal{O}_{S;3}}^{(2)} \Big|_{\text{pure}} &= \text{Li}_3(u) + \text{Li}_3(1-u) - \frac{1}{4} \log^2(u) \log\left(\frac{vw}{(1-u)^2}\right) + \frac{1}{3} \log(u) \log(v) \log(w) \\ &\quad + \zeta_2 \log(u) - \frac{5}{3} \zeta_3 + 2 \zeta_2 \log(-q^2) + \text{perms}(u, v, w). \end{aligned} \quad (4.5.8)$$

Interestingly, this result can be related to another known quantity, the remainder function of the operator $\mathcal{O}_{\mathcal{B}}$ calculated in Chapter 3:

$$\mathcal{R}_{\mathcal{O}_{S;3}}^{(2)} \Big|_{\text{pure}} = \frac{1}{2} \mathcal{R}_{\text{non-BPS};3}^{(2)} + 2 \zeta_2 \log(uvw) - 12 \zeta_3, \quad (4.5.9)$$

where $\mathcal{R}_{\text{non-BPS};3}^{(2)}$ is given in (3.4.8). The term with coefficient u/w in the “non-pure” part of the transcendentality-three piece is

$$\begin{aligned} \mathcal{R}_{\mathcal{O}_{S;3}}^{(2)} \Big|_{u/w} &= \left[-\text{Li}_3\left(-\frac{u}{w}\right) + \log(u) \text{Li}_2\left(\frac{v}{1-u}\right) - \frac{1}{2} \log(1-u) \log(u) \log\left(\frac{w^2}{1-u}\right) \right. \\ &\quad \left. + \frac{1}{2} \text{Li}_3\left(-\frac{uv}{w}\right) + \frac{1}{2} \log(u) \log(v) \log(w) + \frac{1}{12} \log^3(w) + (u \leftrightarrow v) \right] \\ &\quad + \text{Li}_3(1-v) - \text{Li}_3(u) + \frac{1}{2} \log^2(v) \log\left(\frac{1-v}{u}\right) - \zeta_2 \log\left(\frac{uv}{w}\right). \end{aligned} \quad (4.5.10)$$

The coefficients of the other factors in the list (4.5.7) are obtained by taking the appropriate permutations of the function above.

Transcendentality two: The degree-two part contains terms with kinematic-dependent prefactors taken from the list

$$\left\{ \frac{u^2}{v^2}, \frac{v^2}{u^2}, \frac{u^2}{w^2}, \frac{v^2}{w^2}, \frac{w^2}{u^2}, \frac{w^2}{v^2} \right\}. \quad (4.5.11)$$

The pure part reads

$$\mathcal{R}_{\mathcal{O}_{S;2}}^{(2)} \Big|_{\text{pure}} = -\text{Li}_2(1-u) - \log^2(u) + \frac{1}{2} \log(u) \log(v) - \frac{13}{2} \zeta_2 + \text{perms}(u, v, w), \quad (4.5.12)$$

while the coefficient of the u^2/w^2 part is given by

$$\mathcal{R}_{\mathcal{O}_{S;2}}^{(2)} \Big|_{u^2/w^2} = \text{Li}_2(1-u) + \text{Li}_2(1-v) + \log(u) \log(v) - \zeta_2. \quad (4.5.13)$$

Again, the coefficients of the other terms in (4.5.11) are obtained through permutations of the function above.

Transcendentality one and zero: The transcendentality-one slice is simply given by

$$\mathcal{R}_{\mathcal{O}_S;1}^{(2)} = \left(-4 + \frac{v}{w} + \frac{u^2}{2vw}\right) \log(u) + \left(-4 - \frac{1}{3uvw}\right) \log(-q^2) + \text{perms}(u, v, w). \quad (4.5.14)$$

Finally, the degree-zero part of the remainder is

$$\mathcal{R}_{\mathcal{O}_S;0}^{(2)} = 7 \left(12 + \frac{1}{uvw}\right). \quad (4.5.15)$$

4.5.3 The remainder of \mathcal{O}_C

Moving on to discuss the remainder of the two-loop form factor of the component operator \mathcal{O}_C we note the following properties:

1. We recall from Section 4.4.6 that the difference between the form factors of operators \mathcal{O}_S and \mathcal{O}_C , denoted as $\Delta_{\mathcal{N}=4}$ in (4.4.36) contained only terms of order $1/\epsilon$ and a constant. As a result, also for $\mathcal{R}_{\mathcal{O}_C}^{(2)}$ all poles in $1/\epsilon^k$ vanish for $k > 1$, as expected.
2. The $1/\epsilon$ pole has a coefficient of

$$\mathcal{R}_{\mathcal{O}_C}^{(2)} \Big|_{\frac{1}{\epsilon}} = 9 - \pi^2 + \frac{1}{uvw}, \quad (4.5.16)$$

again indicative of mixing, see the corresponding discussion for the supersymmetric operator in point **2.** of Section 4.5.2.

3. Even more strikingly, we find that the two-loop remainder function of the operator \mathcal{O}_C is almost identical to that of operator \mathcal{O}_S , namely

$$\mathcal{R}_{\mathcal{O}_C;i}^{(2)} = \mathcal{R}_{\mathcal{O}_S;i}^{(2)}, \quad i = 4, 3, 2. \quad (4.5.17)$$

At lower transcendentality, we find that

$$\mathcal{R}_{\mathcal{O}_C;1}^{(2)} = \mathcal{R}_{\mathcal{O}_S;1}^{(2)} + 2 \log(uvw) + 6 \log(-q^2), \quad (4.5.18)$$

$$\mathcal{R}_{\mathcal{O}_C;0}^{(2)} = \mathcal{R}_{\mathcal{O}_S;0}^{(2)} - \frac{51}{2}. \quad (4.5.19)$$

4.6 Discussion

In this final section we summarise some of the observations regarding the results we have presented.

Firstly, a particular feature of the remainder described in the previous section is that the “non-pure” terms at transcendentality three, two and one come with rational

coefficients v/u , v^2/u^2 and vw/u^2 respectively. At first sight they are problematic as they could potentially lead to unphysical simple or even double poles in the limit where one or two of the three kinematic ratios, u , v and w , tend to zero. This may either occur in the collinear limit *e.g.* $p_1||p_2$, where $u \rightarrow 0$, or in the soft limit *e.g.* $p_2 \rightarrow 0$ where we have $u \rightarrow 0$ and $v \rightarrow 0$. The soft and collinear limits of the maximally transcendental terms were studied in [123].

Let us begin by looking at the “non-pure” transcendentality-three terms given by (4.5.10) (plus permutations of (u, v, w)) which are multiplied by rational coefficients such as v/u . To study the collinear limit $u \rightarrow 0$ (but with $v \neq 0, 1$) we simply expand (4.5.10) around $u=0$. Keeping only the terms which are diverging in the limit we find

$$\begin{aligned} \frac{u}{w} \mathcal{R}_{\mathcal{O}_{S^3}}^{(2)} \Big|_{u/w} + \text{perms}(u, v, w) \xrightarrow{u \rightarrow 0} \log(u) \left[\frac{v^2(\log(v) \log(1-v) - \zeta_2) + (2v-1) \text{Li}_2(v)}{v(1-v)} \right] \\ - \frac{1}{2} \log^2(u) \left[\frac{v^2 \log(v) + (1-v)^2 \log(1-v)}{v(1-v)} \right] + \text{finite} , \end{aligned} \quad (4.6.1)$$

which displays logarithmic divergences only. Importantly, all potential simple poles have cancelled out, and since the overall tree-level form factor (4.2.1) vanishes in this limit, these contributions to the form factor vanish in the limit.

Similarly, for the soft limit $p_2 \rightarrow 0$ we need to expand around $u = v = 0$ with the result

$$\begin{aligned} \frac{u}{w} \mathcal{R}_{\mathcal{O}_{S^3}}^{(2)} \Big|_{u/w} + \text{perms}(u, v, w) \xrightarrow{u, v \rightarrow 0} 2(1 + \zeta_2) - \log(u) - \log(v) \\ + \frac{\log^2(u)}{2} + \frac{\log^2(v)}{2} . \end{aligned} \quad (4.6.2)$$

Again there are only logarithmic divergences and the dangerous poles have cancelled.

Next let us consider the transcendentality-two terms given by (4.5.13) (plus permutations of (u, v, w)) which potentially contain even more problematic double poles, as they are multiplied by ratios such as u^2/w^2 . Following the same procedure as for the transcendentality-three terms one finds now not only logarithmic singularities – the simple poles do not cancel. Naively one would expect that terms of different degree of transcendentality separately have the correct kinematic limits and this would be a serious problem. However, it turns out that we have to add the transcendentality-one terms (4.5.14) in order to cancel the dangerous poles. Doing so, in the collinear limit

$u \rightarrow 0$ we find only logarithmic divergences

$$\begin{aligned} \frac{u^2}{w^2} \mathcal{R}_{\mathcal{O}_S;2}^{(2)} \Big|_{u^2/w^2} + \mathcal{R}_{\mathcal{O}_S;1}^{(2)} + \text{perms}(u, v, w) \xrightarrow{u \rightarrow 0} \\ \log(u) \left[\frac{v(1-v)(1-10v(1-v)) + v^4 \log(v) + (1-v)^4 \log(1-v)}{v^2(1-v)^2} \right] + \text{finite} , \end{aligned} \quad (4.6.3)$$

while in the soft limit $p_2 \rightarrow 0$ we expand around $u=v=0$

$$\frac{u^2}{w^2} \mathcal{R}_{\mathcal{O}_S;2}^{(2)} \Big|_{u^2/w^2} + \mathcal{R}_{\mathcal{O}_S;1}^{(2)} + \text{perms}(u, v, w) \xrightarrow{u,v \rightarrow 0} -\frac{1}{2} [1 + 15 \log(uv)] . \quad (4.6.4)$$

Hence we find that the transcendentality-two and -one terms of the remainder conspire in a way as to cancel all unphysical poles, leaving only logarithmic singularities in both collinear and soft limits. This provides a strong consistency check of our results and explains the necessity of the peculiar rational factors appearing in (4.5.14). We note that the $1/(uvw)$ term in (4.5.15) is harmless as it is due to mixing with the operator \mathcal{O}_M whose tree-level form factor develops poles in soft and collinear limits. We also note that the same holds for both operators considered in this chapter, namely \mathcal{O}_C and \mathcal{O}_S , since their two-loop remainders differ only by terms without rational prefactors, as shown in (4.5.17)-(4.5.19).

Secondly, the authors of [156] discuss the idea of assigning a degree of transcendentality to harmonic numbers, already explored in *e.g.* [157] and propose the concept of “hidden maximal transcendentality” of the remainder function. For our purposes, we are particularly interested in assigning transcendentality to ratios of Mandelstam invariants which multiply the “non-pure” pieces of the remainder, presented in (4.5.10) and (4.5.13). It turns out that we can think of ratios of invariants such as $(1-v)/w$ as having transcendentality degree one, due to the expansion

$$\lim_{m \rightarrow \infty} \sum_{k=1}^m \frac{1}{k} \left(\frac{1-v}{w} \right)^k = -\log \left(1 - \frac{1-v}{w} \right) . \quad (4.6.5)$$

In order to see the hidden maximal transcendentality manifest itself in the (part of) our result we rewrite the ratios of Mandelstam invariants multiplying the transcendentality-three piece in (4.5.10) using the fact that $u+v+w=1$, for example

$$\frac{u}{w} = \frac{1-v-w}{w} = \frac{1-v}{w} - 1 . \quad (4.6.6)$$

Upon such trivial rewriting, it turns out that the pure transcendentality-three part of

the remainder (almost) cancels out, namely

$$\mathcal{R}_{\mathcal{O}_{\mathcal{S};3}}^{(2)} \Big|_{u/w} + \text{perms}(u, v, w) = \mathcal{R}_{\mathcal{O}_{\mathcal{S};3}}^{(2)} \Big|_{\text{pure}} - 4\zeta_2 \log(uvw) + 6\zeta_3, \quad (4.6.7)$$

leaving “non-pure” terms, now multiplied by ratios such as $(1 - v)/w$ – resulting in uniform transcendentality four.

Finally, we note that the constant part of the remainder in (4.5.15), when multiplied by $-4a/7$ gives the value of the two-loop Konishi anomalous dimension, *i.e.* $\gamma_{\mathcal{K}} = -48a$. The same feature was first noted in [52] for remainders of operators in the $SU(2)$ sector.

4.7 Summary

In this chapter we have considered two-loop form factors of operators $\mathcal{O}_{\mathcal{C}} \propto \text{Tr}(F^3)$ and the supersymmetric descendant of the Konishi operator $\mathcal{O}_{\mathcal{S}}$, which contains $\mathcal{O}_{\mathcal{C}}$. In this final section we wish to briefly summarise the main findings so far:

1. The one-loop minimal form factor has been calculated in (4.3.5) and it is identical for the two operators $\mathcal{O}_{\mathcal{C}}$ and $\mathcal{O}_{\mathcal{S}}$. From this result the one-loop anomalous dimension has been found, $\gamma_{\mathcal{O}_{\mathcal{S}}, \mathcal{O}_{\mathcal{C}}}^{(1)} = 12a$, which is the same as the one-loop anomalous dimension of the scalar operator $\mathcal{O}_{\mathcal{B}}$ studied in Chapter 3 and the Konishi operator $\mathcal{O}_{\mathcal{K}}$.
2. Generalised unitarity, applied to form factors, has been used to find the two-loop integrands for the minimal form factors of $\mathcal{O}_{\mathcal{C}}$ and $\mathcal{O}_{\mathcal{S}}$. The two-particle cuts and the three-particle cut in the q^2 -channel are the same for both operators but for the three-particle cut in the s_{23} -channel a distinction between $\mathcal{O}_{\mathcal{C}}$ and $\mathcal{O}_{\mathcal{S}}$ had to be made. For $\mathcal{O}_{\mathcal{C}}$, this cut has been computed by considering all the possible helicity assignments on the internal loop legs, *i.e.* by working in components. For $\mathcal{O}_{\mathcal{S}}$, the cut has been evaluated using the fact that this operator is a supersymmetric descendant of the Konishi and as a result a super-cut, with the Konishi super MHV form factor (4.2.9) as an ingredient, has been used.
3. Due to dependence on high powers of momenta in the numerators, the two-loop integrand has not been manipulated analytically. Instead, a numerical program for finding the integrand from an ansatz has been implemented. The numerators of integrals which appear in multiple cut channels have been carefully merged, as described in Section 4.4.4.
4. The two-loop remainder functions of the form factors of $\mathcal{O}_{\mathcal{S}}$ and $\mathcal{O}_{\mathcal{C}}$ have been computed in Section 4.5.2 and 4.5.3 respectively. They both contain terms of transcendentality ranging from four to zero and some terms appear multiplied by

kinematic prefactors *e.g.* u/v . The maximally transcendental part is equal to the two-loop remainder of \mathcal{O}_{BPS} , the behaviour which we have already observed for $\mathcal{O}_{\mathcal{B}}$ in Chapter 3. Surprisingly, the two remainders are very similar, with differences listed in (4.5.18) and (4.5.19) solely of transcendental degree one and zero.

5. An operator with a definite anomalous dimension, *i.e.* solution to the mixing problem at two loops, has been found in (4.5.3). Its two-loop anomalous dimension, $\gamma_{\mathcal{O}_S}^{(2)} = -48 a^2$ is in agreement with the anomalous dimension of the Konishi multiplet at this loop order.
6. An interesting observation regarding the “non-pure” pieces of the remainder is that despite containing potentially problematic single and double poles in collinear and soft limits, they are actually well-behaved. In particular, while transcendentality-three terms display the correct behaviour by themselves, for terms of lower transcendentality a delicate cancellation across different degrees leads to vanishing of unphysical poles. The knowledge of behaviour of the remainder in the soft and collinear limits, together with the “hidden maximal transcendentality” hypothesis and universality of the maximally transcendental part, could in the future allow us to bootstrap the remainder of an operator under consideration. We leave this as a direction for future studies.

In the next chapter we move on to consider two-loop form factors and remainder functions of operators \mathcal{O}_S and \mathcal{O}_C computed in theories with less-than-maximal supersymmetry. We will seek to find further similarities and eventually make connections between quantities computed in $\mathcal{N}=4$ SYM and QCD.

Chapter 5

Form factors of $\text{Tr}(F^3)$ in $\mathcal{N} < 4$ super Yang-Mills

5.1 Introduction

In this chapter we extend the study of form factors of the operators $\mathcal{O}_C \propto \text{Tr}(F_{\text{ASD}}^3)$ and \mathcal{O}_S , the supersymmetric descendant of the Konishi operator, initiated in Chapter 4 at two loops and with three external positive-helicity gluons to theories with less-than-maximal ($\mathcal{N} < 4$) supersymmetry. Our main goal is to identify universal structures in the expressions for such form factors for various amounts of supersymmetry. Indeed, in this chapter we show that the maximally transcendental part of these two-loop form factors is universal across theories with *any* amount of supersymmetry, including pure Yang-Mills and QCD, and also, as in the case of $\mathcal{N} = 4$ SYM, identical for \mathcal{O}_S and \mathcal{O}_C . We will quantify these findings by providing explicit expressions for the remainder functions in $\mathcal{N} = 2$ and $\mathcal{N} = 1$ SYM, both for the component operator \mathcal{O}_C and for the appropriate $\mathcal{N} < 4$ supersymmetric version of \mathcal{O}_S .

Scattering amplitudes in $\mathcal{N} < 4$ SYM

Tree-level form factors of \mathcal{O}_S in $\mathcal{N} < 4$ SYM needed for the present computation can be simply obtained by an appropriate truncation of the tree-level MHV super form factor (4.2.9), inspired by the analogous procedure for superamplitudes [158, 159].

The $\mathcal{N} = 4$ SYM Nair super-annihilation operator [74] has been introduced in (2.4.7) and reads

$$\Phi_{\mathcal{N}=4} = g^{(+)}(p) + \psi^A(p) \eta_A + \frac{1}{2} \phi^{AB}(p) \eta_A \eta_B + \frac{1}{3!} \bar{\psi}^{ABC}(p) \eta_A \eta_B \eta_C + g^{(-)}(p) \eta_1 \cdots \eta_4,$$

where $A, B, C = 1, \dots, 4$ and where $g^{(+)}(p)$, $\psi^A(p)$, $\phi^{AB}(p)$, $\bar{\psi}^{ABC}(p)$ and $g^{(-)}(p)$, denote the ladder operators for the various fields of $\mathcal{N} = 4$ SYM, as reviewed in Table 2.

In this formalism, the $(n \geq 4)$ -point $\mathcal{N} = 4$ tree-level MHV superamplitude introduced in (2.4.10) reads

$$A_n^{(0)\text{MHV}}(\lambda_i, \tilde{\lambda}_i, \eta_i) = i \frac{\delta^{(4)}\left(\sum_{i=1}^n \lambda_i \tilde{\lambda}_i\right) \delta^{(8)}\left(\sum_{k=1}^n \lambda_k \eta_k\right)}{\langle 12 \rangle \langle 23 \rangle \cdots \langle n1 \rangle},$$

where the $\delta^{(8)}$ imposes super-momentum conservation. Analogous objects can be constructed for $\mathcal{N} = 2$ and $\mathcal{N} = 1$ SYM by truncating the spectrum of the $\mathcal{N} = 4$ SYM theory.³⁷ In particular, the unitarity cuts of $\mathcal{N} < 4$ SYM are subsets of the $\mathcal{N} = 4$ SYM ones [158], obtained by systematically dropping contributions according to their R -charges.

$\mathcal{N} = 2$ SYM can be obtained from the spectrum of $\mathcal{N} = 4$ SYM by eliminating one $\mathcal{N} = 2$ hypermultiplet *i.e.* two complex scalars and two Weyl fermions. In terms of representations of the $SU(4)$ R -symmetry group this is achieved by re-expressing them in terms of representations of $SU(2) \times SU(2) \times U(1)$ and restricting the spectrum to states transforming trivially under one of the $SU(2)$ factors. We may choose to truncate indices 3 and 4, leaving the new $SU(2)$ R -symmetry index $A = 1, 2$ and leading to the super-annihilation operator

$$\Phi_{\mathcal{N}=2} = g^{(+)}(p) + \psi^A(p) \eta_A + \phi^{12}(p) \eta_1 \eta_2 + \left(\bar{\phi}^{34}(p) + \bar{\psi}^{A34}(p) \eta_A + g^{(-)}(p) \eta_1 \eta_2 \right) \eta_3 \eta_4. \quad (5.1.1)$$

Indices 3 and 4 in the expression above are kept as labels and in order to keep notation uniform with the $\mathcal{N} = 4$ SYM case (2.4.7) but they no longer play the role of group indices.

Similarly, $\mathcal{N} = 1$ SYM can be obtained from the $\mathcal{N} = 2$ SYM spectrum by further dropping one chiral multiplet *i.e.* one complex scalar and one Weyl fermion, which is achieved by requiring that fields transform trivially for example in the 2, 3 and 4 directions. This fixes the only remaining index $A = 1$ and leads to the super-annihilation operator

$$\Phi_{\mathcal{N}=1} = g^{(+)}(p) + \psi^1(p) \eta_1 + \left(\bar{\psi}^{234}(p) + g^{(-)}(p) \eta_1 \right) \eta_2 \eta_3 \eta_4. \quad (5.1.2)$$

Finally by truncating *all* of the fields carrying R -charges we can reduce $\mathcal{N} = 4$ SYM to pure ($\mathcal{N} = 0$) Yang-Mills theory. The differences in the field content of the $\mathcal{N} < 4$ SYM theories are summarised in Table 7.

³⁷On shell, $\mathcal{N} = 3$ SYM and $\mathcal{N} = 4$ SYM are equivalent [160–162].

Symbol	Field	$\mathcal{N}=4$	$\mathcal{N}=2$	$\mathcal{N}=1$	$\mathcal{N}=0$
$g^{(+)}$	gluon	1	1	1	1
ψ	gluino	4	2	1	0
ϕ	real scalar	6	2	0	0
$\bar{\psi}$	anti-gluino	4	2	1	0
$g^{(-)}$	gluon	1	1	1	1

Table 7: Field contents of $\mathcal{N}=4$, $\mathcal{N}=2$ and $\mathcal{N}=1$ SYM.

The $n \geq 4$ -point $\mathcal{N} \leq 4$ tree-level MHV superamplitude is given by [158]

$$A_n^{(0)\mathcal{N}}(\lambda_i, \tilde{\lambda}_i, \eta_i) = i \frac{\delta^{(4)}\left(\sum_{j=1}^n \lambda_j \tilde{\lambda}_j\right)}{\langle 12 \rangle \langle 23 \rangle \cdots \langle n1 \rangle} \left[\prod_{A=1}^{\mathcal{N}} \delta^{(2)}\left(\sum_{i=1}^n \lambda_i \eta_{iA}\right) \right] \left[\sum_{k < l}^n \langle kl \rangle^{4-\mathcal{N}} \prod_{B=\mathcal{N}+1}^4 \eta_{kB} \eta_{lB} \right], \quad (5.1.3)$$

and once the desired number of supersymmetries \mathcal{N} has been fixed, we extract component amplitudes by integrating over appropriate fermionic variables η in analogy with the $\mathcal{N}=4$ prescription (2.4.15). We will need $\mathcal{N} < 4$ component amplitudes extracted from (5.1.3) in calculation of the two-loop form factor of \mathcal{O}_C . For \mathcal{O}_S we will require both the $\mathcal{N} < 4$ superamplitude (5.1.3) and a similar truncation applied to form factors.

The rest of the chapter is organised as follows. In Section 5.2 we briefly describe the $\mathcal{N} < 4$ SYM truncation of the supersymmetric form factor (4.2.9). Section 5.3 contains summary of the one-loop calculation while in Section 5.4 we move on to calculate the two-loop minimal form factors in theories with less than maximal supersymmetry. In Section 5.5 we compute the Catani two-loop form factor remainder functions in $\mathcal{N}=2$ and $\mathcal{N}=1$ SYM. We conclude in Section 5.6 with a discussion of our results and a number of consistency checks.

5.2 Operators and tree-level form factors in $\mathcal{N} < 4$ SYM

As explained in detail in Chapter 4, a central point of our discussion consists of appropriately translating the operator $\mathcal{O}_C \propto \text{Tr}(F_{\text{ASD}}^3)$ to a supersymmetric completion $\mathcal{O}_S = \mathcal{O}_C + \mathcal{O}(g)$. In Chapter 4 we have identified \mathcal{O}_S in $\mathcal{N}=4$ SYM as a Supersymmetric descendant of the Konishi, generated by acting with tree-level $\mathcal{N}=4$ supercharges on the lowest-dimensional operator in the multiplet. The Component operator \mathcal{O}_C is contained within \mathcal{O}_S . Similar supersymmetric completions of \mathcal{O}_C can be obtained in $\mathcal{N}=2$ and $\mathcal{N}=1$ SYM by an appropriate truncation [159], analogous to that described for amplitudes in Section 5.1. We will see shortly that for the concrete calculations in this

chapter, we will only need \mathcal{O}_S in $\mathcal{N}=2$ SYM.

For both operators, the tree-level minimal form factor with the external state of three positive-helicity gluons is given by (4.2.1) and equal to

$$F_{\mathcal{O}_S, \mathcal{O}_C}^{(0)}(1^+, 2^+, 3^+; q) = -[12][23][31].$$

The tree-level MHV super form factors of the full Konishi multiplet in $\mathcal{N}=4$ SYM are expressed in a compact formula (4.2.8). The MHV form factors of $\overline{\mathcal{O}}_S$ are obtained by extracting an appropriate component of (4.2.8), namely, as given in (4.2.9)

$$\begin{aligned} F_{\mathcal{O}_S, \text{MHV}}^{(0)}(1, 2, \dots, n; q) &= \\ &= \frac{1}{144} \frac{\delta^{(8)}(\sum_{i=1}^n \eta_i \lambda_i)}{\langle 12 \rangle \dots \langle n1 \rangle} \sum_{i \leq j < k \leq l} (2 - \delta_{ij})(2 - \delta_{kl}) \epsilon^{ABCD} \eta_{iA} \eta_{jB} \eta_{kC} \eta_{lD} \langle jk \rangle \langle li \rangle. \end{aligned}$$

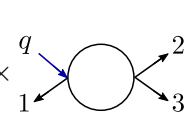
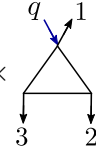
Following the prescription for amplitudes [159] reviewed in Section 5.1, we can truncate the formula (4.2.9) to find the corresponding quantity in $\mathcal{N}=2$ SYM, which will contain the operator \mathcal{O}_C with appropriate additional $\mathcal{N}=2$ completion terms. In order to do so, we have to appropriately project out the superfields for each external particle. In practice this means that we drop all terms which are linear in η_3 or η_4 for each field in the $\mathcal{N}=4$ super form factor and super amplitude. The state sums in unitarity cuts are still performed using $\int d^4\eta$ for each internal leg.

We can apply the same procedure to the case of $\mathcal{N}=1$ SYM, however the supersymmetric completion of \mathcal{O}_C would only introduce additional four-gluino terms. At two-loop order and with the external state of three gluons these cannot contribute and hence are dropped. As a result, the tree-level form factors of \mathcal{O}_S and \mathcal{O}_C in $\mathcal{N}=1$ SYM coincide and will lead to the same result for the two-loop remainder function.

5.3 One-loop minimal form factors

For the reader's convenience we quote here the one-loop correction to the minimal form factor of the operators \mathcal{O}_S and \mathcal{O}_C , calculated in (4.3.5)

$$F_{\mathcal{O}_S, \mathcal{O}_C}^{(1)}(1^+, 2^+, 3^+; q) = i F_{\mathcal{O}_S, \mathcal{O}_C}^{(0)}(1^+, 2^+, 3^+; q) \left(2 \times \text{[Diagram 1]} + s_{23} \times \text{[Diagram 2]} + \text{cyclic}(1, 2, 3) \right).$$

For the purpose of the current discussion an important observation is in order here. The result for the one-loop form factor of the two operators \mathcal{O}_C and \mathcal{O}_S is not only operator-

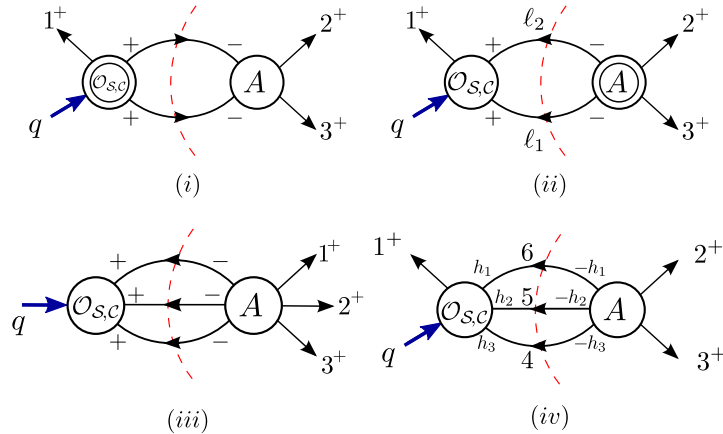
independent, as discussed in Section 4.3, but also theory-independent, *i.e.* the same whether computed in pure or supersymmetric Yang-Mills. This is due to the fact that both the tree-level form factor (4.2.1) and the four-gluon tree-level amplitude (4.3.1) entering the one-loop cut are identical in any Yang-Mills theory. Theory-dependence will manifest itself at two and higher loops where the differences in matter content of the theories will become important.

5.4 Two-loop minimal form factors in $\mathcal{N} < 4$ SYM

We now compute the minimal form factors $F_{\mathcal{O}_S}(1^+, 2^+, 3^+; q)$ and $F_{\mathcal{O}_C}(1^+, 2^+, 3^+; q)$ at two loops and in theories with less-than-maximal supersymmetry.

5.4.1 An effective supersymmetric decomposition

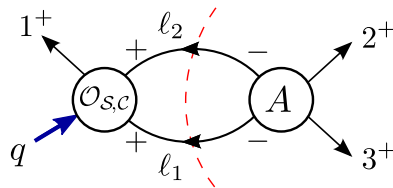
There are two modifications one needs to take into account when decreasing the number of supersymmetries, \mathcal{N} , from the maximal value of $\mathcal{N} = 4$.



Firstly, in computing the two-loop remainder functions the subtraction of the universal IR divergences (2.9.5) for theories with less-than-maximal supersymmetry must be substituted by a more general formula introduced by Catani [118], featuring the non-zero beta function of the theory.

Secondly, the two-loop integrand constructed in Chapter 4 using the generalised unitarity cuts presented in Figure 34 and repeated above for reader's convenience may receive contributions from different states depending on the field content of the theory. As reviewed in Section 5.1, the various supersymmetric Yang-Mills theories differ by the number of scalars and fermions in the vector multiplet. Hence, the key to understanding the difference between two-loop form factors in these theories lies in computing the individual contributions of scalars and fermions to the two- and three-particle cuts shown in Figure 34.

However, inspecting the cuts in Figure 34 carefully, it is clear that only (ii) and (iv) are sensitive to the field content of the theory since they feature a non-minimal form factor or a one-loop amplitude. Indeed, cut (iii) involves only a tree-level form factor and an amplitude with gluons as external states, rendering it independent of the field content of the theory. Cut (i) is slightly more subtle as it features a one-loop form factor which can in principle involve fermions and scalars running in the loop. For this particular configuration of external states, however, the cut of the one-loop form factor consists solely of tree-level quantities with gluons as external states, as shown in Figure 33, again repeated here for convenience. Thus we conclude that only cuts (ii) and (iv) are sensitive to the amount of supersymmetry.



Cut (ii) depends on the field content only through the one-loop amplitude, whose cut-constructible part receives additional contributions proportional to bubble integrals compared to the $\mathcal{N}=4$ SYM case [14]. We will show this explicitly for different values of \mathcal{N} in Section 5.4.2.

The last cut, (iv), also depends on the particular matter content due to the non-trivial sum over internal fermions and scalars running in the loops. However, for the operator \mathcal{O}_C the only possible matter-dependent contributions to this cut involve an internal state with a positive-helicity gluon and two *adjacent* scalars or fermions.³⁸ Hence, the situation is entirely parallel to that of cut (ii) as the matter content dependence is restricted to one-loop sub-diagrams. This allows us to use the supersymmetric decomposition (2.7.16) for one-loop amplitudes. This is a remarkable and important simplification which does not apply to generic two-loop amplitudes. In the following we will obtain the result of this cut for the operator \mathcal{O}_C as a function of c_B (the number of real scalar fields) and c_F (the number of Weyl fermions) in each theory. This computation will be presented in detail in Section 5.4.3.

In Table 8 we briefly summarise what we know about the contributions from the individual cuts so far, and in the next Section we discuss modifications arising from the two- and three-particle cuts in turn.

³⁸Recall discussion in Section 4.2.2 where non-minimal tree-level form factors of \mathcal{O}_S and \mathcal{O}_C were given. Tree-level form factors with non-adjacent scalars, *e.g.* (4.2.19) and (4.2.20), or fermions, *e.g.* (4.2.21), vanish for \mathcal{O}_C but are non-vanishing for \mathcal{O}_S .

		Theory-independent?	\mathcal{O}_S same as \mathcal{O}_C ?
Two-particle cut	$F^{(0)} \times A^{(1)}$	\times	\checkmark
	$F^{(1)} \times A^{(0)}$	\checkmark	\checkmark
Three-particle cut	q^2 -channel	\checkmark	\checkmark
	s_{23} -channel	\times	\times

Table 8: Summary of the theory- and operator-dependence of the unitarity cuts of the two-loop form factor.

5.4.2 Modifications to the two-particle cut

The two-particle cut with $F^{(0)} \times A^{(1)}$, presented in Figure 34(ii) contains a four-point one-loop amplitude. If the matter content is changed compared to that of $\mathcal{N} = 4$ SYM the amplitude will be modified by additional bubble integrals [14, 163, 164]. Fortunately, for the four-point amplitude the modification is very simple. Explicitly, we have [14, 95]:

$$A_{\mathcal{N} \leq 4}^{(1)}(\ell_1^-, \ell_2^-, 2^+, 3^+) = A_{\mathcal{N} = 4}^{(1)}(\ell_1^-, \ell_2^-, 2^+, 3^+) - \beta_0 A_{\mathcal{N} = 1 \text{ chiral}}^{(1)}(\ell_1^-, \ell_2^-, 2^+, 3^+), \quad (5.4.1)$$

where β_0 is the first coefficient of the beta function of the theory in question,³⁹ and

$$A_{\mathcal{N} = 1 \text{ chiral}}^{(1)}(\ell_1^-, \ell_2^-, 2^+, 3^+) = A^{(0)}(\ell_1^-, \ell_2^-, 2^+, 3^+) \times \begin{array}{c} \begin{array}{c} 2 \\ \swarrow \quad \searrow \\ \text{---} \text{---} \text{---} \\ \nwarrow \quad \nearrow \\ \ell_2 \quad \ell_1 \end{array} \end{array}. \quad (5.4.2)$$

Once multiplied by the usual tree-level form factor (4.2.1), this additional contribution gives rise to a new topology, absent in $\mathcal{N} = 4$ SYM:

$$F_{\mathcal{O}_S, \mathcal{O}_C}^{(0)}(1^+, -\ell_2^+, -\ell_1^+; q) \times A_{\mathcal{N} = 1 \text{ chiral}}^{(1)}(\ell_1^-, \ell_2^-, 2^+, 3^+) = \frac{\text{Tr}_+(1 \ell_2 \ell_1 1 3 2)}{s_{12} s_{13}} \times \begin{array}{c} \begin{array}{c} \text{---} \text{---} \text{---} \\ \uparrow \quad \downarrow \\ \ell_2 \quad \ell_1 \\ \downarrow \quad \uparrow \\ q_1 \quad 3 \end{array} \end{array}. \quad (5.4.3)$$

We note that this integral is free of any ambiguities as numerator terms involving powers of ℓ_1^2 or ℓ_2^2 would lead to scaleless integrals. Moreover, we do not expect to observe this integral in any of the other cut channels we considered – thus, we can simply add it to the integrand of the two-loop form factor. Finally, as indicated in Table 8, this cut is universal for both operators \mathcal{O}_S and \mathcal{O}_C and therefore its contribution to the integrands of both form factors is the same.

The important point we wish to make here is that, upon integral reduction, such an additional contribution can only produce two-loop integrals of sub-maximal transcen-

³⁹See Table 9 for its values in our conventions.

dentiality. As a consequence, the maximally transcendental part of the result remains unaltered by modifications of this cut [2].

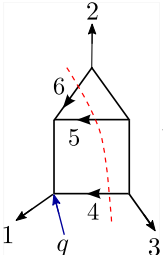
5.4.3 Modifications to the three-particle cut

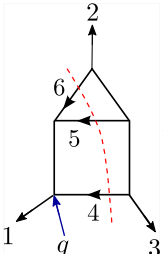
Having considered all modifications to two-particle cuts arising from studying different supersymmetric Yang-Mills theories, it remains to inspect the individual contributions of scalars and fermions to the calculation of the s_{23} -channel three-particle cut, presented in Figure 34(iv). We focus our discussion on the operator \mathcal{O}_C .

Using the relevant expressions for tree-level form factors and amplitudes explicitly quoted in (4.4.19)-(4.4.25) and leaving the multiplicities unspecified as c_F for fermions and c_B for scalars, after some manipulation we can bring all the scalar and fermion terms to a compact form:

$$\begin{aligned}
 F_{\mathcal{O}_C}^{(2)}(1^+, 2^+, 3^+; q) \Big|_{3, s_{23}}^{\text{scalars, fermions}} &= \frac{\langle 46 \rangle}{\langle 23 \rangle \langle 34 \rangle \langle 62 \rangle} \left[\frac{1}{s_{56}} \left([1|54|1] (c_F s_{45} - \frac{1}{2} c_B s_{46}) \right. \right. \\
 &+ [1|64|1] (c_F s_{46} - \frac{1}{2} c_B s_{45}) \Big) + \frac{1}{s_{45}} \left([1|65|1] (c_F s_{56} - \frac{1}{2} c_B s_{46}) + [1|64|1] (c_F s_{46} - \frac{1}{2} c_B s_{56}) \right) \Big].
 \end{aligned} \tag{5.4.4}$$

See Appendix C.3 for a detailed derivation. We can then draw the corresponding integrals in this expression term-by-term:

$$\begin{aligned}
 \text{First term} &= \left(\text{Diagram} \right) \frac{F_{\mathcal{O}_S, \mathcal{O}_C}^{(0)}(1^+, 2^+, 3^+; q)}{s_{12} s_{23} s_{31}} \left(-c_F s_{45} + \frac{1}{2} c_B s_{46} \right) \text{Tr}_+(26431541),
 \end{aligned} \tag{5.4.5}$$


$$\begin{aligned}
 \text{Second term} &= \left(\text{Diagram} \right) \frac{F_{\mathcal{O}_S, \mathcal{O}_C}^{(0)}(1^+, 2^+, 3^+; q)}{s_{12} s_{23} s_{31}} \left(c_F s_{46} - \frac{1}{2} c_B s_{45} \right) \text{Tr}_+(16413462),
 \end{aligned} \tag{5.4.6}$$


$$\text{Third term} = \left[\text{Diagram} \right] \frac{F_{\mathcal{O}_S, \mathcal{O}_C}^{(0)}(1^+, 2^+, 3^+; q)}{s_{12}s_{23}s_{31}} \left(-c_F s_{56} + \frac{1}{2} c_B s_{46} \right) \text{Tr}_+(34621561), \tag{5.4.7}$$

$$\text{Fourth term} = \left[\text{Diagram} \right] \frac{F_{\mathcal{O}_S, \mathcal{O}_C}^{(0)}(1^+, 2^+, 3^+; q)}{s_{12}s_{23}s_{31}} \left(c_F s_{46} - \frac{1}{2} c_B s_{56} \right) \text{Tr}_+(14612643). \tag{5.4.8}$$

The reduction of these integrals with complicated-looking numerators leads to surprisingly simple results. For example, the term in (5.4.5)⁴⁰ reduces to

$$\begin{aligned}
 & - \frac{c_B(6d + 4d^2 - 5d^3 + d^4) + c_F(40d - 40d^2 + 14d^3 - 2d^4)}{24(d-4)^2(d-3)(d-2)(d-1)(p_2 \cdot p_3)} \times \text{Diagram 1} \\
 & - \frac{c_B(-96 + 137d - 53d^2 + 6d^3) + c_F(-96 + 84d - 12d^2)}{12(d-4)(d-1)(3d-8)} \times \text{Diagram 2}, \tag{5.4.9}
 \end{aligned}$$

which, after explicit evaluation, turns out to be of transcendentality three and lower. We hence see that regardless of the number of fermions and scalars present in the theory, their contribution is sub-maximal in transcendentality. As a result, we arrive at the important conclusion that the maximally transcendental part of the two-loop form factor is universal for Yang-Mills theories with any amount of supersymmetry. As far as QCD is concerned the same conclusion holds – the presence of fermions in the fundamental representation alters only the group theory factors and does not lead to new types of integrals.

An important observation is that in (5.4.9), which is the result of the integral reduction of (5.4.5), we see two two-loop master topologies arising. While the first topology is consistent with the cut we are considering – three-particle in the s_{23} -channel, the second topology arising from the reduction does not have a cut in this channel. De-

⁴⁰Where we omit the tree-level form factor as in the remainder we are always concerned with the helicity blind ratio function, see discussion after (2.9.5).

manding consistency of the cut and the topology it gives rise to, we conclude that such contribution is inconsistent and therefore we drop it from the result.

5.5 Remainder functions in $\mathcal{N} < 4$ SYM

5.5.1 Catani form factor remainder and renormalisation

For theories with $\mathcal{N} < 4$ supersymmetry, which have non-vanishing beta function, one must take into account renormalisation. Catani's remainder, which we will use for theories with $\mathcal{N} < 4$, is expressed in terms of renormalised quantities, and hence we need to first discuss how these are related to the bare quantities which we calculate.

We begin by noting that in the $\overline{\text{MS}}$ scheme, the bare coupling constant as a function of the renormalised coupling at a scale μ_R , denoted by $a(\mu_R)$, is given by [118]

$$a^U S_\epsilon = \left(\frac{\mu_R}{\mu}\right)^{2\epsilon} a(\mu_R) \left[1 - a(\mu_R) \frac{\beta_0}{\epsilon} + a^2(\mu_R) \left(\frac{\beta_0^2}{\epsilon^2} - \frac{\beta_1}{2\epsilon} \right) \right] + \mathcal{O}(a^4(\mu_R)), \quad (5.5.1)$$

where $S_\epsilon := (4\pi)^\epsilon e^{-\gamma_E \epsilon}$ and β_0, β_1 are the first two coefficients of the beta function for the 't Hooft coupling,

$$\beta(a(\mu_R)) := \mu_R \frac{\partial a(\mu_R)}{\partial \mu_R}, \quad (5.5.2)$$

$\beta(a) = -2a\epsilon - 2a^2\beta_0 - 2a^3\beta_1 + \mathcal{O}(a^4)$ and the 't Hooft coupling a has been defined in (2.4.1). The values of β_0 are well-known for any $SU(N)$ gauge theory [165]

$$\beta_0 = \frac{11}{3} - \frac{1}{6} \sum_i \frac{C_i}{N} - \frac{2}{3} \sum_j \frac{\tilde{C}_j}{N}, \quad (5.5.3)$$

where the first sum is over all real scalars and the second sum over all Weyl fermions with quadratic Casimirs C_i and \tilde{C}_j respectively. Since we are dealing with Yang-Mills theories without fundamental matter, all fields are in the adjoint representation and thus $C_j = \tilde{C}_j = N$. In Table 9 we list the values of β_0 and β_1 for $\mathcal{N} = 4, 2, 1, 0$.

\mathcal{N}	4	2	1	0
β_0	0	2	3	11/3
β_1	0	0	6	34/3

Table 9: Values of β_0 and β_1 for Yang-Mills theories with $\mathcal{N} = 4, 2, 1, 0$ supersymmetry.

As discussed in Chapter 1, we can think of a form factor as an additional operator \mathcal{O} added to the Lagrangian of the theory with a coupling λ that also undergoes

renormalisation,

$$\lambda^U = \lambda(\mu_R) \left[1 - a(\mu_R) \frac{\gamma_0}{\epsilon} + \frac{a^2(\mu_R)}{2} \left(\frac{\rho_0^2}{\epsilon^2} - \frac{\rho_1}{\epsilon} \right) \right] + \mathcal{O}(a^4(\mu_R)) . \quad (5.5.4)$$

Thus, we can write a renormalised form factor in two ways, either as functions of bare or renormalised quantities. Up two loops we have

$$\begin{aligned} F_{\mathcal{O}}^R &= \lambda(\mu_R) \left[(F_{\mathcal{O}}^R)^{(0)} + a(\mu_R)(F_{\mathcal{O}}^R)^{(1)} + a^2(\mu_R)(F_{\mathcal{O}}^R)^{(2)} \right] + \mathcal{O}(a^4(\mu_R)) \\ &= \lambda^U \left[(F_{\mathcal{O}}^U)^{(0)} + a^U(F_{\mathcal{O}}^U)^{(1)} + (a^U)^2(F_{\mathcal{O}}^U)^{(2)} \right] + \mathcal{O}((a^U)^4) . \end{aligned} \quad (5.5.5)$$

Using (5.5.1) and (5.5.4) in the above equation, we can solve for the renormalised form factors in terms of the bare ones, arriving at the following relations:

$$(F_{\mathcal{O}}^R)^{(0)} = (F_{\mathcal{O}}^U)^{(0)} , \quad (5.5.6)$$

$$(F_{\mathcal{O}}^R)^{(1)} = \left(\frac{\mu_R}{\mu} \right)^{2\epsilon} \frac{(F_{\mathcal{O}}^U)^{(1)}}{S_\epsilon} - \frac{\gamma_0}{\epsilon} (F_{\mathcal{O}}^U)^{(0)} , \quad (5.5.7)$$

$$(F_{\mathcal{O}}^R)^{(2)} = \left(\frac{\mu_R}{\mu} \right)^{4\epsilon} \frac{(F_{\mathcal{O}}^U)^{(2)}}{S_\epsilon^2} - \frac{1}{\epsilon} \left[(\beta_0 + \gamma_0) \left(\frac{\mu_R}{\mu} \right)^{2\epsilon} \frac{(F_{\mathcal{O}}^U)^{(1)}}{S_\epsilon} + \frac{\rho_1}{2} (F_{\mathcal{O}}^U)^{(0)} \right] + (F_{\mathcal{O}}^U)^{(0)} \frac{\rho_0^2}{2\epsilon^2} , \quad (5.5.8)$$

where the superscripts U and R stand for unrenormalised and renormalised.

We are now ready to use these expressions and define finite remainders. Having removed UV divergences through renormalisation, the final step is to remove the universal IR ones. At one loop, the finite remainder is defined as

$$\mathcal{R}^{(1)}(\epsilon) := (\mathcal{F}_{\mathcal{O}}^R)^{(1)} - I^{(1)}(\epsilon) , \quad (5.5.9)$$

where $\mathcal{F}_{\mathcal{O}}^{R(L)} := (F_{\mathcal{O}}^R)^{(L)} / (F_{\mathcal{O}})^{(0)}$ is the usual L -loop helicity blind ratio function, $(F_{\mathcal{O}}^R)^{(1)}$ is the one-loop renormalised form factor defined in (5.5.7), and the expression for $I^{(1)}(\epsilon)$ for n gluons is [166–169],

$$I^{(1)}(\epsilon) = -\frac{e^{\epsilon\gamma}}{\Gamma(1-\epsilon)} \left(\frac{1}{\epsilon^2} + \frac{\beta_0}{2\epsilon} \right) \sum_{i=1}^n \left(-\frac{s_{ii+1}}{\mu_R^2} \right)^{-\epsilon} . \quad (5.5.10)$$

Next we introduce the two-loop Catani remainder [118] in the the formulation of [16]. This is given by

$$\begin{aligned} \mathcal{R}^{(2)}(\epsilon) &:= (\mathcal{F}_{\mathcal{O}}^R)^{(2)}(\epsilon) - \frac{1}{2} \left[(\mathcal{F}_{\mathcal{O}}^R)^{(1)}(\epsilon) \right]^2 + \frac{\beta_0}{\epsilon} (\mathcal{F}_{\mathcal{O}}^R)^{(1)}(\epsilon) \\ &\quad - e^{-\gamma_E \epsilon} \frac{\Gamma(1-2\epsilon)}{\Gamma(1-\epsilon)} (\mathcal{F}_{\mathcal{O}}^R)^{(1)}(2\epsilon) \left(\frac{\beta_0}{\epsilon} + K \right) + \frac{n e^{\gamma_E \epsilon}}{4\epsilon \Gamma(1-\epsilon)} H^{(2)} , \end{aligned} \quad (5.5.11)$$

where n is the number of legs and $n=3$ for the case in question. The particular values of K and $H^{(2)}$ required in order to guarantee the IR finiteness of the remainder are

$$K_{\text{SYM}} = 2[(4 - \mathcal{N}) - \zeta_2], \quad (5.5.12)$$

$$H_{\text{SYM}}^{(2)} = 2\zeta_3 + \frac{(4 - \mathcal{N})}{2}\zeta_2, \quad (5.5.13)$$

where \mathcal{N} is the number of supersymmetries.⁴¹

Away from $\mathcal{N}=4$ SYM, the values of parameters γ_0 , ρ_0 and ρ_1 appearing in (5.5.7) and (5.5.8) are not yet determined. We are now going to fix γ_0 , which in turn is related to the one-loop anomalous dimensions of the operators. We defer fixing the remaining parameters to the next sections as it requires two-loop data.

The constant γ_0 can be determined by requiring the finiteness of the one-loop remainder (5.5.9) with the one-loop unrenormalised minimal form factor (4.3.5) as an input. Demanding cancellation of $1/\epsilon$ terms leads to the relation

$$\gamma_0 = -6 + \frac{3}{2}\beta_0. \quad (5.5.14)$$

Note that this result is the same for the two operators \mathcal{O}_S and \mathcal{O}_C . The one-loop anomalous dimension is related to the UV counterterm according to (3.2.15) and given by

$$\gamma_{\mathcal{O}_S, \mathcal{O}_C}^{(1)} = -2\gamma_0 a = (12 - 3\beta_0)a. \quad (5.5.15)$$

In pure Yang-Mills $\beta_0 = 11/3$ and we get $\gamma_{\mathcal{O}_S, \mathcal{O}_C}^{(1)} = a$, in agreement with [170]. For $\mathcal{N}=4$ we get $\gamma_{\mathcal{O}_S, \mathcal{O}_C}^{(1)} = 12a$, which agrees with our earlier result (4.3.6) [130, 131].

5.5.2 $\mathcal{N}=2$ SYM

In this section we evaluate the two-loop form factors and the Catani remainder functions of the operators \mathcal{O}_S and \mathcal{O}_C in $\mathcal{N}=2$ SYM.

The $\mathcal{N}=2$ SYM form factors

As indicated by the summary in Table 8, in order to obtain the two-loop form factor integrand in $\mathcal{N}=2$ SYM we need to reconsider two types of cuts as they are theory-dependent: the two particle cut involving a one-loop amplitude and the three-particle cut in the s_{23} -channel.

There are two possible ways of finding the contribution of the s_{23} -channel three-particle cut to the two-loop integrand of form factor of \mathcal{O}_C in $\mathcal{N} < 4$ SYM. We can either

⁴¹This choice is not unique however. Compared with the conventions of (A.27) and (A.32) of [16] for $\mathcal{N}=1$ SYM, we have shifted an $\mathcal{O}(\epsilon)$ term from K_{SYM} to $H_{\text{SYM}}^{(2)}$. Therefore the latter is shifted by a rational constant with respect to [16].

follow the strategy described in Section 4.4.3 of Chapter 4 and solve this cut numerically, or we can use the result for $\mathcal{N} = 4$ SYM and appropriately subtract the contributions of scalars and fermions described in Section 5.4.3. In the case of $\mathcal{N} = 2$ SYM we subtract the contribution of 2 Weyl fermions and 4 real scalars from the $\mathcal{N} = 4$ SYM integrand, which amounts to subtracting the integral topologies (5.4.5)-(5.4.8) with $c_F = 2$ and $c_B = 4$. We have performed the calculation using both methods, arriving at the same result. For operator \mathcal{O}_S only the first method applies and we solve the super-cut numerically, using the $\mathcal{N} = 2$ truncation of the super form factor (4.2.9).

The procedure follows that of Section 4.4.3 of Chapter 4, with an important modification of the power counting imposed on the numerator loop momenta. Specifically, the no-triangle property of $\mathcal{N} = 4$ SYM discussed in Section 2.7 strongly restricts the power counting of the loop momenta belonging to a one-loop sub-amplitude. For example, for the cut topology presented in Figure 49, p_6 cannot feature in the numerator since the sub-amplitude can only contain scalar boxes.

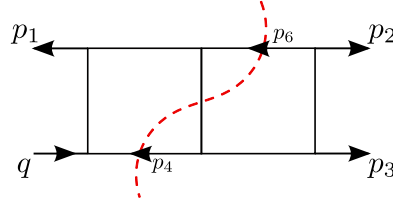


Figure 49: One of the cuts of the maximal topology used to solve the s_{23} -channel triple cut. Note that p_6 is part of a one-loop sub-amplitude.

In $\mathcal{N} < 4$ SYM the no-triangle property does not apply and p_6 can now appear in the numerator. Solving for the $\mathcal{N} = 2$ SYM integrand, we indeed observe new integral topologies which were previously forbidden by the no-triangle property of $\mathcal{N} = 4$ SYM, shown as I_{13} and I_{14} in Table 10.

The full integrand for the two-loop form factor of \mathcal{O}_S computed in $\mathcal{N} = 2$ SYM, including the additional contributions from the modified two- and three-particle cuts, can be expressed in terms the $\mathcal{N} = 4$ SYM result (4.4.35) plus an offset term:

$$F_{\mathcal{N}=2\mathcal{O}_S}^{(2)}(1^+, 2^+, 3^+; q) = F_{\mathcal{N}=4\mathcal{O}_S}^{(2)}(1^+, 2^+, 3^+; q) + \Delta_{\mathcal{N}=2\mathcal{O}_S},$$

$$\Delta_{\mathcal{N}=2\mathcal{O}_S} = F_{\mathcal{O}_S, \mathcal{O}_C}^{(0)}(1^+, 2^+, 3^+; q) \sum_{i=5}^{15} N'_i \times I_i + \text{cyclic}(1, 2, 3), \quad (5.5.16)$$

with the numerators presented in (E.3.2) of Appendix E and the integrals listed in Table 10. As discussed in Section 5.4.2, the modification identified from two-particle cuts is directly added to the integrand and is denoted as topology I_{15} . Similarly, the full integrand for the two-loop form factor of \mathcal{O}_C computed in $\mathcal{N} = 2$ SYM can be expressed

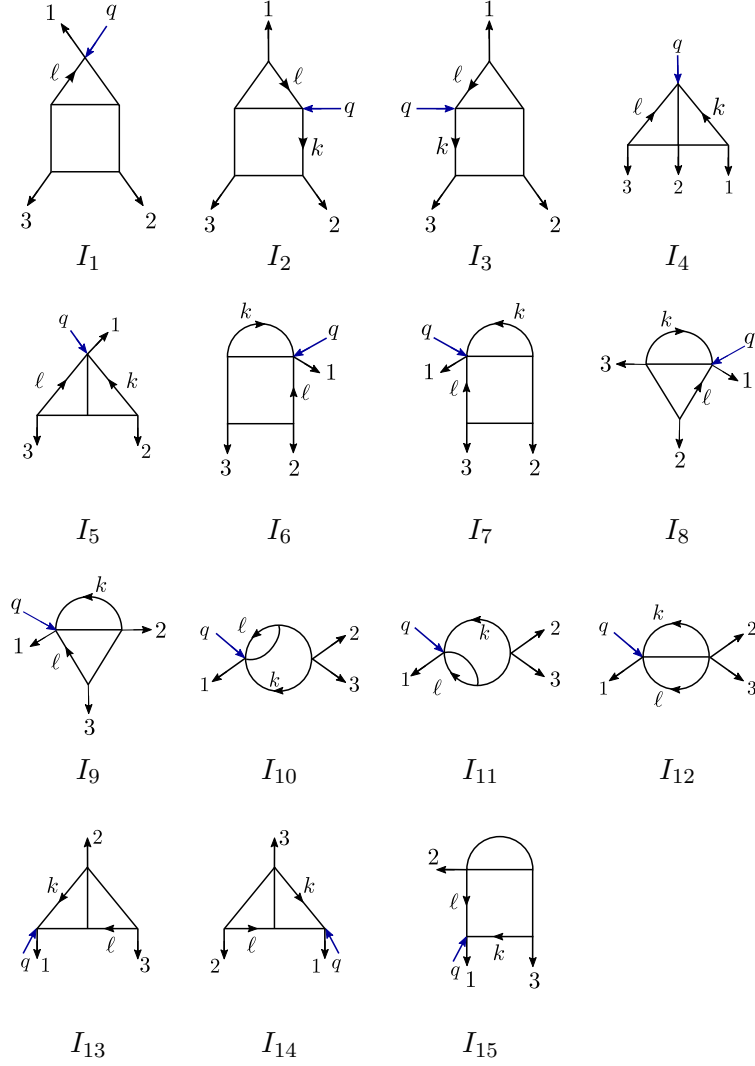


Table 10: Integrals contributing to the integrand of the two-loop form factor $F_{\mathcal{O}_S, \mathcal{O}_C}^{(2)}(1^+, 2^+, 3^+; q)$ in $\mathcal{N} < 4$ SYM.

in terms of its difference from the $\mathcal{N} = 4$ SYM result (4.4.36) as

$$\begin{aligned}
 F_{\mathcal{N}=2\mathcal{O}_C}^{(2)}(1^+, 2^+, 3^+; q) &= F_{\mathcal{N}=4\mathcal{O}_C}^{(2)}(1^+, 2^+, 3^+; q) + \Delta_{\mathcal{N}=2\mathcal{O}_C}, \\
 \Delta_{\mathcal{N}=2\mathcal{O}_C} &= F_{\mathcal{O}_S, \mathcal{O}_C}^{(0)}(1^+, 2^+, 3^+; q) \sum_{i=5}^{15} \hat{N}_i \times I_i + \text{cyclic}(1, 2, 3),
 \end{aligned} \tag{5.5.17}$$

with the numerators presented in (E.4.2).

Having obtained the integrand for the two-loop form factors of operators \mathcal{O}_S and \mathcal{O}_C in $\mathcal{N} = 2$ SYM, we follow the usual procedure of reduction to master integrals with the help of LiteRed [141, 142] and evaluation using the known expressions of the master integrals of [139, 140].

The $\mathcal{N}=2$ SYM remainders

We now evaluate the two-loop remainder function defined in (5.5.11) for the operators \mathcal{O}_S and \mathcal{O}_C , using the renormalised form factors (5.5.6)–(5.5.8) as input.

The first observation to make is that demanding the finiteness of the two-loop remainder to all orders in ϵ we fix the parameters appearing in the renormalised expressions, with the results:

$$\gamma_0 = -3, \quad \rho_0^2 = 3, \quad \rho_{1,\mathcal{O}_S} = -2, \quad \rho_{1,\mathcal{O}_C} = -3. \quad (5.5.18)$$

In order to present the finite $\mathcal{N}=2$ SYM remainder efficiently and at the same time highlight its main features, in Table 11 below we quote the difference between the $\mathcal{N}=2$ and $\mathcal{N}=4$ SYM remainders, slice by slice in transcendentality degree. In fact, we will need a small modification to the $\mathcal{N}=4$ SYM results given in Section 4.5, since in this chapter we are using the Catani definition of the remainder function, while in Chapter 4 we used the BDS definition, which is standard in $\mathcal{N}=4$ SYM. The $\mathcal{N}=4$ SYM Catani remainder is related to the BDS remainder as

$$\mathcal{R}_{\mathcal{O},\text{Catani}}^{(2)} = \mathcal{R}_{\mathcal{O},\text{BDS}}^{(2)} - \zeta_3 [\log(q^2) + \log(uvw) - 6] - \frac{33}{8}\zeta_4, \quad \mathcal{O} = \mathcal{O}_S, \mathcal{O}_C. \quad (5.5.19)$$

In this chapter, all remainders are computed in the Catani formulation (5.5.11) and Table 11 shows the difference between remainder functions computed in $\mathcal{N}=2$ and $\mathcal{N}=4$ SYM.

Degree	$\mathcal{R}_{\mathcal{N}=2\mathcal{O}_S}^{(2)} - \mathcal{R}_{\mathcal{N}=4\mathcal{O}_S}^{(2)}$	$\mathcal{R}_{\mathcal{N}=2\mathcal{O}_C}^{(2)} - \mathcal{R}_{\mathcal{N}=4\mathcal{O}_C}^{(2)}$
4	0	0
3	$-\frac{5}{2}\zeta_2 [\log(uvw) + 3\log(-q^2)] - \frac{11}{2}\zeta_3$	$-\frac{5}{2}\zeta_2 [\log(uvw) + 3\log(-q^2)] - \frac{11}{2}\zeta_3$
2	$18\zeta_2$	$18\zeta_2$
1	$\frac{14}{3} [\log(uvw) + 3\log(-q^2)]$	$3 [\log(uvw) + 3\log(-q^2)]$
0	$-\frac{65}{2}$	$-\frac{45}{4}$

Table 11: Difference between two-loop Catani remainders of operators \mathcal{O}_S and \mathcal{O}_C when calculated in $\mathcal{N}=4$ and $\mathcal{N}=2$ SYM, split by transcendentality degree.

Table 11 immediately shows the main feature of the result: the $\mathcal{N}=2$ SYM remainders are almost identical to those obtained in $\mathcal{N}=4$ SYM. The transcendentality-four slices of the remainders for \mathcal{O}_S and \mathcal{O}_C are identical and equal to the maximally-transcendental part of the result in the $\mathcal{N}=4$ SYM, *i.e.* this quantity is universal across theories and operators studied, with the universality extending also to pure Yang-Mills and QCD.

The difference between the remainders of operators when computed in $\mathcal{N} < 4$ and

$\mathcal{N} = 4$ SYM is limited to a small number of terms as detailed in the table. Recalling the result of Chapter 4 for the $\mathcal{N} = 4$ SYM remainder, we see that the $\mathcal{N} = 2$ SYM expression also contains “pure” terms, *i.e.* purely transcendental functions, as well as “non-pure” terms, which have rational prefactors. Strikingly, such non-pure terms in the $\mathcal{N} = 2$ SYM remainder are exactly the same as in $\mathcal{N} = 4$ SYM quoted in (4.5.10) and (4.5.13). As Table 11 shows, only pure logarithms, ζ_2 and ζ_3 terms appear in the difference, without any rational prefactor. In Section 4.6 it was shown that the rational prefactors in the $\mathcal{N} = 4$ SYM result do not lead to unphysical soft or collinear singularities in the remainder function. That discussion applies also to the present context, since the additional terms we find for reduced supersymmetry do not have any new pole singularity in such kinematic limits.

Finally, inspecting Table 11 we can further infer that the difference between the remainders of \mathcal{O}_S and \mathcal{O}_C when computed in $\mathcal{N} = 2$ SYM only contains terms of transcendentality degree one and zero, as was the case for the two remainders in $\mathcal{N} = 4$ SYM, see (4.5.17).

5.5.3 $\mathcal{N} = 1$ SYM

In this section we evaluate the two-loop form factors and the Catani remainder functions of the operators \mathcal{O}_S and \mathcal{O}_C in $\mathcal{N} = 1$ SYM.

The $\mathcal{N} = 1$ SYM form factors

For $\mathcal{N} = 1$ SYM, the operators \mathcal{O}_S and \mathcal{O}_C have the same tree-level form factors and as such their remainders are identical. As discussed in Section 5.2 the supersymmetric completion of \mathcal{O}_C can only involve additional four-gluino terms which cannot contribute at two-loop order and with the chosen external state. As a result, the integrand for the two-loop form factor of \mathcal{O}_S and \mathcal{O}_C computed in $\mathcal{N} = 1$ SYM can be expressed in terms of its difference with respect to the $\mathcal{N} = 4$ SYM result for \mathcal{O}_C , as

$$\begin{aligned}
 F_{\mathcal{N}=1, \mathcal{O}_S, \mathcal{O}_C}^{(2)}(1^+, 2^+, 3^+; q) &= F_{\mathcal{N}=4, \mathcal{O}_C}^{(2)}(1^+, 2^+, 3^+; q) + \Delta_{\mathcal{N}=1}, \\
 \Delta_{\mathcal{N}=1} &= F_{\mathcal{O}_S, \mathcal{O}_C}^{(0)}(1^+, 2^+, 3^+; q) \sum_{i=5}^{15} N_i'' \times I_i + \text{cyclic}(1, 2, 3),
 \end{aligned}
 \tag{5.5.20}$$

with the numerators listed in (E.5.2).

The $\mathcal{N} = 1$ SYM remainders

Similarly to the $\mathcal{N} = 2$ SYM case, by demanding the finiteness of the remainder function we can fix the parameters γ_0 , ρ_0 and ρ_1 appearing in the renormalised remainders, with

the result:

$$\gamma_0 = -\frac{3}{2}, \quad \rho_0^2 = -\frac{9}{4}, \quad \rho_1 = -\frac{9}{2}. \quad (5.5.21)$$

In Table 12 we present our result in terms of the difference between the remainder computed in $\mathcal{N}=1$ SYM and those computed in $\mathcal{N}=4$ SYM.

Degree	$\mathcal{R}_{\mathcal{N}=1 \mathcal{O}_S, \mathcal{O}_C}^{(2)} - \mathcal{R}_{\mathcal{N}=4 \mathcal{O}_S}^{(2)}$	$\mathcal{R}_{\mathcal{N}=1 \mathcal{O}_S, \mathcal{O}_C}^{(2)} - \mathcal{R}_{\mathcal{N}=4 \mathcal{O}_C}^{(2)}$
4	0	0
3	$-\frac{15}{4}\zeta_2 [\log(uvw) + 3\log(-q^2)] - \frac{33}{4}\zeta_3$	$-\frac{15}{4}\zeta_2 [\log(uvw) + 3\log(-q^2)] - \frac{33}{4}\zeta_3$
2	$\frac{243}{8}\zeta_2$	$\frac{243}{8}\zeta_2$
1	$\frac{13}{2} [\log(uvw) + 3\log(-q^2)]$	$\frac{9}{2} [\log(uvw) + 3\log(-q^2)]$
0	$-\frac{339}{8}$	$-\frac{135}{8}$

Table 12: Difference between two-loop Catani remainders of operators \mathcal{O}_S and \mathcal{O}_C when calculated in $\mathcal{N}=4$ and $\mathcal{N}=1$ SYM, split by transcendentality degree.

Inspecting Table 12, we realise that the discussion in Section 5.5.2 can be repeated almost verbatim. The transcendentality-four part of the $\mathcal{N}=1$ remainder is identical to that in the $\mathcal{N}=4$ SYM theory, confirming its universality. The difference between the remainders of operators is limited only to a small number of pure terms, *i.e.* terms without rational prefactors of the type u/v or u^2/v^2 (and permutations thereof), with all the non-pure terms in the $\mathcal{N}=1$ SYM remainder the same as in $\mathcal{N}=4$ and $\mathcal{N}=2$ SYM, given in (4.5.10) and (4.5.13). Only pure logarithms, and ζ_2 and ζ_3 terms make an appearance in the difference, without rational prefactors. Again, this is consistent with the absence of unphysical soft and collinear singularities in the remainder function, as discussed in Section 5.5.2.

5.6 Consistency checks

In this section we present the consistency checks of our results for the remainder functions of the operators \mathcal{O}_S and \mathcal{O}_C in the less-than-maximally supersymmetric theories.

We perform the following consistency check of the values of the parameters γ_0 and ρ_0 entering the Catani remainder (5.5.11), which we have obtained by demanding the finiteness of the remainder function. We consider the beta function for the operator coupling λ introduced in (5.5.4). Since the left-hand side of that expression is independent of μ , the following renormalisation group equation must hold:

$$0 = \mu_R \frac{\partial}{\partial \mu_R} \left\{ \lambda(\mu_R) \left[1 - a(\mu_R) \frac{\gamma_0}{\epsilon} + \frac{a(\mu_R)^2}{2} \left(\frac{\rho_0^2}{\epsilon^2} - \frac{\rho_1}{\epsilon} \right) \right] + \mathcal{O}(a^4(\mu_R)) \right\}. \quad (5.6.1)$$

Defining γ_λ through

$$\mu_R \frac{\partial \lambda(\mu_R)}{\partial \mu_R} := \lambda(\mu_R) \gamma_\lambda, \quad (5.6.2)$$

we find that (5.6.1) leads to the two relations

$$\gamma_\lambda = -2a(\mu_R) \left[\gamma_0 + a(\mu_R) \rho_1 \right], \quad (5.6.3)$$

and

$$\gamma_0^2 + \beta_0 \gamma_0 = \rho_0^2. \quad (5.6.4)$$

Here (5.6.4) follows from demanding the cancellation of ϵ^{-1} poles in the expression for γ_λ and is a constraint that must be obeyed by ρ_0 and γ_0 . The values we have determined, quoted in (5.5.18) and (5.5.21) for $\mathcal{N} = 2$ and $\mathcal{N} = 1$ SYM, respectively, obey (5.6.4), thereby providing a strong consistency check of our result.

As another consistency check, our calculation has independently confirmed the values of K and $H^{(2)}$ which enter the two-loop Catani remainder (5.5.11) for $\mathcal{N} = 4, 2, 1$ SYM [171, 172], *cf.* (A.27) and (A.32) of [16] for the $\mathcal{N} = 1$ values. The particular values of these constants are crucial to ensure the IR finiteness of the renormalised remainder.

5.7 Summary

In this chapter we have discussed two-loop form factors of $\mathcal{O}_C \propto \text{Tr}(F_{\text{ASD}}^3)$ and the supersymmetric descendant of the Konishi operator \mathcal{O}_S computed in Yang-Mills theories with less-than-maximal supersymmetry. Here we wish to summarise the main findings of the chapter:

1. We find that the two-loop form factors of operator \mathcal{O}_C in $\mathcal{N} < 4$ SYM can be found using the $\mathcal{N} = 4$ result by performing small changes to some of the unitarity cuts. Modifications to two-particle cut have been discussed in Section 5.4.2 and to three-particle cut in Section 5.4.3. Two loop form factors of \mathcal{O}_S has been found using super-cuts with an appropriate truncation of the $\mathcal{N} = 4$ tree-level MHV form factor (4.2.9) as described in Section 5.2.
2. In Section 5.5 we have renormalised the form factors and computed their Catani remainders. In doing so, we have discovered yet another appearance of the principle of universality of the maximally transcendental part of the two-loop remainder. The transcendentality four part of the result for the remainders in $\mathcal{N} = 1$, $\mathcal{N} = 2$ and pure Yang-Mills is universal and equal to that in the $\mathcal{N} = 4$ SYM theory. We find that the difference between the remainders of operators is restricted to pure

terms, without rational prefactors of the type u/v or u^2/v^2 . Such differences for the $\mathcal{N}=2$ SYM and $\mathcal{N}=1$ SYM remainders are listed in Tables 11 and 12. Terms which appear in the difference are logarithms, ζ_2 and ζ_3 terms.

3. In (5.5.15) we find the one-loop anomalous dimension, universal for operators \mathcal{O}_C and \mathcal{O}_S , as a function of the first coefficient of the beta function of the given Yang-Mills theory. After substitution of appropriate values of β_0 , this agrees with known results for pure Yang-Mills and $\mathcal{N}=4$ SYM.
4. The constant ρ_1 in (5.5.18) and (5.5.21) is the two-loop anomalous dimension of the operators considered here, provided that the μ^2 -terms do not alter the $\mathcal{O}(1/\epsilon)$ part of our result,⁴² see discussion of rational terms in Section 2.7. It would be interesting to check the values of ρ_1 and the corresponding anomalous dimensions determined in this chapter with an independent calculation.

In the next, final section we conclude the thesis by summarising its main findings and providing outlook for future research directions.

⁴²Note that we have used four-dimensional generalised unitarity throughout.

Chapter 6

Conclusions

In this final chapter we would like to emphasise the main findings of the thesis, briefly describe extension of the results beyond supersymmetric Yang-Mills theories and propose possible further research directions arising from the present work.

6.1 Summary of the key results

In this thesis we considered two-loop form factors of a number of non-protected operators. In Chapter 3 we focused on operators formed out of fields of the $SU(2|3)$ sector of $\mathcal{N} = 4$ SYM, the scalar $\mathcal{O}_B = \text{Tr}(X[Y, Z])$ and the fermionic $\mathcal{O}_F = 1/2 \text{Tr}(\psi\psi)$. In Chapter 4 we have discussed two operators, $\mathcal{O}_C \propto \text{Tr}(F_{\text{ASD}}^3)$ and a supersymmetric descendant of the Konishi operator, \mathcal{O}_S , both in $\mathcal{N} = 4$ SYM. Finally in Chapter 5 we have considered \mathcal{O}_C and \mathcal{O}_S in theories with less-than-maximal supersymmetry, namely $\mathcal{N} = 2$ and $\mathcal{N} = 1$ SYM. The main results of these three chapters can be summarised as follows:

1. The one-loop anomalous dimension of the three operators \mathcal{O}_B , \mathcal{O}_C and \mathcal{O}_S is the same and equal to that of the Konishi operator [130, 131],

$$\gamma_{\mathcal{O}_K}^{(1)} = \gamma_{\mathcal{O}_B}^{(1)} = \gamma_{\mathcal{O}_C}^{(1)} = \gamma_{\mathcal{O}_S}^{(1)} = 12a. \quad (6.1.1)$$

The one-loop minimal form factors of operators \mathcal{O}_B , \mathcal{O}_C and \mathcal{O}_S coincide up to factoring out the respective tree-level form factors.

2. The maximally transcendental part of the two-loop form factor remainder of \mathcal{O}_B in $\mathcal{N} = 4$ SYM and \mathcal{O}_C , \mathcal{O}_S in $\mathcal{N} = 4, 2, 1$ SYM and pure Yang-Mills is universal and equal to the result for the two-loop form factor remainder of $\mathcal{O}_{\text{BPS}} = \text{Tr}(X^3)$ quoted in (2.9.6). The same universal transcendentality-four slice of the remainder was observed for the Konishi operator [173] and operators in the $SU(2)$ [52] and $SL(2)$ [156] sectors of $\mathcal{N} = 4$ SYM.

3. We further conclude that the maximally transcendental part of the form factor of \mathcal{O}_C , which enters the Higgs effective Lagrangian (1.0.11), computed in QCD is equal to the $\mathcal{N}=4$ SYM value (2.9.6). Form factors of half-BPS operators in $\mathcal{N}=4$ SYM compute the maximally transcendental part of the effective $m_t \gg m_H$ limit Higgs amplitudes in QCD.
4. The lower-transcendentality parts of the two-loop remainder functions share many similarities, both across the operators studied and the different supersymmetric theories. We observe an emergence of certain universal building blocks of two-loop remainder functions. The differences between the remainders of operators are restricted to terms without rational prefactors of the type u/v or u^2/v^2 and contain only products of ζ_2 , ζ_3 and logarithms, *i.e.* no polylogarithms.
5. Solutions to the mixing problem at two-loops for operators belonging to the closed $SU(2|3)$ sector and for \mathcal{O}_S have been found, leading to diagonal operators with definite two-loop anomalous dimension, again in agreement with that of the Konishi operator,

$$\gamma_{\mathcal{O}_K}^{(2)} = \gamma_{\mathcal{O}_{\bar{K}}}^{(2)} = \gamma_{\mathcal{O}_S}^{(2)} = -48 a^2. \quad (6.1.2)$$

6. The requirement of cancellation of unphysical poles in the soft and collinear limits connects the terms of different degree of transcendentality in the remainder. In particular for operators \mathcal{O}_C and \mathcal{O}_S , transcendentality-two and -one terms must be considered together in the limits in order to ensure that no unphysical poles appear.

6.2 Pure Yang-Mills

As described in Section 2.7, computation of loop quantities in non-supersymmetric theories is complicated by the need to include rational terms if, for example, a one-loop amplitude enters the unitarity cut. At the time of preparation of publications [3] and [4], results of which constitute Chapters 4 and 5 of this thesis, a parallel work [174] has appeared. Therein, the authors compute the two-loop remainder function of the form factor of \mathcal{O}_C in pure Yang-Mills theory using D -dimensional unitarity method [175], in contrast to four dimensional cuts employed throughout this work.

This explicit computation confirms the observation made in Chapter 5 that the maximally transcendental part of the two-loop form factor remainder in pure Yang-Mills is the usual \mathcal{O}_{BPS} result (2.9.6). Moreover, the differences between lower-transcendentality slices of the remainder are constrained to products of logarithms, ζ_2 and ζ_3 , again a

feature observed in Chapter 5. In particular,⁴³

$$\begin{aligned}
 \mathcal{R}_{\mathcal{O}_c;4}^{(2)\mathcal{N}=0} &= \mathcal{R}_{\mathcal{O}_c;4}^{(2)\mathcal{N}=4}, \\
 \mathcal{R}_{\mathcal{O}_c;3}^{(2)\mathcal{N}=0} &= \mathcal{R}_{\mathcal{O}_c;3}^{(2)\mathcal{N}=4} - \frac{11}{12} \zeta_2 [\log(uvw) + 3 \log(-q^2)] + \frac{143}{12} \zeta_3, \\
 \mathcal{R}_{\mathcal{O}_c;2}^{(2)\mathcal{N}=0} &= \mathcal{R}_{\mathcal{O}_c;2}^{(2)\mathcal{N}=4} - \left[\frac{55}{48} \log^2(u) - \frac{73}{72} \log(u) \log(v) - \frac{23}{6} \zeta_2 + \text{perms}(u, v, w) \right] \\
 &\quad - \frac{19}{36} \log(uvw) \log(-q^2) - \frac{19}{24} \log^2(-q^2) \\
 \mathcal{R}_{\mathcal{O}_c;1}^{(2)\mathcal{N}=0} &= \mathcal{R}_{\mathcal{O}_c;1}^{(2)\mathcal{N}=4} + \frac{173}{9} [\log(uvw) + 3 \log(-q^2)], \\
 \mathcal{R}_{\mathcal{O}_c;0}^{(2)\mathcal{N}=0} &= \frac{487}{72} \frac{1}{uvw} - \frac{14075}{216}.
 \end{aligned} \tag{6.2.1}$$

This is, by all means, a remarkable result – a significant part of the two-loop Higgs plus three gluons amplitude in the EFT is computed through $\mathcal{N} = 4$ SYM. It would certainly be very interesting to compute the same result using the four dimensional cuts, as advocated in this thesis, with potentially very small, localised modifications needed in order to account for the appearance of rational terms.

6.3 Further work

There are several natural continuations of the work presented in this thesis, which we list here divided into broad categories.

Full QCD calculation

An immediate extension of the work contained in this thesis and of the results in [174] would be to perform the full QCD computation involving massless quarks running in the loops and on the external lines. As argued in Chapter 5, presence of quarks in the fundamental representation will not affect the universality of the maximally transcendental part of the remainder function. It would be fascinating to see what effect inclusion of quarks will have on terms of lower transcendentality and to what degree the $\mathcal{N} = 4$ SYM results remain relevant.

Higher-dimensional operators

Another important avenue to follow is to investigate the universality of the maximally transcendental part of the two-loop remainder for higher-dimensional operators, with

⁴³Note that authors of [174] use the definition of Catani remainder of [118]. Since no explicit result for transcendentality-one part of $\mathcal{N} = 4$ Catani remainder has been presented in the paper, we make a comparison to our value (4.5.18).

the hope of a similar recurrence of the remainder of the relevant protected operator. Dimension-nine operators, contributing at the next order in the EFT Lagrangian (1.0.11) could be a potential candidate for future considerations.

Remainder bootstrap

The knowledge of the behaviour of form factor remainder in the soft and collinear limits, together with the “hidden maximal transcendentality” hypothesis and universality of the maximally transcendental part could in the future allow us to bootstrap the remainder of an operator under consideration. To this end, it would be very useful to study further the soft and collinear behaviour of minimal form factors as they do not follow the standard, general factorisation of amplitudes or non-minimal form factors.

Integrability and dilatation operator

It would be interesting to consider wider classes of non-protected operators than those studied in this thesis also for another reason, namely that it could lead to new insights and approaches to integrability. For example, [128] established a direct link between minimal one-loop form factors of general operators and Zwiebel’s form of the one-loop dilatation operator [127]. In [176] it was shown, using this form of the dilatation operator, how the Yangian symmetry of the tree-level S -matrix of $\mathcal{N}=4$ SYM implies the Yangian symmetry of the one-loop dilatation operator, which in turn is related to its integrability [177]. It would also be very interesting to generalise this result to higher loops.

Supersymmetric Ward identities

Supersymmetric Ward identities were used in [25] to relate form factors of all the different operators in the protected stress tensor multiplet to form factors of the chiral primary operator $\text{Tr}(X^2)$ at any loop order. This led naturally to the definition of super form factors extending the Nair on-shell superspace used for amplitudes in $\mathcal{N}=4$ SYM. It would be interesting to extend this result to non-protected operators contained in larger multiplets. Technically this is more challenging but first important steps in this direction have been taken in recent papers [178, 179] and [180] where tree-level MHV form factors for arbitrary unprotected operators were constructed using twistor-string theory and Lorentz harmonic chiral superspace, respectively.

We expect that in all these considerations supersymmetry will emerge as a powerful organisational principle and that results for form factors in QCD will reveal further remarkable similarities with $\mathcal{N}=4$ SYM.

Appendix A

Spinor conventions

In this appendix we list the conventions for manipulating spinor-helicity variables, introduced in Section 2.1 and used extensively throughout the thesis. We follow closely the conventions of [54].

A.1 Spinor manipulations

The Pauli sigma matrices are defined as

$$\sigma_1 = \begin{pmatrix} 0 & 1 \\ 1 & 0 \end{pmatrix}, \quad \sigma_2 = \begin{pmatrix} 0 & -i \\ i & 0 \end{pmatrix}, \quad \sigma_3 = \begin{pmatrix} 1 & 0 \\ 0 & -1 \end{pmatrix}, \quad (\text{A.1.1})$$

and often it is useful to package those into vectors as

$$(\bar{\sigma}_\mu)^{\dot{\alpha}\alpha} = (\mathbf{1}, \sigma_i), \quad (\sigma_\mu)_{\alpha\dot{\alpha}} = (\mathbf{1}, -\sigma_i), \quad (\text{A.1.2})$$

$$(\bar{\sigma}^\mu)^{\dot{\alpha}\alpha} = (\mathbf{1}, -\sigma_i), \quad (\sigma^\mu)_{\alpha\dot{\alpha}} = (\mathbf{1}, \sigma_i). \quad (\text{A.1.3})$$

We raise and lower spinorial indices $\alpha, \dot{\alpha}$ and construct invariant quantities using the antisymmetric invariant Levi-Civita tensors

$$\epsilon_{\alpha\beta} = (i\sigma_2)_{\alpha\beta} = \begin{pmatrix} 0 & 1 \\ -1 & 0 \end{pmatrix}, \quad \epsilon^{\dot{\alpha}\dot{\beta}} = -(i\sigma_2)^{\dot{\alpha}\dot{\beta}} = \begin{pmatrix} 0 & -1 \\ 1 & 0 \end{pmatrix}, \quad (\text{A.1.4})$$

with the following contractions

$$\epsilon_{\alpha\beta}\epsilon^{\beta\gamma} = \delta_\alpha^\gamma, \quad \epsilon_{\dot{\alpha}\dot{\beta}}\epsilon^{\dot{\beta}\dot{\gamma}} = \delta_{\dot{\alpha}}^{\dot{\gamma}}. \quad (\text{A.1.5})$$

The four momentum has been defined in (2.1.11) as a product of two two-component spinors,

$$p_i^{\dot{\alpha}\alpha} = (\bar{\sigma}_\mu)^{\dot{\alpha}\alpha} p_i^\mu = \tilde{\lambda}_i^{\dot{\alpha}} \lambda_i^\alpha, \quad (\text{A.1.6})$$

where i is the particle label and we raise and lower the spinor indices according to

$$\begin{aligned} \lambda_\alpha &:= \epsilon_{\alpha\beta} \lambda^\beta, & \lambda^\alpha &= \epsilon^{\alpha\beta} \lambda_\beta, \\ \tilde{\lambda}_{\dot{\alpha}} &:= \epsilon_{\dot{\alpha}\dot{\beta}} \tilde{\lambda}^{\dot{\beta}}, & \tilde{\lambda}^{\dot{\alpha}} &= \epsilon^{\dot{\alpha}\dot{\beta}} \tilde{\lambda}_{\dot{\beta}}. \end{aligned} \quad (\text{A.1.7})$$

In these conventions, as introduced in (2.1.15) and (2.1.16), we can form the Lorentz invariant, antisymmetric brackets

$$\begin{aligned} \langle ij \rangle &:= \lambda_i^\alpha \lambda_{j\alpha} = \epsilon_{\alpha\beta} \lambda_i^\alpha \lambda_j^\beta = -\langle ji \rangle, \\ [ij] &:= \tilde{\lambda}_{i\dot{\alpha}} \tilde{\lambda}_j^{\dot{\alpha}} = \epsilon^{\dot{\alpha}\dot{\beta}} \tilde{\lambda}_{i\dot{\alpha}} \tilde{\lambda}_{j\dot{\beta}} = -[ji]. \end{aligned} \quad (\text{A.1.8})$$

For any two massless on-shell four-momenta p_i and p_j we can form a Mandelstam invariant

$$s_{ij} = (p_i + p_j)^2 = 2(p_i \cdot p_j) = \langle ij \rangle [ji], \quad (\text{A.1.9})$$

and additionally we will often use the following shorthand notations,

$$\begin{aligned} \langle i|j|k \rangle &= \langle ij \rangle [jk], & [i|j|k] &= [ij] \langle jk \rangle, \\ \langle i|jk|l \rangle &= \langle ij \rangle [jk] \langle kl \rangle, & [i|jk|l] &= [ij] \langle jk \rangle [kl]. \end{aligned} \quad (\text{A.1.10})$$

A.2 Spinor traces

We often make use of the following notation

$$\text{Tr}_+(abcd) := [ab] \langle bc \rangle [cd] \langle da \rangle, \quad \text{Tr}_-(abcd) := \langle ab \rangle [bc] \langle cd \rangle [da]. \quad (\text{A.2.1})$$

These traces are evaluated using the fact that for four Pauli sigma matrices,

$$\begin{aligned} \text{Tr}(\sigma^\mu \bar{\sigma}^\nu \sigma^\rho \bar{\sigma}^\tau) &= \frac{1}{2} \text{Tr}(\gamma^\mu \gamma^\nu \gamma^\rho \gamma^\tau (1 - \gamma^5)), \\ \text{Tr}(\bar{\sigma}^\mu \sigma^\nu \bar{\sigma}^\rho \sigma^\tau) &= \frac{1}{2} \text{Tr}(\gamma^\mu \gamma^\nu \gamma^\rho \gamma^\tau (1 + \gamma^5)), \end{aligned} \quad (\text{A.2.2})$$

where in the chiral basis we write the Dirac gamma matrices as

$$\gamma^\mu = \begin{pmatrix} 0 & \sigma^\mu \\ \bar{\sigma}^\mu & 0 \end{pmatrix}, \quad \gamma^5 = \begin{pmatrix} -1 & 0 \\ 0 & 1 \end{pmatrix}. \quad (\text{A.2.3})$$

Then we have

$$\begin{aligned}
 [ab]\langle bc\rangle[cd]\langle da\rangle &= \text{Tr}_+(abcd) = \frac{1}{2} \text{Tr}(\not{a}\not{b}\not{c}\not{d}(1 + \gamma^5)) \\
 &= 2((p_a \cdot p_b)(p_c \cdot p_d) - (p_a \cdot p_c)(p_b \cdot p_d) + (p_b \cdot p_c)(p_a \cdot p_d) - i\epsilon^{\mu\nu\rho\tau} p_{a\mu} p_{b\nu} p_{c\rho} p_{d\tau}),
 \end{aligned} \tag{A.2.4}$$

and similarly for the $\text{Tr}_-(abcd)$.

A.3 Parity on spinors

Finally, we will often need to know the form of the parity conjugate of an expression involving spinor brackets. Under parity, the time component of the four-momentum is invariant while the three spatial components pick up a minus sign. In terms of spinors, this is realised as

$$\mathbb{P}: \begin{cases} \lambda_i^1 \rightarrow \tilde{\lambda}_i^2 \\ \lambda_i^2 \rightarrow -\tilde{\lambda}_i^1 \\ \tilde{\lambda}_i^1 \rightarrow \lambda_i^2 \\ \tilde{\lambda}_i^2 \rightarrow -\lambda_i^1 \end{cases}. \tag{A.3.1}$$

It is straightforward to verify that under (A.3.1) the components of p^μ transform as required, *i.e.* $\mathbb{P}(p^0, p^i) = (p^0, -p^i)$. The action of parity on the spinor brackets is then

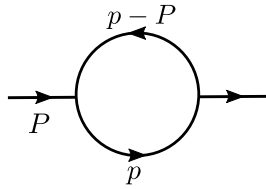
$$\begin{aligned}
 \langle ab \rangle &= \lambda_a^1 \lambda_b^2 - \lambda_a^2 \lambda_b^1 \xrightarrow{\mathbb{P}} -\tilde{\lambda}_a^2 \tilde{\lambda}_b^1 + \tilde{\lambda}_a^1 \tilde{\lambda}_b^2 = -[ab] \\
 [ab] &= \tilde{\lambda}_a^2 \tilde{\lambda}_b^1 - \tilde{\lambda}_a^1 \tilde{\lambda}_b^2 \xrightarrow{\mathbb{P}} -\lambda_a^1 \lambda_b^2 + \lambda_a^2 \lambda_b^1 = -\langle ab \rangle \\
 \mathbb{P}(\langle ab \rangle) &= -[ab], \quad \mathbb{P}([ab]) = -\langle ab \rangle.
 \end{aligned} \tag{A.3.2}$$

Appendix B

Integral functions

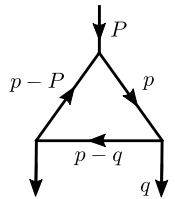
In this appendix we list the conventions for the integral functions used throughout the thesis. The integrals are evaluated in dimensional regularisation with $D = 4 - 2\epsilon$. Upper/lower-case letters correspond to massive/massless momenta and we follow the conventions of [14].

B.1 One-loop scalar integrals



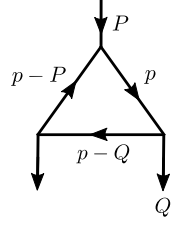
$$\equiv I_2(P^2)$$

$$= \int \frac{d^{4-2\epsilon}p}{(2\pi)^{4-2\epsilon}} \frac{1}{p^2(p-P)^2} = i \frac{c_\Gamma}{\epsilon(1-2\epsilon)} (-P^2)^{-\epsilon}, \quad (\text{B.1.1})$$

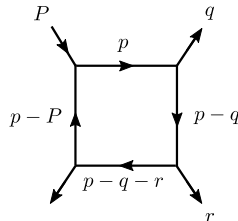


$$\equiv I_3^{1\text{m}}(P^2)$$

$$= \int \frac{d^{4-2\epsilon}p}{(2\pi)^{4-2\epsilon}} \frac{1}{p^2(p-q)^2(p-P)^2} = -i \frac{c_\Gamma}{\epsilon^2} (-P^2)^{-\epsilon-1}, \quad (\text{B.1.2})$$



$$\begin{aligned}
 &\equiv I_3^{2m}(P^2, Q^2) \\
 &= \int \frac{d^{4-2\epsilon}p}{(2\pi)^{4-2\epsilon}} \frac{1}{p^2(p-Q)^2(p-P)^2} \\
 &= -i \frac{c_\Gamma}{\epsilon^2} \frac{(-P^2)^{-\epsilon} - (-Q^2)^{-\epsilon}}{(-P^2) - (-Q^2)}, \tag{B.1.3}
 \end{aligned}$$

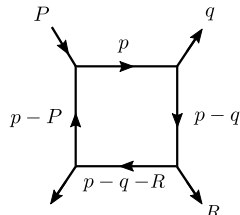


$$\begin{aligned}
 &\equiv I_4^{1m}(s, t, P^2) \\
 &= \int \frac{d^{4-2\epsilon}p}{(2\pi)^{4-2\epsilon}} \frac{1}{p^2(p-q)^2(p-q-r)^2(p-P)^2} \\
 &= -i \frac{2c_\Gamma}{st} \left\{ -\frac{1}{\epsilon^2} \left[(-s)^{-\epsilon} + (-t)^{-\epsilon} - (-P^2)^{-\epsilon} \right] \right. \\
 &\quad \left. + \text{Li}_2\left(1 - \frac{P^2}{s}\right) + \text{Li}_2\left(1 - \frac{P^2}{t}\right) + \frac{1}{2} \log^2\left(\frac{s}{t}\right) + \frac{\pi^2}{6} \right\}, \tag{B.1.4}
 \end{aligned}$$

where $s = (q+r)^2$, $t = (P-q)^2$ and where

$$c_\Gamma = \frac{\Gamma(1+\epsilon)\Gamma(1-\epsilon)^2}{(4\pi)^{2-\epsilon}\Gamma(1-2\epsilon)}. \tag{B.1.5}$$

For the so-called ‘‘two-mass-easy’’ box integral



$$\begin{aligned}
 &\equiv I_4^{2me}(s, t, P^2, R^2) \\
 &= \int \frac{d^{4-2\epsilon}p}{(2\pi)^{4-2\epsilon}} \frac{1}{p^2(p-q)^2(p-q-R)^2(p-P)^2}, \tag{B.1.6}
 \end{aligned}$$

it is more useful to define the *two-mass-easy box function* $F_4^{2\text{me}}$, related to $I_4^{2\text{me}}$ as

$$F_4^{2\text{me}} = -\frac{1}{2\epsilon\Gamma}(P^2 R^2 - st) I_4^{2\text{me}} \quad (\text{B.1.7})$$

and given by

$$\begin{aligned} F_4^{2\text{me}}(s, t, P^2, R^2) &= -i \frac{1}{\epsilon^2} \left[(-s)^{-\epsilon} + (-t)^{-\epsilon} - (-P^2)^{-\epsilon} - (-R^2)^{-\epsilon} \right] \\ &+ \text{Fin}^{2\text{me}}(s, t, P^2, R^2). \end{aligned} \quad (\text{B.1.8})$$

Here $s = (q + R)^2$, $t = (P - q)^2$ and the finite part is given by [66, 181]

$$\text{Fin}^{2\text{me}}(s, t, P^2, R^2) = \text{Li}_2(1 - aP^2) + \text{Li}_2(1 - aR^2) - \text{Li}_2(1 - as) - \text{Li}_2(1 - at), \quad (\text{B.1.9})$$

with

$$a = \frac{P^2 + R^2 - s - t}{P^2 R^2 - st}. \quad (\text{B.1.10})$$

Appendix C

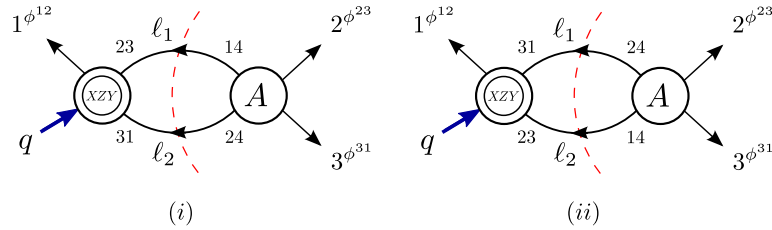
Integrands

In this appendix we present detailed analytic derivation of the integrands of two-loop form factors of $\langle \bar{X}\bar{Y}\bar{Z}|\mathcal{O}_B|0\rangle$ and $\langle g^+g^+g^+|\mathcal{O}_C|0\rangle$. First, in Section C.1 we focus on the operator $\mathcal{O}_{\text{offset}}$, whose form factor contributes to that of \mathcal{O}_B and derive the integrand resulting from the two-particle cut in the s_{23} -channel. Next, in Section C.2 we provide details of the derivation of the integrand of the two-loop minimal form factor of \mathcal{O}_C from the three-particle cut in the q^2 -channel. Finally, in Section C.3 we consider the individual contributions to the integrand of the two-loop form factor of \mathcal{O}_C from scalars and fermions running in the loops of the s_{23} -channel three-particle cut.

C.1 Integrands for the form factor $\langle \bar{X}\bar{Y}\bar{Z}|\mathcal{O}_B|0\rangle$

Two-particle cut in s_{23} -channel with scalars in the loop

First, we focus on the case presented in Figure 16, which we repeat below for reader's convenience.



In this instance, scalar particles are running in the loop and we have the following one-loop form factors, derived in (3.2.6) for Figure 16(i) and in (3.2.19) for Figure 16(ii),

and the tree-level amplitudes given in (3.3.4):

$$(i) : F_{\mathcal{O}_{\text{offset}}}^{(1)}(1^{\phi^{12}}, \ell_1^{\phi^{23}}, \ell_2^{\phi^{31}}; q) = 2i \times \text{bubble}(q, \ell_1, \ell_2) + \text{cyclic}(1, \ell_1, \ell_2),$$

$$(ii) : F_{\mathcal{O}_{\text{offset}}}^{(1)}(1^{\phi^{12}}, \ell_1^{\phi^{31}}, \ell_2^{\phi^{23}}; q) = -2i \times \text{bubble}(q, \ell_1, \ell_2) - 2i s_{\ell_1 \ell_2} \times \text{triangle}(q, \ell_1, \ell_2) + \text{cyclic}(1, \ell_1, \ell_2),$$

$$(i) : A^{(0)}(2^{\phi^{23}}, 3^{\phi^{31}}, \ell_2^{\phi^{24}}, \ell_1^{\phi^{14}}) = -i \times \text{bubble}(\ell_1, \ell_2, 2, 3) - 2i s_{23} \times \text{triangle}(\ell_2, \ell_1, 2, 3),$$

$$(ii) : A^{(0)}(2^{\phi^{23}}, 3^{\phi^{31}}, \ell_2^{\phi^{14}}, \ell_1^{\phi^{24}}) = i \times \text{bubble}(\ell_1, \ell_2, 2, 3).$$

We derive the integrands for the two diagrams separately.

Diagram (i)

For the first diagram we multiply the whole expression by an additional factor of i^2 corresponding to the two cut propagators. We have:

$$\begin{aligned} F_{\mathcal{O}_{\text{offset}}}^{(2)}(1^{\phi^{12}}, \ell_1^{\phi^{23}}, \ell_2^{\phi^{31}}; q) \Big|_{2, s_{23}}^{\text{scalars}^{(i)}} &= i^2 F_{\mathcal{O}_{\text{offset}}}^{(1)}(1^{\phi^{12}}, \ell_1^{\phi^{23}}, \ell_2^{\phi^{31}}; q) \times A^{(0)}(2^{\phi^{23}}, 3^{\phi^{31}}, \ell_2^{\phi^{24}}, \ell_1^{\phi^{14}}) \\ &= -2 \left[\text{bubble}(q, \ell_1, \ell_2) + \text{bubble}(q, \ell_2, \ell_1) + \text{bubble}(q, \ell_1, 1) + \text{bubble}(q, \ell_1, 2) \right] \times \left[\text{bubble}(\ell_1, \ell_2, 2, 3) + 2s_{23} \times \text{triangle}(\ell_2, \ell_1, 2, 3) \right] \\ &= -2 \left[\text{bubble}(q, \ell_1, \ell_2) + \text{bubble}(q, \ell_2, \ell_1) + s_{23} \times \text{triangle}(q, \ell_1, \ell_2, 2, 3) + \text{triangle}(q, \ell_1, \ell_2, 2, 3) \right] \\ &\quad + s_{23} \left[\text{triangle}(q, \ell_2, \ell_1, 2, 3) + \text{triangle}(q, \ell_2, \ell_1, 3, 2) + s_{23} \times \text{triangle}(q, \ell_2, \ell_1, 2, 3) \right], \end{aligned} \tag{C.1.1}$$

where in order to see the emergent integrals we simply “join” the two constituent integrals by their cut propagators ℓ_1 and ℓ_2 . For example, the third line of the expression above is a result of joining together two bubbles, where we insert the second bubble appropriately, depending on location of ℓ_1 and ℓ_2 on the first bubble.

Diagram (ii)

For the second diagram, where the same multiplication by an additional factor of i^2 has been performed, we have:

$$\begin{aligned}
 F_{\mathcal{O}_{\text{offset}}}^{(2)}(1^{\phi^{12}}, \ell_1^{\phi^{23}}, \ell_2^{\phi^{31}}; q) \Big|_{2, s_{23}}^{\text{scalars (ii)}} &= i^2 F_{\mathcal{O}_{\text{offset}}}^{(1)}(1^{\phi^{12}}, \ell_1^{\phi^{31}}, \ell_2^{\phi^{23}}; q) \times A^{(0)}(2^{\phi^{23}}, 3^{\phi^{31}}, \ell_2^{\phi^{14}}, \ell_1^{\phi^{24}}) \\
 &= -2 \left[\begin{array}{c} q \rightarrow \text{circle} \left(\begin{array}{l} \text{left: } 1 \\ \text{right: } \ell_1, \ell_2 \end{array} \right) + q \rightarrow \text{circle} \left(\begin{array}{l} \text{left: } \ell_2 \\ \text{right: } 1, \ell_1 \end{array} \right) + q \rightarrow \text{circle} \left(\begin{array}{l} \text{left: } \ell_1 \\ \text{right: } \ell_2, 1 \end{array} \right) \\
 + s_{\ell_1 \ell_2} \times \begin{array}{c} q \rightarrow \text{triangle} \left(\begin{array}{l} \text{top: } 1 \\ \text{bottom: } \ell_2, \ell_1 \end{array} \right) + s_{1\ell_1} \times \begin{array}{c} q \rightarrow \text{triangle} \left(\begin{array}{l} \text{top: } \ell_2 \\ \text{bottom: } \ell_1, 1 \end{array} \right) + s_{1\ell_2} \times \begin{array}{c} q \rightarrow \text{triangle} \left(\begin{array}{l} \text{top: } \ell_1 \\ \text{bottom: } 1, \ell_2 \end{array} \right) \end{array} \right] \times \begin{array}{c} \ell_1 \rightarrow \text{circle} \left(\begin{array}{l} \text{left: } \ell_2 \\ \text{right: } 2, 3 \end{array} \right) \end{array} \\
 = -2 \times \left[\begin{array}{c} q \rightarrow \text{circle} \left(\begin{array}{l} \text{left: } 1 \\ \text{right: } 2, 3 \end{array} \right) \text{ with } \ell_1, \ell_2 \text{ loop} + q \rightarrow \text{circle} \left(\begin{array}{l} \text{left: } \ell_2 \\ \text{right: } 1, 3 \end{array} \right) \text{ with } \ell_1, \ell_2 \text{ loop} + q \rightarrow \text{circle} \left(\begin{array}{l} \text{left: } \ell_1 \\ \text{right: } 1, 2 \end{array} \right) \text{ with } \ell_1, \ell_2 \text{ loop} \\
 + s_{23} \times \begin{array}{c} q \rightarrow \text{triangle} \left(\begin{array}{l} \text{top: } 1 \\ \text{bottom: } 1, 2, 3 \end{array} \right) \text{ with } \ell_1, \ell_2 \text{ loop} + s_{1\ell_1} \times \begin{array}{c} q \rightarrow \text{triangle} \left(\begin{array}{l} \text{top: } 1 \\ \text{bottom: } 1, 2, 3 \end{array} \right) \text{ with } \ell_1, \ell_2 \text{ loop} + s_{1\ell_2} \times \begin{array}{c} q \rightarrow \text{triangle} \left(\begin{array}{l} \text{top: } 1 \\ \text{bottom: } 1, 2, 3 \end{array} \right) \text{ with } \ell_1, \ell_2 \text{ loop} \end{array} \right]. \end{array} \tag{C.1.2}
 \end{aligned}$$

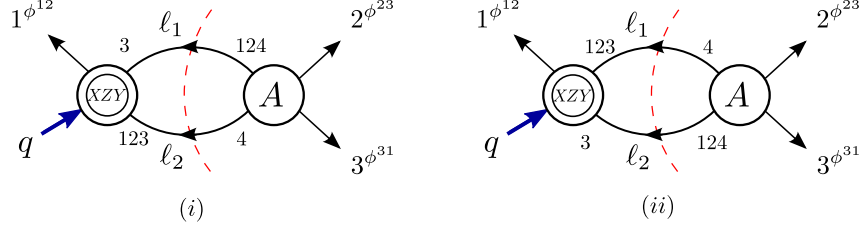
Diagram (i) + Diagram (ii)

Adding the contributions of the two diagrams together finally leads to the integrand quoted in (3.3.5) for the two-particle cut of the contribution to the two-loop form factor where we let scalars run in the loop:

$$\begin{aligned}
 F_{\mathcal{O}_{\text{offset}}}^{(2)}(1^{\phi^{12}}, 2^{\phi^{23}}, 3^{\phi^{31}}; q) \Big|_{2, s_{23}}^{\text{scalars}} &= (\text{C.1.1}) + (\text{C.1.2}) \\
 &= -4 \times \left[\begin{array}{c} q \rightarrow \text{circle} \left(\begin{array}{l} \text{left: } 1 \\ \text{right: } 2, 3 \end{array} \right) \text{ with } \ell_1, \ell_2 \text{ loop} + q \rightarrow \text{circle} \left(\begin{array}{l} \text{left: } \ell_2 \\ \text{right: } 1, 3 \end{array} \right) \text{ with } \ell_1, \ell_2 \text{ loop} + q \rightarrow \text{circle} \left(\begin{array}{l} \text{left: } \ell_1 \\ \text{right: } 1, 2 \end{array} \right) \text{ with } \ell_1, \ell_2 \text{ loop} \end{array} \right] \\
 - 2 \times \left[\begin{array}{c} s_{1\ell_2} \times \begin{array}{c} q \rightarrow \text{triangle} \left(\begin{array}{l} \text{top: } 1 \\ \text{bottom: } 1, 2, 3 \end{array} \right) \text{ with } \ell_1, \ell_2 \text{ loop} + s_{1\ell_1} \times \begin{array}{c} q \rightarrow \text{triangle} \left(\begin{array}{l} \text{top: } 1 \\ \text{bottom: } 1, 2, 3 \end{array} \right) \text{ with } \ell_1, \ell_2 \text{ loop} \end{array} \right] \tag{C.1.3} \\
 - 2 s_{23} \times \left[\begin{array}{c} q \rightarrow \text{triangle} \left(\begin{array}{l} \text{top: } 1 \\ \text{bottom: } 1, 2, 3 \end{array} \right) \text{ with } \ell_1, \ell_2 \text{ loop} + q \rightarrow \text{circle} \left(\begin{array}{l} \text{left: } 1 \\ \text{right: } 2, 3 \end{array} \right) \text{ with } \ell_1, \ell_2 \text{ loop} + q \rightarrow \text{circle} \left(\begin{array}{l} \text{left: } \ell_2 \\ \text{right: } 1, 3 \end{array} \right) \text{ with } \ell_1, \ell_2 \text{ loop} + q \rightarrow \text{circle} \left(\begin{array}{l} \text{left: } \ell_1 \\ \text{right: } 1, 2 \end{array} \right) \text{ with } \ell_1, \ell_2 \text{ loop} \end{array} \right].
 \end{aligned}$$

Two-particle cut in s_{23} -channel with fermions in the loop

For the case presented in Figure 17, which we duplicate below for reader's convenience, we use the expressions for the one-loop form factors given in (3.2.21) and tree-level amplitudes given in (3.3.6):



$$(i) : F_{\mathcal{O}_{\text{offset}}}^{(1)}(1^{\phi^{12}}, -\ell_1^{\psi^3}, -\ell_2^{\bar{\psi}^{123}}; q) = 2i[\ell_1|\ell_4|\ell_2] \times \begin{array}{c} q \quad 1 \\ \diagdown \quad \diagup \\ \ell_3 \quad \ell_4 \\ \diagup \quad \diagdown \\ \ell_2 \quad \ell_1 \end{array},$$

$$(ii) : F_{\mathcal{O}_{\text{offset}}}^{(1)}(1^{\phi^{12}}, -\ell_1^{\bar{\psi}^{123}}, -\ell_2^{\psi^3}; q) = 2i\langle \ell_1|\ell_3|\ell_2 \rangle \times \begin{array}{c} q \quad 1 \\ \diagdown \quad \diagup \\ \ell_3 \quad \ell_4 \\ \diagup \quad \diagdown \\ \ell_2 \quad \ell_1 \end{array},$$

$$(i) : A^{(0)}(2^{\phi^{23}}, 3^{\phi^{31}}, \ell_2^{\psi^4}, \ell_1^{\bar{\psi}^{124}}) = -i[\ell_2|3|\ell_1] \times \begin{array}{c} \ell_2 \quad \ell_1 \\ \uparrow \quad \uparrow \\ \text{---} \\ \downarrow \quad \downarrow \\ 3 \quad 2 \end{array},$$

$$(ii) : A^{(0)}(2^{\phi^{23}}, 3^{\phi^{31}}, \ell_2^{\bar{\psi}^{124}}, \ell_1^{\psi^4}) = -i\langle \ell_2|2|\ell_1 \rangle \times \begin{array}{c} \ell_2 \quad \ell_1 \\ \uparrow \quad \uparrow \\ \text{---} \\ \downarrow \quad \downarrow \\ 3 \quad 2 \end{array}.$$

We note that we have added an extra minus sign to every one-loop form factor expression to take into account the reversal of direction of ℓ_1 and ℓ_2 according to the prescription of [182] where $\lambda_{-P} = -\lambda_P$, $\tilde{\lambda}_{-P} = \tilde{\lambda}_P$, $\eta_{-P} = \eta_P$. We also note that in this case no cyclic permutation of the external state is taken into account in the expression for the one-loop form factor. This is due to the fact that this is the only permutation which results in a non-zero amplitude on the right-hand side of the cut once the external state of the two-loop form factor has been fixed as $\langle \bar{X}\bar{Y}\bar{Z} |$. We obtain the following results for the cuts shown in Figure 17.

Diagram (i)

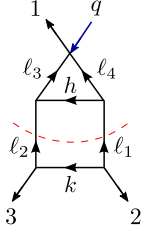
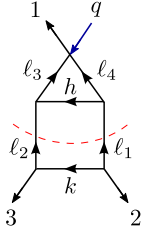
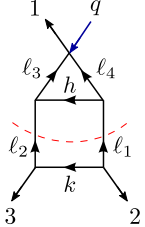
$$\begin{aligned}
 & F_{\mathcal{O}_{\text{offset}}}^{(2)}(1^{\phi^{12}}, \ell_1^{\phi^{23}}, \ell_2^{\phi^{31}}; q) \Big|_{2, s_{23}}^{\text{fermions (i)}} \\
 &= -i^2 F_{\mathcal{O}_{\text{offset}}}^{(1)}(1^{\phi^{12}}, -\ell_1^{\psi^3}, -\ell_2^{\bar{\psi}^{123}}; q) \times A^{(0)}(2^{\phi^{23}}, 3^{\phi^{31}}, \ell_2^{\psi^4}, \ell_1^{\bar{\psi}^{124}}) \\
 &= 2 [\ell_1 | \ell_4 | \ell_2] [\ell_2 | 3 | \ell_1] \times \text{Diagram (i)}
 \end{aligned} \tag{C.1.4}$$


Diagram (ii)

$$\begin{aligned}
 & F_{\mathcal{O}_{\text{offset}}}^{(2)}(1^{\phi^{12}}, \ell_1^{\phi^{23}}, \ell_2^{\phi^{31}}; q) \Big|_{2, s_{23}}^{\text{fermions (ii)}} \\
 &= -i^2 F_{\mathcal{O}_{\text{offset}}}^{(1)}(1^{\phi^{12}}, -\ell_1^{\bar{\psi}^{123}}, -\ell_2^{\psi^3}; q) \times A^{(0)}(2^{\phi^{23}}, 3^{\phi^{31}}, \ell_2^{\bar{\psi}^{124}}, \ell_1^{\psi^4}) \\
 &= 2 \langle \ell_1 | \ell_3 | \ell_2 \rangle \langle \ell_2 | 2 | \ell_1 \rangle \times \text{Diagram (ii)},
 \end{aligned} \tag{C.1.5}$$


where for convenience we have labeled the additional internal momenta as k and h , and we have multiplied the result of the cut by the usual fermionic loop factor of (-1) . Note that in the above ℓ_1 and ℓ_2 are cut, while ℓ_3 , ℓ_4 , k and h are off-shell.

Combining (C.1.4) and (C.1.5) we obtain

$$(C.1.4) + (C.1.5) = 2 \left[\text{Tr}_+(2 \ell_1 \ell_4 \ell_2) + \text{Tr}_+(2 \ell_2 \ell_4 \ell_1) \right] \times \text{Diagram (i)}, \tag{C.1.6}$$


where we use the notation introduced in (A.2.1), momentum conservation

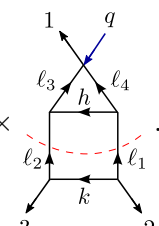
$$\ell_1 + \ell_2 = \ell_3 + \ell_4 = -p_2 - p_3, \tag{C.1.7}$$

and the fact that on the cut $s_{2\ell_1} = s_{3\ell_2}$. Next we evaluate the traces in (C.1.6) using

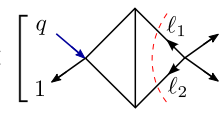
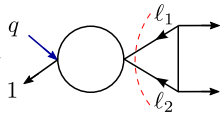
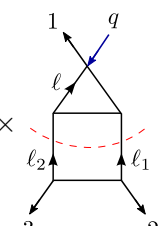
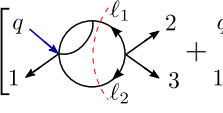
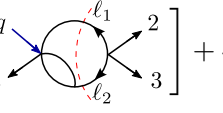
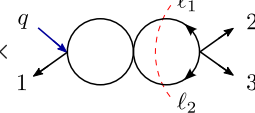
the identity (A.2.4) and expand the emergent scalar products in terms of the inverse propagators appearing in the main topology in (C.1.6), specifically using

$$\begin{aligned}
 2(\ell_2 \cdot \ell_3) &= 2(\ell_1 \cdot \ell_4) + \ell_3^2 - \ell_4^2 = -h^2 + \ell_3^2, \\
 2(\ell_4 \cdot \ell_2) &= s_{23} + h^2 - \ell_3^2, \\
 2(p_2 \cdot \ell_2) &= -2(p_2 \cdot \ell_1) - s_{23} = -k^2 - s_{23},
 \end{aligned} \tag{C.1.8}$$

where $k^2 = (p_2 + \ell_1)^2 = 2(p_2 \cdot \ell_1)$ and $h^2 = (\ell_1 - \ell_4)^2 = -2(\ell_1 \cdot \ell_4) + \ell_4^2$. Doing so, we can rewrite (C.1.6) and obtain the fermionic contribution to the two-particle cut of the two-loop form factors of $\mathcal{O}_{\text{offset}}$,

$$\begin{aligned}
 &F_{\mathcal{O}_{\text{offset}}}^{(2)}(1^{\phi^{12}}, 2^{\phi^{23}}, 3^{\phi^{31}}; q) \Big|_{2, s_{23}}^{\text{fermions}} \\
 &= 2 \left[2k^2 h^2 + s_{23}(k^2 + h^2) - k^2(\ell_3^2 + \ell_4^2) - s_{23}s_{2\ell_4} \right] \times \text{Diagram} \tag{C.1.9}
 \end{aligned}$$


From (C.1.9) we can now proceed to work out the cut integrals contributing to the two-loop form factor of $\mathcal{O}_{\text{offset}}$. Each of the numerator factors will be used to cancel one or two propagators of the master topology, “shrinking” it to a smaller integral with less propagators. Proceeding in this way, we arrive at the result presented in (3.3.7),

$$\begin{aligned}
 &F_{\mathcal{O}_{\text{offset}}}^{(2)}(1^{\phi^{12}}, 2^{\phi^{23}}, 3^{\phi^{31}}; q) \Big|_{2, s_{23}}^{\text{fermions}} \\
 &= 2s_{23} \times \left[\text{Diagram 1} + \text{Diagram 2} \right] - 2s_{23}s_{3\ell} \times \text{Diagram 3} \\
 &\quad - 2 \times \left[\text{Diagram 4} + \text{Diagram 5} \right] + 4 \times \text{Diagram 6} \tag{C.1.10}
 \end{aligned}$$







C.2 Integrands for the form factor $\langle g^+ g^+ g^+ | \mathcal{O}_C | 0 \rangle$

In this section we provide details of the derivation of the integrand of the two-loop minimal form factor of \mathcal{O}_C . In particular, we focus on the manipulations of the three-particle cut in the q^2 -channel, the results of which are presented in Section 4.4.2.

Three-particle cut in the q^2 -channel

In this section we consider the three-particle cut of the two-loop form factor in the q^2 -channel presented in Figure 50, reproduced here for reader's convenience.

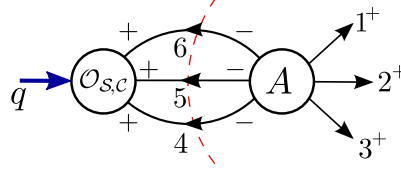


Figure 50: Triple-cut of the two-loop form factor in the q^2 -channel. Only one possible helicity assignment exists.

The tree-level form factor is that of (4.2.13), *i.e.*

$$F_{\mathcal{O}_S}^{(0)}(-6^+, -5^+, -4^+; q) = -[65][54][46],$$

and for the six-point tree-level gluon amplitude we use the expression of (4.4.11), which reads

$$A^{(0)}(1^+, 2^+, 3^+, 4^-, 5^-, 6^-) = i \left[\frac{\overbrace{([23]\langle 56 \rangle [1|p_2 + p_3|4])^2}^{\beta^2}}{s_{234}s_{23}s_{34}s_{56}s_{61}} + \frac{\overbrace{([12]\langle 45 \rangle [3|p_1 + p_2|6])^2}^{\gamma^2}}{s_{345}s_{34}s_{45}s_{61}s_{12}} \right. \\ \left. + \frac{\overbrace{s_{123}[23]\langle 56 \rangle [1|p_2 + p_3|4][12]\langle 45 \rangle [3|p_1 + p_2|6]}^{\beta\gamma}}{s_{12}s_{23}s_{34}s_{45}s_{56}s_{61}} \right],$$

β^2 -term: The first term in (4.4.11) gives rise to a previously-detected topology. In particular, we have

$$F_{\mathcal{O}_S}^{(2)}(1^+, 2^+, 3^+; q) \Big|_{3, q^2}^{\beta^2} = i^3 F_{\mathcal{O}_S}^{(0)}(-6^+, -5^+, -4^+; q) \times A^{(0)}(1^+, 2^+, 3^+, 4^-, 5^-, 6^-) \Big|_{\beta^2} \\ = F_{\mathcal{O}_S}^{(0)}(1^+, 2^+, 3^+; q) \frac{[65][54][46]}{[12][23][31]} \frac{([23]\langle 56 \rangle [1|p_2 + p_3|4])^2}{s_{234}s_{23}s_{34}s_{56}s_{16}} \\ = \frac{F_{\mathcal{O}_S}^{(0)}(1^+, 2^+, 3^+; q)}{s_{234}s_{23}s_{34}s_{16}} \frac{[54][46]}{[12][31]} [23]\langle 56 \rangle [1|q|4]^2 \\ = \frac{F_{\mathcal{O}_S}^{(0)}(1^+, 2^+, 3^+; q)}{s_{234}s_{34}s_{16}s_{23}s_{12}s_{13}} [1|q|4]\langle 45 \rangle \langle 56 \rangle [64]\langle 4|q|1 \rangle [12][23]\langle 31 \rangle$$

$$= F_{\mathcal{O}_S}^{(0)}(1^+, 2^+, 3^+; q) \frac{\text{Tr}_+(1 q 4 5 6 4 q 1 2 3)}{s_{12}s_{23}s_{13}} \times q \times \text{Diagram} \quad (\text{C.2.1})$$

After an appropriate relabelling, it is straightforward to see that the numerator becomes identical to that of (4.4.10), obtained from the two-particle cut.

γ^2 -term: Considering the second term in (4.4.11) we similarly detect a familiar topology. In particular,

$$\begin{aligned}
 F_{\mathcal{O}_S}^{(2)}(1^+, 2^+, 3^+; q) \Big|_{3, q^2}^{\gamma^2} &= i^3 F_{\mathcal{O}_S}^{(0)}(-6^+, -5^+, -4^+; q) \times A^{(0)}(1^+, 2^+, 3^+, 4^-, 5^-, 6^-) \Big|_{\gamma^2} \\
 &= F_{\mathcal{O}_S}^{(0)}(1^+, 2^+, 3^+; q) \frac{[65][54][46] ([12]\langle 45 \rangle [3|p_1+p_2|6])^2}{[12][23][31] s_{345}s_{34}s_{45}s_{16}s_{12}} \\
 &= \frac{F_{\mathcal{O}_S}^{(0)}(1^+, 2^+, 3^+; q)}{s_{345}s_{12}s_{34}s_{16}} \frac{[65][46]}{[23][31]} [12]\langle 45 \rangle [3|q|6]^2 \\
 &= \frac{F_{\mathcal{O}_S}^{(0)}(1^+, 2^+, 3^+; q)}{s_{345}s_{34}s_{16}s_{23}s_{12}s_{13}} [3|q|6][65]\langle 54 \rangle [46]\langle 6|q|3 \rangle \langle 32 \rangle \langle 21 \rangle \langle 13 \rangle
 \end{aligned}$$

$$= F_{\mathcal{O}_S}^{(0)}(1^+, 2^+, 3^+; q) \frac{\text{Tr}_+(3 q 6 5 4 6 q 3 2 1)}{s_{12}s_{23}s_{13}} \times \text{Diagram} \quad (\text{C.2.2})$$

After an appropriate relabelling, it is again easy to see that the numerator becomes identical to that of (4.4.9), obtained from a two-particle cut.

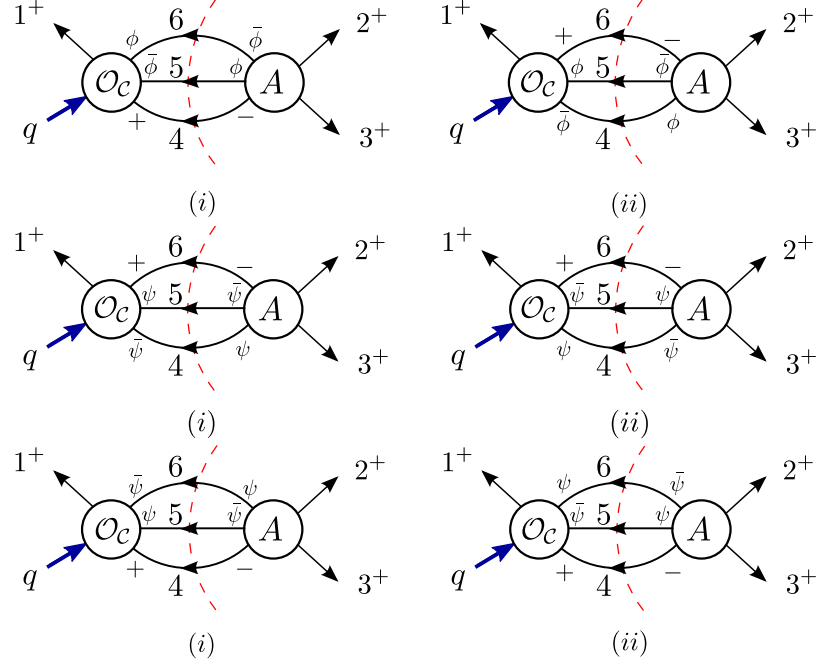
$\beta\gamma$ -term: Finally, we consider the third term in (4.4.11), for which we obtain

$$\begin{aligned}
 F_{\mathcal{O}_S}^{(2)}(1^+, 2^+, 3^+; q) \Big|_{3, q^2}^{\beta\gamma} &= i^3 F_{\mathcal{O}_S}^{(0)}(-6^+, -5^+, -4^+; q) \times A^{(0)}(1^+, 2^+, 3^+, 4^-, 5^-, 6^-) \Big|_{\beta\gamma} \\
 &= F_{\mathcal{O}_S}^{(0)}(1^+, 2^+, 3^+; q) \frac{[65][54][46] s_{123}[23]\langle 56 \rangle [1|p_2+p_3|4][12]\langle 45 \rangle [3|p_1+p_2|6]}{[12][23][31] s_{12}s_{23}s_{34}s_{45}s_{56}s_{16}} \\
 &= \frac{F_{\mathcal{O}_S}^{(0)}(1^+, 2^+, 3^+; q)}{s_{34}s_{16}s_{12}s_{23}s_{13}} s_{123} [1|q|4][46]\langle 6|q|3 \rangle \langle 13 \rangle
 \end{aligned}$$

$$= F_{\mathcal{O}_S}^{(0)}(1^+, 2^+, 3^+; q) \frac{s_{123}}{s_{12}s_{23}s_{13}} \text{Tr}_+(1 q 6 4 q 3) \times \text{Diagram} \quad (\text{C.2.3})$$

C.3 Scalar and fermion contributions to $\langle g^+ g^+ g^+ | \mathcal{O}_c | 0 \rangle$

In this section we isolate the individual contributions to the integrand of the two-loop form factor $\langle g^+ g^+ g^+ | \mathcal{O}_c | 0 \rangle$ from scalars and fermions running in the loops of the s_{23} -channel three-particle cut. The contributing cuts have been presented in Figures 42-44 and we quote them below for reader's convenience.



The relevant expressions for tree-level form factors were given in (4.4.19), (4.4.21), (4.4.22) and (4.4.24) and read

$$F_{\mathcal{O}_c}^{(0)}(1^+, -6^\phi, -5^{\bar{\phi}}, -4^+; q) = -\frac{1}{2} \frac{[14]}{[65]} ([54][16] + [51][46]),$$

$$F_{\mathcal{O}_c}^{(0)}(1^+, -6^+, -5^\phi, -4^{\bar{\phi}}; q) = -\frac{1}{2} \frac{[16]}{[54]} ([46][51] + [41][56]),$$

$$F_{\mathcal{O}_c}^{(0)}(1^+, -6^+, -5^\psi, -4^{\bar{\psi}}; q) = -\frac{[51][56][16]}{[54]},$$

$$F_{\mathcal{O}_c}^{(0)}(1^+, -6^+, -5^{\bar{\psi}}, -4^\psi; q) = \frac{[41][46][16]}{[54]},$$

$$F_{\mathcal{O}_c}^{(0)}(1^+, -6^{\bar{\psi}}, -5^\psi, -4^+; q) = \frac{[54][51][41]}{[65]},$$

$$F_{\mathcal{O}_c}^{(0)}(1^+, -6^\psi, -5^{\bar{\psi}}, -4^+; q) = -\frac{[64][61][41]}{[65]},$$

and where the two other form factors for the opposite assignment of the scalar pair

are identical to those presented. The corresponding tree-level amplitudes were given in (4.4.20), (4.4.21), (4.4.23) and (4.4.25) and read

$$\begin{aligned}
 A^{(0)}(2^+, 3^+, 4^-, 5^\phi, 6^{\bar{\phi}}) &= i \frac{\langle 45 \rangle \langle 46 \rangle^2}{\langle 23 \rangle \langle 34 \rangle \langle 56 \rangle \langle 62 \rangle}, \\
 A^{(0)}(2^+, 3^+, 4^\phi, 5^{\bar{\phi}}, 6^-) &= i \frac{\langle 56 \rangle \langle 46 \rangle^2}{\langle 23 \rangle \langle 34 \rangle \langle 45 \rangle \langle 62 \rangle}, \\
 A^{(0)}(2^+, 3^+, 4^\psi, 5^{\bar{\psi}}, 6^-) &= i \frac{\langle 56 \rangle^2 \langle 46 \rangle}{\langle 23 \rangle \langle 34 \rangle \langle 45 \rangle \langle 62 \rangle}, \\
 A^{(0)}(2^+, 3^+, 4^{\bar{\psi}}, 5^\psi, 6^-) &= -i \frac{\langle 46 \rangle^3}{\langle 23 \rangle \langle 34 \rangle \langle 45 \rangle \langle 62 \rangle}, \\
 A^{(0)}(2^+, 3^+, 4^-, 5^{\bar{\psi}}, 6^\psi) &= -i \frac{\langle 45 \rangle^2 \langle 46 \rangle}{\langle 23 \rangle \langle 34 \rangle \langle 56 \rangle \langle 62 \rangle}, \\
 A^{(0)}(2^+, 3^+, 4^-, 5^\psi, 6^{\bar{\psi}}) &= i \frac{\langle 46 \rangle^3}{\langle 23 \rangle \langle 34 \rangle \langle 56 \rangle \langle 62 \rangle}.
 \end{aligned}$$

In the case of $\mathcal{N}=4$ SYM calculation we would have multiplied the scalar diagrams by 6 and fermion diagrams by 4 to account for the possible ways of assigning the $SU(4)$ R -symmetry indices. In the present calculation, however, we leave the R -symmetry multiplicities unspecified as c_F for fermions and c_B for scalars, in order to derive generic expressions which can be then used for any amount of supersymmetry \mathcal{N} . Taking into account the usual fermion loop minus sign and factor of i^3 from three cut propagator legs, multiplying the expressions together we obtain

$$\begin{aligned}
 F_{\mathcal{O}_c}^{(2)}(1^+, 2^+, 3^+; q) \Big|_{3, s_{23}}^{\text{scalar, fermion}} &= \\
 &= \frac{\langle 46 \rangle}{\langle 23 \rangle \langle 34 \rangle \langle 62 \rangle} \left[-\frac{1}{2} \frac{c_B}{s_{56}} \left(s_{45} [1|64|1] + s_{46} [1|54|1] \right) - \frac{1}{2} \frac{c_B}{s_{45}} \left(s_{46} [1|65|1] + s_{56} [1|64|1] \right) \right. \\
 &\quad \left. + \frac{c_F}{s_{45}} s_{56} [1|65|1] + \frac{c_F}{s_{45}} s_{46} [1|64|1] + \frac{c_F}{s_{56}} s_{45} [1|54|1] + \frac{c_F}{s_{56}} s_{46} [1|64|1] \right] \\
 &= \frac{\langle 46 \rangle}{\langle 23 \rangle \langle 34 \rangle \langle 62 \rangle} \left[\frac{1}{s_{56}} \left([1|54|1] (c_F s_{45} - \frac{1}{2} c_B s_{46}) + [1|64|1] (c_F s_{46} - \frac{1}{2} c_B s_{45}) \right) \right. \\
 &\quad \left. + \frac{1}{s_{45}} \left([1|65|1] (c_F s_{56} - \frac{1}{2} c_B s_{46}) + [1|64|1] (c_F s_{46} - \frac{1}{2} c_B s_{56}) \right) \right]. \tag{C.3.1}
 \end{aligned}$$

We can then draw the corresponding integrals in this expression term-by-term:

$$\text{First term} = (c_F s_{45} - \frac{1}{2} c_B s_{46}) \frac{1}{s_{56}} \frac{F_{\mathcal{O}_S, \mathcal{O}_c}^{(0)}(1^+, 2^+, 3^+; q)}{[12][23][13]} \frac{\langle 46 \rangle [1|54|1]}{\langle 23 \rangle \langle 34 \rangle \langle 62 \rangle}$$

$$\begin{aligned}
 &= \frac{F_{\mathcal{O}_S, \mathcal{O}_C}^{(0)}(1^+, 2^+, 3^+; q)}{s_{12}s_{23}s_{31}} \left(-c_F s_{45} + \frac{1}{2} c_B s_{46}\right) \frac{[26]\langle 64\rangle[43]\langle 31\rangle[15]\langle 54\rangle[41]\langle 12\rangle}{s_{26}s_{34}s_{56}} \\
 &= \begin{array}{c} \text{Diagram 1} \\ \text{Diagram 2} \end{array} \times \frac{F_{\mathcal{O}_S, \mathcal{O}_C}^{(0)}(1^+, 2^+, 3^+; q)}{s_{12}s_{23}s_{31}} \left(c_F s_{45} - \frac{1}{2} c_B s_{46}\right) \text{Tr}_+(26431451), \quad (\text{C.3.2})
 \end{aligned}$$

$$\begin{aligned}
 \text{Second term} &= \left(c_F s_{46} - \frac{1}{2} c_B s_{45}\right) \frac{1}{s_{56}} \frac{F_{\mathcal{O}_S, \mathcal{O}_C}^{(0)}(1^+, 2^+, 3^+; q)}{[12][23][13]} \frac{\langle 46\rangle[1|64|1]}{\langle 23\rangle\langle 34\rangle\langle 62\rangle} \\
 &= \frac{F_{\mathcal{O}_S, \mathcal{O}_C}^{(0)}(1^+, 2^+, 3^+; q)}{s_{12}s_{23}s_{31}} \left(c_F s_{46} - \frac{1}{2} c_B s_{45}\right) \frac{[16]\langle 64\rangle[41]\langle 13\rangle[34]\langle 46\rangle[62]\langle 21\rangle}{s_{26}s_{34}s_{56}} \\
 &= \begin{array}{c} \text{Diagram 1} \\ \text{Diagram 2} \end{array} \times \frac{F_{\mathcal{O}_S, \mathcal{O}_C}^{(0)}(1^+, 2^+, 3^+; q)}{s_{12}s_{23}s_{31}} \left(c_F s_{46} - \frac{1}{2} c_B s_{45}\right) \text{Tr}_+(16413462), \quad (\text{C.3.3})
 \end{aligned}$$

$$\begin{aligned}
 \text{Third term} &= \left(c_F s_{56} - \frac{1}{2} c_B s_{46}\right) \frac{1}{s_{45}} \frac{F_{\mathcal{O}_S, \mathcal{O}_C}^{(0)}(1^+, 2^+, 3^+; q)}{[12][23][13]} \frac{\langle 46\rangle[1|65|1]}{\langle 23\rangle\langle 34\rangle\langle 62\rangle} \\
 &= \frac{F_{\mathcal{O}_S, \mathcal{O}_C}^{(0)}(1^+, 2^+, 3^+; q)}{s_{12}s_{23}s_{31}} \left(-c_F s_{56} + \frac{1}{2} c_B s_{46}\right) \frac{[34]\langle 46\rangle[62]\langle 21\rangle[15]\langle 56\rangle[61]\langle 13\rangle}{s_{26}s_{34}s_{45}} \\
 &= \begin{array}{c} \text{Diagram 1} \\ \text{Diagram 2} \end{array} \times \frac{F_{\mathcal{O}_S, \mathcal{O}_C}^{(0)}(1^+, 2^+, 3^+; q)}{s_{12}s_{23}s_{31}} \left(c_F s_{56} - \frac{1}{2} c_B s_{46}\right) \text{Tr}_+(34621651), \quad (\text{C.3.4})
 \end{aligned}$$

$$\begin{aligned}
 \text{Fourth term} &= \left(c_F s_{46} - \frac{1}{2} c_B s_{56}\right) \frac{1}{s_{45}} \frac{F_{\mathcal{O}_S, \mathcal{O}_C}^{(0)}(1^+, 2^+, 3^+; q)}{[12][23][13]} \frac{\langle 46\rangle[1|64|1]}{\langle 23\rangle\langle 34\rangle\langle 62\rangle} \\
 &= \frac{F_{\mathcal{O}_S, \mathcal{O}_C}^{(0)}(1^+, 2^+, 3^+; q)}{s_{12}s_{23}s_{31}} \left(c_F s_{46} - \frac{1}{2} c_B s_{56}\right) \frac{[14]\langle 46\rangle[61]\langle 12\rangle[26]\langle 64\rangle[43]\langle 31\rangle}{s_{26}s_{34}s_{45}} \\
 &= \begin{array}{c} \text{Diagram 1} \\ \text{Diagram 2} \end{array} \times \frac{F_{\mathcal{O}_S, \mathcal{O}_C}^{(0)}(1^+, 2^+, 3^+; q)}{s_{12}s_{23}s_{31}} \left(c_F s_{46} - \frac{1}{2} c_B s_{56}\right) \text{Tr}_+(14612643). \quad (\text{C.3.5})
 \end{aligned}$$

Appendix D

Non-minimal form factors

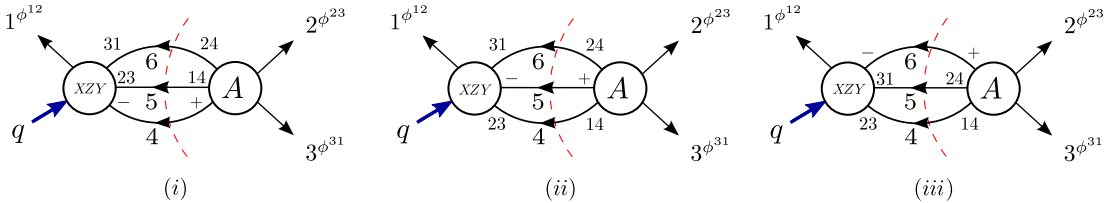
In this appendix we present details of the computations of non-minimal tree-level form factors using the method of MHV diagrams, which was introduced in Section 2.3. First, in Section D.1 we find non-minimal form factors required for computation of the s_{23} -channel three-particle cut of the two-loop form factor $\langle \bar{X}\bar{Y}\bar{Z}|\mathcal{O}_{\mathcal{B}}|0\rangle$ performed in Section 3.3.2. In Section D.2 we find the non-minimal tree-level form factor necessary for the calculation of the two-loop form factor $\langle g^+g^+g^+|\mathcal{O}_{\mathcal{C}}|0\rangle$ in Section 4.4.3.

D.1 Non-minimal form factors contributing to $\langle \bar{X}\bar{Y}\bar{Z}|\mathcal{O}_{\mathcal{B}}|0\rangle$

As discussed in Section 3.3.2, for the s_{23} -channel three-particle cut of the two loop form factor $\langle \bar{X}\bar{Y}\bar{Z}|\mathcal{O}_{\mathcal{B}}|0\rangle$ there are several possible helicity assignments for the particles running in the loops. In order to be able to evaluate this cut we need to compute the non-minimal, four-point tree-level form factors where either one of the legs is a gluon or two of the legs are fermionic. We tackle these two cases in turn.

Gluons in the loop

First, we find the non-minimal tree-level form factors contributing to the cuts presented in Figure 19, which we repeat below for reader's convenience.



We use MHV diagrams, introduced in Section 2.3 in order to find the tree-level form factors contributing to these cuts. The two MHV diagrams which we need to consider to find the non-minimal tree-level form factor in Figure 19(i) are presented in Figure 51.

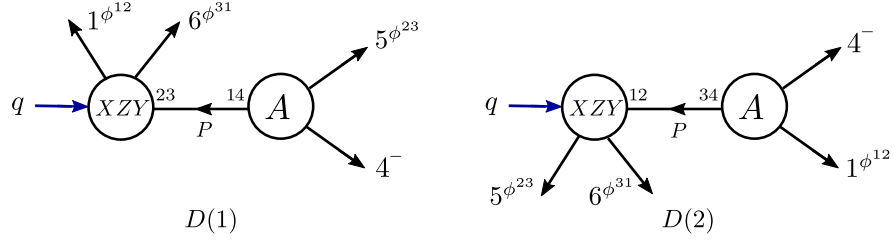


Figure 51: Two MHV diagrams for the non-minimal tree-level form factors contributing to unitarity cuts presented in in Figure 19(i).

We evaluate the two diagrams in turn. First, for $D(1)$ we have

$$\begin{aligned} D(1) &= F_{\mathcal{O}_{\text{offset}}}^{(0)}(1^{\phi^{12}}, 6^{\phi^{31}}, -P^{\phi^{23}}; q) \times \frac{1}{s_{45}} \times A_{\text{MHV}}^{(0)}(4^-, P^{\phi^{14}}, 5^{\phi^{23}}) \\ &= -2 \frac{1}{\langle 45 \rangle [54]} \times \frac{\langle 45 \rangle \langle 4 | P | \xi \rangle}{\langle 5 | P | \xi \rangle} = 2 \frac{1}{[54]} \frac{[5\xi]}{[4\xi]}, \end{aligned}$$

where we have used the off-shell continuation, $\lambda_P^\alpha \rightarrow \lambda_P^\alpha[P\xi]$ and the three-point momentum conservation, $P + p_4 + p_5 = 0$. Diagram $D(2)$ is given by

$$\begin{aligned} D(2) &= F_{\mathcal{O}_{\text{offset}}}^{(0)}(-P^{\phi^{12}}, 6^{\phi^{31}}, 5^{\phi^{23}}; q) \times \frac{1}{s_{14}} \times A_{\text{MHV}}^{(0)}(4^-, 1^{\phi^{12}}, P^{\phi^{34}}) \\ &= -2 \frac{1}{\langle 14 \rangle [41]} \times \frac{\langle 14 \rangle \langle 4 | P | \xi \rangle}{\langle 1 | P | \xi \rangle} = 2 \frac{1}{[41]} \frac{[1\xi]}{[4\xi]}, \end{aligned}$$

and summing the two together we arrive at

$$\begin{aligned} F_{\mathcal{O}_{\text{offset}}}^{(0)}(1^{\phi^{12}}, 6^{\phi^{31}}, 5^{\phi^{23}}, 4^-; q) &= D(1) + D(2) = \frac{2}{[4\xi]} \left(\frac{[5\xi]}{[54]} + \frac{[1\xi]}{[41]} \right) \\ &= \frac{2}{[4\xi]} \frac{[4\xi][51]}{[54][41]} = 2 \frac{[51]}{[54][41]}. \end{aligned} \quad (\text{D.1.1})$$

In order to find the non-minimal tree-level form factor in Figure 19(ii) we consider two MHV diagrams presented in Figure 52.

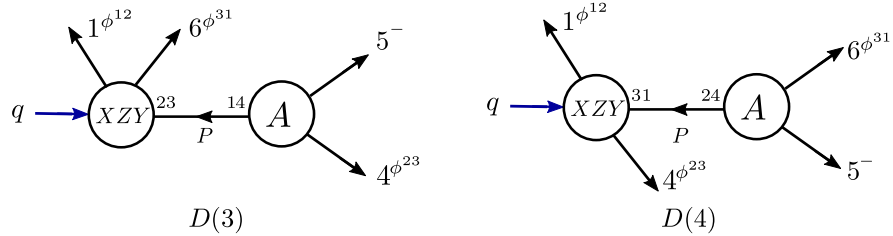


Figure 52: Two MHV diagrams for the non-minimal tree-level form factors contributing to unitarity cuts presented in in Figure 19(ii).

Performing the off-shell continuation, for $D(3)$ we have

$$\begin{aligned} D(3) &= F_{\mathcal{O}_{\text{offset}}}^{(0)}(1^{\phi^{12}}, 6^{\phi^{31}}, -P^{\phi^{23}}; q) \times \frac{1}{s_{45}} \times A_{\text{MHV}}^{(0)}(5^-, 4^{\phi^{23}}, P^{\phi^{14}}) \\ &= -2 \frac{1}{\langle 45 \rangle [54]} \times \frac{\langle 45 \rangle \langle 5 | P | \xi \rangle}{\langle 4 | P | \xi \rangle} = 2 \frac{1}{[54]} \frac{[4\xi]}{[5\xi]}, \end{aligned}$$

while $D(4)$ is given by

$$\begin{aligned} D(4) &= F_{\mathcal{O}_{\text{offset}}}^{(0)}(1^{\phi^{12}}, -P^{\phi^{31}}, 4^{\phi^{23}}; q) \times \frac{1}{s_{56}} \times A_{\text{MHV}}^{(0)}(5^-, P^{\phi^{24}}, 6^{\phi^{31}}) \\ &= -2 \frac{1}{\langle 56 \rangle [65]} \times \frac{\langle 56 \rangle \langle 5 | P | \xi \rangle}{\langle 6 | P | \xi \rangle} = 2 \frac{1}{[65]} \frac{[6\xi]}{[5\xi]}, \end{aligned}$$

and summing the two contributions together we arrive at

$$\begin{aligned} F_{\mathcal{O}_{\text{offset}}}^{(0)}(1^{\phi^{12}}, 6^{\phi^{31}}, 5^-, 4^{\phi^{23}}; q) &= D(3) + D(4) = \frac{2}{[5\xi]} \left(\frac{[4\xi]}{[54]} + \frac{[6\xi]}{[65]} \right) \\ &= \frac{2}{[5\xi]} \frac{[5\xi][64]}{[54][65]} = 2 \frac{[64]}{[65][54]}. \end{aligned} \quad (\text{D.1.2})$$

In order to find the non-minimal tree-level form factor in Figure 19(iii) we consider two MHV diagrams presented in Figure 53.

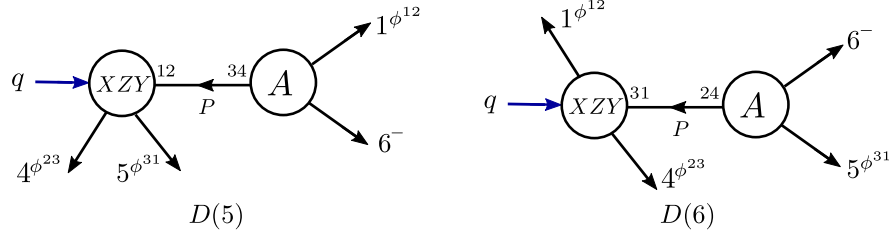


Figure 53: Two MHV diagrams for the non-minimal tree-level form factors contributing to unitarity cuts presented in Figure 19(iii).

For $D(5)$ we have

$$\begin{aligned} D(5) &= F_{\mathcal{O}_{\text{offset}}}^{(0)}(-P^{\phi^{12}}, 5^{\phi^{31}}, 4^{\phi^{23}}; q) \times \frac{1}{s_{16}} \times A_{\text{MHV}}^{(0)}(6^-, P^{\phi^{34}}, 1^{\phi^{12}}) \\ &= -2 \frac{1}{\langle 16 \rangle [61]} \times \frac{\langle 61 \rangle \langle 6 | P | \xi \rangle}{\langle 1 | P | \xi \rangle} = 2 \frac{1}{[16]} \frac{[1\xi]}{[6\xi]}, \end{aligned}$$

while $D(6)$ is given by

$$\begin{aligned} D(6) &= F_{\mathcal{O}_{\text{offset}}}^{(0)}(1^{\phi^{12}}, -P^{\phi^{31}}, 4^{\phi^{23}}; q) \times \frac{1}{s_{56}} \times A_{\text{MHV}}^{(0)}(5^{\phi^{31}}, P^{\phi^{24}}, 6^-) \\ &= -2 \frac{1}{\langle 56 \rangle [65]} \times \frac{\langle 56 \rangle \langle 6 | P | \xi \rangle}{\langle 5 | P | \xi \rangle} = 2 \frac{1}{[65]} \frac{[5\xi]}{[6\xi]}, \end{aligned}$$

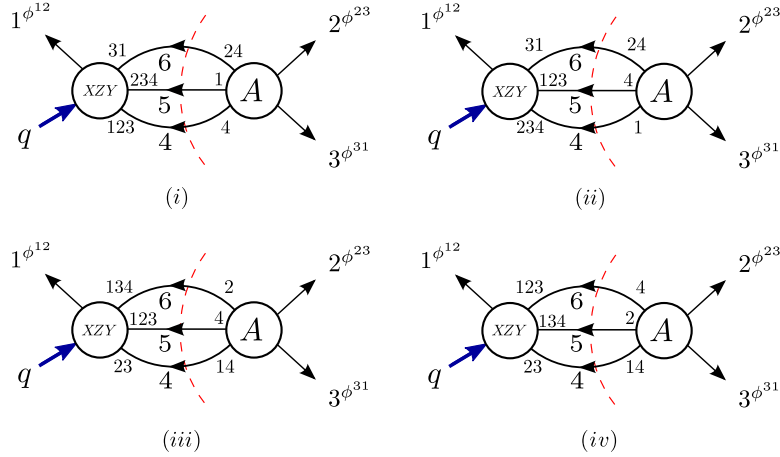
and summing the two diagrams together we arrive at

$$\begin{aligned}
 F_{\mathcal{O}_{\text{offset}}}^{(0)}(1^{\phi^{12}}, 6^-, 5^{\phi^{31}}, 4^{\phi^{23}}; q) &= D(5) + D(6) = \frac{2}{[6\xi]} \left(\frac{[1\xi]}{[16]} + \frac{[5\xi]}{[65]} \right) \\
 &= \frac{2}{[6\xi]} \frac{[6\xi][15]}{[16][65]} = 2 \frac{[15]}{[16][65]}. \tag{D.1.3}
 \end{aligned}$$

For the cuts presented in Figure 19 we need to find tree-level form factors with momenta p_4, p_5 and p_6 flowing into the form factor, *i.e.* with opposite direction to that in (D.1.1)-(D.1.3). Fortunately, these form factors are functions of square spinorial brackets only and as such, using the practical prescription of [182] where $\lambda_{-P} = -\lambda_P$, $\tilde{\lambda}_{-P} = \tilde{\lambda}_P$, $\eta_{-P} = \eta_P$, the expressions remain unchanged.

Fermions in the loop

Next, we find the non-minimal tree-level form factors contributing to the cuts presented in Figures 20 and 21, which we repeat below for reader's convenience.



Again, we use MHV diagrams to find the non-minimal tree-level form factors. In this case, however, to each of the non-minimal form factors corresponds only one MHV diagram. These are collectively presented in Figure 54.

Using the diagram in Figure 54(i), the first form factor is given by

$$\begin{aligned}
 F_{\mathcal{O}_{\text{offset}}}^{(0)}(1^{\phi^{12}}, 6^{\phi^{31}}, 5^{\bar{\psi}^{234}}, 4^{\bar{\psi}^{123}}; q) &= \\
 &= F_{\mathcal{O}_{\text{offset}}}^{(0)}(1^{\phi^{12}}, 6^{\phi^{31}}, -P^{\phi^{23}}; q) \times \frac{1}{s_{45}} \times A_{\text{MHV}}^{(0)}(4^{\bar{\psi}^{123}}, P^{\phi^{14}}, 5^{\bar{\psi}^{234}}) \\
 &= -2 \frac{1}{\langle 45 \rangle [54]} \times \langle 45 \rangle = \frac{2}{[45]}, \tag{D.1.4}
 \end{aligned}$$

and using the diagram in Figure 54(ii), the second form factor reads

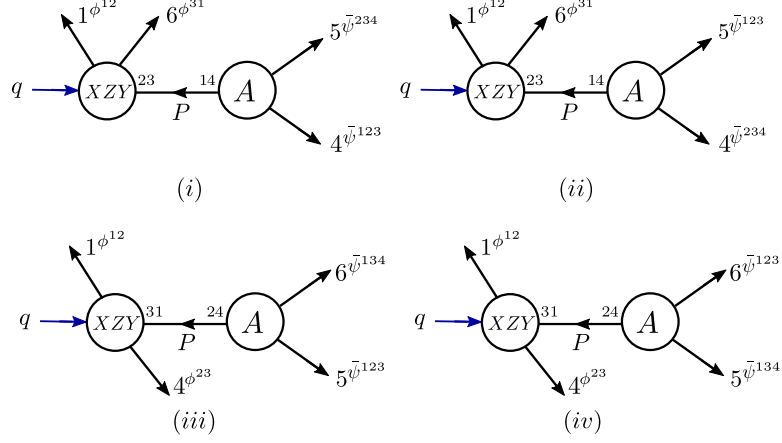


Figure 54: Four MHV diagrams for the non-minimal tree-level form factors contributing to unitarity cuts presented in in Figure 20 and Figure 21.

$$\begin{aligned}
 F_{\mathcal{O}_{\text{offset}}}^{(0)}(1^{\phi^{12}}, 6^{\phi^{31}}, 5^{\bar{\psi}^{123}}, 4^{\bar{\psi}^{234}}; q) &= \\
 &= F_{\mathcal{O}_{\text{offset}}}^{(0)}(1^{\phi^{12}}, 6^{\phi^{31}}, -P^{\phi^{23}}; q) \times \frac{1}{s_{45}} \times A_{\text{MHV}}^{(0)}(4^{\bar{\psi}^{234}}, P^{\phi^{14}}, 5^{\bar{\psi}^{123}}) \\
 &= -2 \frac{1}{\langle 45 \rangle [54]} \times \langle 54 \rangle = \frac{2}{[54]}. \tag{D.1.5}
 \end{aligned}$$

Just as simply, we use the diagrams in Figure 54(*iii*) and (*iv*) to obtain the third and fourth form factor,

$$\begin{aligned}
 F_{\mathcal{O}_{\text{offset}}}^{(0)}(1^{\phi^{12}}, 6^{\bar{\psi}^{134}}, 5^{\bar{\psi}^{123}}, 4^{\phi^{23}}; q) &= \\
 &= F_{\mathcal{O}_{\text{offset}}}^{(0)}(1^{\phi^{12}}, -P^{\phi^{31}}, 4^{\phi^{23}}; q) \times \frac{1}{s_{56}} \times A_{\text{MHV}}^{(0)}(5^{\bar{\psi}^{123}}, P^{\phi^{24}}, 6^{\bar{\psi}^{134}}) \\
 &= -2 \frac{1}{\langle 56 \rangle [65]} \times \langle 65 \rangle = \frac{2}{[65]}, \tag{D.1.6}
 \end{aligned}$$

$$\begin{aligned}
 F_{\mathcal{O}_{\text{offset}}}^{(0)}(1^{\phi^{12}}, 6^{\bar{\psi}^{123}}, 5^{\bar{\psi}^{134}}, 4^{\phi^{23}}; q) &= \\
 &= F_{\mathcal{O}_{\text{offset}}}^{(0)}(1^{\phi^{12}}, -P^{\phi^{31}}, 4^{\phi^{23}}; q) \times \frac{1}{s_{56}} \times A_{\text{MHV}}^{(0)}(5^{\bar{\psi}^{134}}, P^{\phi^{24}}, 6^{\bar{\psi}^{123}}) \\
 &= -2 \frac{1}{\langle 56 \rangle [65]} \times \langle 56 \rangle = \frac{2}{[56]}. \tag{D.1.7}
 \end{aligned}$$

D.2 Non-minimal form factors contributing to $\langle g^+ g^+ g^+ | \mathcal{O}_C | 0 \rangle$

In this section we perform an independent check of the expression for the four-point non-minimal form factor of \mathcal{O}_C with the external state made up of positive-helicity gluons,

which we use in Section 4.4.3. Its expression has been calculated in [38] and reads

$$F_{\mathcal{O}_c}^{(0)}(1^+, 2^+, 3^+, 4^+; q) = \frac{[12][23][34][41]}{s_{12}} \left(1 + \frac{[31][4|q|3]}{s_{23}[41]} \right) + \text{cyclic}(1, 2, 3, 4). \quad (\text{D.2.1})$$

We re-derive this expression using the method of MHV diagrams, reviewed in Section 2.3, which we modify to a version more suitable to the present calculation with positive-helicity fields in the external state. In particular, we perform the off-shell continuation $\tilde{\lambda}_P^\alpha \rightarrow \tilde{\lambda}_P^\alpha \langle P\xi \rangle$ and use the (anti-)MHV diagram presented in Figure 55 to which we add three others, with the external legs cyclically permuted. The tree-level minimal form factor is given by (4.2.1) and the tree-level $\overline{\text{MHV}}$ amplitude is given in (2.2.9).

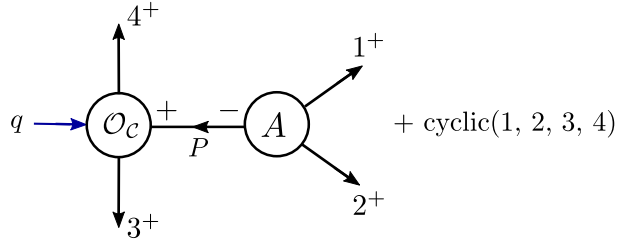


Figure 55: Four MHV diagrams for the non-minimal tree-level form factor (4.2.6).

The whole diagram in Figure 55 is then given by

$$\begin{aligned} F_{\mathcal{O}_c}^{(0)}(1^+, 2^+, 3^+, 4^+; q) &= \\ &= F_{\mathcal{O}_c}^{(0)}(4^+, -P^+, 3^+; q) \times \frac{1}{s_{12}} \times A_{\overline{\text{MHV}}}^{(0)}(2^+, P^-, 1^+) + \text{cyclic}(1, 2, 3, 4) \\ &= -[4|P|\xi]\langle\xi|P|3\rangle[34] \times \frac{1}{\langle 21\rangle[12]} \times \frac{[21]^3}{\langle\xi|P|1\rangle[2|P|\xi]} + \text{cyclic}(1, 2, 3, 4) \\ &= \frac{[4|P|\xi][3|P|\xi][34][12]^2}{[1|P|\xi][2|P|\xi]\langle 21\rangle} + \text{cyclic}(1, 2, 3, 4) \\ &= \frac{[4|1+2|\xi][3|1+2|\xi][34][12]^2}{[1|2|\xi][2|1|\xi]\langle 21\rangle} + \text{cyclic}(1, 2, 3, 4) \\ &= \frac{([41]\langle 1\xi\rangle + [42]\langle 2\xi\rangle)([31]\langle 1\xi\rangle + [32]\langle 2\xi\rangle)[34]}{\langle 2\xi\rangle\langle 1\xi\rangle\langle 12\rangle} + \text{cyclic}(1, 2, 3, 4) \\ &= \left(\frac{[41][31]\langle 1\xi\rangle}{\langle 2\xi\rangle} + [41][32] + [42][31] + \frac{[42][32]\langle 2\xi\rangle}{\langle 1\xi\rangle} \right) \frac{[34]}{\langle 12\rangle} + \text{cyclic}(1, 2, 3, 4) \end{aligned} \quad (\text{D.2.2})$$

Let us first isolate the ξ -dependent terms in (D.2.2) and sum over all of the cyclic permutations:

$$F_{\mathcal{O}_c}^{(0)}(1^+, 2^+, 3^+, 4^+; q) \Big|_{\xi} = \frac{[41][31][34]\langle 1\xi\rangle}{\langle 2\xi\rangle\langle 12\rangle} + \frac{[42][32][34]\langle 2\xi\rangle}{\langle 1\xi\rangle\langle 12\rangle} + \frac{[12][42][41]\langle 2\xi\rangle}{\langle 3\xi\rangle\langle 23\rangle}$$

$$\begin{aligned}
 & + \frac{[13][43][41]\langle 3\xi \rangle}{\langle 2\xi \rangle \langle 23 \rangle} + \frac{[23][13][12]\langle 3\xi \rangle}{\langle 4\xi \rangle \langle 34 \rangle} + \frac{[24][14][12]\langle 4\xi \rangle}{\langle 3\xi \rangle \langle 34 \rangle} + \frac{[34][24][23]\langle 4\xi \rangle}{\langle 1\xi \rangle \langle 41 \rangle} + \frac{[31][21][23]\langle 1\xi \rangle}{\langle 4\xi \rangle \langle 41 \rangle} \\
 & = \frac{[42][32][34]}{\langle 1\xi \rangle} \left(\frac{\langle 2\xi \rangle}{\langle 12 \rangle} + \frac{\langle 4\xi \rangle}{\langle 41 \rangle} \right) + \frac{[41][31][34]}{\langle 2\xi \rangle} \left(\frac{\langle 1\xi \rangle}{\langle 12 \rangle} + \frac{\langle 3\xi \rangle}{\langle 23 \rangle} \right) \\
 & + \frac{[42][12][41]}{\langle 3\xi \rangle} \left(\frac{\langle 2\xi \rangle}{\langle 23 \rangle} + \frac{\langle 4\xi \rangle}{\langle 34 \rangle} \right) + \frac{[23][13][12]}{\langle 4\xi \rangle} \left(\frac{\langle 3\xi \rangle}{\langle 34 \rangle} + \frac{\langle 1\xi \rangle}{\langle 41 \rangle} \right) \\
 & = \frac{[42][32][34]}{\langle 1\xi \rangle} \frac{\langle 1\xi \rangle \langle 42 \rangle}{\langle 12 \rangle \langle 41 \rangle} + \frac{[41][31][34]}{\langle 2\xi \rangle} \frac{\langle 2\xi \rangle \langle 13 \rangle}{\langle 12 \rangle \langle 23 \rangle} \\
 & + \frac{[42][12][41]}{\langle 3\xi \rangle} \frac{\langle 3\xi \rangle \langle 24 \rangle}{\langle 23 \rangle \langle 34 \rangle} + \frac{[23][13][12]}{\langle 4\xi \rangle} \frac{\langle 4\xi \rangle \langle 31 \rangle}{\langle 34 \rangle \langle 41 \rangle} \\
 & = s_{24} \frac{[23][34]}{\langle 12 \rangle \langle 41 \rangle} + s_{31} \frac{[41][34]}{\langle 12 \rangle \langle 23 \rangle} + s_{24} \frac{[12][41]}{\langle 23 \rangle \langle 34 \rangle} + s_{13} \frac{[23][12]}{\langle 34 \rangle \langle 41 \rangle} \tag{D.2.3}
 \end{aligned}$$

where in the second step we have used the Schouten identity (2.1.21). We can see that the reference spinor dependence has cancelled out as expected and we can recombine the terms in (D.2.3) with the ξ -independent leftover of (D.2.2) (plus cyclic permutations).

$$\begin{aligned}
 F_{\mathcal{O}_c}^{(0)}(1^+, 2^+, 3^+, 4^+; q) & = \\
 & = ([41][32] + [42][31]) \frac{[34]}{\langle 12 \rangle} + s_{31} \frac{[41][34]}{\langle 12 \rangle \langle 23 \rangle} + ([12][43] + [13][42]) \frac{[41]}{\langle 23 \rangle} + s_{24} \frac{[12][41]}{\langle 23 \rangle \langle 34 \rangle} \\
 & + ([23][14] + [24][13]) \frac{[12]}{\langle 34 \rangle} + s_{13} \frac{[23][12]}{\langle 34 \rangle \langle 41 \rangle} + ([34][21] + [31][24]) \frac{[23]}{\langle 41 \rangle} + s_{24} \frac{[23][34]}{\langle 12 \rangle \langle 41 \rangle} \\
 & = ([41][32] + [42][31]) \frac{[34]}{\langle 12 \rangle} + s_{31} \frac{[41][34]}{\langle 12 \rangle \langle 23 \rangle} + \text{cyclic}(1, 2, 3, 4) \\
 & = \frac{[31][34]}{\langle 12 \rangle \langle 23 \rangle} ([42]\langle 23 \rangle + [41]\langle 13 \rangle) + \frac{[41][32][34]}{\langle 12 \rangle} + \text{cyclic}(1, 2, 3, 4) \\
 & = \frac{[34]}{\langle 12 \rangle} \left(\frac{[31][4|q|3]}{\langle 23 \rangle} + [41][32] \right) + \text{cyclic}(1, 2, 3, 4) \\
 & = [12][23][34][41] \left(\frac{[31][4|q|3]}{\langle 12 \rangle [12] \langle 23 \rangle [23][41]} - \frac{1}{\langle 12 \rangle [12]} \right) + \text{cyclic}(1, 2, 3, 4) \\
 & = \frac{[12][23][34][41]}{s_{12}} \left(1 + \frac{[31][4|q|3]}{s_{23}[41]} \right) + \text{cyclic}(1, 2, 3, 4), \tag{D.2.4}
 \end{aligned}$$

which is the expression quoted in (4.2.6).

Appendix E

Numerators

In this appendix we present the numerators of the integral topologies which constitute the two loop integrands for form factors of \mathcal{O}_S and \mathcal{O}_C in $\mathcal{N}=4, 2, 1$ SYM. The integral topologies, denoted as I_i , $i = 1, \dots, 15$ are presented in Table 10.

E.1 Two-loop integrand for $\langle g^+ g^+ g^+ | \mathcal{O}_S | 0 \rangle$ in $\mathcal{N}=4$ SYM

The integrand of the two-loop minimal form factor of the Konishi descendant operator \mathcal{O}_S is given by

$$F_{\mathcal{O}_S}^{(2)}(1^+, 2^+, 3^+; q) = F_{\mathcal{O}_S, \mathcal{O}_C}^{(0)}(1^+, 2^+, 3^+; q) \sum_{i=1}^{12} N_i \times I_i + \text{cyclic}(1, 2, 3), \quad (\text{E.1.1})$$

where⁴⁴

$$N_1 = \frac{1}{2} \frac{s_{23}}{s_{12}s_{13}} \left[2s_{12}s_{23}s_{13} - 2p_1 \cdot (p_3 + \ell) s_{23}(s_{12} - s_{13}) + (s_{12} + s_{13})^2 (p_3 + \ell)^2 \right],$$

$$N_2 = \frac{\text{Tr}(1 q k q \ell k q 1 3 2)}{s_{12}s_{23}s_{13}},$$

$$N_3 = N_2 \Big|_{p_2 \leftrightarrow p_3},$$

$$N_4 = \frac{s_{123}}{s_{12}s_{23}s_{13}} \text{Tr}(1 q \ell k q 3),$$

$$N_5 = \frac{1}{2} \left[-3(s_{2\ell} + s_{23} + s_{1k}) - \frac{s_{23}^3 + 2s_{23}s_{3k}s_{1\ell} + s_{23}s_{3k}s_{2\ell} + 2s_{23}^2(s_{1k} + s_{2\ell})}{2s_{12}s_{13}} \right. \\ \left. - \frac{s_{23}(s_{1k} + s_{2\ell} + 2s_{3k} + 4s_{1\ell} + 2s_{23}) + s_{13}(s_{3k} + s_{1\ell} - 3s_{2\ell} + s_{23})}{s_{12}} \right]$$

⁴⁴Note that the N_1 quoted here is before the PV reduction, in contrast to (4.4.34). PV reduction procedure relates the two, but it affects the numerators N_6 and N_7 accordingly.

$$\begin{aligned}
 & + \left. \frac{2s_{1k}s_{2\ell} + s_{3k}(s_{1\ell} + s_{2\ell})}{s_{12}} + \frac{s_{12}s_{3k} - s_{1k}s_{2\ell}}{s_{23}} + \frac{s_{12}s_{3k}(s_{12} - s_{1\ell})}{s_{13}s_{23}} \right] \\
 & + (p_2 \leftrightarrow p_3, k \leftrightarrow \ell), \\
 N_6 & = s_{23} \left(\frac{s_{1\ell}}{s_{12}} - \frac{s_{1\ell}}{s_{13}} + \frac{s_{13}}{2s_{12}} - \frac{s_{12}}{s_{13}} - \frac{1}{2} \right), \\
 N_7 & = N_6 \Big|_{p_2 \leftrightarrow p_3}, \\
 N_8 & = -2 + \frac{s_{23}(s_{1\ell} - s_{23})}{2s_{12}s_{13}} + \frac{s_{12}s_{1\ell}}{2s_{13}s_{23}} + \frac{s_{1\ell} - 2s_{23} - s_{13}}{2s_{12}} + \frac{2s_{1\ell} - s_{23} + 2s_{12}}{2s_{13}} \\
 & + \frac{s_{1\ell} - s_{12} - s_{13}}{2s_{23}}, \\
 N_9 & = N_8 \Big|_{p_2 \leftrightarrow p_3}, \\
 N_{10} & = -\frac{(s_{12} + s_{13})^2}{s_{12}s_{13}}, \\
 N_{11} & = N_{10}, \\
 N_{12} & = \frac{s_{12} + s_{23} + s_{13}}{2s_{12}s_{13}}. \tag{E.1.2}
 \end{aligned}$$

E.2 Two-loop integrand for $\langle g^+ g^+ g^+ | \mathcal{O}_c | 0 \rangle$ in $\mathcal{N} = 4$ SYM

The two-loop integrand of the form factor of the component operator \mathcal{O}_c can be conveniently expressed in terms that of the supersymmetric operator \mathcal{O}_S plus an offset term:

$$\begin{aligned}
 F_{\mathcal{O}_c}^{(2)}(1^+, 2^+, 3^+; q) & = F_{\mathcal{O}_S}^{(2)}(1^+, 2^+, 3^+; q) + \Delta_{\mathcal{N}=4}, \\
 \Delta_{\mathcal{N}=4} & = F_{\mathcal{O}_S, \mathcal{O}_c}^{(0)}(1^+, 2^+, 3^+; q) \sum_{i=5}^{12} \tilde{N}_i \times I_i + \text{cyclic}(1, 2, 3), \tag{E.2.1}
 \end{aligned}$$

$$\begin{aligned}
 \tilde{N}_5 & = \frac{s_{3k}s_{2\ell}}{s_{23}} - \frac{s_{3k}s_{1\ell}}{s_{13}} - \frac{s_{1k}s_{3k}s_{2\ell}}{s_{12}s_{23}} + \frac{s_{3k}^2}{2s_{23}} + \frac{5s_{3k}}{2} - \frac{3s_{1k}s_{3k}}{2s_{12}} - \frac{3s_{23}s_{1k}}{2s_{12}} \\
 & + s_{23} + (p_2 \leftrightarrow p_3, k \leftrightarrow \ell), \\
 \tilde{N}_6 & = \frac{s_{2k}s_{1\ell}}{2s_{13}} - \frac{s_{3k}s_{1\ell}}{2s_{12}} - \frac{s_{23}s_{1k}}{2s_{13}} + \frac{s_{2k}}{2} + \frac{s_{3k}}{2} + \frac{s_{12}(s_{2k} + s_{3k})}{2s_{13}}, \\
 \tilde{N}_7 & = \tilde{N}_6 \Big|_{p_2 \leftrightarrow p_3}, \\
 \tilde{N}_8 & = 4 + \frac{s_{2k}s_{1\ell}}{s_{12}s_{23}} + \frac{4s_{2k} + 3s_{3k} + 6s_{3\ell}}{2s_{23}} + \frac{s_{2k}s_{1\ell} + s_{12}(s_{2k} + s_{3k} + s_{3\ell})}{s_{13}s_{23}}
 \end{aligned}$$

$$\begin{aligned}
 & -\frac{s_{1k}}{s_{13}} - \frac{3s_{1\ell}}{s_{12}} + \frac{3s_{12}}{2s_{13}}, \\
 \tilde{N}_9 &= \tilde{N}_8 \Big|_{p_2 \leftrightarrow p_3}, \\
 \tilde{N}_{10} &= -\frac{s_{1k}}{2s_{12}} + \frac{s_{2k}}{s_{23}} + \frac{s_{13}s_{2k}}{2s_{12}s_{23}} + \frac{s_{12}s_{2k}}{2s_{13}s_{23}} + (p_2 \leftrightarrow p_3), \\
 \tilde{N}_{11} &= \tilde{N}_{10}, \\
 \tilde{N}_{12} &= \frac{3s_{12} - s_{1k}}{s_{13}s_{23}} + \frac{3s_{13} - s_{1\ell}}{s_{12}s_{23}} + \frac{8}{s_{23}}. \tag{E.2.2}
 \end{aligned}$$

E.3 Two-loop integrand for $\langle g^+ g^+ g^+ | \mathcal{O}_S | 0 \rangle$ in $\mathcal{N}=2$ SYM

The integrand for the two-loop form factor of \mathcal{O}_S computed in $\mathcal{N}=2$ SYM can be expressed in terms of its difference with respect to the $\mathcal{N}=4$ SYM result as

$$\begin{aligned}
 F_{\mathcal{N}=2\mathcal{O}_S}^{(2)}(1^+, 2^+, 3^+; q) &= F_{\mathcal{N}=4\mathcal{O}_S}^{(2)}(1^+, 2^+, 3^+; q) + \Delta_{\mathcal{N}=2\mathcal{O}_S}, \\
 \Delta_{\mathcal{N}=2\mathcal{O}_S} &= F_{\mathcal{O}_S, \mathcal{O}_c}^{(0)}(1^+, 2^+, 3^+; q) \sum_{i=5}^{15} N'_i \times I_i + \text{cyclic}(1, 2, 3), \tag{E.3.1}
 \end{aligned}$$

with the numerators

$$\begin{aligned}
 N'_5 &= \frac{2s_{3k}s_{2\ell}}{3s_{23}} - \frac{s_{1k}s_{2\ell}}{s_{12}} + \frac{5s_{3k}}{3} - \frac{4s_{23}s_{1k}}{3s_{12}} - \frac{s_{1k}s_{3k}}{3s_{12}} + \frac{s_{2\ell}^2}{3s_{23}} + \frac{2s_{23}}{3} + (p_2 \leftrightarrow p_3, k \leftrightarrow \ell), \\
 N'_6 &= \frac{s_{2k}s_{1\ell} + s_{12}s_{2k} + s_{12}s_{3k} - s_{23}s_{1k}}{3s_{13}} - \frac{s_{3k}s_{1\ell}}{3s_{12}} + \frac{s_{2k} + s_{3k}}{3} - \frac{s_{23}s_{1\ell}}{s_{12}}, \\
 N'_7 &= N'_6 \Big|_{p_2 \leftrightarrow p_3}, \\
 N'_8 &= 3 - \frac{s_{1\ell}}{3s_{12}} + \frac{s_{1\ell}}{s_{13}} + \frac{4s_{12}}{3s_{13}} + \frac{2s_{2k} + s_{3k} + 4s_{3\ell}}{3s_{23}}, \\
 N'_9 &= N'_8 \Big|_{p_2 \leftrightarrow p_3}, \\
 N'_{10} &= 1 + \frac{2(s_{2k} + s_{3k})}{3s_{23}} + \frac{s_{12}s_{2k} + s_{12}s_{3k}}{3s_{13}s_{23}} + \frac{s_{13}s_{2k} + s_{13}s_{3k}}{3s_{12}s_{23}} - \frac{s_{1k} + 3s_{13}}{3s_{12}} - \frac{s_{1k} + 3s_{1\ell}}{3s_{13}}, \\
 N'_{11} &= N'_{10} \Big|_{p_2 \leftrightarrow p_3}, \\
 N'_{12} &= \frac{2}{s_{23}} + \frac{4s_{12}}{3s_{13}s_{23}} + (p_2 \leftrightarrow p_3, k \leftrightarrow \ell), \\
 N'_{13} &= s_{2\ell} + \frac{(s_{1k} + s_{13})s_{2\ell} - (s_{2k} + s_{23})s_{1\ell}}{s_{12}} - \frac{s_{1\ell}(s_{2k} + s_{23})}{s_{13}}, \\
 N'_{14} &= N'_{13} \Big|_{p_2 \leftrightarrow p_3},
 \end{aligned}$$

$$N'_{15} = 2 \frac{\text{Tr}_+(1 \ell k 1 3 2)}{s_{12} s_{13}}. \quad (\text{E.3.2})$$

E.4 Two-loop integrand for $\langle g^+ g^+ g^+ | \mathcal{O}_c | 0 \rangle$ in $\mathcal{N} = 2$ SYM

The integrand for the two-loop form factor of \mathcal{O}_c computed in $\mathcal{N} = 2$ SYM can be expressed in terms of its difference with respect to the $\mathcal{N} = 4$ SYM result as

$$\begin{aligned} F_{\mathcal{N}=2 \mathcal{O}_c}^{(2)}(1^+, 2^+, 3^+; q) &= F_{\mathcal{N}=4 \mathcal{O}_c}^{(2)}(1^+, 2^+, 3^+; q) + \Delta_{\mathcal{N}=2 \mathcal{O}_c}, \\ \Delta_{\mathcal{N}=2 \mathcal{O}_c} &= F_{\mathcal{O}_S, \mathcal{O}_c}^{(0)}(1^+, 2^+, 3^+; q) \sum_{i=5}^{15} \hat{N}_i \times I_i + \text{cyclic}(1, 2, 3), \end{aligned} \quad (\text{E.4.1})$$

with the numerators

$$\begin{aligned} \hat{N}_5 &= \frac{s_{1k} s_{2\ell} s_{3k}}{s_{12} s_{23}} + \frac{s_{1k} s_{3k}}{s_{12}} + (p_2 \leftrightarrow p_3, k \leftrightarrow \ell), \\ \hat{N}_6 &= -\frac{s_{23} s_{1\ell}}{s_{12}}, \\ \hat{N}_7 &= \hat{N}_6 \Big|_{p_2 \leftrightarrow p_3}, \\ \hat{N}_8 &= \frac{2s_{1\ell}}{s_{12}} + \frac{s_{1k} + s_{1\ell}}{s_{13}} - \frac{s_{2k} + s_{3k} + s_{3\ell}}{s_{23}} - \frac{s_{1\ell} s_{2k}}{s_{12} s_{23}} - \frac{(s_{1\ell} + s_{12}) s_{2k} + (s_{3k} + s_{3\ell}) s_{12}}{s_{13} s_{23}}, \\ \hat{N}_9 &= \hat{N}_8 \Big|_{p_2 \leftrightarrow p_3}, \\ \hat{N}_{10} &= 1 - \frac{s_{1\ell}}{s_{13}} + \frac{s_{13}}{s_{12}}, \\ \hat{N}_{11} &= \hat{N}_{10} \Big|_{p_2 \leftrightarrow p_3}, \\ \hat{N}_{12} &= \frac{s_{1\ell}}{s_{12} s_{23}} - \frac{s_{12}}{s_{13} s_{23}} - \frac{1}{s_{23}} + (p_2 \leftrightarrow p_3, k \leftrightarrow \ell), \\ \hat{N}_{13} &= s_{2\ell} + \frac{s_{1k} s_{2\ell} - s_{1\ell} s_{2k} - s_{1\ell} s_{23} + s_{13} s_{2\ell}}{s_{12}} - \frac{s_{1\ell} (s_{2k} + s_{23})}{s_{13}}, \\ \hat{N}_{14} &= \hat{N}_{13} \Big|_{p_2 \leftrightarrow p_3}, \\ \hat{N}_{15} &= 2 \frac{\text{Tr}_+(1 \ell k 1 3 2)}{s_{12} s_{13}}. \end{aligned} \quad (\text{E.4.2})$$

E.5 Two-loop integrand for $\langle g^+ g^+ g^+ | \mathcal{O}_S | 0 \rangle$ and $\langle g^+ g^+ g^+ | \mathcal{O}_c | 0 \rangle$ in $\mathcal{N} = 1$ SYM

Finally, we quote the result for the two-loop form factors calculated in $\mathcal{N} = 1$ SYM. As explained in Section 4.2, there is no difference between the form factors of the

supersymmetric and component operators for our particular external state. As a result, the integrand for the two-loop form factor of $\mathcal{O}_S, \mathcal{O}_C$ computed in $\mathcal{N}=1$ SYM can be expressed in terms of its difference with respect to the $\mathcal{N}=4$ SYM result for \mathcal{O}_C as

$$\begin{aligned}
 F_{\mathcal{N}=1, \mathcal{O}_S, \mathcal{O}_C}^{(2)}(1^+, 2^+, 3^+; q) &= F_{\mathcal{N}=4, \mathcal{O}_C}^{(2)}(1^+, 2^+, 3^+; q) + \Delta_{\mathcal{N}=1}, & (E.5.1) \\
 \Delta_{\mathcal{N}=1} &= F_{\mathcal{O}_S, \mathcal{O}_C}^{(0)}(1^+, 2^+, 3^+; q) \sum_{i=5}^{15} N_i'' \times I_i + \text{cyclic}(1, 2, 3),
 \end{aligned}$$

with the numerators

$$N_i'' = \frac{3}{2} \hat{N}_i, \quad i = 5, \dots, 15. \quad (E.5.2)$$

Bibliography

- [1] A. Brandhuber, M. Kostacińska, B. Penante, G. Travaglini and D. Young, *The $SU(2|3)$ dynamic two-loop form factors*, *JHEP* **08** (2016) 134 [1606.08682].
- [2] A. Brandhuber, M. Kostacińska, B. Penante and G. Travaglini, *Higgs amplitudes from $\mathcal{N} = 4$ super Yang-Mills theory*, *Phys. Rev. Lett.* **119** (2017) 161601 [1707.09897].
- [3] A. Brandhuber, M. Kostacinska, B. Penante and G. Travaglini, *Higgs amplitudes from supersymmetric form factors Part I: $\mathcal{N} = 4$ super Yang-Mills*, 1804.05703.
- [4] A. Brandhuber, M. Kostacinska, B. Penante and G. Travaglini, *Higgs amplitudes from supersymmetric form factors Part II: $\mathcal{N} < 4$ super Yang-Mills*, 1804.05828.
- [5] CMS collaboration, S. Chatrchyan et al., *Observation of a new boson at a mass of 125 GeV with the CMS experiment at the LHC*, *Phys. Lett.* **B716** (2012) 30 [1207.7235].
- [6] ATLAS collaboration, G. Aad et al., *Observation of a new particle in the search for the Standard Model Higgs boson with the ATLAS detector at the LHC*, *Phys. Lett.* **B716** (2012) 1 [1207.7214].
- [7] F. Englert and R. Brout, *Broken Symmetry and the Mass of Gauge Vector Mesons*, *Phys. Rev. Lett.* **13** (1964) 321.
- [8] P. W. Higgs, *Broken Symmetries and the Masses of Gauge Bosons*, *Phys. Rev. Lett.* **13** (1964) 508.
- [9] G. S. Guralnik, C. R. Hagen and T. W. B. Kibble, *Global Conservation Laws and Massless Particles*, *Phys. Rev. Lett.* **13** (1964) 585.
- [10] H. Lehmann, K. Symanzik and W. Zimmerman, *Zur Formulierung quantisierter Feldtheorien*, *Nuovo Cimento* **1(1)** (1955) 205.
- [11] M. L. Mangano and S. J. Parke, *Multiparton amplitudes in gauge theories*, *Phys. Rept.* **200** (1991) 301 [hep-th/0509223].

-
- [12] S. J. Parke and T. R. Taylor, *An Amplitude for n Gluon Scattering*, *Phys. Rev. Lett.* **56** (1986) 2459.
- [13] Z. Bern, L. J. Dixon, D. C. Dunbar and D. A. Kosower, *One loop n point gauge theory amplitudes, unitarity and collinear limits*, *Nucl. Phys.* **B425** (1994) 217 [hep-ph/9403226].
- [14] Z. Bern, L. J. Dixon, D. C. Dunbar and D. A. Kosower, *Fusing gauge theory tree amplitudes into loop amplitudes*, *Nucl. Phys.* **B435** (1995) 59 [hep-ph/9409265].
- [15] Z. Bern and A. G. Morgan, *Massive loop amplitudes from unitarity*, *Nucl. Phys.* **B467** (1996) 479 [hep-ph/9511336].
- [16] Z. Bern, L. J. Dixon and D. A. Kosower, *Two-loop $g \rightarrow gg$ splitting amplitudes in QCD*, *JHEP* **08** (2004) 012 [hep-ph/0404293].
- [17] E. Witten, *Perturbative gauge theory as a string theory in twistor space*, *Commun. Math. Phys.* **252** (2004) 189 [hep-th/0312171].
- [18] R. Penrose, *Twistor algebra*, *J. Math. Phys.* **8** (1967) 345.
- [19] R. Britto, F. Cachazo, B. Feng and E. Witten, *Direct proof of tree-level recursion relation in Yang-Mills theory*, *Phys. Rev. Lett.* **94** (2005) 181602 [hep-th/0501052].
- [20] F. Cachazo, P. Svrcek and E. Witten, *MHV vertices and tree amplitudes in gauge theory*, *JHEP* **09** (2004) 006 [hep-th/0403047].
- [21] W. L. van Neerven, *Infrared Behavior of On-shell Form-factors in a $N = 4$ Supersymmetric Yang-Mills Field Theory*, *Z. Phys.* **C30** (1986) 595.
- [22] L. F. Alday and J. Maldacena, *Comments on gluon scattering amplitudes via AdS/CFT*, *JHEP* **11** (2007) 068 [0710.1060].
- [23] J. Maldacena and A. Zhiboedov, *Form factors at strong coupling via a Y-system*, *JHEP* **11** (2010) 104 [1009.1139].
- [24] A. Brandhuber, B. Spence, G. Travaglini and G. Yang, *Form Factors in $N=4$ Super Yang-Mills and Periodic Wilson Loops*, *JHEP* **01** (2011) 134 [1011.1899].
- [25] A. Brandhuber, O. Gürdoğan, R. Mooney, G. Travaglini and G. Yang, *Harmony of Super Form Factors*, *JHEP* **10** (2011) 046 [1107.5067].
- [26] B. Penante, B. Spence, G. Travaglini and C. Wen, *On super form factors of half-BPS operators in $N=4$ super Yang-Mills*, *JHEP* **1404** (2014) 083 [1402.1300].

-
- [27] A. Brandhuber, E. Hughes, R. Panerai, B. Spence and G. Travaglini, *The connected prescription for form factors in twistor space*, *JHEP* **11** (2016) 143 [1608.03277].
- [28] L. V. Bork, D. I. Kazakov and G. S. Vartanov, *On form factors in $N=4$ sym*, *JHEP* **02** (2011) 063 [1011.2440].
- [29] T. Gehrmann, J. M. Henn and T. Huber, *The three-loop form factor in $N=4$ super Yang-Mills*, *JHEP* **03** (2012) 101 [1112.4524].
- [30] A. Brandhuber, G. Travaglini and G. Yang, *Analytic two-loop form factors in $\mathcal{N}=4$ SYM*, *JHEP* **05** (2012) 082 [1201.4170].
- [31] A. Brandhuber, O. Gurdogan, D. Korres, R. Mooney and G. Travaglini, *Two-loop Sudakov Form Factor in ABJM*, *JHEP* **11** (2013) 022 [1305.2421].
- [32] D. Young, *Form Factors of Chiral Primary Operators at Two Loops in $ABJ(M)$* , *JHEP* **06** (2013) 049 [1305.2422].
- [33] L. Bianchi and M. S. Bianchi, *Nonplanarity through unitarity in the ABJM theory*, *Phys. Rev.* **D89** (2014) 125002 [1311.6464].
- [34] L. J. Dixon and Y. Shadmi, *Testing gluon selfinteractions in three jet events at hadron colliders*, *Nucl. Phys.* **B423** (1994) 3 [hep-ph/9312363].
- [35] T. Cohen, H. Elvang and M. Kiermaier, *On-shell constructibility of tree amplitudes in general field theories*, *JHEP* **04** (2011) 053 [1010.0257].
- [36] J. Broedel and L. J. Dixon, *Color-kinematics duality and double-copy construction for amplitudes from higher-dimension operators*, *JHEP* **10** (2012) 091 [1208.0876].
- [37] D. Neill, *Two-Loop Matching onto Dimension Eight Operators in the Higgs-Glue Sector*, 0908.1573.
- [38] S. Dawson, I. M. Lewis and M. Zeng, *Effective field theory for Higgs boson plus jet production*, *Phys. Rev.* **D90** (2014) 093007 [1409.6299].
- [39] F. Wilczek, *Decays of Heavy Vector Mesons Into Higgs Particles*, *Phys. Rev. Lett.* **39** (1977) 1304.
- [40] M. A. Shifman, A. I. Vainshtein, M. B. Voloshin and V. I. Zakharov, *Low-Energy Theorems for Higgs Boson Couplings to Photons*, *Sov. J. Nucl. Phys.* **30** (1979) 711.

-
- [41] S. Dawson, *Radiative corrections to Higgs boson production*, *Nucl. Phys.* **B359** (1991) 283.
- [42] M. Spira, A. Djouadi, D. Graudenz and P. M. Zerwas, *Higgs boson production at the LHC*, *Nucl. Phys.* **B453** (1995) 17 [hep-ph/9504378].
- [43] L. J. Dixon, E. W. N. Glover and V. V. Khoze, *MHV rules for Higgs plus multi-gluon amplitudes*, *JHEP* **12** (2004) 015 [hep-th/0411092].
- [44] S. D. Badger, E. W. N. Glover and V. V. Khoze, *MHV rules for Higgs plus multi-parton amplitudes*, *JHEP* **03** (2005) 023 [hep-th/0412275].
- [45] S. D. Badger and E. W. N. Glover, *One-loop helicity amplitudes for $H \rightarrow$ gluons: The All-minus configuration*, *Nucl. Phys. Proc. Suppl.* **160** (2006) 71 [hep-ph/0607139].
- [46] S. D. Badger, E. W. N. Glover and K. Risager, *One-loop phi-MHV amplitudes using the unitarity bootstrap*, *JHEP* **07** (2007) 066 [0704.3914].
- [47] S. Badger, E. W. Nigel Glover, P. Mastrolia and C. Williams, *One-loop Higgs plus four gluon amplitudes: Full analytic results*, *JHEP* **01** (2010) 036 [0909.4475].
- [48] W. Buchmuller and D. Wyler, *Effective Lagrangian Analysis of New Interactions and Flavor Conservation*, *Nucl. Phys.* **B268** (1986) 621.
- [49] D. Neill, *Analytic Virtual Corrections for Higgs Transverse Momentum Spectrum at $O(\alpha_s^2/m_t^3)$ via Unitarity Methods*, 0911.2707.
- [50] R. V. Harlander and T. Neumann, *Probing the nature of the Higgs-gluon coupling*, *Phys. Rev.* **D88** (2013) 074015 [1308.2225].
- [51] T. Gehrmann, M. Jaquier, E. W. N. Glover and A. Koukoutsakis, *Two-Loop QCD Corrections to the Helicity Amplitudes for $H \rightarrow 3$ partons*, *JHEP* **02** (2012) 056 [1112.3554].
- [52] F. Loebbert, D. Nandan, C. Sieg, M. Wilhelm and G. Yang, *On-Shell Methods for the Two-Loop Dilatation Operator and Finite Remainders*, *JHEP* **10** (2015) 012 [1504.06323].
- [53] H. Elvang and Y.-t. Huang, *Scattering Amplitudes*, 1308.1697.
- [54] J. M. Henn and J. C. Plefka, *Scattering Amplitudes in Gauge Theories, Lect. Notes Phys.* **883** (2014) pp.1.

-
- [55] F. A. Berends and W. T. Giele, *Recursive Calculations for Processes with n Gluons*, *Nucl. Phys.* **B306** (1988) 759.
- [56] M. L. Mangano, S. J. Parke and Z. Xu, *Duality and Multi - Gluon Scattering*, *Nucl. Phys.* **B298** (1988) 653.
- [57] R. Britto, F. Cachazo and B. Feng, *New recursion relations for tree amplitudes of gluons*, *Nucl. Phys.* **B715** (2005) 499 [[hep-th/0412308](#)].
- [58] B. Feng, J. Wang, Y. Wang and Z. Zhang, *BCFW Recursion Relation with Nonzero Boundary Contribution*, *JHEP* **01** (2010) 019 [[0911.0301](#)].
- [59] Q. Jin and B. Feng, *Recursion Relation for Boundary Contribution*, *JHEP* **06** (2015) 018 [[1412.8170](#)].
- [60] Q. Jin and B. Feng, *Boundary Operators of BCFW Recursion Relation*, *JHEP* **04** (2016) 123 [[1507.00463](#)].
- [61] A. Brandhuber, P. Heslop and G. Travaglini, *A Note on dual superconformal symmetry of the $N=4$ super Yang-Mills S -matrix*, *Phys.Rev.* **D78** (2008) 125005 [[0807.4097](#)].
- [62] N. Arkani-Hamed, J. L. Bourjaily, F. Cachazo, S. Caron-Huot and J. Trnka, *The All-Loop Integrand For Scattering Amplitudes in Planar $N=4$ SYM*, *JHEP* **01** (2011) 041 [[1008.2958](#)].
- [63] G. Georgiou and V. V. Khoze, *Tree amplitudes in gauge theory as scalar MHV diagrams*, *JHEP* **05** (2004) 070 [[hep-th/0404072](#)].
- [64] H. Elvang, D. Z. Freedman and M. Kiermaier, *Recursion Relations, Generating Functions, and Unitarity Sums in $N=4$ SYM Theory*, *JHEP* **04** (2009) 009 [[0808.1720](#)].
- [65] H. Elvang, D. Z. Freedman and M. Kiermaier, *Proof of the MHV vertex expansion for all tree amplitudes in $N=4$ SYM theory*, *JHEP* **06** (2009) 068 [[0811.3624](#)].
- [66] A. Brandhuber, B. J. Spence and G. Travaglini, *One-loop gauge theory amplitudes in $N=4$ super Yang-Mills from MHV vertices*, *Nucl. Phys.* **B706** (2005) 150 [[hep-th/0407214](#)].
- [67] J. M. Maldacena, *The Large N limit of superconformal field theories and supergravity*, *Int. J. Theor. Phys.* **38** (1999) 1113 [[hep-th/9711200](#)].

-
- [68] J. M. Maldacena, *TASI 2003 lectures on AdS / CFT*, in *Progress in string theory. Proceedings, Summer School, TASI 2003, Boulder, USA, June 2-27, 2003*, pp. 155–203, 2003, [hep-th/0309246](#).
- [69] G. 't Hooft, *A Planar Diagram Theory for Strong Interactions*, *Nucl. Phys.* **B72** (1974) 461.
- [70] C.-N. Yang and C. P. Yang, *Thermodynamics of one-dimensional system of bosons with repulsive delta function interaction*, *J. Math. Phys.* **10** (1969) 1115.
- [71] A. B. Zamolodchikov, *Thermodynamic Bethe Ansatz in Relativistic Models. Scaling Three State Potts and Lee-yang Models*, *Nucl. Phys.* **B342** (1990) 695.
- [72] N. Beisert et al., *Review of AdS/CFT Integrability: An Overview*, *Lett. Math. Phys.* **99** (2012) 3 [[1012.3982](#)].
- [73] L. Brink, J. H. Schwarz and J. Scherk, *Supersymmetric Yang-Mills Theories*, *Nucl. Phys.* **B121** (1977) 77.
- [74] V. P. Nair, *A Current Algebra for Some Gauge Theory Amplitudes*, *Phys. Lett.* **B214** (1988) 215.
- [75] M. T. Grisaru, H. N. Pendleton and P. van Nieuwenhuizen, *Supergravity and the S Matrix*, *Phys. Rev.* **D15** (1977) 996.
- [76] M. T. Grisaru and H. N. Pendleton, *Some Properties of Scattering Amplitudes in Supersymmetric Theories*, *Nucl. Phys.* **B124** (1977) 81.
- [77] J. Drummond, J. Henn, G. Korchemsky and E. Sokatchev, *Dual superconformal symmetry of scattering amplitudes in $N=4$ super-Yang-Mills theory*, *Nucl. Phys.* **B828** (2010) 317 [[0807.1095](#)].
- [78] J. M. Drummond, J. M. Henn and J. Plefka, *Yangian symmetry of scattering amplitudes in $N=4$ super Yang-Mills theory*, *JHEP* **0905** (2009) 046 [[0902.2987](#)].
- [79] N. Beisert, *The complete one loop dilatation operator of $N=4$ superYang-Mills theory*, *Nucl. Phys.* **B676** (2004) 3 [[hep-th/0307015](#)].
- [80] N. Beisert, *The $su(2|3)$ dynamic spin chain*, *Nucl. Phys.* **B682** (2004) 487 [[hep-th/0310252](#)].
- [81] J. Minahan and K. Zarembo, *The Bethe ansatz for $N=4$ superYang-Mills*, *JHEP* **0303** (2003) 013 [[hep-th/0212208](#)].

-
- [82] N. Beisert and M. Staudacher, *The $N=4$ SYM integrable super spin chain*, *Nucl.Phys.* **B670** (2003) 439 [[hep-th/0307042](#)].
- [83] B. Eden, *A Two-loop test for the factorised S-matrix of planar $N = 4$* , *Nucl. Phys.* **B738** (2006) 409 [[hep-th/0501234](#)].
- [84] A. V. Belitsky, G. P. Korchemsky and D. Mueller, *Integrability of two-loop dilatation operator in gauge theories*, *Nucl. Phys.* **B735** (2006) 17 [[hep-th/0509121](#)].
- [85] G. Georgiou, V. Gili and J. Plefka, *The two-loop dilatation operator of $N=4$ super Yang-Mills theory in the $SO(6)$ sector*, *JHEP* **12** (2011) 075 [[1106.0724](#)].
- [86] B. Eden, C. Jarczak and E. Sokatchev, *Three-loop test of the dilatation operator and integrability in $N = 4$ SYM*, *Fortsch. Phys.* **53** (2005) 610.
- [87] C. Sieg, *Superspace calculation of the three-loop dilatation operator of $N=4$ SYM theory*, *Phys. Rev.* **D84** (2011) 045014 [[1008.3351](#)].
- [88] N. Beisert, T. McLoughlin and R. Roiban, *The Four-loop dressing phase of $N=4$ SYM*, *Phys. Rev.* **D76** (2007) 046002 [[0705.0321](#)].
- [89] M. D. Schwartz, *Quantum Field Theory and the Standard Model*. Cambridge University Press, 2014.
- [90] R. E. Cutkosky, *Singularities and discontinuities of Feynman amplitudes*, *J. Math. Phys.* **1** (1960) 429.
- [91] G. Passarino and M. J. G. Veltman, *One Loop Corrections for $e^+ e^-$ Annihilation Into $\mu^+ \mu^-$ in the Weinberg Model*, *Nucl. Phys.* **B160** (1979) 151.
- [92] G. 't Hooft and M. J. G. Veltman, *Regularization and Renormalization of Gauge Fields*, *Nucl. Phys.* **B44** (1972) 189.
- [93] W. Pauli and F. Villars, *On the Invariant regularization in relativistic quantum theory*, *Rev. Mod. Phys.* **21** (1949) 434.
- [94] G. 't Hooft and M. J. G. Veltman, *DIAGRAMMAR*, *NATO Sci. Ser. B* **4** (1974) 177.
- [95] N. Arkani-Hamed, F. Cachazo and J. Kaplan, *What is the Simplest Quantum Field Theory?*, *JHEP* **09** (2010) 016 [[0808.1446](#)].

-
- [96] A. Brandhuber, S. McNamara, B. J. Spence and G. Travaglini, *Loop amplitudes in pure Yang-Mills from generalised unitarity*, *JHEP* **10** (2005) 011 [hep-th/0506068].
- [97] Z. Bern, J. S. Rozowsky and B. Yan, *Two loop four gluon amplitudes in $N=4$ superYang-Mills*, *Phys. Lett.* **B401** (1997) 273 [hep-ph/9702424].
- [98] C. Anastasiou, Z. Bern, L. J. Dixon and D. A. Kosower, *Planar amplitudes in maximally supersymmetric Yang-Mills theory*, *Phys. Rev. Lett.* **91** (2003) 251602 [hep-th/0309040].
- [99] Z. Bern, L. J. Dixon and V. A. Smirnov, *Iteration of planar amplitudes in maximally supersymmetric Yang-Mills theory at three loops and beyond*, *Phys. Rev.* **D72** (2005) 085001 [hep-th/0505205].
- [100] Z. Bern, M. Czakon, D. A. Kosower, R. Roiban and V. A. Smirnov, *Two-loop iteration of five-point $N=4$ super-Yang-Mills amplitudes*, *Phys. Rev. Lett.* **97** (2006) 181601 [hep-th/0604074].
- [101] F. Cachazo, M. Spradlin and A. Volovich, *Iterative structure within the five-particle two-loop amplitude*, *Phys. Rev.* **D74** (2006) 045020 [hep-th/0602228].
- [102] A. B. Goncharov, *Multiple polylogarithms, cyclotomy and modular complexes*, *Math. Res. Lett.* **5** (1998) 497 [1105.2076].
- [103] H. Gangl, A. B. Goncharov and A. Levin, *Multiple polylogarithms, polygons, trees and algebraic cycles*, *Proc. Symp. Pure Math.* **80** (2009) 547 [arXiv:math.NT/0508066].
- [104] C. Duhr, H. Gangl and J. R. Rhodes, *From polygons and symbols to polylogarithmic functions*, *JHEP* **10** (2012) 075 [1110.0458].
- [105] A. B. Goncharov, M. Spradlin, C. Vergu and A. Volovich, *Classical Polylogarithms for Amplitudes and Wilson Loops*, *Phys.Rev.Lett.* **105** (2010) 151605 [1006.5703].
- [106] V. Del Duca, C. Duhr and V. A. Smirnov, *An Analytic Result for the Two-Loop Hexagon Wilson Loop in $N = 4$ SYM*, *JHEP* **03** (2010) 099 [0911.5332].
- [107] V. Del Duca, C. Duhr and V. A. Smirnov, *The Two-Loop Hexagon Wilson Loop in $N = 4$ SYM*, *JHEP* **05** (2010) 084 [1003.1702].
- [108] D. Gaiotto, J. Maldacena, A. Sever and P. Vieira, *Pulling the straps of polygons*, *JHEP* **12** (2011) 011 [1102.0062].

-
- [109] S. Caron-Huot, *Superconformal symmetry and two-loop amplitudes in planar $N=4$ super Yang-Mills*, *JHEP* **12** (2011) 066 [1105.5606].
- [110] L. J. Dixon, J. M. Drummond and J. M. Henn, *Bootstrapping the three-loop hexagon*, *JHEP* **11** (2011) 023 [1108.4461].
- [111] P. Heslop and V. V. Khoze, *Wilson Loops @ 3-Loops in Special Kinematics*, *JHEP* **11** (2011) 152 [1109.0058].
- [112] L. J. Dixon, J. M. Drummond and J. M. Henn, *Analytic result for the two-loop six-point NMHV amplitude in $N=4$ super Yang-Mills theory*, *JHEP* **01** (2012) 024 [1111.1704].
- [113] A. Prygarin, M. Spradlin, C. Vergu and A. Volovich, *All Two-Loop MHV Amplitudes in Multi-Regge Kinematics From Applied Symbology*, *Phys. Rev.* **D85** (2012) 085019 [1112.6365].
- [114] P. Cvitanovic and T. Kinoshita, *Sixth Order Magnetic Moment of the electron*, *Phys. Rev.* **D10** (1974) 4007.
- [115] S. Laporta and E. Remiddi, *The Analytical value of the electron ($g-2$) at order α^{*3} in QED*, *Phys. Lett.* **B379** (1996) 283 [hep-ph/9602417].
- [116] B. Eden, P. Heslop, G. P. Korchemsky and E. Sokatchev, *The super-correlator/super-amplitude duality: Part I*, *Nucl. Phys.* **B869** (2013) 329 [1103.3714].
- [117] C. R. Schmidt, *$H \rightarrow g g g$ ($g q$ anti- q) at two loops in the large $M(t)$ limit*, *Phys. Lett.* **B413** (1997) 391 [hep-ph/9707448].
- [118] S. Catani, *The Singular behavior of QCD amplitudes at two loop order*, *Phys. Lett.* **B427** (1998) 161 [hep-ph/9802439].
- [119] A. V. Kotikov and L. N. Lipatov, *DGLAP and BFKL equations in the $N = 4$ supersymmetric gauge theory*, *Nucl. Phys.* **B661** (2003) 19 [hep-ph/0208220].
- [120] A. V. Kotikov, L. N. Lipatov, A. I. Onishchenko and V. N. Velizhanin, *Three loop universal anomalous dimension of the Wilson operators in $N = 4$ SUSY Yang-Mills model*, *Phys. Lett.* **B595** (2004) 521 [hep-th/0404092].
- [121] S. Moch, J. A. M. Vermaseren and A. Vogt, *The Three loop splitting functions in QCD: The Nonsinglet case*, *Nucl. Phys.* **B688** (2004) 101 [hep-ph/0403192].
- [122] A. Vogt, S. Moch and J. A. M. Vermaseren, *The Three-loop splitting functions in QCD: The Singlet case*, *Nucl. Phys.* **B691** (2004) 129 [hep-ph/0404111].

-
- [123] A. Brandhuber, B. Penante, G. Travaglini and C. Wen, *The last of the simple remainders*, *JHEP* **1408** (2014) 100 [1406.1443].
- [124] L. Koster, V. Mitev and M. Staudacher, *A Twistorial Approach to Integrability in $\mathcal{N} = 4$ SYM*, *Fortsch.Phys.* **63** (2015) 142 [1410.6310].
- [125] A. Brandhuber, B. Penante, G. Travaglini and D. Young, *Integrability and unitarity*, *JHEP* **1505** (2015) 005 [1502.06627].
- [126] A. Brandhuber, B. Penante, G. Travaglini and D. Young, *Integrability and MHV diagrams in $N=4$ supersymmetric Yang-Mills theory*, *Phys.Rev.Lett.* **114** (2015) 071602 [1412.1019].
- [127] B. I. Zwiebel, *From Scattering Amplitudes to the Dilatation Generator in $N=4$ SYM*, *J.Phys.* **A45** (2012) 115401 [1111.0083].
- [128] M. Wilhelm, *Amplitudes, Form Factors and the Dilatation Operator in $\mathcal{N} = 4$ SYM Theory*, *JHEP* **1502** (2015) 149 [1410.6309].
- [129] J. L. Bourjaily, *Efficient Tree-Amplitudes in $N=4$: Automatic BCFW Recursion in Mathematica*, 1011.2447.
- [130] D. Anselmi, M. T. Grisaru and A. Johansen, *A Critical behavior of anomalous currents, electric - magnetic universality and CFT in four-dimensions*, *Nucl. Phys.* **B491** (1997) 221 [hep-th/9601023].
- [131] M. Bianchi, S. Kovacs, G. Rossi and Y. S. Stanev, *On the logarithmic behavior in $N=4$ SYM theory*, *JHEP* **08** (1999) 020 [hep-th/9906188].
- [132] K. Konishi, *Anomalous Supersymmetry Transformation of Some Composite Operators in SQCD*, *Phys. Lett.* **135B** (1984) 439.
- [133] K.-i. Konishi and K.-i. Shizuya, *Functional Integral Approach to Chiral Anomalies in Supersymmetric Gauge Theories*, *Nuovo Cim.* **A90** (1985) 111.
- [134] D. Amati, K. Konishi, Y. Meurice, G. C. Rossi and G. Veneziano, *Nonperturbative Aspects in Supersymmetric Gauge Theories*, *Phys. Rept.* **162** (1988) 169.
- [135] L. Andrianopoli and S. Ferrara, *K - K excitations on $AdS(5) \times S^{*5}$ as $N=4$ 'primary' superfields*, *Phys. Lett.* **B430** (1998) 248 [hep-th/9803171].
- [136] L. Andrianopoli and S. Ferrara, *'Nonchiral' primary superfields in the $AdS(d+1)$ / $CFT(d)$ correspondence*, *Lett. Math. Phys.* **46** (1998) 265 [hep-th/9807150].

- [137] L. Andrianopoli and S. Ferrara, *On short and long $SU(2,2/4)$ multiplets in the AdS / CFT correspondence*, *Lett. Math. Phys.* **48** (1999) 145 [[hep-th/9812067](#)].
- [138] M. Bianchi, S. Kovacs, G. Rossi and Y. S. Stanev, *Properties of the Konishi multiplet in $N=4$ SYM theory*, *JHEP* **05** (2001) 042 [[hep-th/0104016](#)].
- [139] T. Gehrmann and E. Remiddi, *Differential equations for two loop four point functions*, *Nucl. Phys.* **B580** (2000) 485 [[hep-ph/9912329](#)].
- [140] T. Gehrmann and E. Remiddi, *Two loop master integrals for $\gamma^* \rightarrow 3$ jets: The planar topologies*, *Nucl. Phys.* **B601** (2001) 248 [[hep-ph/0008287](#)].
- [141] R. N. Lee, *Presenting LiteRed: a tool for the Loop InTEgrals REDuction*, 1212.2685.
- [142] R. N. Lee, *LiteRed 1.4: a powerful tool for reduction of multiloop integrals*, *J. Phys. Conf. Ser.* **523** (2014) 012059 [[1310.1145](#)].
- [143] A. V. Smirnov, *Algorithm FIRE - Feynman Integral REDuction*, *JHEP* **10** (2008) 107 [[0807.3243](#)].
- [144] A. von Manteuffel and C. Studerus, *Reduze 2 - Distributed Feynman Integral Reduction*, 1201.4330.
- [145] S. Laporta, *High precision calculation of multiloop Feynman integrals by difference equations*, *Int. J. Mod. Phys.* **A15** (2000) 5087 [[hep-ph/0102033](#)].
- [146] B. Eden, P. Heslop, G. P. Korchemsky and E. Sokatchev, *The super-correlator/super-amplitude duality: Part I*, *Nucl. Phys.* **B869** (2013) 329 [[1103.3714](#)].
- [147] M. Bianchi, S. Kovacs, G. Rossi and Y. S. Stanev, *Anomalous dimensions in $N=4$ SYM theory at order g^{*4}* , *Nucl. Phys.* **B584** (2000) 216 [[hep-th/0003203](#)].
- [148] K. A. Intriligator and W. Skiba, *Bonus symmetry and the operator product expansion of $N=4$ SuperYang-Mills*, *Nucl. Phys.* **B559** (1999) 165 [[hep-th/9905020](#)].
- [149] B. Eden, C. Jarczak, E. Sokatchev and Ya. S. Stanev, *Operator mixing in $N = 4$ SYM: The Konishi anomaly revisited*, *Nucl. Phys.* **B722** (2005) 119 [[hep-th/0501077](#)].
- [150] B. Eden, *Operator mixing in $N = 4$ SYM: The Konishi anomaly re-re-visited*, *Nucl. Phys.* **B843** (2011) 223 [[0911.4884](#)].

-
- [151] C. Anastasiou and K. Melnikov, *Higgs boson production at hadron colliders in NNLO QCD*, *Nucl. Phys.* **B646** (2002) 220 [hep-ph/0207004].
- [152] A. Djouadi, M. Spira and P. M. Zerwas, *Production of Higgs bosons in proton colliders: QCD corrections*, *Phys. Lett.* **B264** (1991) 440.
- [153] A. Djouadi, *The Anatomy of electro-weak symmetry breaking. I: The Higgs boson in the standard model*, *Phys. Rept.* **457** (2008) 1 [hep-ph/0503172].
- [154] S. Dawson, I. M. Lewis and M. Zeng, *Usefulness of effective field theory for boosted Higgs production*, *Phys. Rev.* **D91** (2015) 074012 [1501.04103].
- [155] D. Chicherin and E. Sokatchev, *Composite operators and form factors in $\mathcal{N} = 4$ SYM*, *J. Phys.* **A50** (2017) 275402 [1605.01386].
- [156] F. Loebbert, C. Sieg, M. Wilhelm and G. Yang, *Two-Loop $SL(2)$ Form Factors and Maximal Transcendentality*, *JHEP* **12** (2016) 090 [1610.06567].
- [157] J. Fleischer, A. V. Kotikov and O. L. Veretin, *Analytic two loop results for selfenergy type and vertex type diagrams with one nonzero mass*, *Nucl. Phys.* **B547** (1999) 343 [hep-ph/9808242].
- [158] Z. Bern, J. J. M. Carrasco, H. Ita, H. Johansson and R. Roiban, *On the Structure of Supersymmetric Sums in Multi-Loop Unitarity Cuts*, *Phys. Rev.* **D80** (2009) 065029 [0903.5348].
- [159] H. Elvang, Y.-t. Huang and C. Peng, *On-shell superamplitudes in $\mathcal{N} < 4$ SYM*, *JHEP* **09** (2011) 031 [1102.4843].
- [160] W. Nahm, *Supersymmetries and their Representations*, *Nucl. Phys.* **B135** (1978) 149.
- [161] E. Witten, *An Interpretation of Classical Yang-Mills Theory*, *Phys. Lett.* **77B** (1978) 394.
- [162] A. Galperin, E. Ivanov, S. Kalitsyn, V. Ogievetsky and E. Sokatchev, *$N = 3$ SUPERSYMMETRIC GAUGE THEORY*, *Phys. Lett.* **B151** (1985) 215.
- [163] Z. Bern, L. J. Dixon and D. A. Kosower, *One loop corrections to five gluon amplitudes*, *Phys. Rev. Lett.* **70** (1993) 2677 [hep-ph/9302280].
- [164] J. Bedford, A. Brandhuber, B. J. Spence and G. Travaglini, *Non-supersymmetric loop amplitudes and MHV vertices*, *Nucl. Phys.* **B712** (2005) 59 [hep-th/0412108].

-
- [165] D. J. Gross and F. Wilczek, *Asymptotically Free Gauge Theories. 1*, *Phys. Rev.* **D8** (1973) 3633.
- [166] W. T. Giele and E. W. N. Glover, *Higher order corrections to jet cross-sections in $e^+ e^-$ annihilation*, *Phys. Rev.* **D46** (1992) 1980.
- [167] Z. Kunszt, A. Signer and Z. Trocsanyi, *Singular terms of helicity amplitudes at one loop in QCD and the soft limit of the cross-sections of multiparton processes*, *Nucl. Phys.* **B420** (1994) 550 [[hep-ph/9401294](#)].
- [168] S. Catani and M. H. Seymour, *The Dipole formalism for the calculation of QCD jet cross-sections at next-to-leading order*, *Phys. Lett.* **B378** (1996) 287 [[hep-ph/9602277](#)].
- [169] S. Catani and M. H. Seymour, *A General algorithm for calculating jet cross-sections in NLO QCD*, *Nucl. Phys.* **B485** (1997) 291 [[hep-ph/9605323](#)].
- [170] G. Ferretti, R. Heise and K. Zarembo, *New integrable structures in large- N QCD*, *Phys. Rev.* **D70** (2004) 074024 [[hep-th/0404187](#)].
- [171] Z. Bern, A. De Freitas and L. J. Dixon, *Two loop helicity amplitudes for gluon-gluon scattering in QCD and supersymmetric Yang-Mills theory*, *JHEP* **03** (2002) 018 [[hep-ph/0201161](#)].
- [172] Z. Bern, A. De Freitas and L. J. Dixon, *Two loop helicity amplitudes for quark gluon scattering in QCD and gluino gluon scattering in supersymmetric Yang-Mills theory*, *JHEP* **06** (2003) 028 [[hep-ph/0304168](#)].
- [173] P. Banerjee, P. K. Dhani, M. Mahakhud, V. Ravindran and S. Seth, *Finite remainders of the Konishi at two loops in $\mathcal{N} = 4$ SYM*, *JHEP* **05** (2017) 085 [[1612.00885](#)].
- [174] Q. Jin and G. Yang, *Analytic Two-loop Higgs Amplitudes in Effective Field Theory and Maximal Transcendentality Principle*, [1804.04653](#).
- [175] C. Anastasiou, R. Britto, B. Feng, Z. Kunszt and P. Mastrolia, *D-dimensional unitarity cut method*, *Phys. Lett.* **B645** (2007) 213 [[hep-ph/0609191](#)].
- [176] A. Brandhuber, P. Heslop, G. Travaglini and D. Young, *Yangian Symmetry of Scattering Amplitudes and the Dilatation Operator in $N = 4$ Supersymmetric Yang-Mills Theory*, *Phys. Rev. Lett.* **115** (2015) 141602 [[1507.01504](#)].
- [177] L. Dolan, C. R. Nappi and E. Witten, *A Relation between approaches to integrability in superconformal Yang-Mills theory*, *JHEP* **10** (2003) 017 [[hep-th/0308089](#)].

- [178] L. Koster, V. Mitev, M. Staudacher and M. Wilhelm, *Composite Operators in the Twistor Formulation of $\mathcal{N} = 4$ Supersymmetric Yang-Mills Theory*, *Phys. Rev. Lett.* **117** (2016) 011601 [1603.04471].
- [179] L. Koster, V. Mitev, M. Staudacher and M. Wilhelm, *All tree-level MHV form factors in $\mathcal{N} = 4$ SYM from twistor space*, *JHEP* **06** (2016) 162 [1604.00012].
- [180] D. Chicherin and E. Sokatchev, *Composite operators and form factors in $N=4$ SYM*, 1605.01386.
- [181] G. Duplancic and B. Nizic, *Dimensionally regulated one loop box scalar integrals with massless internal lines*, *Eur. Phys. J.* **C20** (2001) 357 [hep-ph/0006249].
- [182] J. J. M. Carrasco, *Gauge and Gravity Amplitude Relations*, 1506.00974.